

# **Studies on the Role of Tropospheric Biennial Oscillation in the Interannual Variability of Indian Summer Monsoon**

Thesis submitted to the

**Cochin University of Science and Technology**

*in partial fulfillment of the requirement for the Degree of*

**DOCTOR OF PHILOSOPHY**

in

**ATMOSPHERIC SCIENCE**



by

**PRASANTH A PILLAI**

**Department of Atmospheric Sciences  
Cochin University of Science and Technology  
Cochin - 682 016, India**

October 2008



**COCHIN UNIVERSITY OF SCIENCE AND TECHNOLOGY**  
**DEPARTMENT OF ATMOSPHERIC SCIENCES**

Lakeside Campus, Fine Arts Avenue, Cochin - 682 016, India.

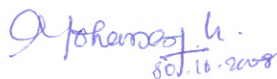
**Dr. K. Mohankumar M.Sc., Ph.D.**  
Dean, Faculty of Marine Sciences &  
Hon. Director, Centre for Space Research

**CERTIFICATE**

This is to certify that the thesis entitled *Studies on the Role of Tropospheric Biennial Oscillation in the Interannual Variability of Indian Summer Monsoon* is an authentic record of research work done by **Mr. Prasanth A Pillai** under my supervision in the Department of Atmospheric Sciences, Cochin University of Science and Technology. I also certify that the subject matter of the thesis has not formed the basis for the award of any Degree or Diploma of any University or Institution.

I also certify that **Mr. Prasanth A Pillai** has passed the Ph. D qualifying examination conducted by the Department of Atmospheric Sciences, Cochin University of Science and Technology in August 2006

Cochin 682 016  
October 29, 2008

  
**K. Mohankumar**  
Supervising Guide

## DECLARATION

I hereby declare that this thesis entitled *Studies on the Role of Tropospheric Biennial Oscillation in the Interannual Variability of Indian Summer Monsoon* is a genuine record of research work carried out by me and no part of this thesis has been submitted to any University or Institution for the award of any Degree or Diploma.

Prasanth

**PRASANTH A PILLAI**  
Research Scholar,  
Department of Atmospheric Sciences  
Cochin University of Science and Technology

Cochin 682 016  
October 29, 2008

## ACKNOWLEDGEMENT

I take this opportunity to express my sincere gratitude together with respect to my supervising guide Prof (Dr). K. Mohankuamr, Dean, Faculty of Marine Sciences. Sir introduced me to this new subject as thesis topic and is the real force for the timely completion of the work. I express my sincere and deep admiration for his patience and enthusiasm to make me write my research outputs and to correct them many time to send for publications, inspite of his busy academic and administrative schedules. Words fail to convey my respect and thanks to him.

I acknowledge Dr. K.R Santosh, Head, Deaprtment of Atmospheric Sciences and former heads Dr. C.K Rajan and Dr. C.A Babu for the assistance provided from the department during the research period.

Prof. P.V. Josph, Professor of Emeritus, Departemnt of Atmosphereic Sciences, helped me at the initial discussion of the research topic. I express my sincere gratitude to him also.

I am indebted to Dr. Anu Simon who helped me a lot during the initial stage of my research with useful suggestions and to Dr. Venu G Nair for all time help throughout the research period.

I also acknowledge all the faculty and staff of the Department of Atmospheric Sciences, for the help they gave me during these years of research. I also express my sincere gratitude to the research scholars of the department for their co-operation, especially to Mr. Jayakrishnan, Mr. Nithin and Mr. Sivaprasad for final arrangement of the thesis.

I thank University Grand commission, India for the financial support provided for the research in the form of research fellowship.

At last I thank my parents for their patience and confidence shown over me and to the god for making it in a smooth tone.

**Prasanth A Pillai**

## **PREFACE**

Indian summer monsoon exhibits wide range of variabilities in different time scales, in which interannual time scale is the most interesting and extensively studied. Interannual variability was studied in detail with the effect of El Nino southern Oscillation to the monsoon and was considered as major cause for interannual variability. But the weakening of the reverse monsoon-ENSO relationship in recent decades and normal rainfall in some of the recent El Nino years stress the need for other factors affecting the monsoon variability. This leads to the well-known biennial periodicity of Indian summer monsoon rainfall to relate with the tropospheric biennial oscillation (TBO) of tropical ocean-atmosphere system. TBO cycle and monsoon interannual cycle associated with the TBO is studied and reported in this thesis.

The thesis consists of eight chapters, in which the first chapter contains general introduction of Asian summer monsoon, factors making it and its different scales of variabilities. It also gives description of TBO, recent studies on TBO and different theories proposed to explain TBO phenomena. NCEP/ NCAR reanalysis data sets for the period 1950-2005 are main data sets used in the study along with NCEP SST, NOAA OLR, Indian summer monsoon rainfall Index, CMAP precipitation data and ECMWF wind and temperature. Chapter 2 gives the difference in association of SST and lower level wind to interannual variability of Indian summer monsoon in both biennial and low frequencies. It also describes the cycle of anomalies of sea surface temperature, convection, wind, sea level pressure and Indian Ocean fluxes associated with interannual variability of Indian summer monsoon.

Third chapter explains the circulation features of TBO. It describes equatorial Walker circulation, mean meridional circulation and local Hadley circulation during TBO cycle and monsoon. Eventhough ENSO has 2-7 year periodicity, it also has a biennial periodicity and most of the ENSO years are coinciding with TBO years. Chapter 4 analyses the difference of TBO cycle when it is associated with ENSO, in absence of ENSO and also with Indian Ocean Dipole. This analysis gives the interannual

variability of Indian summer monsoon in the presence and absence of ENSO and IOD. The biennial oscillation of Indian summer monsoon has significant changes along with the factors determining TBO. Chapter 5 identifies the major periodicities of intraseasonal oscillation during TBO years for OLR and zonal wind. It also identifies the variance of major periodicities in different TBO years and their propagation.

The chapter 6 links the stratospheric QBO and tropospheric biennial oscillation over Indian and Australian monsoon region, especially in TBO years. Vertical structure of zonal wind and temperature has unique structure over Indian monsoon region in TBO cycle. The pattern is quite different in Australian monsoon region. But these two monsoon regions linked with the zonal wind and sea surface temperature over Indian Ocean and Pacific Ocean in QBO scale. The seventh chapter is about the changes occurred to TBO cycle and interannual variability of monsoon due to the climate regime shift of 1976. Role of local and remote forcing on monsoon along with in phase Indian to Australian monsoon transition is investigated.

Final chapter (chapter 8) summarises the results of above chapters and gives scope for future works. References in alphabetical order are included at the end of the thesis. List of research publications in journals and conferences during the period of research along with abbreviations used in the thesis are also presented in the thesis.

## CONTENTS

		PAGE No
<b>Chapter 1</b>	<b>Introduction</b>	1
1.1	The monsoon	1
1.1.1	The monsoon makers	2
1.1.2	The annual cycle and mean monsoon	3
1.2	The Indian summer monsoon	7
1.3	Variability of the monsoon	9
1.3.1	Intraseasonal variability	9
1.3.2	Interannual variability	10
1.3.3	Interdecadal variability	12
1.4	Modes of Interannual variability	12
1.4.1	Tropospheric Biennial Oscillation	15
1.4.1.1	Role of Oceans and Asian-Australian monsoon in TBO	15
1.4.1.2	Theories of TBO	17
<b>Chapter 2</b>	<b>Biennial Oscillation of Tropical Ocean-Atmosphere System Associated with Indian Summer Monsoon</b>	
2.1	Introduction	24
2.2	Objectives of the study	26
2.3	Data and methodology	26
2.4	Results	29
2.4.1	Indian summer monsoon rainfall in TBO and ENSO scale	29
2.4.2	Seasonal evolution of SST and wind in TBO and ENSO scale	30
2.4.3	Relative contribution of TBO and ENSO scale variations to monsoon rainfall	30
2.4.4	Ocean- atmosphere processes in TBO transition	35
2.5	Discussion	44
2.6	Conclusion	46
<b>Chapter 3</b>	<b>Salient Features of Atmospheric circulation associated with TBO</b>	
3.1	Introduction	48
3.2	Objectives of the study	50
3.3	Data and methodology	50
3.4	Results	51
3.4.1	Anomalous Walker circulation associated with TBO	51
3.4.2	Mean meridional circulation during TBO cycle	58

3.4.3	Local monsoon Hadley circulation during the TBO cycle	60
3.4.4	Temporal variation of local Hadley circulation	61
3.4.5	Discussion and conclusion	62
<b>Chapter 4</b>	<b>Influence of El Nino Southern Oscillation and Indian Ocean Dipole in Biennial Oscillation of Indian Summer Monsoon</b>	
4.1	Introduction	64
4.2	Objectives of the study	67
4.3	Data and methodology	68
4.4	Results	68
4.4.1	Effect of ENSO on TBO	68
4.4.1.1	Evolution of ENSO anomalies in the Pacific Ocean	69
4.4.1.2	TBO mechanism in presence and absence of ENSO	70
4.4.2	Role of IOD in TBO	77
4.4.2.1	In phase and out of phase association of TBO and IOD	78
4.4.3	TBO cycle in absence of both IOD and ENSO (pure TBO)	82
4.5	Discussion and Summary	83
<b>Chapter 5</b>	<b>Investigation of Common Mode of Variability in Boreal summer intraseasonal Oscillation and Tropospheric Biennial Oscillation</b>	
5.1	Introduction	87
5.2	Objectives of the study	89
5.3	Data and methodology	89
5.4	Results	90
5.4.1	Wavelet analysis of TBO years	90
5.4.2	Dominant patterns of ISO and TBO	92
5.4.3	Propagation of convection in TBO years	98
5.5	Conclusion	103
<b>Chapter 6</b>	<b>Linkage of stratospheric QBO and tropospheric biennial oscillation of Asian-Australian monsoon system</b>	
6.1	Introduction	105
6.2	Objectives of the study	107
6.3	Data and Methodology	108
6.4	Results	109
6.4.1	Wavelet analysis of zonal wind over Indian monsoon region	109
6.4.2	Zonal wind structure in QBO scale	110
6.4.3	Propagation of zonal wind anomalies in QBO scale	111



6.4.4	Vertical profile of zonal wind during TBO cycle	115
6.4.5	Zonal temperature anomalies in TBO cycle	118
6.4.6	Relationship of zonal wind in QBO scale and SST in TBO cycle	119
6.4.7	Effect of QBO on ISMR in TBO cycle	124
6.5	Discussion	126
6.6	Conclusion	127
<b>Chapter 7</b>	<b>Effect of late 1970's Climate Shift on Interannual Variability of Indian Summer Monsoon Associated with TBO</b>	
7.1	Introduction	128
7.2	Objectives of the study	129
7.3	Data and methodology	130
7.4	Results and Discussion	131
7.4.1	EOF analysis	131
7.4.2	TBO mechanism before and after the climate shift	135
7.4.3	Effect of ENSO on TBO cycle	140
7.4.4	Asian-Australian monsoon relationship	144
7.4.5	SST-latent heat relationship in Indian Ocean	145
7.5	Discussion	146
7.6	Conclusion	148
<b>Chapter 8</b>	<b>Summary and Conclusion</b>	149
8.1	Scope for future work	152
	<b>References</b>	154
	List of Publications	165
	List of Abbreviations	167

---

# INTRODUCTION

---

### 1.1 The monsoon

The term 'monsoon' is derived from the Arabic word *mausam*, which means seasons. The term monsoon is widely used to denote any annual climate cycle with seasonal wind reversal in both tropical and subtropical regions resulting seasonal changes in both atmospheric circulation and associated precipitation. These changes arise from the reversal in heating and temperature gradient between continents and adjacent oceans with the progress of seasons. The extremes in the seasons are denoted as summer and winter. The name southwest monsoon is used for the rain and southwesterly winds of summer season and northeast monsoon to the winter.

Ramage (1971) formulated four criteria to define the monsoon areas as:

- i. the prevailing wind direction shifts by at least  $120^{\circ}$  between January and July;
- ii. the average frequency of prevailing wind direction in January and July exceeds 40%;
- iii. the mean resultant wind in at least one of the months exceeds  $3\text{ms}^{-1}$  and;
- iv. fewer than one cyclone-anticyclone alternation occurs every two years in either months in a  $5^{\circ}$  latitude-longitude rectangle.

Based on the above criteria, monsoon regions include almost half of the African continent, south and east Asia and northern Australia (shaded portions in figure 1.1), in which more than half of the world population resides.

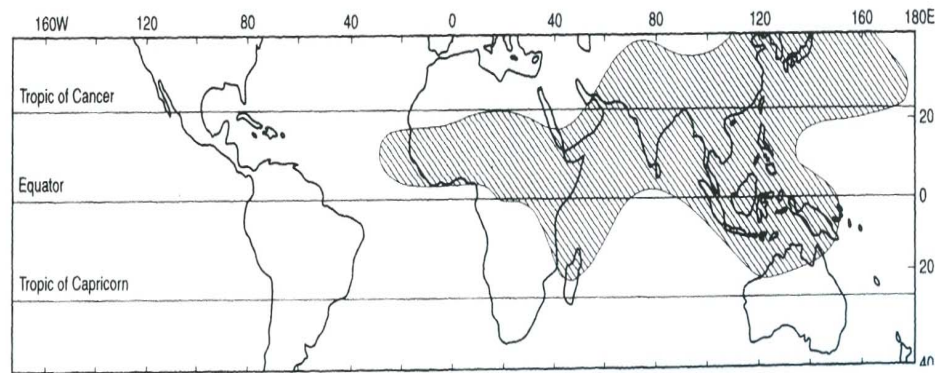


Figure 1.1 Monsoon areas (shaded portions) from criteria of Ramage. (Figure from Monsoon Meteorology (Ramage 1979), Academic press, New York)

As monsoons are such dominant features, the social and economic welfare of many tropical countries is intimately linked to the vagaries of monsoon cycle.

### 1.1.1 The monsoon makers

The three general mechanisms account for the cause and existence of monsoons are as follows

- i. ***The differential heating of the oceans and continents:*** Over the vast ocean regions, tropical circulation has little variations, but over continents it has a seasonal rhythm. The relative warming of land over ocean produces heat lows, which gradually forms regions of convergence. The air is drawn into the low from the winter hemisphere crossing the equator. In winter the condition reverses. Thus the tropical oceans and continents experience a semi-annual reversal in wind direction, which characterises the monsoon.
- ii. ***Moisture processes in the atmosphere:*** As moist warm air rises over summer time heated land surfaces, the moisture eventually condense, releasing energy in the form of latent heat of condensation. This extra energy raises summer land-ocean pressure differences adding vigor to monsoon.
- iii. ***Earth's rotation:*** As the earth rotates on its own axis and produces a rotation force called Coriolis force, air in the monsoon currents moves in curved paths. Inter-hemispheric difference in Coriolis force also causes wind to change direction as they cross the equator.

### 1.1.2 The annual cycle and mean monsoon

The Asian monsoon system contains two distinct seasons: the *wet* and the *dry*. The wet occurs during the boreal summer when warm and moist winds blow across south Asia from southwest. During dry winter season, the winds reverse, blowing cool and dry air from the winter continent across Indian subcontinent from the northeast. The two conditions are expressed schematically in figure 1.2

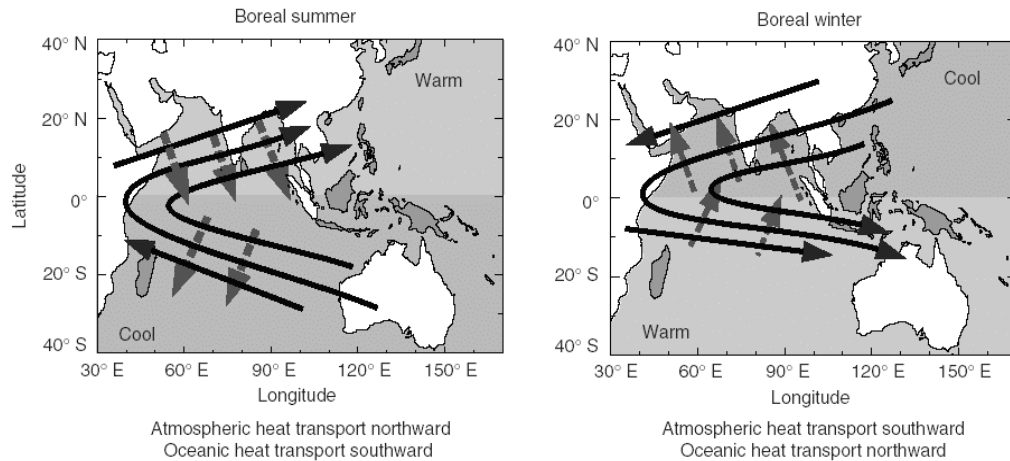


Figure 1.2 Boreal summer and winter season wind pattern and ocean heat transport.

The relationship between the general mechanism that generate monsoon, the seasonal climate cycle and monsoon annual cycle is described by Webster (1987). In the transition months between the southern and northern hemisphere summer (April and May), the intertropical convergence zone (ITCZ), which is the region of surface low pressure, rising air movements and convergence of air masses is located in the equatorial region, which is the region of maximum heating at this time. At this period of seasonal cycle, the northern hemisphere tropical-subtropical latitudes are beginning to warm up with weak vertical motions. The northern hemisphere Hadley cell is still predominates with offshore air flow. With the northward movement of the Sun in May to June, heating in the northern hemisphere land masses increases strengthening vertical motion. Northern hemisphere moisture content increases as a result of intensification of southern hemisphere Hadley cell and predominant wind direction is offshore. By this time ITCZ and associated precipitation has moved well north of the equator along with the onset of monsoon in many areas.

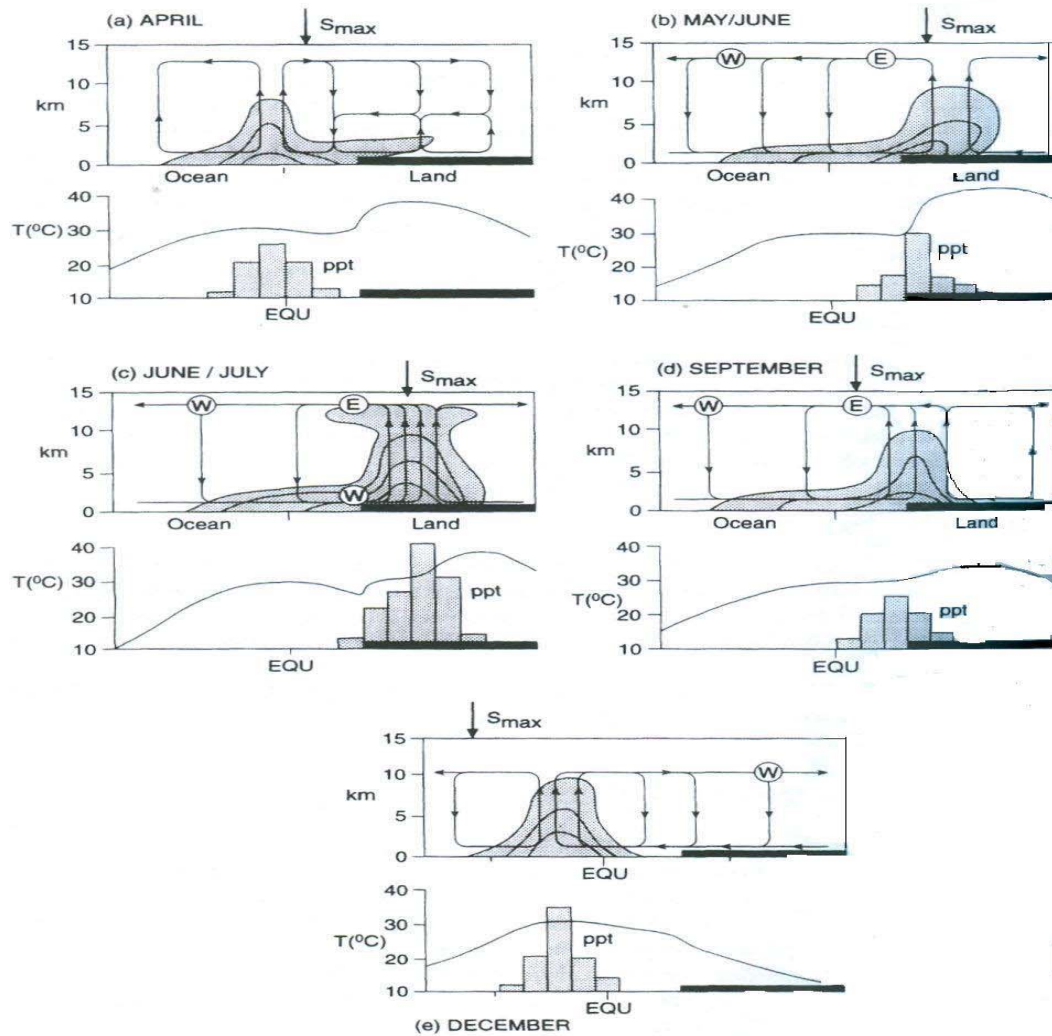


Figure 1.3 Annual monsoon cycle (Webster 1987)

During June-July period sensible heat input at surface becomes maximum, as vertical motion and moisture content over land masses. The monsoon attains its maximum intensity with maximum precipitation and northward extent. By September the heating again comes close to equator as in the April period. This indicates the cessation of northern hemisphere wet monsoon season. By December, maximum heating and ITCZ has moved well south of the equator. Northern hemisphere Hadley cell starts strengthening and zone of maximum heating attains its maximum southward position.

The schematic model of annual cycle described here is for mean annual conditions. But in reality, there is a considerable variation in onset, duration and magnitude of monsoon.

The seasonal climatology of precipitation and wind at 850 hPa during the summer (June to September, JJAS) and winter (December to February, DJF) are illustrated in figure 1.4. During northern summer, the low level circulation over Indian Ocean and the subcontinent is dominated by strong cross equatorial flow and southwesterly winds. The monsoonal circulation acts as a moisture *conveyer belt*, transporting moisture from the south Indian Ocean and the Arabian Sea towards the south Asian land masses and the Bay of Bengal (Fasullo and Webster, 1999). The relatively steady moist, unstable air advected over the south Asian landmasses enhances convection and precipitation across south Asian monsoon region. Heavy rainfall experiences over south and southeast Asian region as well as through much of the northern Indian Ocean including the eastern Arabian Sea and Bay of Bengal. Maximum precipitation is also found in the winter hemisphere just south of the equator.

The mean convection and precipitation during the northern winter shifts from southern Asia to along and south of the equator over the maritime continent and northern Australia and extending into the South Pacific Convergence Zone (SPCZ). The 850 hPa circulation has northeasterly winds over the Indian subcontinent and cross equatorial flow from north to south over the maritime continent which provides moisture for the Australian monsoon rainfall (figure 1.4b) The boreal summer south Asian monsoon tends to be stronger than boreal winter Australian monsoon both in terms of precipitation and the strength of monsoon circulation. The difference is in large part due to the presence of an elevated heat source in the form of Tibetan Plateau affecting the south Asian monsoon. The onset of summer monsoon is coincident with the reversal of the meridional temperature gradient in the upper troposphere south of the Tibetan Plateau (Flohn 1957; Li and Yanai, 1996). In the southern hemisphere the reversal of temperature gradient is not evident. But still the cross-equatorial pressure gradient that drives the winter monsoon are the result of intense radiative cooling over north Asia during winter (Webster et al. 1998).

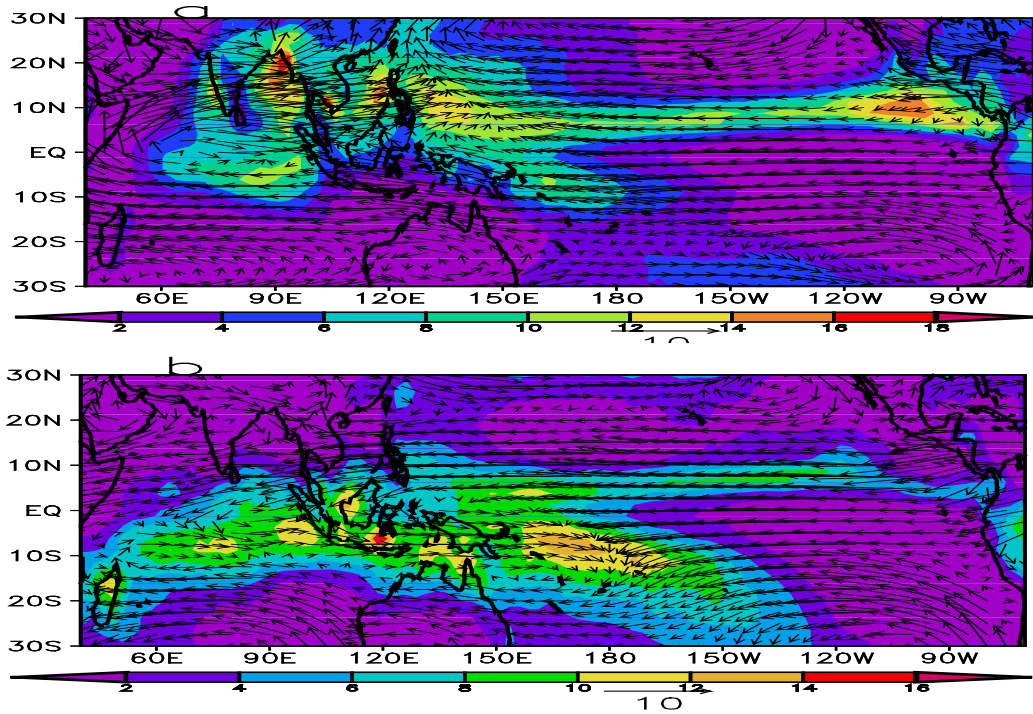


Figure 1.4: Seasonal climatology of precipitation (shaded,  $\text{mmday}^{-1}$ ) and 850 hpa wind (vector,  $\text{ms}^{-1}$ ) for (a) summer season (June to September) and (b) winter (December to February).

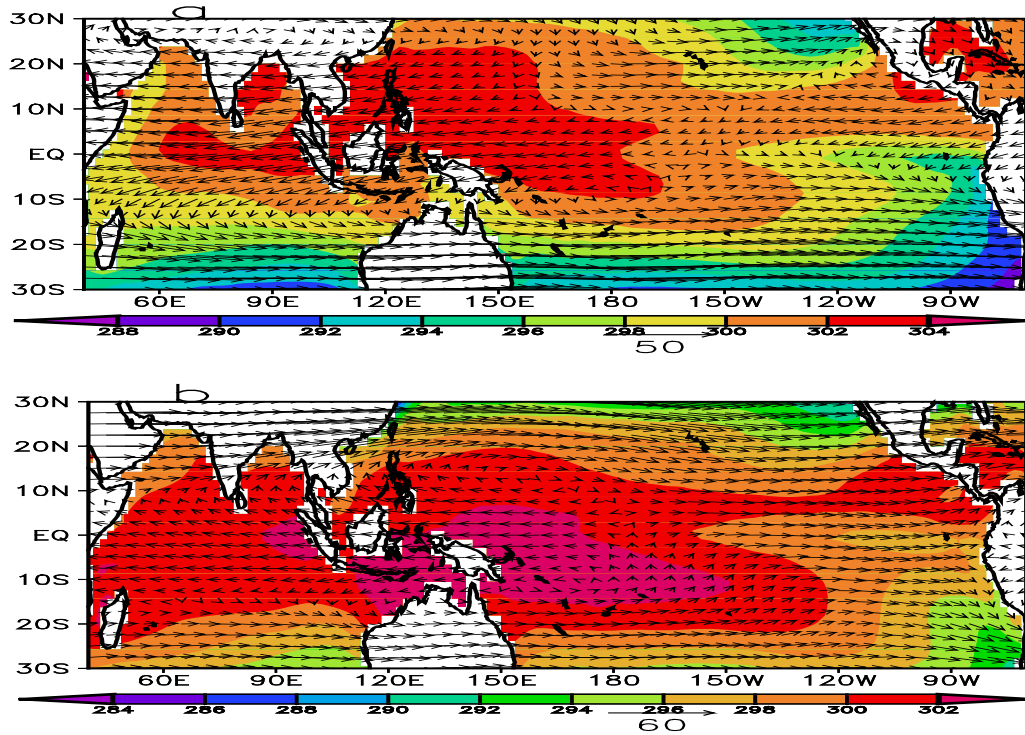


Figure 1.5: seasonal climatology of sea surface temperature (shaded, K) and 200 hpa wind (vector,  $\text{ms}^{-1}$ ) for (a) summer season (June to September) and (b) winter (December to February).

The climatology of 200 hPa wind and Indian and Pacific Ocean sea surface temperature (SST) are shown in figure 1.5 for both the seasons considered above. The predominant feature of 200 hPa wind is the persistent upper level westerly jet poleward of  $20^{\circ}$  latitude in both the hemispheres. Over South Asia and Africa, there is an upper level easterly jet during summer that is replaced by an upper level westerly jet during the winter. Thus on average the flows in both the seasons are generally opposite in direction to low level flow yielding an easterly wind shear during summer and westerly wind shear during winter. Cross-equatorial return flow is also evident during summer, large part of which is divergent contributing to the local Hadley cell (Krishnamurthi, 1971).

Mean SSTs in excess of  $28^{\circ}\text{C}$  are confined to equatorial latitudes. In the Indian Ocean basin and western Pacific Ocean, a clear latitudinal shift of warm SSTs into the summer hemisphere is evident. The entire Bay of Bengal and the eastern Arabian Sea possess warm SSTs during summer and is evenly distributed along the equator in the winter season. The expansion of warm SST eastward in the central equatorial Pacific Ocean and westward in the Indian Ocean during the northern winter is evident in the figure 15a and b.

## 1.2 The Indian summer monsoon

Indian summer monsoon, which is an active part of south Asian monsoon, gives more than 75% of the annual rainfall to the Indian land masses affecting the agriculture and thus economy of the country. The Indian summer monsoon is made up of the following components suggested by Krishnamurthi and Bhalme (1976) and is shown in figure 1.6

- 1) *The monsoon trough over north India*- It is formed in the summer months as extension of global ITCZ and is region of surface low pressure and wind shear. South of the trough has southeasterly winds and north has northwesterly winds.
- 2) *The Mascarene anticyclone system and cross-equatorial jet*- It is high pressure system formed over southeast Indian Ocean. From this high large outflow of air takes place and it crosses the equator as cross-equatorial Somali jet and becomes southwesterly wind. Reaching at maximum



intensity in the summer months, it crosses the southern Arabian Sea and reach over central western and southern coast of India. Variation in the intensity of this jet is important in determining the rainfall over India.

- 3) *The Tibetan high pressure system*- This is an upper level anticyclone found above the surface monsoon trough located over north India. By July it is established over Tibetan High lands and is well developed at 200 hPa level. It remains upto the end of summer season and then moves south-southeast direction with the movement of maximum heating to south.
- 4) *The tropical easterly jet*- The outflow of air from the southern flank of Tibetan anticyclone gives rise to tropical easterly jet and it remains from June to September.
- 5) *Monsoon cloudiness and rainfall*- Cloud cover is the manifestation of moist convective processes over the Indian subcontinent and it varies both in space and time. During active phase of monsoon, cloud cover is maximum in a belt running from western shore of Bay of Bengal to northern shore of Arabian Sea and minimum over foot hills of Himalaya, south India and Sri Lanka. The pattern reverses during break phase. Rainfall distribution closely flows the cloud distribution.

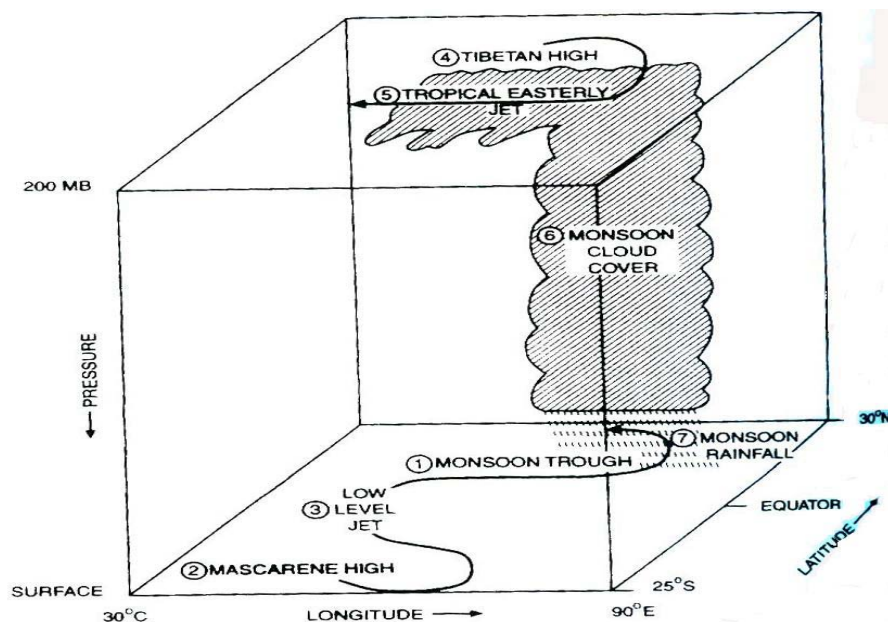


Figure 1.6 : Components of Indian summer monsoon system (Krishnamurthi and Bhalme, 1976)

### 1.3 Variability of the monsoon

The Asian monsoon exhibits high amplitude variability on all time scales from synoptic to interdecadal. The main causes for the variations are internal dynamics and boundary forcing (Shukla, 1987). Internal dynamics controlling monsoon includes a variety of aperiodic variations in the atmospheric circulations such as traveling disturbances, thermal and orographic forcing, non-linear interaction between different scales of atmospheric motions etc. Boundary forcing refers to changes in surface conditions, like spatial extent of snow cover, surface hydrological effects and sea surface variations. These changes can alter the geographical distribution of sources and sinks of heat and moisture in the atmosphere and thus patterns of tropical winds.

On the basis of time scales of variation summer monsoon variability can be divided generally into three categories:

- *Intraseasonal* (with in the season)
- *Interannual* (between years)
- *Inter decadal* (more than a decade)

#### 1.3.1 Intraseasonal variability

While defining the variability of a monsoon system in its seasonal character, its variability about a typical season is of most interest and important. The southwest monsoon is marked by episodes of prolonged abundant precipitation, active periods separated by periods of reduced rainfall, break days. The transition from active to break periods and vice versa evolve slowly such that typically 3 to 4 active periods are seen over a typical single monsoon season (Webster et al., 1998). Relative frequency of occurrence of active and break phases could influence the seasonal mean and contribute to interannual variability of intraseasonal oscillation (ISO).

The active and break periods of south Asian monsoon or the wet and dry spells over the Indian continent, are manifestation of repeated northward propagation of the Tropical Convergence Zone (TCZ) from the equatorial position to the continental position (Yasunari, 1979; Sikka and Gadgil, 1980) and results from superposition of a 10-20 day and a 30-60 day oscillations. Both the 10-20 day oscillation and the 30-

60 day oscillation contribute almost equally to the total intraseasonal variability in this region. While 30-60 day oscillation has a very large zonal scale encompassing both the south and east Asian and west Pacific monsoon regions, the 10-20 day oscillation has a smaller zonal scale and is regional in character. The 30-60 day mode is characterized by a northward propagation, while the 10-20 day mode is characterized by a westward propagation.

Two mechanisms seem to contribute to the temporal scale selection of the 30-60 day mode. One is a 'convection-thermal relaxation feedback mechanism' (Goswami and Shukla, 1984), according to which convective activity results in an increase of static stability, which depresses convection itself. As convection weakens, dynamical processes and radiative relaxation decreases moist static stability and brings the atmosphere to a new convectively unstable state. This mechanism does not involve wave dynamics and may be responsible for the northward propagating 30-60 day oscillations not associated with eastward propagation of convection in the equatorial region. The other mechanism involves eastward propagation of convection the equatorial Indian Ocean in the form of a Kelvin wave and west northwest propagation of Rossby waves emanated from the equatorial convection over the western Pacific (Wang and Xie, 1997). The time scale is determined in this case by propagation time of the moist Kelvin wave from the eastern Indian Ocean to western Pacific, the moist Rossby waves from western Pacific to the Arabian Sea where they decay and a new equatorial perturbation is generated.

The monsoon ISO is crucial building blocks of the Asian summer monsoon. Through multi-scale interactions with synoptic activity on one hand and the seasonal cycle on the other, they determine not only the probability of occurrence of daily precipitation but also the interannual variability of the seasonal mean. Thus, the ISOs also have the potential to produce interannual variability of the seasonal mean precipitation.

### **1.3.2 Interannual variability**

Among the wide range of variabilities of Asian summer monsoon, the interannual variability (IAV) is most extensively studied. The interannual variability of Asian monsoon is the yearly deviation of seasonal transition from mean annual cycle. The

interannual variability is characterized by a set of seasonally and spatially varying characteristic features. Many large-scale phenomena like ENSO which affect the monsoon also fluctuates significantly in interannual time scales. The interannual variability of the south Asian monsoon is rather modest with the interannual standard deviation being about 10% of the seasonal mean. However, larger excess or deficit of all India rainfall are associated with large spatial scale covering most of the country (Shukla, 1987). Extremes in monsoon rainfall leads to devastating floods and droughts (Shukla, 1987; Webster et al., 1998) leading to enormous economic loss and human misery. Therefore, understanding of the physical processes responsible for the observed IAV of south Asian monsoon is crucial for advancing the capability for predicting the IAV.

Although the variability of the monsoon is largely controlled by the internal dynamics of the atmosphere, which is related to the amount and distribution of solar energy, the slowly varying boundary forcing from underlying ocean and land also plays a major role in affecting the interannual variability of monsoon. The seasonal mean tropical circulation is thought to be influenced to a greater extent by the boundary conditions rather than internal dynamics (Charney and Shukla, 1981; Shukla, 1981).

Among the external causes of interannual variability of Asian monsoon, sea surface temperature (SST) is perhaps the leading impacting factor (Chao and Chen, 2001). Effect of SST on monsoon can be the *remote effect* from tropical central and east Pacific and *local effect* from oceans near Asian continent. There are several studies, both observational and modelling indicating that the interannual variability of Indian summer season (June to September) monsoon rainfall is linked to the SST variation in Pacific (Rasmusson and Carpenter, 1983; Mooley and Parthasarathy, 1983; Ju and Slingo, 1995; Soman and Slingo, 1997). The relationship between the east Pacific SST and monsoon can be regarded as problems of ENSO-monsoon relationship. There is a tendency for the El Nino to be associated with drought and La Nina to be associated with above normal conditions over India. This interaction is primarily through the change in the equatorial Walker circulation influencing the regional Hadley circulation associated with the Asian monsoon (Webster et al., 1998, Goswami, 1998; Lau and Nath, 2000).

SSTs in the west Pacific and Indian Ocean are also believed to be important for South Asian monsoon. Although the variabilities of these regional SSTs are not independent from ENSO, there is considerable effect of regional SST on interannual variability of monsoon. Regional SSTs influence monsoon through changes in surface heat and moisture fluxes, direct moisture supply, thermal difference between land and ocean and waves generated anomalous atmospheric heat sources.

### **1.3.3 Interdecadal variability**

The south Asian monsoon (SAM) precipitation does not seem to have any climatic trend but has epochs of roughly three decades when the precipitation has the tendency to be more above than below normal followed by a roughly three decades when it has the tendency to be more below than above normal. The large scale circulation changes associated with the interdecadal variability may lead to change in teleconnection patterns in these time scales. For example, the ENSO-monsoon relationship is known to undergo low frequency variations in these time scales. It may be noted that the simultaneous as well as the lag relationship between all India rainfall and *Nino3* SST anomalies has undergone major changes during the recent years compared to earlier decades. Our understanding of the interdecadal variability of the SAM remains much poorer than our understanding of the mean annual cycle and its intraseasonal and interannual variabilities. Modulation of interannual variability by interdecadal variability influences the predictability of seasonal mean monsoon. Correlation between several predictors and Indian summer monsoon has been found to undergo interdecadal variability (Kumar et al., 1999). A better understanding of interdecadal variability may therefore, be very important in improving the predictability of mean seasonal monsoon climate.

### **1.4 Modes of interannual variability**

In the periodicities longer than annual cycle, we have interannual variability corresponding to biennial periodicity (Yasunari, 1987; 1991; Rasmusson et al., 1990; Barnett, 1991) and multiyear variability corresponding to ENSO scale (see figure 1.6 b).

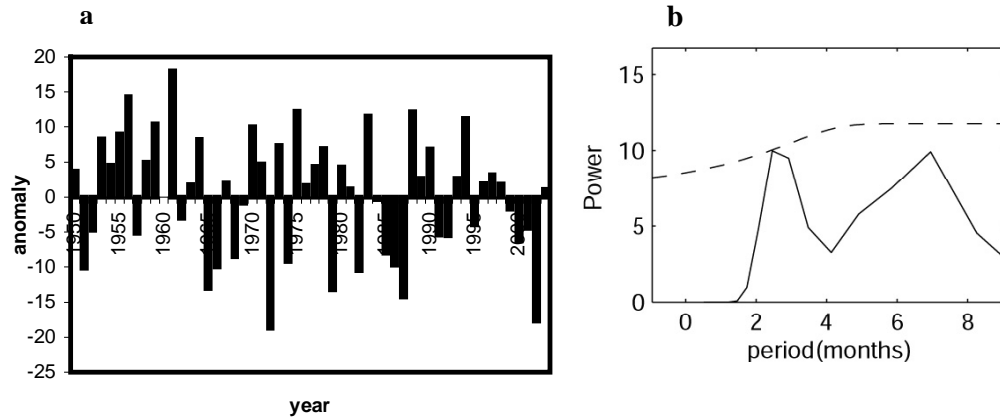


Figure 1.6: (a) Indian summer monsoon rainfall anomaly (cm) from 1950-2004. (b) wavelet analysis of ISMR anomalies from 1950-2004, dotted line indicates 95% significance level.

One notable connection with the interannual variability of the south Asian monsoon is that with the ENSO. The occurrence of El Niño is generally associated with a weak monsoon, and La Niña is associated with a strong monsoon (e.g., Webster and Yang, 1992). During normal periods, the warm pool (SST > 27°C) extends from the eastern Indian Ocean to the western Pacific Ocean and is associated with a broad precipitation maximum. During an El Niño event, the locus of maximum SST in the Pacific Ocean shifts eastward, typically bringing more precipitation over the central and eastern Pacific Ocean. During these periods the eastern Indian Ocean, Indonesia, and south Asia are in the subsiding part of the Walker circulation that has shifted eastward from its climatological position (Webster et al., 1998). The strong heat source associated with the south Asian monsoon could indeed influence the atmospheric circulation in a significant way and could modify the surface stresses over the central and western Pacific and influence the strength and evolution of the ENSO (Yasunari, 1990; Chung and Nigam, 1999; Kirtman and Shukla, 2000). These independent studies of ENSO influence on the ASM and ASM influence on the ENSO, made it clear that the ENSO and the ASM are not independent phenomena but part of a coupled ocean-atmosphere oscillation.

While a connection between the south Asian monsoon and the ENSO exists, but it is not possible to predict the strength of the monsoon solely from the phase of ENSO, as these monsoon-ENSO correlations have variable lag-lead times (Webster and Yang, 1992). It is worth noting here that many droughts and floods of the south Asian monsoon occur without El Niño or La Niña. The correlation between Indian

rainfall and Pacific Oceans SST varies from 0.4 to 0.8 for different decades from 1900 through to the present (Torrence and Webster, 1999). Kumar et al., (1999) gives the evidence of weakening of the reverse monsoon-ENSO relationship during the last two decades.

The failure of ENSO-monsoon relationship in the recent decades forced to look into the relationship of monsoon with the newly discovered tropical phenomena like tropospheric biennial oscillation (TBO) and Indian Ocean Dipole (IOD). The biennial tendency of IAV of the Asian summer monsoon has been known for a long time (Mooley and Parthasarathy, 1984; Yasunari, 1990; Clarke et al., 1998; Webster et al., 1998). Meehl (1987) first identified the quasi-biennial signal in summertime all India rainfall. Subsequent studies identify the spectral peak that exists in AIR between 2.5 and 3 yr and interpret it as a tendency for the monsoon to alternate often between successive “strong” and “weak” years, a sequence attributed to large-scale coupled land–ocean–atmosphere interactions in the Indian and Pacific Ocean regions (e.g. Meehl 1997).

Both observational (Yasunari, 1990; 1991; Ropelewski et al., 1992; Yasunari and Seki, 1992; Kane, 1995; Yang et al., 1996; Tomita and Yasunari, 1996; Harzallah and Sadourny, 1997; Webster et al., 1998) and modeling (Goswami, 1998; Ogasawara et al., 1999; Kitoh et al., 1999; Chang and Li, 2000; Li et al., 2001) studies have documented characteristics of tropical biennial variations. Strong biennial signal is observed in both precipitation and circulation features of Asian summer monsoon. Numerous conceptual models of the oscillation have also been developed (Meehl, 1987; 1993; 1994; Goswami, 1995; Webster et al., 1998; Kawamura et al., 2001; Clarke et al., 1998; Loschnigg and Webster, 2000; Kim and Lau, 2001; Loschnigg et al., 2003). More recently, an active role for equatorial eastern Pacific Ocean interactions has also been incorporated (Meehl and Arblaster 2002a, b; Sahai et al. 2003; Wang et al. 2003).

Various mechanisms have been proposed for the TBO (e.g. Nicholls, 1978; Meehl, 1987; Meehl, 1993; Clarke et al., 1998; Goswami, 1995; Chang and Li., 2000). The modeling studies mentioned above provides a synthesis of the TBO studies and the ENSO-monsoon connection studies and shows that they are linked and part of the

same air-sea coupled oscillation involving both the Indian Ocean and the Pacific Ocean basins

### **1.4.1 Tropospheric Biennial Oscillation**

The tropospheric biennial oscillation (TBO) is defined as the tendency for a relatively strong monsoon to be followed by a relatively weak one, and vice versa, with the transitions occurring in the season prior to the monsoon involving coupled land–atmosphere–ocean processes over a large area of the Indo-Pacific region (Meehl, 1997, Meehl and Arblaster, 2002a; Meehl et al., 2003). Thus the TBO is more a tendency for the system to flip-flop back and forth from year to year, and not so much an oscillation. The more of these interannual flip-flops or transitions, the more biennial the system. One of the most remarkable features of TBO is its characteristic seasonal progression and dynamically coherent spatial structure. The conditions of a strong (or weak) monsoon over India and southeast Asia in the northern summer often continues to the succeeding autumn and winter over the maritime continent and Australia monsoon region. So that a strong (weak) Asian monsoon is often followed by a strong (weak) Australian monsoon.

The TBO has become recognized as a candidate for understanding some of the processes that can contribute to interannual variability of a variety of parameters in the Indian and Pacific regions in both observations (Yasunari, 1990; Ropelewski et al., 1992; Yasunari and Seki, 1992; Yang et al., 1996; Tomita and Yasunari, 1996; Meehl, 1997; Meehl and Arblaster, 2001) and models (Ogasawara et al., 1999; Chang and Li, 2000). Coupled climate interactions between ocean and atmosphere contribute to a mechanism that produces biennial variability (TBO) in the troposphere and upper Ocean in the tropical Indian and Pacific Ocean regions. The TBO is associated with modulations of seasonal cycle, with maximum in the TBO is manifested as warm (El Niño) and cool (La Niña) in the tropical Pacific and have connections to Indian monsoon.

#### **1.4.1.1 Role of Oceans and Asian-Australian monsoon in TBO**

An important part of any biennial mechanism is anomalous heat storage in the ocean and the associated SST anomalies that can occur in certain regions. Thus, the ocean retains the “memory” of ocean–atmosphere interaction over the course of a



year to affect the atmosphere the following year (e.g., Brier, 1978; Nicholls, 1978; Meehl, 1987; 1993; Chang and Li, 2000; Li et al., 2001). Several studies have suggested that coupled ocean dynamics plays a role in the formation and maintenance of these heat content and SST anomalies associated with the TBO (Meehl, 1993; Clarke et al., 1998; Webster et al., 1999; Saji et al., 1999; Meehl and Arblaster, 2002a; Loschnigg et al., 2003). Meehl (1993) also noted significant upper-ocean heat content anomalies in regions of the tropical Pacific that contribute to the memory of the system and, thus, the TBO. Yu et al., (2003) through modeling study argued that east Pacific SST is important for inphase Indian to Australian transition in TBO cycle and Indian Ocean plays major role in out of phase transition from Australian to Indian monsoon. Pacific Ocean SST anomalies maintain large amplitude during inphase transition in northern autumn and reverses sign in spring season, in which out of phase transition is occurring. On the other hand, the Indian Ocean SST anomalies maintain large amplitude during out-of-phase transition and reverses sign in northern spring. These seasonally dependent anomalies in these two oceans allow these two oceans to play different role in transition of phase of TBO.

Li et al (2001) and Wu and Kirtman (2007) are of the opinion that biennial transition of Indian summer monsoon can produce through the local air-sea interaction in the northern Indian Ocean when Pacific ENSO is suppressed. Wu and Kirtman (2007) showed that the local SST anomalies in the Indian Ocean induce monsoon transition through low level moisture convergence. Surface evaporation anomalies affect the SST changes. The anomalous condition in the Indian and Pacific Ocean through regional and remote effect in spring season can produce anomalous monsoon conditions.

A plausible mechanism through which ocean-atmosphere coupling leads to a TBO and the role of Asian summer monsoon is given by Wu and Kirtman (2004). A strong Asian summer monsoon (ASM) during boreal summer (June to September) can enhance surface easterlies in the central equatorial Pacific, induces an eastward propagating upwelling Kelvin wave and gives rise to negative SST anomalies in the eastern Pacific that amplifies through air-sea interactions. Colder SST in the eastern Pacific is also associated with warmer SST in the western Pacific. A strong ASM also cools the Indian Ocean through enhanced evaporation and upwelling.

Associated intensification of the Walker circulation leads to divergence of moisture supply in the western Indian Ocean. Reduced moisture supply at low levels together with upper level subsidence leads to a weaker ASM during the next summer. A weak ASM induces opposite affects and can lead to a stronger monsoon next year. Thus, the ocean-atmosphere interaction generates IAV of the ASM via generation of TBO signal.

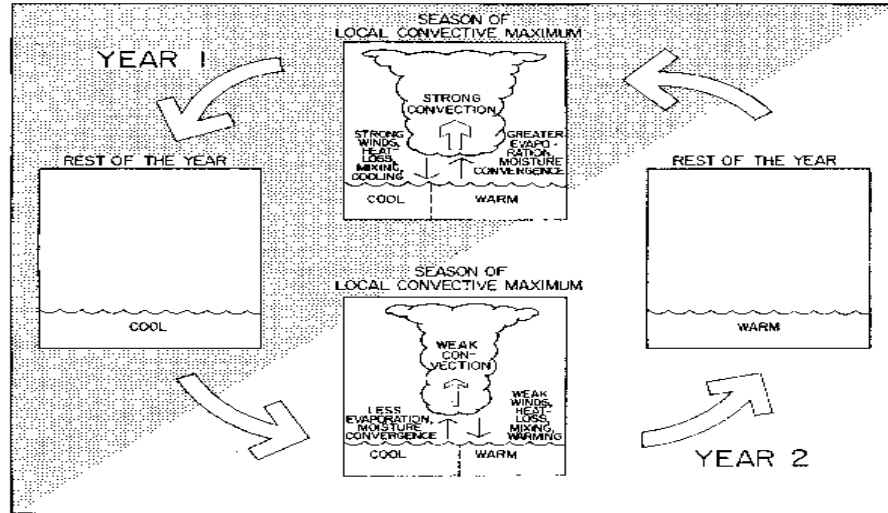
#### **1.4.1.2 Theories of TBO**

Understanding the TBO in the Asian-Australian, the Pacific Ocean and the Indian Ocean sector often relies on the knowledge of variations of Asian-Australian monsoon, ENSO and Indo-Pacific SST as well as the transitions of these phenomena with seasons and geographic locations. The origin of the TBO is a subject of debate. The existing theories on TBO emphasis the following three aspects of ocean-land-atmosphere coupling viz; (a) Local air-sea interaction (Brier, 1978; Nicholls, 1978; Meehl, 1987; Clarke et al., 1998), (b) Remote ocean-atmosphere interaction (Meehl, 1987; Chang and Li, 2000; Kim and Lau, 2001; Li et al., 2001, Meehl and Arblaster, 2002 a,b), and (c) Tropical- extratropical teleconnection (Yasunari and Seki, 1992; Meehl, 1994, 1997; Tomitta and Yasunari, 1996; Ogasawara et al., 1999).

The local air-sea interaction theory emphasizes the importance of basic flow and the interactive processes of atmospheric and oceanic anomalies (see Nicholls, 1978). A westerly wind anomaly superimposed on westerly basic flow intensifies the total wind and cools the ocean. By this same argument, westerly wind anomaly weakens a easterly basic flow and warms upper ocean. The changes in the atmosphere associated with these changes are considered as a delayed feedback of the SST anomaly. On the other hand, Meehl (1987, 1993) stressed the role of initial SST anomalies in local air-sea interaction leading to TBO. Meehl (1997) described an air-sea negative feedback mechanism in which warm spring SSTs in the Indian Ocean enhance atmospheric convection. The ensuing stronger monsoon leads to greater than average wind strength, increased Ekman transports and vertical mixing, and higher heat loss by evaporation throughout the summer monsoon season, which causes subsequent cooling of the ocean surface. The low ocean temperatures persist

for one year until the next pluvial season. The lowered SSTs are associated with less convection than the previous spring, producing weakened winds, and reduced heat loss by evaporation, and less mixing, which leads to higher SSTs than the year before. The cycle is thus repeated. Figure 1.7 shows the biennial cycle due to land-atmosphere and ocean-atmosphere interactions as illustrated by Meehl (1997)

**a) BIENNIAL ATMOSPHERE-OCEAN MECHANISM**



**b) BIENNIAL ATMOSPHERE-LAND MECHANISM**

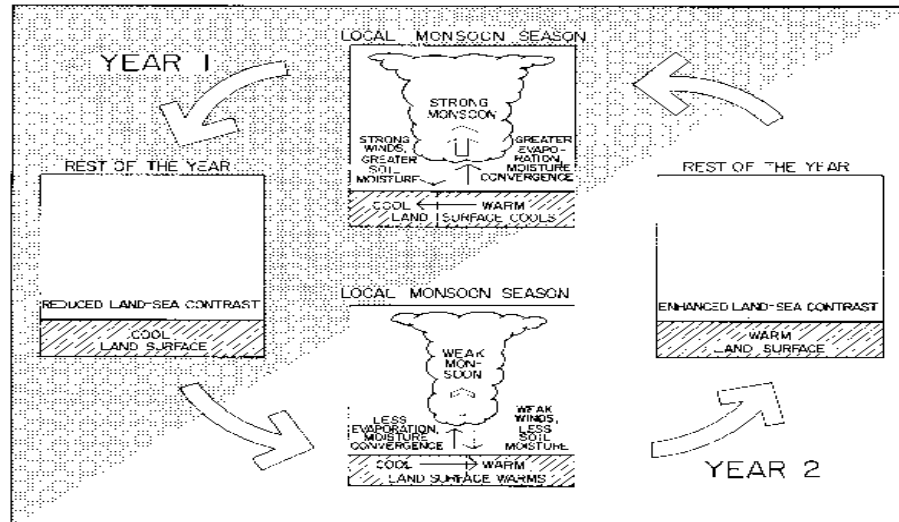


Figure 1.7: Schematics of TBO mechanism (a) ocean-atmosphere mechanism (b) land-atmosphere mechanism (Meehl, 1997).

One of the prominent features of Asian-Australian monsoon system is the migration of monsoon convection from northern Australia to southern Asia from boreal winter to summer and in opposite direction from summer to winter. In this migration

process, a strong (weak) Asian monsoon is followed by a strong (weak) Australian monsoon. Meehl and Arblaster (2002a) proposed a remote forcing mechanism emphasizing the importance of eastern Pacific SST for the large scale east-west circulation and the Asian monsoon. The southeastward migration of a strong Asian monsoon through Australia weakens the south Pacific High and thus the trade winds. This increases eastern Pacific SST and decrease zonal SST gradient and east-west atmospheric cells across tropical Pacific. As a result of the diminished upward motion in the western Pacific weakens next monsoon.

Tropical–extratropical teleconnection mechanism (Meehl, 1997) emphasis the response of extratropical atmosphere to tropical forcing for TBO. The response of the extra tropical circulation causes anomalies in land surface temperature. According to Ogasawara et al. (1999), the convective activity around Indonesia and northern Australia is the main tropical forcing and anomalous atmospheric circulation over Asia is direct Rossby wave response to tropical heating. Favorable interaction between the land and atmosphere processes prolongs the anomalies of the coupled land-atmosphere system.

Using a simple five-box model that considers SST-monsoon, evaporation-wind, monsoon-Walker circulation, and wind-thermocline feedback, Chang and Li (2000) showed that these processes can give rise to the seasonal evolution of TBO. Their theory explains why TBO can maintain the same phase from northern summer to northern winter and why a reversed phase of TBO can last three locally inactive seasons to affect the next year's monsoon. Without the interference from and interaction with motions of other scale, Chang and Li (2000) obtained a pure, regular biennial oscillation. Differ from Meehl (1997), Chang and Li (2000) put importance to Asian monsoon than east Pacific SST for the TBO mechanism. According to them a strong monsoon produces anomalous westerlies in the Indian Ocean and increases east-west circulation in the Pacific. As a result of the westerly anomalies SST cools in the Indian Ocean and it persists to next monsoon making it weak. Increase in west Pacific SST due to the deepening of west Pacific thermocline favoring strong Australian monsoon in the forthcoming boreal winter. In addition, strong trade winds over Pacific decrease east Pacific SST which maintain west Pacific warm through easterly anomaly and shoaling thermocline.

The mechanism proposed by Chang and Li (2000) is given in figure 1.8.

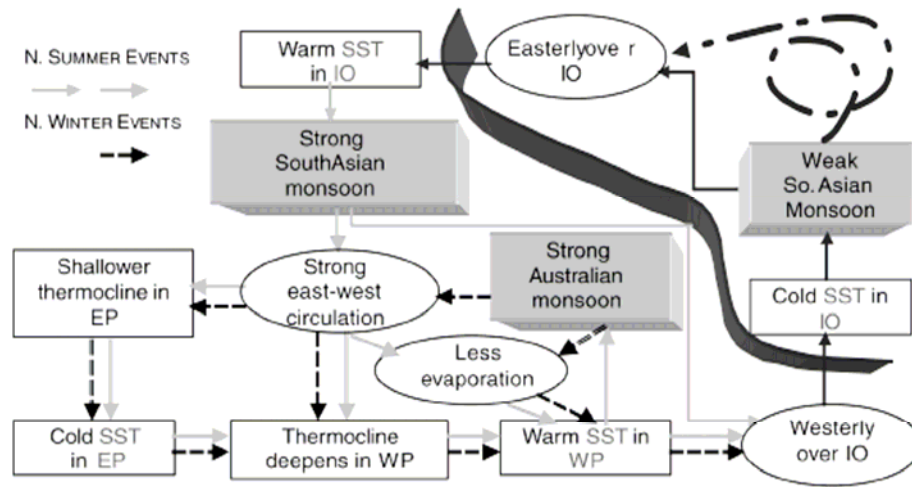


Figure 1.8: Schematic diagram indicating the interactive processes leading to TBO. Land and Ocean regions are shaded. Non shaded boxes indicate atmospheric (oval) and oceanic (rectangular) processes. The strong monsoon phase starts with warm Indian Ocean SST leading to strong south Asian monsoon. The reverse phase is in the upper right corner separated by thick ribbon (Chang and Li,2000)

Another potential explanation for biennial monsoon variability involves land surface processes, especially Eurasian snow cover. Extensive snow cover typically precedes a weak monsoon and light snow cover precedes a strong monsoon (Barnett et al. 1989; Vernekar et al., 1995; Yang, 1996). Large and persistent winter snow cover over Eurasia following a strong monsoon can delay and weaken the spring and summer heating of landmass that is necessary for the establishment of large scale monsoon flow (Shukla, 1987; Barnett et al., 1989; Yasunari et al., 1991). In this manner, snow cover may act as a negative feedback upon the Asian monsoon, imparting biennial variability. Clearly a better understanding of the ocean–atmosphere and land–atmosphere feedbacks that may give rise to the TBO can improve predictions of monsoon strength.

The transitions (from relatively strong to relatively weak monsoon) occur in northern spring for the south Asian or Indian monsoon and northern fall for the Australian monsoon involving coupled land atmosphere–ocean processes over a large area of the Indo-Pacific region. Transitions from March–May (MAM) to June–September (JJAS) tend to set the system for the next year, with opposite sign in the

following year. Indian and Pacific SST forcing are more dominant in the TBO than circulation and meridional temperature gradient anomalies over Asia (Meehl and Arblaster, 2002a). A fundamental element of the TBO is the large-scale east–west atmospheric circulation (Walker circulation) that links anomalous convection and precipitation, winds, and ocean dynamics across the Indian and Pacific sectors. This circulation connects convection over the Asian–Australian monsoon regions both to the central and eastern Pacific (eastern Walker cell), and to the central and western Indian Ocean (western Walker cell). From all these above discussions Meehl and Arblaster (2002b) proposed a mechanism involving convection, SST, wind, extra tropical circulation, east-west circulation etc and is illustrated in figure 1.9 starting from the winter season (DJF) before the strong monsoon to the next winter after the monsoon.

In the winter (DJF) season, warm SST is seen in the Indian Ocean and east Pacific and cool SST is seen north of Australia. This will look like an El Nino condition. Under these circumstances, the Eurasian continent is characterized by less snow and warmer conditions as a result to the tropical heating. In the following spring (MAM) the conditions of coupled ocean-atmosphere system persists because of the memories in the ocean and thermocline conditions. As a result summer monsoon increases. Because of these, the Eurasian land surface is cool and SST decreases in the Indian Ocean and west Pacific. These summer conditions are maintained to next post monsoon season (SON). These above conditions lead to the strong Australian monsoon in the next winter (DJF). The strong convection associated with Australian monsoon and weak convection over the western Indian Ocean and the central Pacific contribute an anomalous trough and cold land temperature over Eurasia (as a Rossby wave response), which are followed by a weak south Asian summer monsoon.

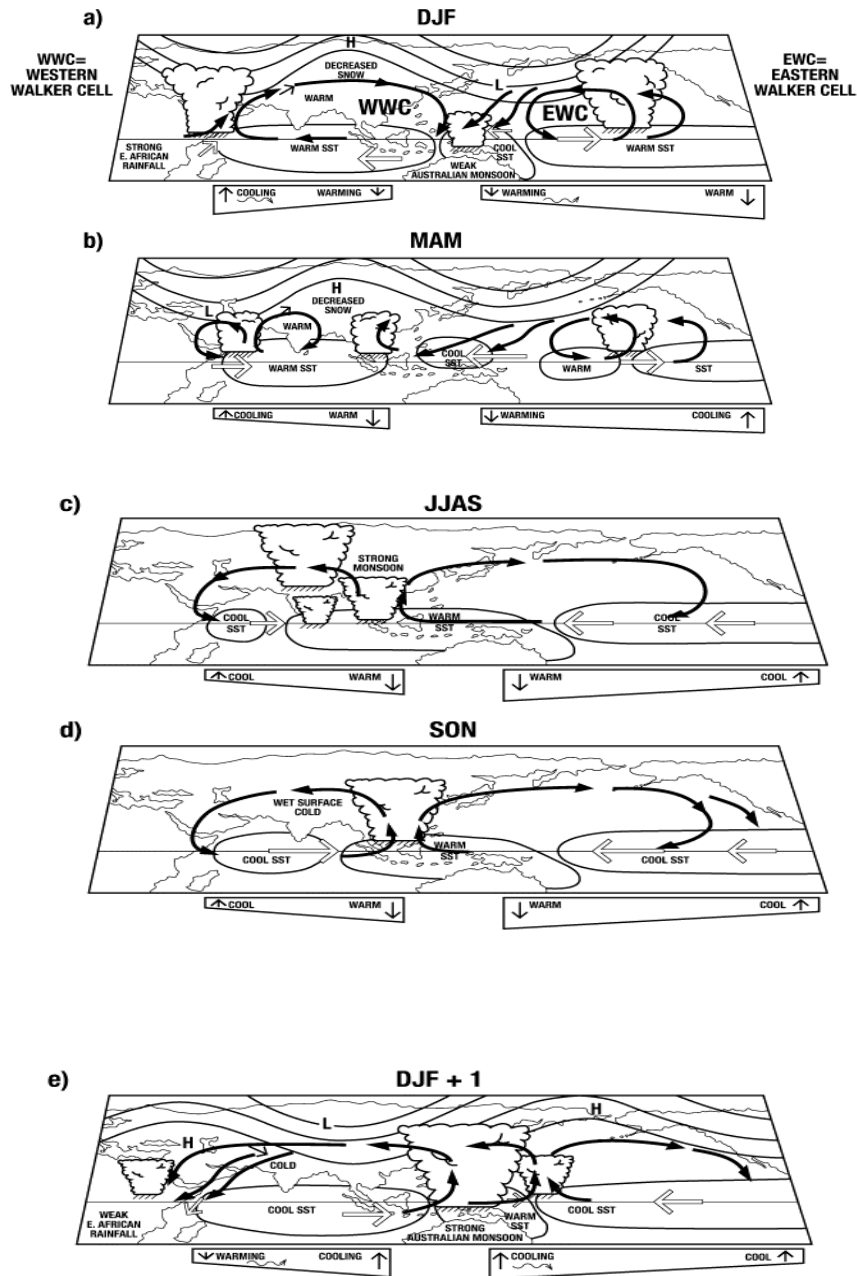


Figure 1.9: schematic picture representing TBO features associated with anomalies of convection, SST, surface winds, extratropical circulation and equatorial Pacific and Indian Ocean thermocline orientations (Meehl and Arblaster 2002b)

But in reality, TBO exhibits a rich, irregular spectrum. Such irregularity may, in large part, result from nonlinear interaction with ENSO. Since TBO is an inherent mode of the coupled ocean-atmosphere system in which monsoon is a major part, the prediction of anomalous rainfall over the Asian-Australian monsoon region based on ENSO forecast must consider the combined effects of TBO and ENSO. The strength of the TBO is modulated by interdecadal variability. For example, Torrence and Webster (1999) find the biennial oscillation to be weaker in some decades than others. Difficulties in fully understanding the relationship between the TBO and monsoon arise at least partly due from lack of understanding the internal and external features of the TBO. The TBO in Asia, Australia and the adjacent tropical regions can be considered as inherent mode of monsoon itself. However, the variability of SST in the tropical central Pacific is also characterized by quasi-biennial signal and is coupled with the Asian-Australian monsoon. It is even more difficult to understand the relationship between the internal monsoon characteristics and external ENSO features of TBO, which is the result of interaction of annual cycle and ENSO cycle. Quantifying the role of these conditions associated with the transition of TBO and their relationship with ENSO and the accurate representation of these in models is needed for better forecasting of monsoon.

Eventhough a good account of TBO mechanism is in the literature, it is not differentiated from ENSO in the Pacific. The role of monsoon, land surface processes, ocean etc are not well studied. The ENSO also has a good biennial cycle. The ENSO- biennial cycle and TBO are not differentiated up to now. The present study tries to answer all these questions by analyzing the following parts of TBO-monsoon relationship

- Mechanism of biennial and low frequency variability of monsoon
- Atmosphere- Ocean pattern associated with TBO
- Circulation features of TBO.
- The difference of TBO in the absence of active Pacific Ocean
- Role of Indian Ocean processes like Indian Ocean Dipole (IOD) in TBO
- Is intraseasonal Oscillation is modified during TBO period?
- Possibility of QBO-TBO interaction
- Effect of climate shift on TBO and interannual variability of Indian summer monsoon



---

## **Biennial Oscillation of Tropical Ocean-Atmosphere System Associated with Indian Summer Monsoon**

---

### **2.1 Introduction**

The Indian summer monsoon displays substantial interannual variability, which can have profound social and economic consequences in the country. Societies worldwide rely on a stable climate and nowhere more so than in those countries affected by the monsoon where the failure or even the delay of the monsoon can make all the difference between famine and plenty. This variability is intimately related to large scale features like the phase of the El Niño Southern Oscillation (e.g. Rasmusson and Carpenter, 1983; Webster and Yang, 1992), but also depends on the regional and intraseasonal behavior of the monsoon (e.g. Krishnamurti and Bhalme, 1976; Gadgil and Asha, 1992). Thus, an understanding of the mechanisms involved in the mean evolution of the monsoon and its spatial and temporal variability is central for future success in seasonal and longer-term prediction. Consequently, considerable research has been conducted in recent years towards understanding the factors that give rise to the observed interannual variability of the monsoon and towards improving our capabilities to predict it (e.g. Brankovic et al., 1994; Webster et al., 1998).

The power spectrum analysis of ISMR in figure 1.3 identifies two prominent peaks corresponding to the quasi-biennial time scale (2-3 year) and to the longer time period (3-7 year). The quasi-biennial periodicity is related to tropospheric biennial oscillation

(TBO) and the longer period to El Nino Southern Oscillation (ENSO) (Li and Zhang, 2002). Similar two prominent peaks are observed for many parameters in the tropical region like meridional wind component, sea level pressure (SLP) difference between Asian continent and northwest Pacific (Lau and Sheu, 1988; Tomitta and Yasunari, 1996). Thus it will be interesting to analyse the effect of different ocean-atmosphere parameters in both the scales to the interannual variability of summer monsoon.

El Nino Southern Oscillation (ENSO) is considered to be a major factor determining the interannual variability of Indian Summer Monsoon Rainfall (ISMR) till two decades back. Several studies have been reported to illustrate the monsoon- ENSO relationship (eg: Yasunari, 1990; Webster and Yang, 1992; Ju and Slingo, 1995). The Indian monsoon tends to have a simultaneous negative correlation with eastern pacific SST (Rasmusson and Carpenter, 1983), although this correlation has been broken down in recent years (Kumar et al., 1999). Wu and Kirtman (2007) demonstrated that ENSO affects the Indian summer monsoon transition by shifting large-scale east-west circulation across the equatorial Indo-Pacific Oceans and by Rossby wave type response over the north Indian Ocean-western north Pacific.

But in the recent studies of interannual variability of monsoon, the biennial variability governed by TBO also comes into a major role. The TBO is associated with modulations of seasonal cycle, with maximum is manifested as El Niño and La Niña. Thus both the TBO and ENSO are related to interannual variability of Indian summer monsoon. Reason et al (2000) is of the opinion that the ENSO episodes with its longer term periodicity may weaken the biennial signal. But the ENSO also has a well-known biennial periodicity, as TBO. Thus it is very difficult to distinguish the effect of both these phenomena to monsoon variability.

Several theories have been proposed to understand the origin of TBO as explained in chapter 1. Some believes TBO as an extreme cause of ENSO, making fundamental cause of TBO and ENSO similar (Meehl, 1997). Others believe that TBO is an inherent monsoon mode, resulting from monsoon-ocean interactions (Chang and Li, 2000). According to Meehl and Arblaster (2002a), dynamic coupling between ocean and

atmosphere in conjunction with seasonal cycle of convection over the tropical Indian and Pacific Oceans and associated large-scale east-west circulation in the atmosphere produces TBO. They proposed factors like SST in the Pacific Ocean and Indian Ocean and 500 hPa height over Asia as important factors for TBO. The TBO phenomena includes both Indian and Australian monsoon regions and has southeast movement from Indian to Australian monsoon region (Meehl and Arblaster 2001; 2002a). The in-phase Indian to Australian monsoon transition and out of phase Australian to Indian monsoon transition is also a main characteristic of TBO. Meehl and Arblaster (2002a) gives importance to boreal spring season for Indian monsoon and boreal autumn season for Australian monsoon TBO transition. Detailed explanation of TBO including the role of northwest Pacific warm pool can be found in Li et al. (2006).

## **2.2 Objectives of the study**

The behavior of the atmosphere-ocean system in the tropical region along with the biennial oscillation of Indian summer monsoon need to be investigated in detail, in order to understand ocean-atmosphere interaction associated with TBO and its role in Indian summer monsoon. The previous description of TBO transition by Meehl and Arblaster 2001; 2002a; Meehl et al., 2003 etc is from one winter season to the next year winter season, not from monsoon and the changes associated with monsoon transition. The analysis of biennial cycle from strong/weak monsoon to next year monsoon should be investigated for various ocean atmosphere parameters of tropical region.

The present chapter describes the pattern of anomalies associated with both the TBO and ENSO periodicities for SST and lower level wind and the relative contribution of different parameters on both the scales to monsoon rainfall. The study also analyses the evolution and movement of anomalies of different ocean-atmosphere parameters associated with interannual variability of Indian summer monsoon in both inphase and out of phase transition of TBO.

## **2.3 Data and methodology**

The present study uses National Centre for Environmental Prediction /National Center for Atmospheric Research (NCEP/NCAR) reanalysis (Kalnay et al., 1996) data sets that

include meridional and zonal wind at 850 hPa, Sea level pressure (SLP) and flux data like specific humidity, latent heat flux and shortwave radiation along with NCEP SST for the time period 1950-2005. The NCEP/NCAR is a joint project between NCEP and NCAR to produce a multi-decadal record of global system that is unchanged (Kalnay et al., 1996). The data assimilation and global forecasting model are based on the global system that implemented operationally at the NCEP in January 1995. The model is run at a horizontal resolution of T62 and with 28 vertical levels. Moist convection is represented by simplified form of Arakawa-schubert parameterization scheme and clouds are diagnosed from model variables using a scheme based on Slingo (1987). The model uses a 3-layer soil scheme in which the temperature of the bottom layer is set to the annual mean climatological value. Data were assimilated using a spectral statistical interpolation/three-dimensional variation analysis method, which requires no nonlinear normal-mode initialization. Monthly mean upper-air data on standard pressure surface have been supplied, already gridded on to a  $2.5^{\circ} \times 2.5^{\circ}$  grid. Surface and 24-hour forecast fields are given on equivalent T62 Gaussian grid.

Atmospheric convection associated with TBO is studied by using outgoing long wave radiation (OLR) data obtained from NOAA for the time period 1974-2005, with a one year gap in the data at 1978. ISMR index, which is the area averaged June to September rainfall of 306 stations well distributed over India, (Parthasarathy et al., 1994) and updated for making it to period 1950-2005 is used to define strong and weak monsoon years. Climate prediction center merged analysis project (CMAP) precipitation data (Xie and Arkin, 1997), which is merged analysis of gauge and satellite observations with model outputs for the period 1979-2005 are also used.

In order to differentiate the process in TBO and ENSO scales, the corresponding frequencies must be picked up separately from the original data sets. A band pass filter Murakami (1979) has been used to separate the data into approximately 2-3 years (TBO) and in 3-7 years (ENSO) windows, with half power points of the response function located at 16 and 36 months and 42 and 86 months respectively for TBO and ENSO scales. Seasonal data sets are used for filtering seasonal summer monsoon rainfall and monthly data sets were used for the other parameters. For both the filters,

the time frequencies of the peak-power point (denoted by  $W_0$ ) and the two lateral half-power points (denoted by  $W_1$  and  $W_2$ ) follow the relationship:

$$W_0^2 = W_1 * W_2 \quad \dots 2.1$$

The resultant peak-power points of these two bands are 2 and 5 years, respectively. Thus, the band pass filter well separates the 2-3 year and 3-7 year windows.

The strong and weak monsoon years in each time scales are selected from the ISMR anomaly filtered on both TBO and ENSO scales, which has standardized anomalies of above  $\pm 1$  standard deviations. The strong minus weak composites of SST and lower level wind are carried out from winter season before the TBO year to next winter after the TBO year. An Empirical Orthogonal Function (EOF) analysis has been carried out for winter and spring season SST anomalies over both Indian and Pacific Oceans and geopotential height at 500 hPa to identify the prominent modes of variabilities in these two windows and the prominent patterns are correlated with rainfall.

To specify the seasonal evolution and movement of different ocean-atmosphere process in the tropical regions, both strong and weak TBO years are identified from original ISMR index as defined by Meehl and Arblaster (2002a).

That is, if  $P_i$  is the area averaged monsoon season precipitation for a given year  $i$ ,

Then a relatively strong monsoon year is defined as;

$$P_{i-1} < P_i > P_{i+1} \quad \dots 2.2$$

and a relatively weak year is defined as;

$$P_{i-1} > P_i < P_{i+1} \quad \dots 2.3$$

Here in the present study ISMR index is used for  $P_i$ .

According to above definition we have 18 strong TBO years and 17 weak TBO years in the 56 year period of the study.

Composite analysis of strong minus weak TBO years is carried out for unfiltered OLR, SST, SLP and 850 hPa wind to investigate the evolution and movement of anomalies in

TBO cycle. The analyses were carried out from previous monsoon season (JJA-1), previous autumn (SON-1), boreal winter before strong monsoon (DJF-1), pre-monsoon (MAM0), present strong monsoon (JJA0), following autumn (SON0), winter (DJF0), spring (MAM+1) and next monsoon (JJA+1). Local changes in the Indian Ocean are analysed from similar composite analysis of latent heat flux, specific humidity and shortwave radiation over the Indian Ocean region for above-mentioned seasons.

## **2.4 Results**

Strong minus weak monsoon year composite analysis of both SST and lower level wind in both TBO and ENSO scale is carried out to investigate the pattern of these parameters in both the scales and their influence to monsoon rainfall. Seasonal cycle of SST, wind, OLR and SLP from previous summer of TBO year to next year summer will enable to understand the TBO cycle associated with monsoon variability.

### ***2.4.1 Indian summer monsoon rainfall in TBO and ENSO scale***

Figure 2.1 shows the time series of standardized anomalies of ISMR index, both unfiltered and filtered in TBO and ENSO scale. From the figure it can be seen that in most of the years all these three are in same phase and in some other years original may have sign of either TBO scale or ENSO scale anomaly and or may differ from both.

From the ISMR index shown in the figure 2.1 strong and weak monsoon years having anomaly above one standard deviation is selected for both ENSO and TBO scales. These strong and weak years are used for composite analysis in both the scales.

Figure 2.2 shows the precipitation composite anomalies of the strong minus weak TBO years for present summer (JJA0) and next year (JJA1) of interannual cycle in both TBO and ENSO scales. During the strong monsoon season (JJA0) precipitation is increased over Indian region, Bay of Bengal and Arabian Sea region close to land and south of the equatorial Indian Ocean in TBO frequency. The north equatorial Indian Ocean has decreased rainfall. In the ENSO frequency, rainfall is enhanced over India and entire north Indian Ocean region. In the next year monsoon (JJA1) anomalies are reversed in the TBO scale, while in the ENSO scale Indian region and western Indian Ocean has reduced precipitation and Bay of Bengal and eastern Indian Ocean has increased

precipitation anomalies. Thus though Indian region has increased (decreased) precipitation in strong (weak) phase of monsoon in both the scales, precipitation pattern is different in both the scales.

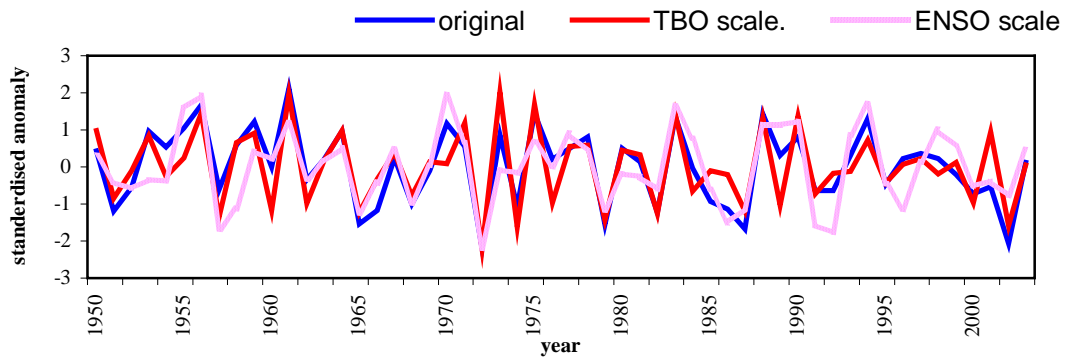


Figure 2.1: Time series of standardized ISMR anomalies of original ISMR index and filtered in both TBO and ENSO scales.

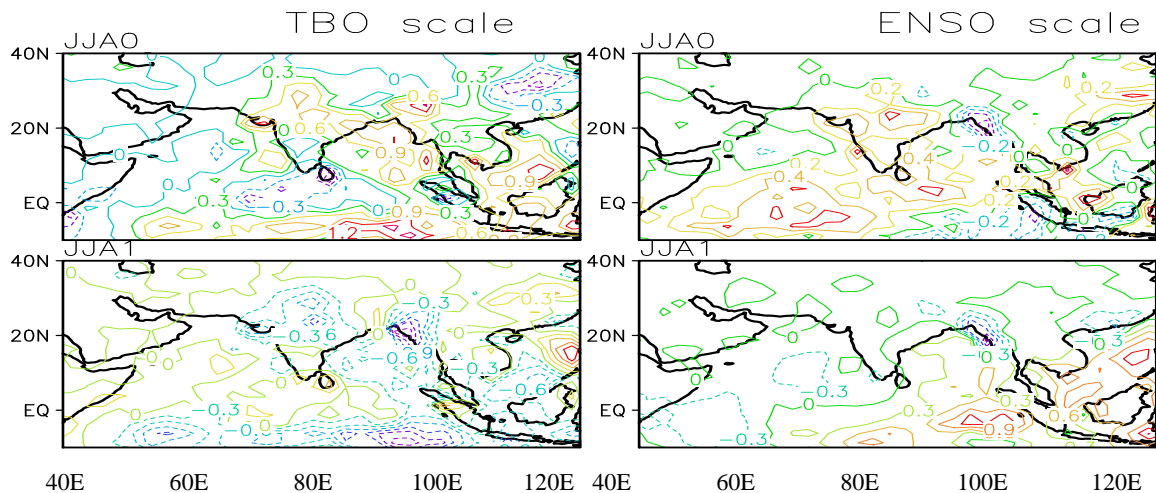


Figure 2.2: strong minus weak monsoon composite of CMAP precipitation (1975-2005, unit mm/day) in TBO scale (left panel) and ENSO scale (right panel). JJA0 denotes strong monsoon and JJA1 denotes next weak monsoon season.

#### 2.4.2 Seasonal evolution of SST and wind in TBO and ENSO scale

In order to review the influence of SST and lower level wind on both these time scales, similar composite analysis is carried out from boreal winter season before the monsoon to next winter after the monsoon in TBO and ENSO window separately.

### 2.4.2.1 SST

Figure 2.3 shows the strong minus weak years composite of SST in both scales from previous winter (DJF-1) season to next year winter (DJF0) of a reference monsoon (JJA0). Left panels are for TBO window and right ones for ENSO window. In the TBO window, entire Indian Ocean and tropical Pacific Ocean becomes warm by DJF-1, while in the low frequency ENSO mode, the central and western Pacific is cool. During the spring season (MAM0) cooling starts in the extreme eastern Pacific and Indian Ocean is warm in TBO scale. In ENSO scale anomalies has not changed much compared to previous winter season. Thus the central equatorial Pacific has opposite anomalies in winter and spring season before a strong monsoon in both quasi-biennial and low frequency scale. Along with the onset of monsoon north Indian Ocean cools and the cooling in the eastern Pacific extends to central Pacific in biennial time scale. In the ENSO time scale, the equatorial eastern Indian Ocean is cool and cooling in the central Pacific extends further east. Entire Indian Ocean is cooled by the post monsoon season (SON0) in TBO mode. Both the Indian Ocean and eastern Pacific are cool in ENSO mode and the cooling pattern continues to next winter season.

### 2.4.2.2 Wind at 850 hPa

Figure 2.4 shows the composite of zonal wind ( $U$ ) at 850 hPa for strong minus weak composites in both the TBO and ENSO frequencies. In the biennial scale winter season before the strong monsoon, westerlies confines to north of  $20^{\circ}\text{N}$  and easterly maximum is over north of Australia extending to north equatorial Pacific and westerlies in the south equatorial Pacific. But in the ENSO scale, the westerly maximum is in the north Indian Ocean extending to India. Easterlies are seen in the south Indian Ocean and equatorial central Pacific. During the spring season easterlies appears in the Tibetan plateau region and strengthens in the south Indian Ocean and north Pacific. In ENSO mode easterlies are strong in the south Pacific and westerlies strengthen in the northwest Indian Ocean. During monsoon season pattern has not much changes in both the windows, with westerly maximum in the northwest Indian Ocean and entire equatorial central Pacific has easterlies and by fall westerlies extend to Indonesian



region also. The pattern is exactly opposite in the TBO cycle from next winter, but the anomalies continues as such in the ENSO scale

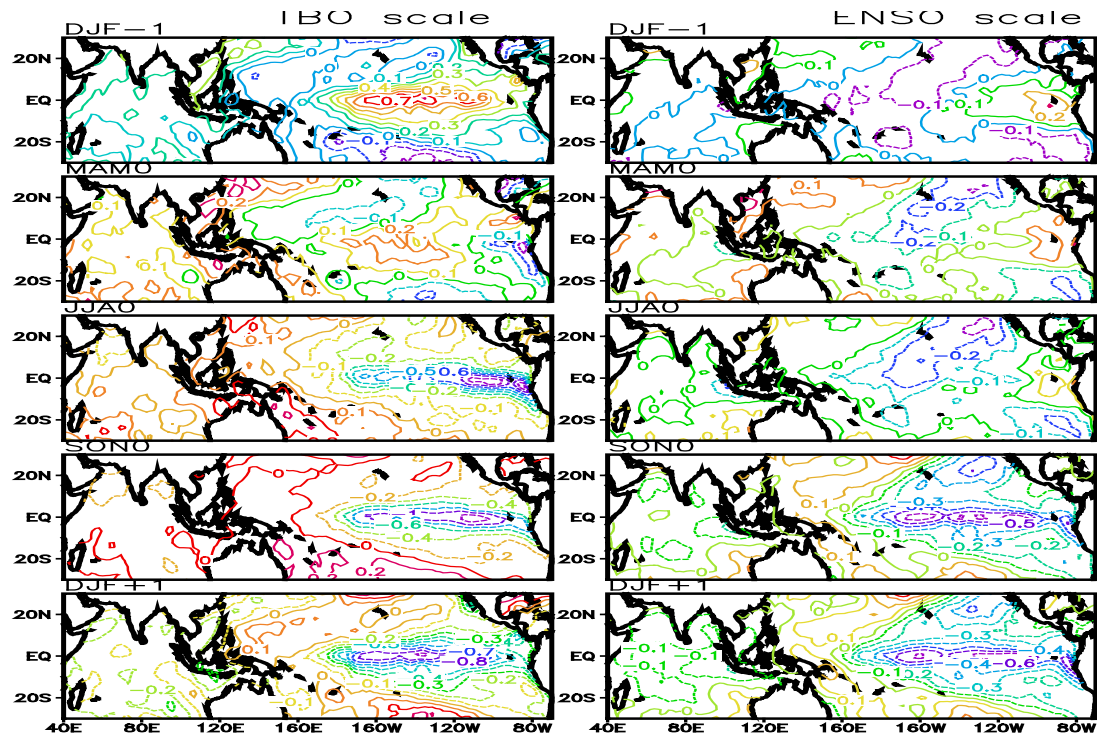


Figure 2. 3: Strong minus weak composite of SST from winter season before monsoon to winter after the monsoon. Left panels are for TBO window and right for ENSO window. In figure DJF-1 corresponding to previous year boreal winter season, MAMO spring season before the monsoon, JJA0 reference monsoon, SON0 post monsoon season and DJF+1 next winter.

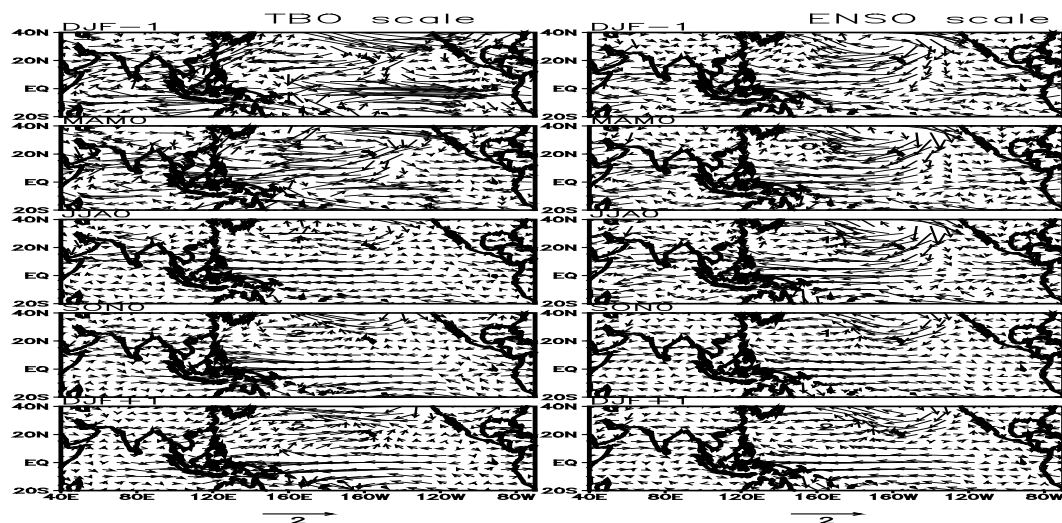


Figure 2. 4: Strong minus weak composite of 850 hPa wind from winter season before monsoon to winter after the monsoon. Left panels are for TBO window and right for ENSO window.

### ***2.4.3 Relative contribution of TBO and ENSO scale variations to monsoon rainfall***

The relative role of oceanic and atmospheric parameters in both the scales to summer (JJAS) monsoon is presented here. EOF analysis of seasonal SST anomalies of both equatorial Indian Ocean ( $20^{\circ}\text{S}$ - $25^{\circ}\text{N}$ ,  $40^{\circ}$ - $110^{\circ}\text{E}$ ), equatorial east Pacific ( $20^{\circ}\text{S}$ - $20^{\circ}\text{N}$ ,  $150^{\circ}\text{E}$ - $80^{\circ}\text{W}$ ), spring season geopotential height at 500 hPa over Asia ( $30^{\circ}$ - $70^{\circ}\text{N}$ ,  $50^{\circ}\text{E}$ - $110^{\circ}\text{E}$ ) are conducted with seasonally filtered data on both the scales. For all the parameters first EOF identifies more than 50% of the variance in both the scales. First prominent pattern in TBO scale looks like the strong minus weak composite of monsoon in TBO scale, shown earlier (see left panels of figure 2.3). Anomalously warm SSTs in the Indian Ocean in the winter and spring season can provide a source for strong monsoon through increased evaporation. Eastern equatorial Pacific SST can influence the monsoon through large scale Walker circulation and positive 500 hPa height over Asia represents the atmospheric circulations and associated enhanced meridional temperature gradient that can strengthen monsoon.

In order to identify the role of these above mentioned parameters on monsoon rainfall, correlation analysis of rainfall and time series of the first EOF have been carried out on both the time scales for the period 1979-2005 and is given in the right panel of Figure 2.5. For positive SSTs in the Indian Ocean in spring season of TBO scale, increased rainfall is noticed over Arabian Sea, Bay of Bengal, northeast India and east equatorial Indian Ocean regions. The positive SSTs in the equatorial eastern Pacific Ocean in spring season is associated with positive correlation in some parts of Arabian Sea, northeast India, Bay of Bengal and east Indian Ocean. Increased 500 hPa height over Asia strengthens rainfall over eastern peninsula and east equatorial Indian Ocean.

In the 3-7 year scale, positive SSTs in the Indian Ocean in winter and spring have positive correlation over the Arabian Sea area. Similarly positive SSTs in the equatorial eastern Pacific also have positive correlation with rainfall over the Arabian Sea region. For 500 hPa geopotential height the effect in rainfall shifts to Indonesian region from the east Indian Ocean.

The above analysis gives the characteristics of SST and wind in both quasi-biennial and low frequency scales and their effect to Indian summer monsoon in both the scales. But the effect of an individual year will be combined from these two scales or difference or independent of these variations. The next section analyses the formation and movement of some ocean-atmosphere parameters contributing to monsoon along with the weak – strong-weak transition of Indian summer monsoon

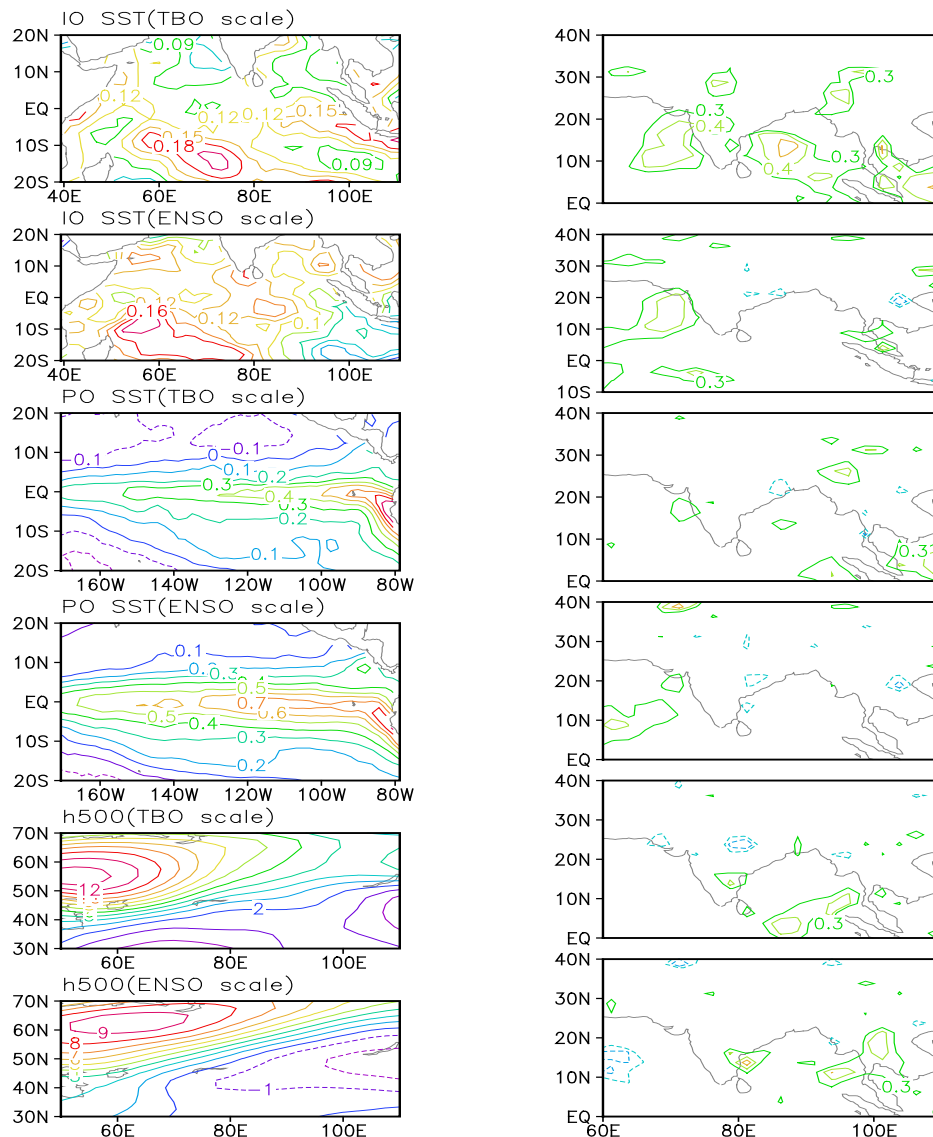


Figure 2.5: Spatial pattern of first EOF of spring season SST of Indian Ocean (20°S-25°N, 40°E-110°E), east Pacific (20°S-20°N, 150°E-80°W) and 500 hPa geopotential height over Asia (30°N-70°N, 50°E-110°E) on both TBO and ENSO scales (Left side) and correlations of corresponding PC's with CMAP rainfall (right panels) for 1979-2005 period.

## **2.4.4 Ocean-atmosphere process in TBO transitions**

### ***2.4.4.1 Large scale processes in the Indo-Pacific region***

It is given that convection, low-level wind, temperature composites provides an over all description of monsoon transition. Strong and weak TBO years are identified from ISMR index by using above definition and strong minus weak composite analysis is carried out for convection (OLR), SST, Sea level pressure and 850 hPa wind from JJA-1 to JJA1.

Figure 2.6 shows the strong minus weak composite of above parameters in the summer season before a strong (weak) monsoon (JJA-1). During this time convection is strong over the southeastern Indian Ocean, equatorial central Pacific and southeast Asian region (figure 2.6a). The SST anomalies are warm in the Indian Ocean and equatorial east Pacific and cool SST is in the west Pacific (figure 2.6b). Sea level pressure is anomalously high in the Indian Ocean and west Pacific and is low in the east Pacific and easterly anomalies are seen over India and north Indian Ocean. Westerly anomalies are observed over equatorial Indian Ocean and equatorial central Pacific. The condition refers to a relatively weak monsoon in JJA-1 season.

In the next season (SON-1), convection remains strong in the central equatorial Pacific and starts in the western Indian Ocean (figure 2.7a) and entire Indian Ocean has warm anomalies along with equatorial east Pacific. Sea level pressure lowers in the western Indian Ocean and easterlies weakens in the north Indian Ocean. Thus the TBO convection, SLP and wind start transition from a weak monsoon to a next year strong monsoon and is illustrated in figure 2.7.

The next season (boreal winter before strong summer monsoon, DJF-1 is given in figure 2.8. Convection in the equatorial Pacific weakens by the DJF-1 and is active over the south Indian Ocean and west of India. Warming increases in the Indian Ocean and warm region in the equatorial Pacific extends west. Sea level pressure is high over Australia and west Pacific and is low west of India and southeast Pacific (figure 2.8). Westerlies starts in the north Indian Ocean and easterlies are seen north of Australia. Reduced convection over Australia, warm SST in the southeast Indian Ocean, cool SST

anomalies in the southwest Pacific along with high SLP and easterly winds over Australia indicates a weak Australian monsoon during this time. This points to the fact that after a weak Indian summer monsoon in JJA-1 is followed by a weak Australian monsoon in DJF-1 indicating an in-phase transition from Indian to Australian monsoon.

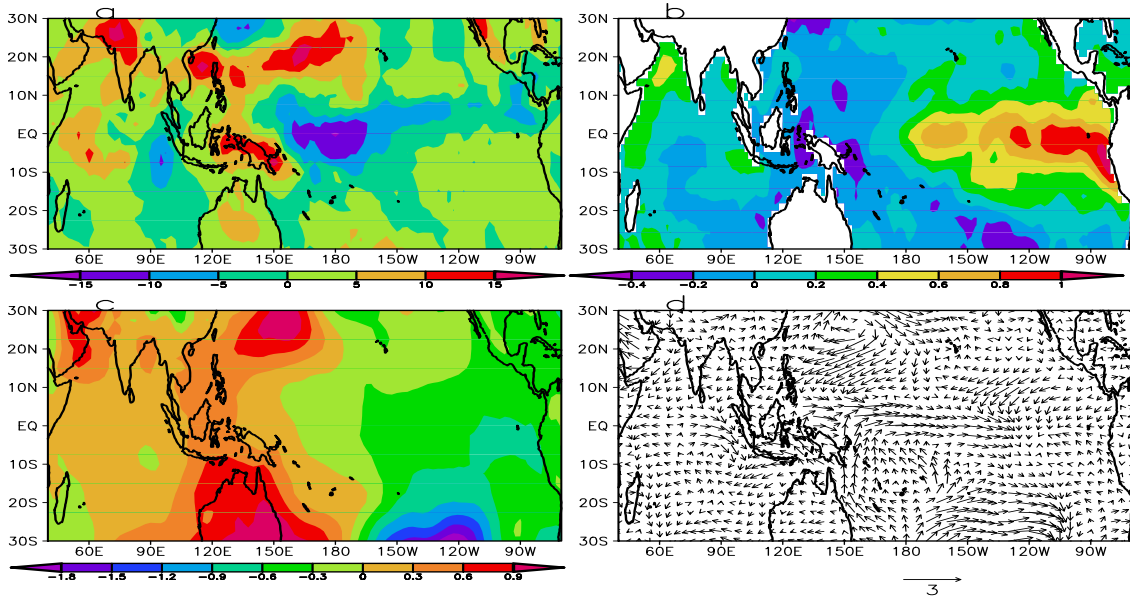


Figure 2.6: Strong minus weak TBO Indian monsoon composite for the previous year summer season (JJA-1) for (a) OLR, (b) SST, (c) SLP and (d) 850 hPa wind.

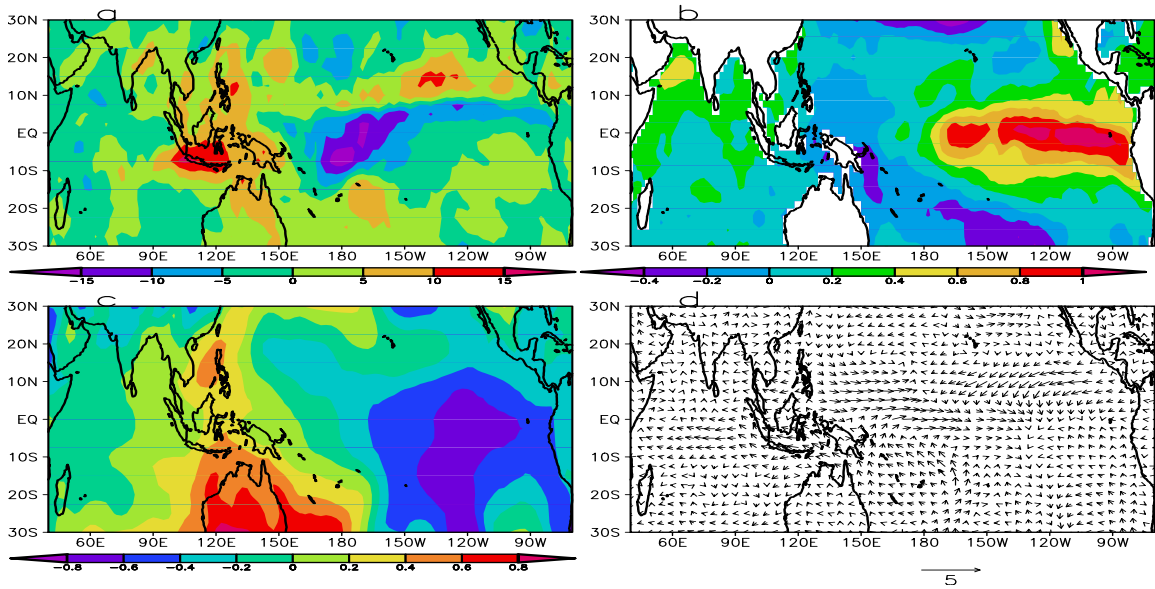


Figure 2.7 Strong minus weak TBO Indian monsoon composite for the previous year post monsoon season (SON-1) for (a) OLR, (b) SST, (c) SLP and (d) 850 hPa wind.

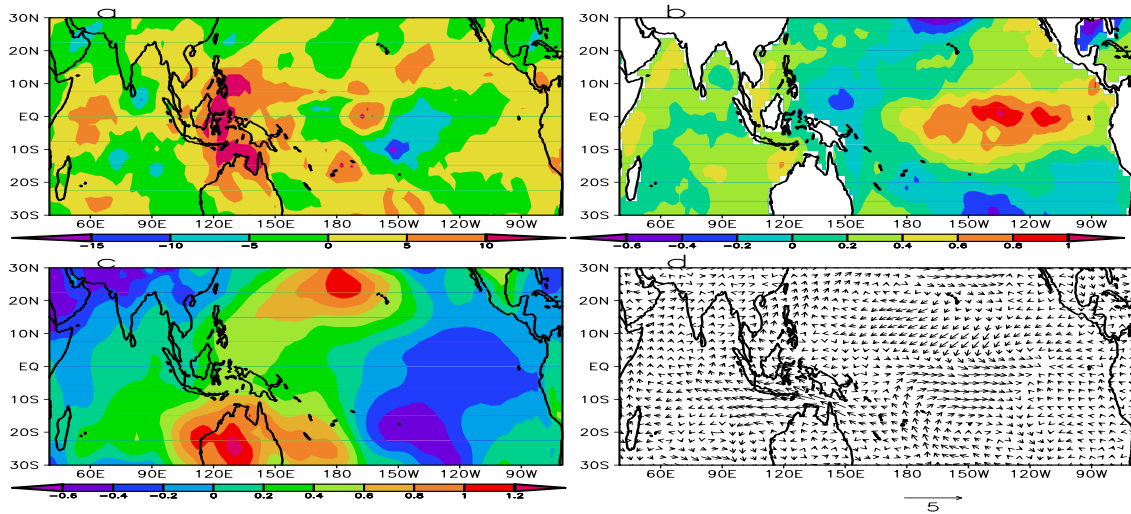


Figure 2.8 Strong minus weak TBO Indian monsoon composite for the previous year boreal winter season (DJF-1) for (a) OLR, (b) SST, (c) SLP and (d) 850 hPa wind.

In the spring season convection is not organized and is seen over north Indian Ocean and east part of Australia and southeast Pacific Ocean (figure 2.9 a). SST remains warm in the Indian Ocean, but anomalies are reduced in the equatorial region due to the increased convection there. SST anomalies in the east Pacific starts reversing in the extreme east (figure 2.9b). Thus in the Pacific anomalies start reversing by the spring season. SLP lowers in the entire Indian Ocean and equatorial Pacific with maximum over India and westerlies in the north Indian Ocean strengthens by this time.

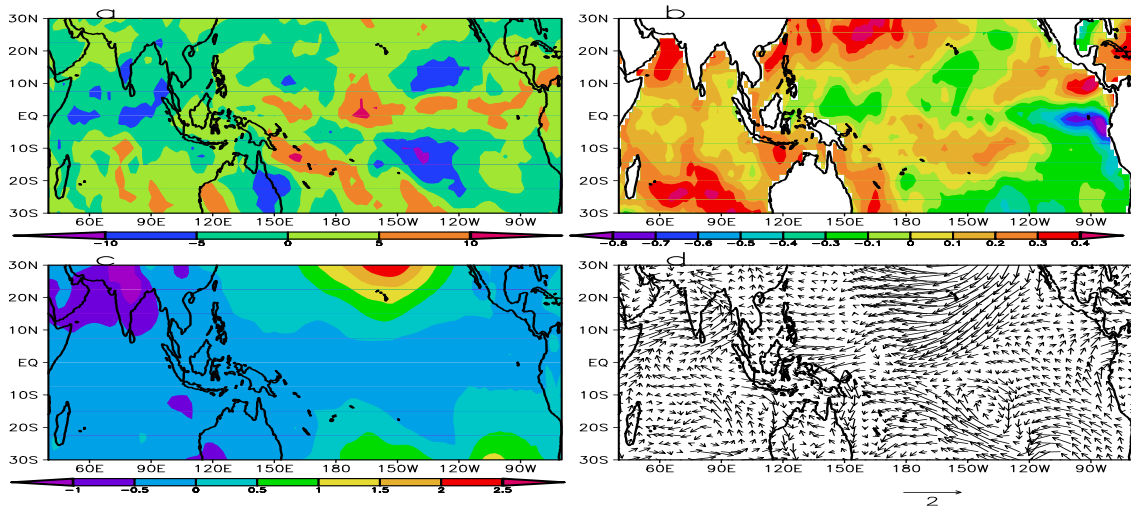


Figure 2.9 Strong minus weak TBO Indian monsoon composite for the spring season (MAM0) before the reference monsoon for (a) OLR, (b) SST, (c) SLP and (d) 850 hPa wind.

The reference summer monsoon (JJA0) season anomalies of OLR, SST, SLP and 850 hPa wind pattern is shown in figure 2.10. During JJA0 OLR anomalies are reduced over India and Arabian Sea region along with western equatorial Indian Ocean and Indonesian region indicating heavy convection in these regions (figure 2.10a). Due to the strong monsoon in these regions, Indian Ocean cools and cooling in the equatorial east Pacific Ocean extends west. Sea level pressure is reduced in the entire Indian Ocean with maximum negative anomaly in the Arabian Sea area. Westerly anomalies are seen over north Indian Ocean and India and are strong in the Arabian Sea. Equatorial easterlies are seen in the Indian Ocean and central Pacific. The JJA0 looks like strong monsoon condition with increased convection over India, cool SST in the Indian Ocean and strong westerlies in the north Indian Ocean and reduced SLP. Thus TBO transition from a weak Australian monsoon in DJF-1 to a strong Indian monsoon in JJA0 takes place.

Comparing figure 2.6 and figure 2.10, which shows boreal summer monsoon composites for two consecutive years we can see that the anomalies of convection, SST, SLP and 850 hPa wind are reverses in almost all the regions considered in the study. Thus clear TBO cycle is seen for Indian summer monsoon from a weak monsoon to a strong monsoon.

Strong minus weak TBO year composite of OLR, SST, SLP and 850 hPa wind for the post monsoon season (SON0) is given in the figure 2.11. After the strong monsoon, convection anomalies weakens over India and north Indian Ocean and is seen in the northwest Pacific and Indonesian region. SST remains cool in the north Indian Ocean and equatorial east Pacific. Warm SST anomalies are noted in the southeast Indian Ocean and south Pacific convergence zone (SPCZ). Sea level pressure remains low over India, east Indian Ocean and Indonesian region. Westerlies weaken in the north Indian Ocean and easterlies are seen in the equatorial central Pacific. Comparing figure 2.7 and figure 2.11, the biennial oscillation is evident between SON-1 and SON0.

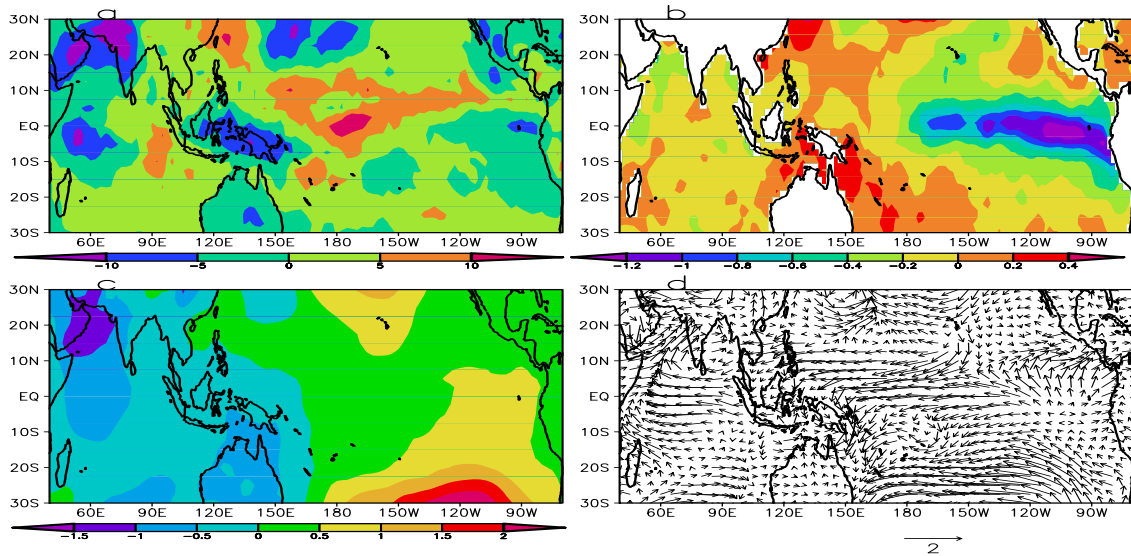


Figure 2.10: Strong minus weak TBO Indian monsoon composite for the reference monsoon season (JJA0) for (a) OLR, (b) SST, (c) SLP and (d) 850 hPa wind.

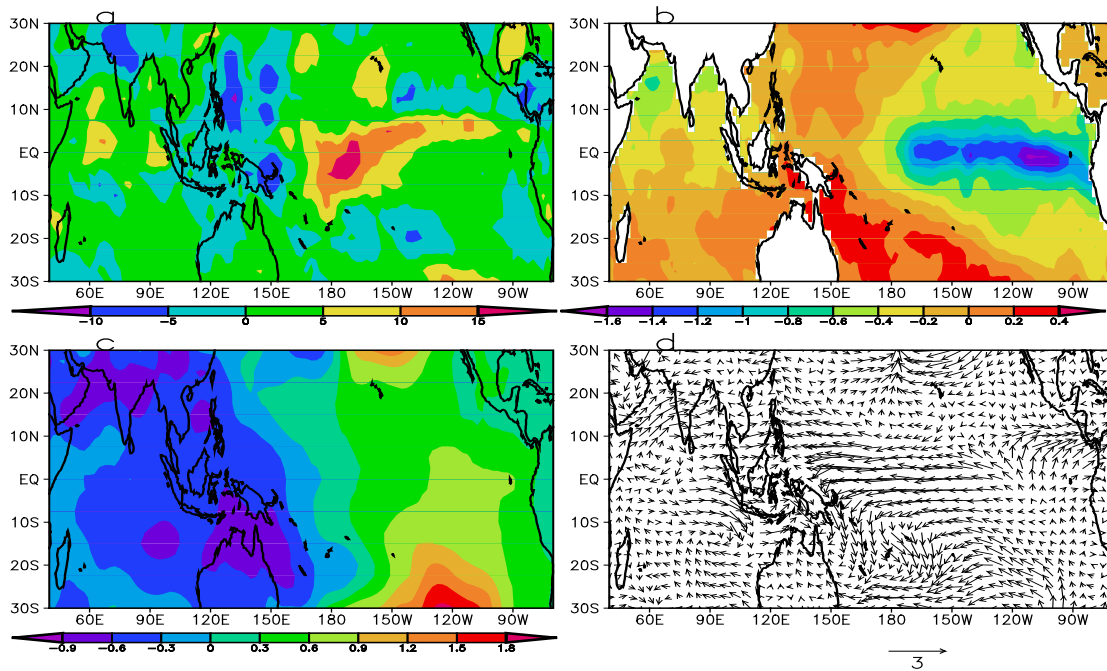


Figure 2.11: Strong minus weak TBO Indian monsoon composite for the post monsoon season (SON0) for (a) OLR, (b) SST, (c) SLP and (d) 850 hPa wind.

The composite pattern for the next boreal winter DJF0 is seen in figure 2.12. By this time convection anomalies concentrate over the equatorial west Pacific and north of Australia. Southeast Indian Ocean and western Indian Ocean cools due to the strong



Australian summer monsoon. Thus entire Indian Ocean region gets cooled by DJF0 and negative maximum in the east Pacific extends west. SLP lowers in the western Pacific and north of Australia and westerlies are seen over north of Australia. Thus Australian monsoon is strengthened in the winter season following the strong Indian summer monsoon. The in phase TBO transition from Indian to Australian monsoon is also evident in this cycle. The ocean atmosphere parameters in the previous winter (DJF0) and the present winter (DJF0) are opposite to each other (see figure 2.8 and figure 2.12)

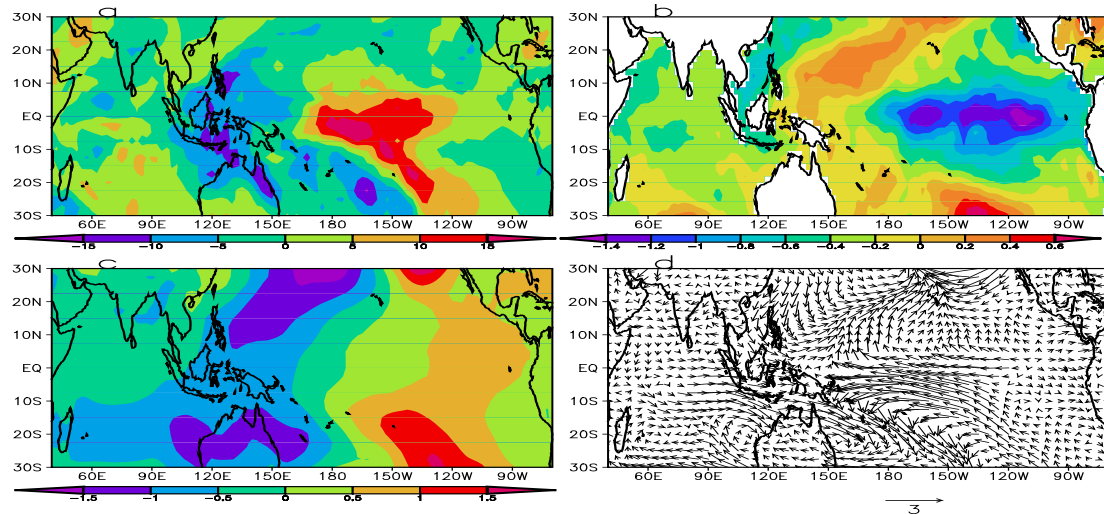


Figure 2.12: Strong minus weak TBO Indian monsoon composite for the preceding winter season (DJF0) for a) OLR, b) SST, c) SLP and d) 850 hPa wind.

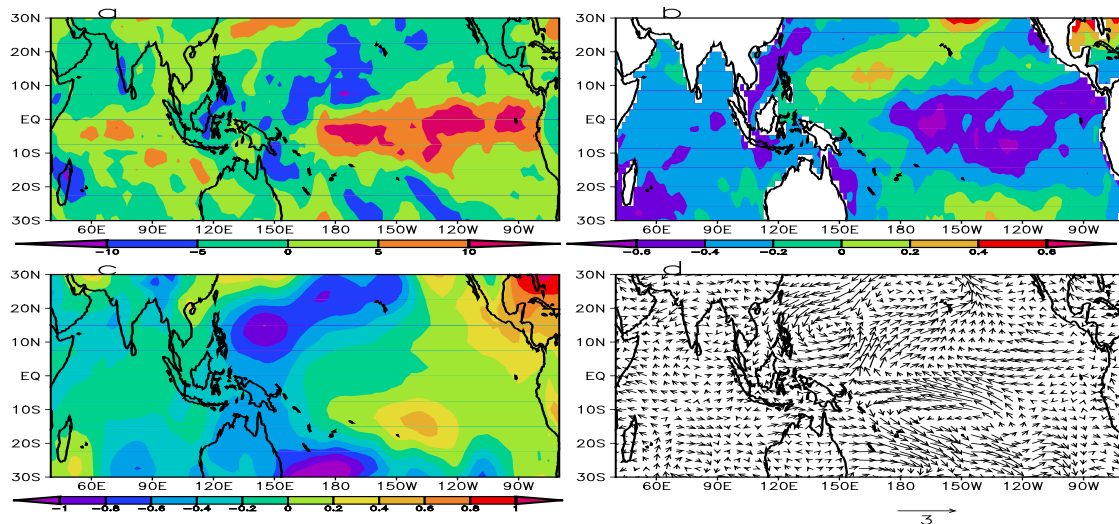


Figure 2.13: Strong minus weak TBO Indian monsoon composite for the next year spring season (MAM1) for (a) OLR, (b) SST, (c) SLP and (d) 850 hPa wind.

The atmosphere–ocean conditions for the next year spring (MAM1) is shown as strong minus weak TBO years composite of OLR, SST, SLP and 850 hPa wind in figure 2.13. In MAM1 convection anomalies moves to central Pacific and minor convection anomalies are seen in the western Indian Ocean and west coast of India. SST is cool in the entire Indian Ocean and equatorial Pacific. SLP minimum is in the western Pacific and weak easterlies are seen in the northwest Indian Ocean. Comparing the spring seasons, MAM0 and MAM1, the anomalies are not reversed completely for all the parameters as observed in the previous seasons. In the case of SST extreme east Pacific starts cooling in the MAM0, but is not reversed to warm anomaly in MAM1.

The strong minus weak composite of TBO years for Indian summer monsoon for the next year summer season (JJA1) is given in figure 2.14 for OLR, SST, SLP and 850 hPa wind respectively. Convection shifts to south China Sea and is also seen in southeast Indian Ocean. Entire Indian Ocean remains cool and warming starts in the equatorial east Pacific. SLP lowers in south China Sea and extreme south Pacific. Weak westerlies are seen in some parts of north Indian Ocean extending to northwest Pacific.

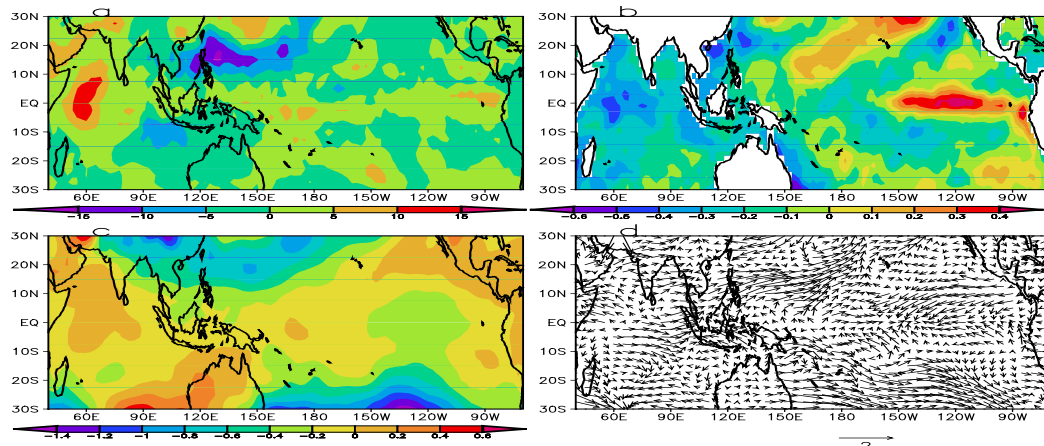


Figure 2.14: Strong minus weak TBO Indian monsoon composite for the next year summer season (JJA1) for (a) OLR, (b) SST, (c) SLP and (d) 850 hPa wind.

Thus in the JJA1 convection shifts to south China Sea compared to strong convection over India in the previous year summer. In the absence of strong monsoon also Indian Ocean remained cool as the JJA0 case, where strong monsoon induced cooling in the north Indian Ocean. Weak westerly anomalies existed in the JJA1, which was strong in JJA0.

Both the Indian and Australian summer monsoon showed reversal in both the phases of TBO with convection strengthening and weakening in adjacent years, showing strong interannual variability. In phase transition from Indian to Australian monsoon and out of phase transition from Australian to Indian monsoon is also observed in these parameters considered for the study.

#### ***2.4.5.2 Indian Ocean fluxes and radiation***

Latent heat flux, shortwave radiation, specific humidity etc lay foundation for understanding external impacts on monsoon transition. These parameters over Indian Ocean are analyzed here for the above mentioned seasons.

##### ***2.4.5.2.1 Latent heat flux***

Latent heat flux anomalies are positive in the western Indian Ocean and Indonesia in JJA-1 season and increases and extend to entire Indian Ocean by MAM0. By the onset of strong monsoon, latent heat flux is negative over equator and southeast Indian Ocean and Indonesian region. The negative value over equator reverses in the next season itself and by next spring south Indian Ocean has negative anomalies and by weak monsoon southwest Indian Ocean has negative anomalies

##### ***2.4.5.2.2 Shortwave radiation***

Shortwave radiation anomalies are positive in the equatorial and south Indian Ocean in JJA-1 and is negative in Arabian Sea and Bay of Bengal. It also becomes positive after the weak monsoon and negative anomalies are over Indonesian region and with onset of strong monsoon positive maximum is in the Arabian Sea and negative anomalies starts at extreme east. Negative anomalies in the south Indian Ocean strengthens and positive anomalies weakens after monsoon and reverses by next summer JJA1.

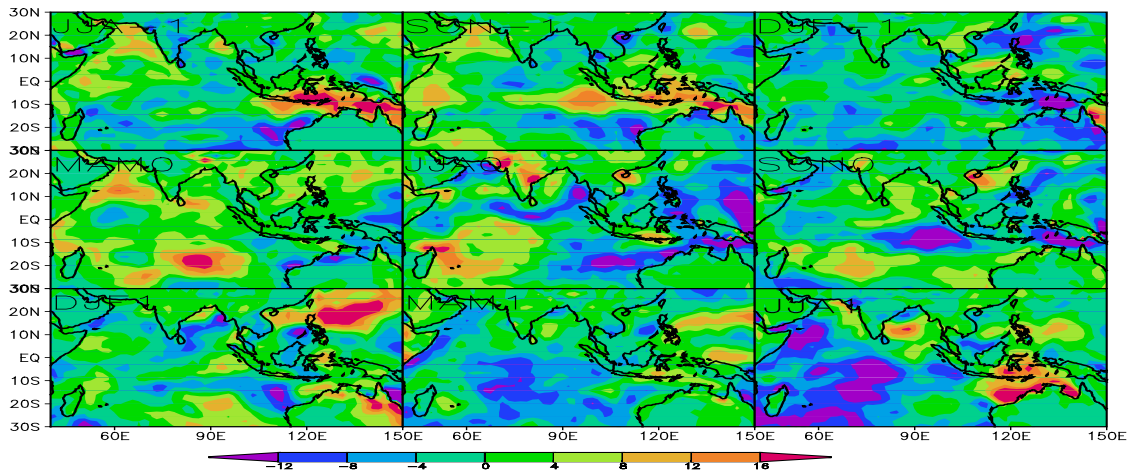


Figure 2.15: strong minus weak composite of latent heat flux over Indian Ocean from JJA-1 to JJA1.

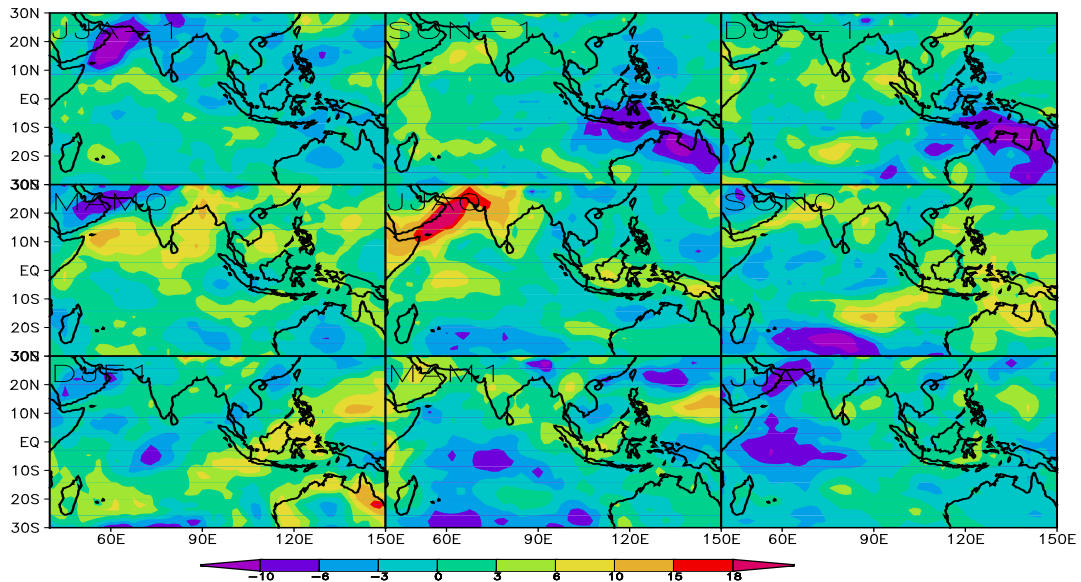


Figure 2.16: Strong minus weak composite of shortwave radiation over Indian Ocean from JJA-1 to JJA1.

### 2.4.5.2 .3 Specific humidity

Specific humidity anomaly is negative in the previous year monsoon over Indian and is positive in the entire Indian Ocean region. The anomaly over the entire region is positive after the monsoon and it strengthens over India by JJA0 and becomes negative in the east Indian Ocean. Entire Indian Ocean becomes negative by MAM1 and Indian land masses by JJA1.

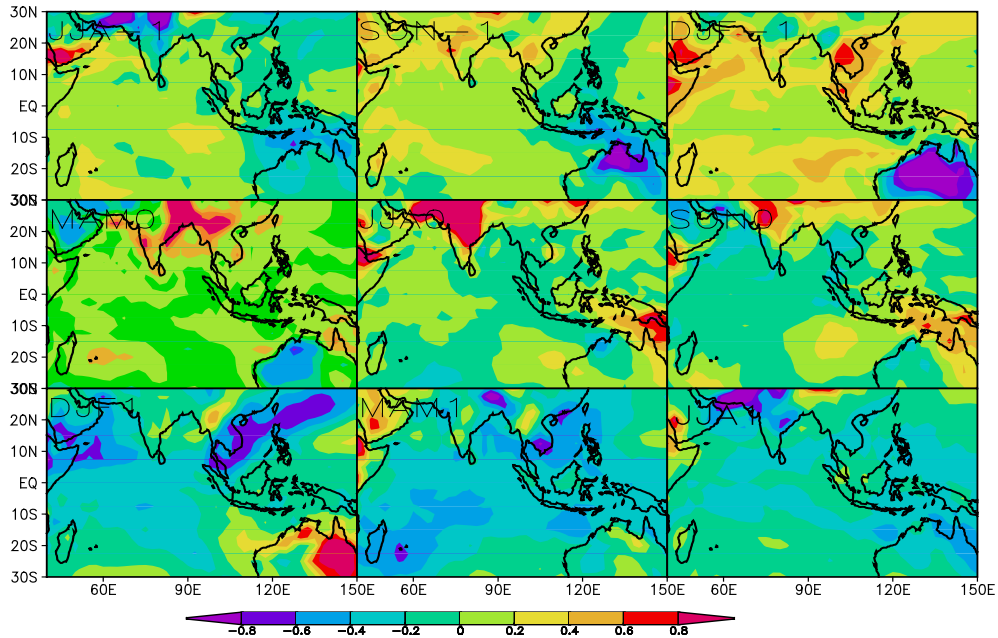


Figure 2.17: strong minus weak composite of specific humidity over Indian Ocean from JJA-1 to JJA1.

## 2.5 Discussion

The present chapter analyses the role of biennial and low frequency oscillation of Indo-Pacific Ocean SST and wind to the interannual variability of Indian summer monsoon. Previous studies by Li and Zhang (2002) identified local SST and moisture over the Indian Ocean has major role in TBO scale and remote SST forcing in the Pacific has major role in ENSO scale processes through modification of Walker circulation. Present observational study identifies different evolution of SST and lower troposphere wind in both the time scales associated with interannual variability of Indian summer monsoon rainfall. Indian Ocean SST has similar pattern in both the scales and Pacific SST has different pattern. In both the scales, Indian Ocean becomes warm before the strong monsoon and starts cooling with the onset of strong monsoon. The east Pacific SST starts cooling in the spring season before the strong monsoon in TBO scale and intensifies with onset of monsoon. But in ENSO scale reversal of SST anomalies are after the summer season.

More over in the TBO scale warm equatorial central Pacific favors strong monsoon and in ENSO scale cool central Pacific favors a strong Indian summer monsoon. 850 hPa

wind over India and Indian Ocean has similar pattern in both the scales, the anomalies and extend is different in both the scales. Strengthening of westerlies over north of Australia in DJF0 is not observed in the ENSO scale. A stationary anticyclone is present in the northeast Pacific in ENSO scale, while it forms in summer in TBO scale. In strong monsoon, rainfall strengthens over India and decreases in equatorial Indian Ocean in TBO scale and reverses in next weak monsoon in TBO scale, while land and ocean region has similar anomalies in ENSO scale. Though the prominent pattern of Indian Ocean SST looks similar in both the scale, its effect on rainfall is different in both the scales. In TBO scale a strong India Ocean SST in spring season will strengthen the rainfall anomalies over western coast and Indian region along with Bay of Bengal.

The filtering technique identifies the difference in processes in both the TBO and ENSO scales. But on an individual year, the anomaly will depend on any of them, both of them or none (Ropelewski et al., 1992). The strong minus weak TBO year composite analysis of different ocean-atmosphere parameter enables to understand the interannual variability of monsoon associated with TBO. In the previous year summer of TBO composite convection is strong in the Pacific indicating a weak Indian summer monsoon and Indian Ocean becomes warm along with equatorial east Pacific Ocean. Easterly winds and high sea level pressure is also present in Indian monsoon region. SLP starts decreasing and westerlies starts setting in the north Indian ocean after the monsoon season, while warm SST persists to next spring season, which is the basic condition needed for TBO.

Australian monsoon also weakens in the boreal winter with warm west Pacific, easterly winds and high SLP over the Australian monsoon region. Thus a weak Australian monsoon follows a weak Indian summer monsoon. East Pacific starts cooling in the spring. In the following summer season convection comes over Indian monsoon region and Indonesia cooling Indian Ocean and SLP is low due to convection and strong westerly flow is also seen over India and north Indian Ocean. Thus along with interannual variability of monsoon, both ocean-atmosphere parameters also reversed indicating biennial oscillation. The convection moves to Australian monsoon region by next winter making it a strong Australian monsoon. The convection moves to west

Pacific in the following seasons and cool SST in the Indian Ocean and equatorial Pacific remains as such. In this phase of monsoon cycle, east Pacific is warmed only in the summer season and Indian Ocean remains cool itself in the next year summer, though the Indian region is less convergent and easterly anomalies are seen over India and north Indian Ocean. Thus in the strong to weak monsoon transition, SST changes in the tropical oceans are delayed by a season.

Shortwave radiation over Indian Ocean shows good interannual variability associated with TBO of Indian summer monsoon, with strengthening/weakening in association with convection and also has southeast movement associated with TBO. Specific humidity over India is low in weak monsoon and is high in strong monsoon showing reversal with monsoon. But over the Indian Ocean it is positive in the weak monsoon and it starts reverses by strong monsoon and completes by next year weak monsoon. According to Yu and Rienecker (1999), the latent heat flux explains the changes in SST in most of the tropical Indian Ocean. If SST changes are introduced by latent heat flux, reduction in latent heat flux can cause progressive warming over tropical Indian Ocean. In the TBO cycle when SST transits from strong to weak phase with onset of strong monsoon, some parts of western Indian Ocean and east Indian Ocean close to Indonesia latent heat flux is not becoming negative. Thus in these areas the SST changes are controlled by external factors like ENSO.

## **2.6 Conclusion**

The study reported in the present chapter identifies the difference in pattern for SST and lower level wind in both TBO and ENSO scale. Indian Ocean has almost similar spatial pattern in both the scales and transition is along with monsoon onset. Equatorial Pacific Ocean has different pattern in both the scales. Spring season strong SST in Indian Ocean enhances rainfall over India and Bay of Bengal in TBO scale. Composite analysis shows southeast movement of convection, lower level wind and SLP from Indian to Australian region from summer to winter season. Indian Ocean SST anomalies retains one year period in interannual monsoon variation periods associated with TBO. Strong to weak monsoon transition of tropical SST is delayed by a season. Local

processes like shortwave radiation follows convection, while is weak for latent heat flux in many areas of Indian Ocean indicting the control of ENSO in SST anomalies of these regions.



---

## **Salient Features of Atmospheric Circulation Associated with TBO**

---

### **3.1 Introduction**

Large-scale tropical circulations, such as Hadley, Walker and monsoon circulations are the strongest driving forces of the general circulation in the low latitudes. Year-to-year variations of these circulations have great impact on climate variability. These changes are arising from reversal of temperature gradient between continents and adjacent oceans. Both the Walker and Hadley cells are the result of thermal contrast and they transport moist static energy. Ferrel cells are indirect cells driven by transient baroclinic eddies and transport heat and momentum poleward (Holton, 1992). Mean meridional circulation has been explained by Lorenz (1967); Oort and Rasmusson (1970); Trenberth et al. (2000), etc. Oort and Rasmusson (1970) analysed the annual variation of monthly mean meridional circulation and their results were well supported by other studies like Newell et al., (1972); Piexoto and Oort (1992); Trenberth et al. (2000); Dima and Wallace (2003) etc. Lindzen and Hou (1988) and Hou and Lindzen (1992) studied the role of concentrated heating on the intensity of Hadley circulation and in turn global climate. Oort and Yienger (1996) observed significant seasonal variation in the strength, latitude and height of maximum stream function for both

Hadley cells. They also noticed significant correlation between the strength of tropical Hadley cells and ENSO.

The Walker circulation has been identified as a main factor connecting the changes in the Pacific Ocean to the globe affecting the global climate variability. It is characterized by rising air in the equatorial western Pacific flowing eastward in the upper troposphere and sinking in the eastern Pacific and returning towards the western Pacific in the lower levels. From the days of Bjerkins (1969), the Walker circulation and its relationship with El Niño-Southern Oscillation (ENSO) has been studied in detail (eg: Philander, 1990; McCreary and Anderson, 1991; Nellin et al., 1998). Wang (2002) studied the atmospheric circulation cells over the Pacific during different phases of ENSO and reported weakening of the Walker cell during the strong phase of ENSO.

Earlier studies of tropospheric biennial oscillation investigated ocean-atmosphere parameters of tropical Indo-Pacific region only (eg, Meehl and Arblaster 2001; 2002a; Meehl et al., 2003; Wu and Kirtman 2004; 2007 etc). Circulation cells connected with TBO has not been studied in detail. Meehl and Arblaster (2002a; b) proposes the influence of east-west atmospheric circulation on the TBO phenomena and Meehl et al. (2003) explained the weakening and strengthening of Walker circulation with the help of vertical velocity. But the seasonal evolution and movement of the Walker circulation cells are not yet studied on the basis of TBO cycle. Earlier studies are concerned with the Hadley circulation as mean meridional circulation of the tropical atmosphere.

But when we are looking for the circulation associated with monsoon and its interannual variability, local meridional circulation is found to be more important than the mean meridional circulation as suggested by Slingo and Annamalai (2000). The definition of Hadley circulation then seems to have extended to any local meridional circulation. For example, Wang (2002) discussed the local Hadley circulation induced by ENSO in the eastern and western Pacific separately. Goswami et al. (1999) discussed local Hadley circulation as part of south Asian monsoon circulation. They also proposed a monsoon Hadley circulation index based on the meridional wind shear between 850 hPa and 200 hPa. averaged over the south Asian monsoon area to measure the strength

of the local Hadley circulation over the monsoon area. Ju and Slingo (1995) and Soman and Slingo (1997) have suggested that changes in local Hadley circulation may have a role in the influence of ENSO on the interannual variability of Asian summer monsoon. Thus it will be interesting to investigate the role of Walker, Hadley and local Hadley circulation associated with biennial oscillation of Indian summer monsoon and thus with TBO.

### 3.2 Objectives of the study

The present chapter analyses the evolution and movement of Walker and mean meridional circulation in the tropical regions associated with TBO. It also studies the role of local Hadley circulation during the monsoon season in strong and weak TBO years.

### 3.3 Data and methodology

The data sets used for the present study are the zonal ( $u$ ), meridional ( $v$ ) and vertical ( $w$ ) component of wind from 1000 hPa to 100 hPa, and vertical velocity at 500 hPa taken from NCEP/NCAR reanalysis (Kalnay et al., 1996) for a period of 54 years (1950-2005). Indian summer monsoon rainfall (ISMR) index (Parthasarathy et al., 1994) is used for the identification of relatively strong and weak TBO years, as defined in chapter 2. The velocity potential and divergence at 850 hPa and 200 hPa along with 500 hPa vertical velocity pattern identifies the divergence/convergence centers associated with upward/downward motions. Equatorial east-west circulation cells are represented by the vertical profile of  $u$  and negative of  $w$  averaged over 10°S-10°N area.

The strength of the mean meridional overturning of mass can be derived from meridional velocity from 1000 hPa to 100 hPa heights (Oort and Yienger 1996). The mass transport is computed using observed zonal mean meridional winds.

Zonally averaged mass continuity equation is computed in the form

$$\frac{\partial[\bar{v}]\cos\phi}{R\cos\phi\partial\phi} + \frac{\partial[\bar{\omega}]}{\partial p} = 0 \quad \dots 3.1$$

Where  $[\bar{v}]$  is temporal and zonal averaged meridional velocity,  $\omega$  is vertical velocity in pressure co ordinates,  $R$  is mean radius of earth and  $p$  is pressure.

Introducing a Stokes stream function  $\psi$ , given by equation

$$[\bar{v}] = g \frac{\partial \psi}{2\pi R \cos \phi \partial p} \quad \dots 3.2$$

We can calculate the  $\psi$  field, assuming  $\psi=0$  at the top of the atmosphere and integrating the equation downward to the surface.

$$\psi = \frac{2\pi R \cos \phi}{g} \int_p^{p_0} [\bar{v}] dp \quad \dots 3.3$$

Using this Stokes stream function, we have calculated the mean mass and examined its seasonal evolution for strong minus weak monsoon year composites for TBO years. We used positive sign for  $\psi$  in the case of clockwise rotation and negative sign for anti-clockwise rotation as represented by Oort and Yienger (1996). According to this sign convention, strengthening of two tropical Hadley cells would mean larger positive values of  $\psi$  in the Northern Hemisphere (NH) tropics and more negative values of  $\psi$  in the Southern Hemisphere (SH) tropics. The difference of mass stream function between two points on a cross section is equal to the amount of mass flowing across a line joining the two points.

The vertical profile of meridional wind ( $v$ ) and vertical velocity ( $w$ ) averaged over Indian monsoon area ( $60^{\circ}\text{E}-95^{\circ}\text{E}$ ) is used to represent the local meridional circulation.

### 3.4 Results

#### 3.4.1 Anomalous Walker circulation associated with TBO cycle

In order to understand the anomalous variation of atmospheric circulation cells, the pattern of lower and upper level convergence/divergence are very important. Atmospheric convergence/divergence centers and associated upward motion can be identified from the lower (850 hPa) and upper (200 hPa) troposphere velocity potential and divergence winds and associated mid-troposphere (500 hPa) vertical velocity

patterns. Divergent (convergent) center at the upper troposphere corresponds to convergent (divergent) centers at the lower level and is associated with upward (downward) motion at the mid troposphere. The Walker circulation cells can be seen from the vertical profile of combined fields of  $u$  and  $w$  averaged over the equatorial region between  $10^{\circ}\text{S}$  and  $10^{\circ}\text{N}$ .

The above parameters for the previous year summer season (JJA-1) of TBO year is given in figure 3.1. During the previous year summer season (JJA-1) upper level (200 hPa) convergence and lower level divergence (850 hPa) is over southwest Pacific Ocean and reverse pattern is over east Pacific (figure 3.1a). 500 hPa vertical velocity shows strong upward motion in the equatorial east Pacific and equatorial west Indian Ocean. 850 hPa has strong divergent center over Indian monsoon region. Equatorial Walker circulation has upward branch in the Pacific Ocean east of  $150^{\circ}\text{W}$  and in the western Indian Ocean and downward motion in eastern Indian Ocean and western Pacific (figure 3.1d). Thus the large scale circulation causes descending motion and divergence over India and western Indian Ocean supporting weak Indian summer monsoon during negative phase of TBO.

In the next season (SON-1), the upper level convergence center is over the southwest and southeast Indian Ocean and divergence is over the equatorial east Pacific Ocean (figure 3.2a). The mid-troposphere has upward motion in the equatorial east Pacific and downward motion in the Indonesian region. 850 hPa has divergent center over north of India and Indonesian region and convergence is over southeast Pacific. Equatorial zonal circulation also has upward branch in the central and east Pacific and downward motion in Indian Ocean and west Pacific Ocean regions.

During the boreal winter before the strong monsoon (DJF-1), upper level convergence, lower level divergence and associated midtroposphere downward motion is over north of Australia (see figure 3.3 a to c). 200 hPa divergent center, lower level convergence center and mid-tropospheric upward motion is over equatorial east Pacific. Equatorial Walker circulation has strong upward motion east of date line and downward motion in the west Pacific region. Indian Ocean also has upward motion anomalies, which is seen in the mid troposphere vertical velocity pattern also. Thus the lower level divergence,

upper level convergence and downward motion is over Australian monsoon region, making it a weak monsoon after a weak Indian monsoon.

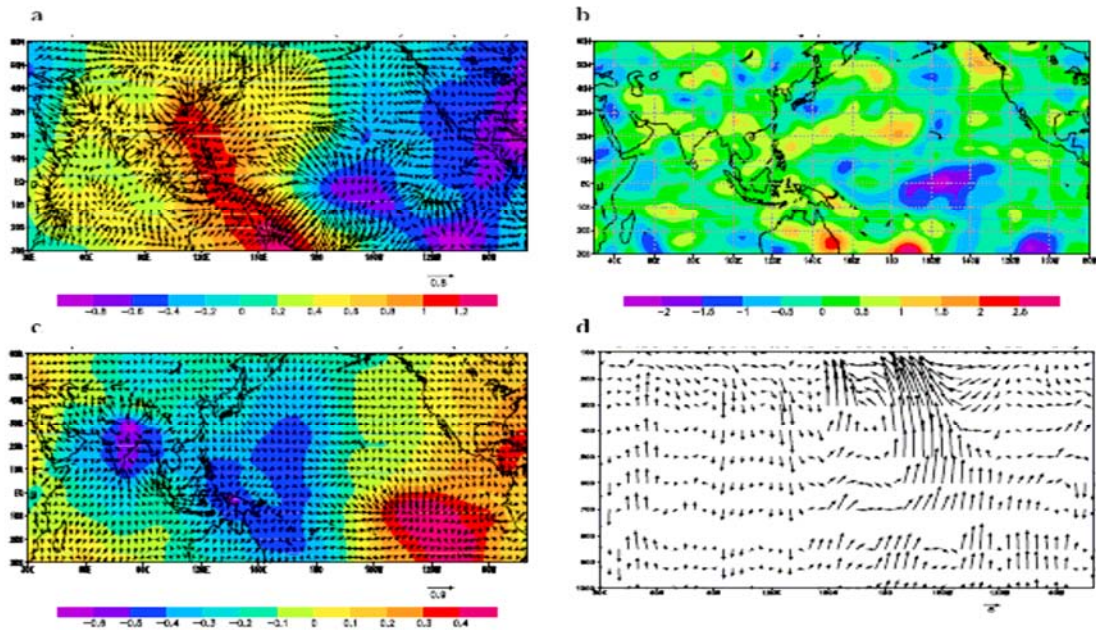


Figure 3.1: Strong minus weak TBO composite of (a) velocity potential (shaded) and convergence (vector) at 200 hPa (b) 500 hPa vertical velocity, (c) velocity potential and convergence at 200 hPa and (d) height–longitude plot of u and w averaged for equatorial belt ( $10^{\circ}\text{S}$ - $10^{\circ}\text{N}$ ) for JJA-1

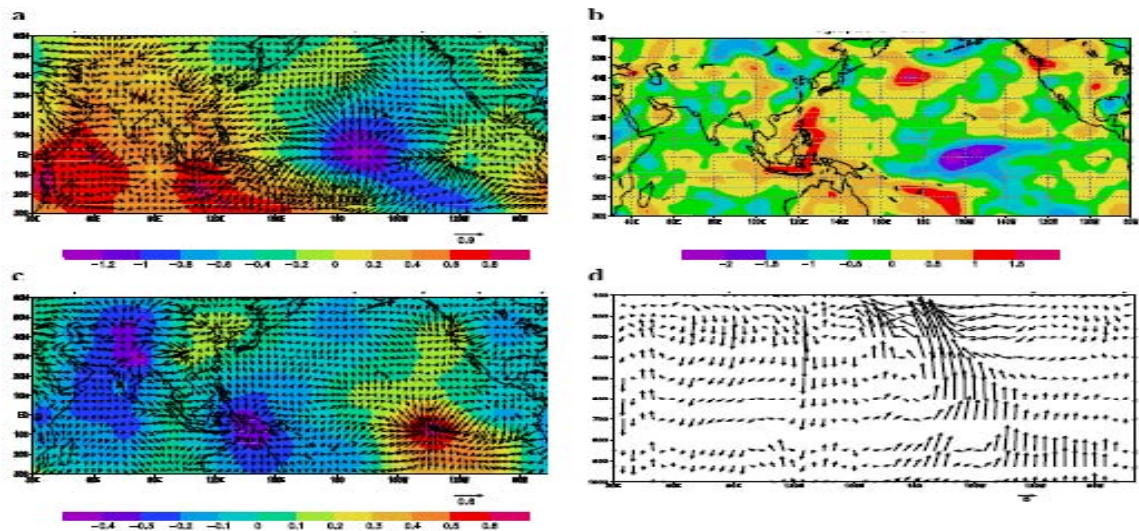


Figure 3.2: Strong minus weak TBO composite of (a) velocity potential (shaded) and convergence (vector) at 200 hPa (b) 500 hPa vertical velocity, (c) velocity potential and convergence at 200 hPa and (d) height–longitude plot of u and w averaged for equatorial belt ( $10^{\circ}\text{S}$ - $10^{\circ}\text{N}$ ) for SON-1

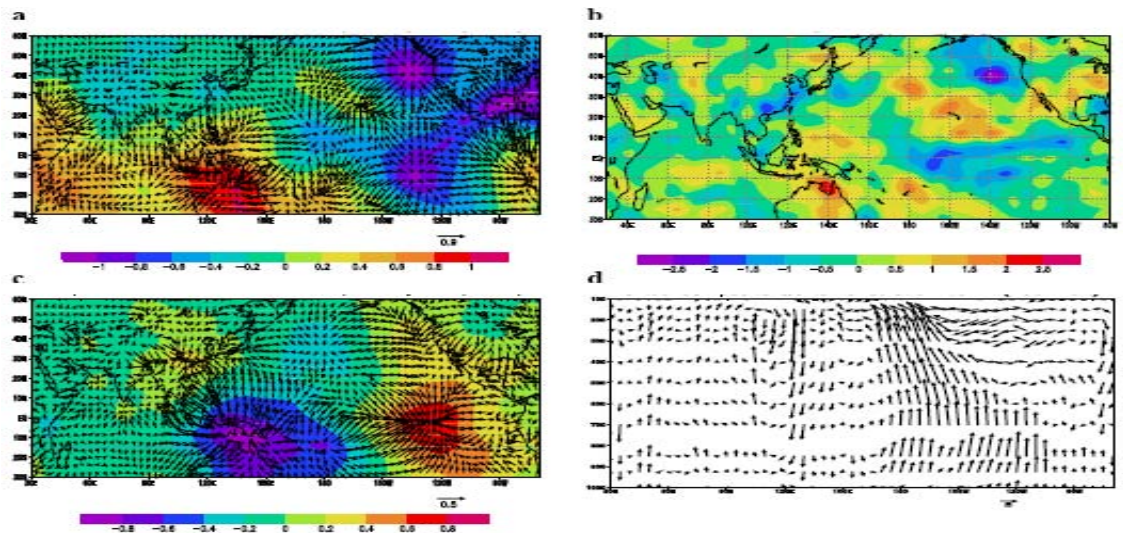


Figure 3.3: Boreal winter season (DJF-1) pattern of strong minus weak TBO composite of (a) velocity potential and convergence at 200 hPa (b) 500 hPa vertical velocity, (c) velocity potential and convergence at 200 hPa and (d) height–longitude plot of  $u$  and  $w$  averaged for equatorial belt ( $10^{\circ}\text{S}$ - $10^{\circ}\text{N}$ )

In the spring season prior to a strong TBO monsoon (MAM0), upper level divergence and lower level convergence moves to southeast Asia making midtropospheric upward motion (see figure 3.4). Upper level convergence and lower level divergence is over the extreme equatorial east Pacific. Equatorial Walker circulation has upward motion anomalies in the dateline and weak downward motion is seen over Indian Ocean region along with strong downward motion in the east Pacific.

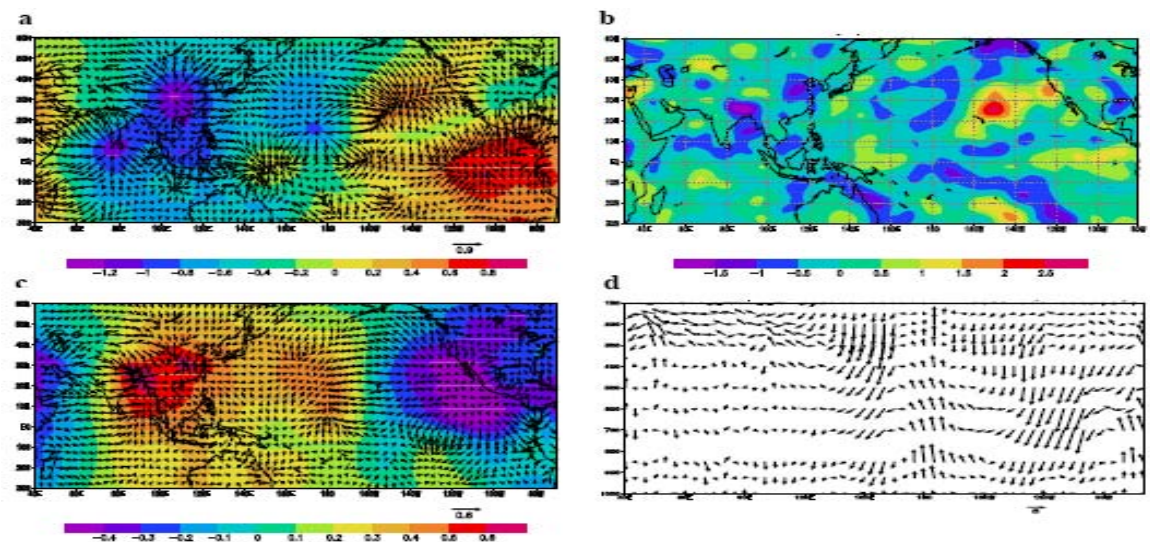


Figure 3.4: Strong minus weak TBO composite of (a) velocity potential and convergence at 200 hPa (b) 500 hPa vertical velocity, (c) velocity potential and convergence at 200 hPa and (d) height–longitude plot of  $u$  and  $w$  averaged for equatorial belt ( $10^{\circ}\text{S}$ - $10^{\circ}\text{N}$ ) for MAM0

During the strong year monsoon season (JJA0), velocity potential and divergence anomalies identifies upper level (200 hPa) divergence center over India and equatorial western Indian Ocean and lower level convergence center over India, along with upward motion anomalies at mid-troposphere (500 hPa) in figure 3.5 a, b, and c. Upper level convergence and lower level divergence anomalies along with mid-troposphere downward motion is seen in the equatorial east Pacific. The convergence and upward motion in Indian monsoon region indicates the strengthened circulation during the positive phase of TBO monsoon period. The Walker circulation has ascending air over western Indian Ocean and western Pacific and descending air over the eastern Indian Ocean and east Pacific.

Thus in the JJA-1 and JJA0 equatorial western Indian Ocean has upward motion eastern side has downward motion, but anomalies reverses in the east and west Pacific

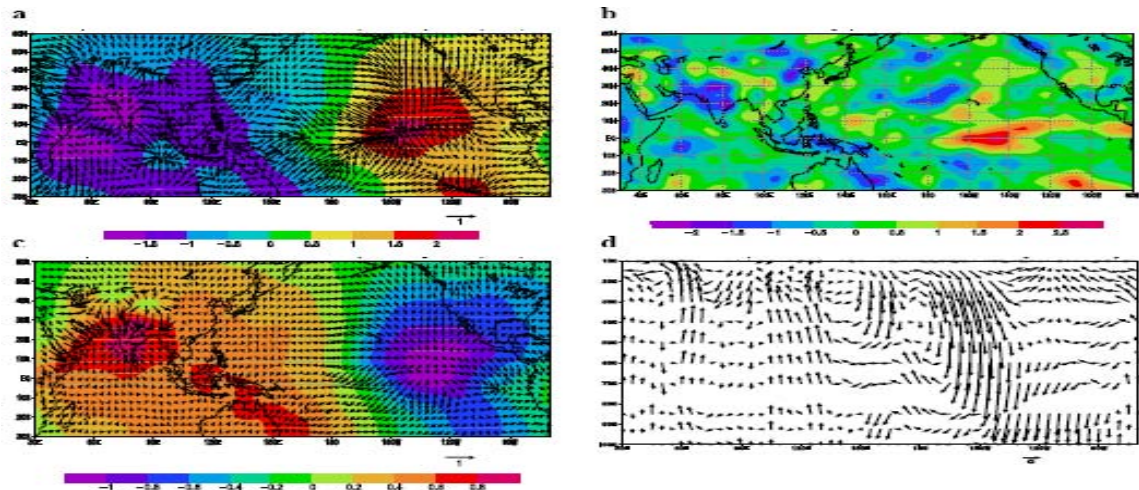


Figure 3.5: Summer season (JJA0) strong minus weak TBO composite of (a) velocity potential and convergence at 200 hPa (b) 500 hPa vertical velocity, (c) velocity potential and convergence at 200 hPa and (d) height–longitude plot of  $u$  and  $w$  averaged for equatorial belt ( $10^{\circ}\text{S}$ - $10^{\circ}\text{N}$ )

The convergence/divergence pattern and Walker circulation for the season after the strong monsoon (SON0) is given in figure 3.6. The upper level divergence center and lower level convergence center moves to Indonesian region along with mid-tropospheric upward motion. 200 hPa convergence and 850 hPa divergence remains in the east Pacific. It is noted that the east-west cell has ascending motion over the west Pacific region and descends over the eastern Pacific and also over Indian Ocean.



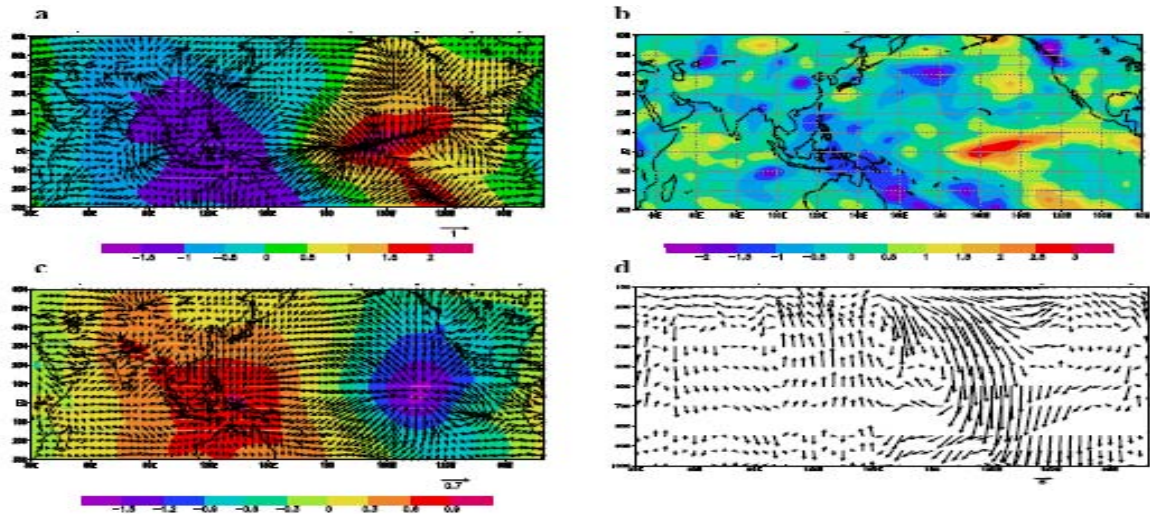


Figure 3.6: Strong minus weak TBO composite of (a) velocity potential and convergence at 200 hPa (b) 500 hPa vertical velocity, (c) velocity potential and convergence at 200 hPa and (d) height–longitude plot of  $u$  and  $w$  averaged for equatorial belt ( $10^{\circ}\text{S}$ - $10^{\circ}\text{N}$ ) for SON0

By the following boreal winter (DJF0), the 200 hPa divergence center, lower level convergence and mid-tropospheric upward motion moves to north of Australia and the western Pacific. Reverse pattern is seen in the eastern Pacific in all the three levels (see figure 3.7 a to c). The equatorial zonal circulation has ascending air over the western Pacific and it moves towards east and descending in the eastern Pacific and Indian Ocean. Thus circulation also strengthens over Australia in the boreal winter following a strong summer monsoon.

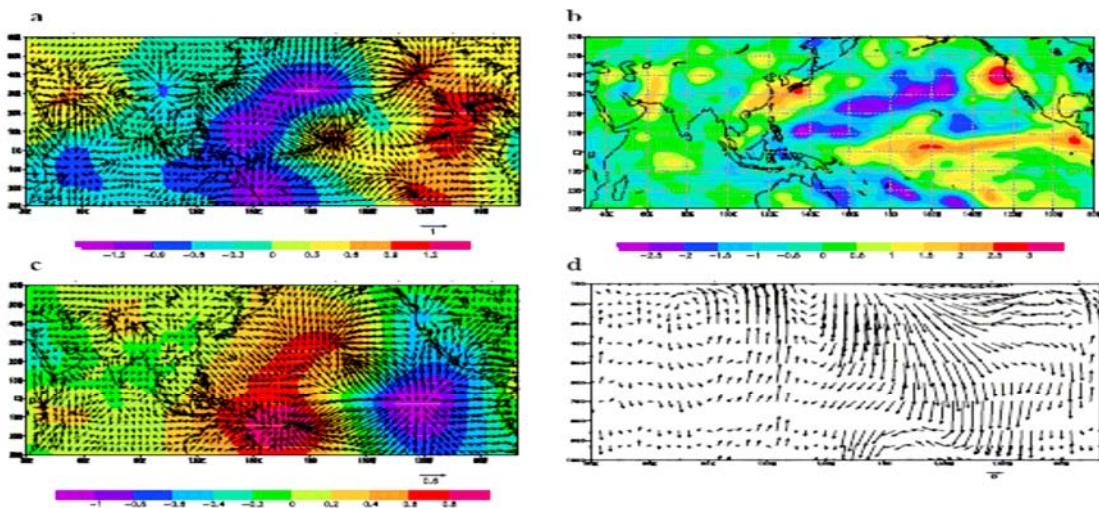


Figure 3.7: strong minus weak TBO composite of (a) velocity potential and convergence at 200 hPa (b) 500 hPa vertical velocity, (c) velocity potential and convergence at 200 hPa and (d) height–longitude plot of  $u$  and  $w$  averaged for equatorial belt ( $10^{\circ}\text{S}$ - $10^{\circ}\text{N}$ ) for DJF0

The convergence/divergence pattern and equatorial Walker circulation for the next spring season (MAM1) is given in figure 3.8. All through the next spring (MAM1) the upper level divergence and lower level convergence in the west Pacific remains as such and it weakens over Australia. But upper level divergence and lower level convergence anomalies appear over Africa. Upper level convergence and lower level divergence is over east Pacific along with mid-tropospheric downward motion. The east-west circulation responds to the convergence/divergence pattern with anomalous air rising in the western Pacific and descending in the eastern Pacific. Ascending air is found in the extreme west and east of Indian Ocean also.

With the onset of next year monsoon (JJA1), velocity potential shows upper level convergence and lower level divergence over the equatorial western Indian Ocean and midtropospheric level shows downward motion in figure 3.9. Upper level divergence and lower level convergence is over the east Pacific and over the equatorial east Indian Ocean. Equatorial Walker circulation also follows the same pattern with rising air in the eastern Pacific and eastern Indian Ocean (figure 6 a-d). The Walker circulation thus reverses with strengthened eastern Walker Cell and weakened western Walker cell.

Thus the zonal circulation is showing biennial oscillation by strengthening in strong TBO phase and weakening in weak phase and has southeast movement.

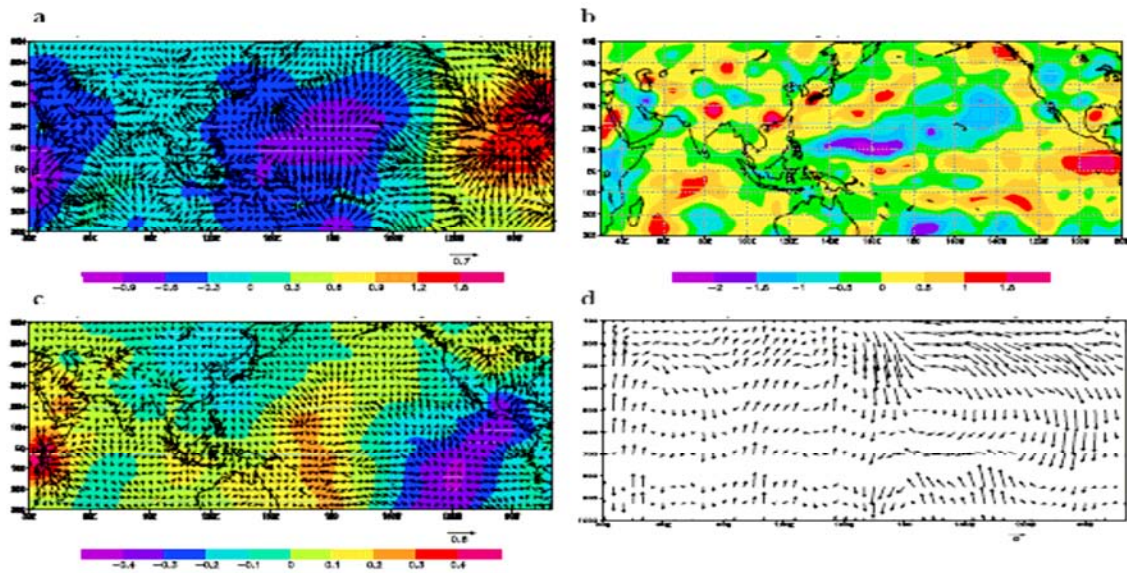


Figure 3.8: Strong minus weak TBO composite of (a) velocity potential and convergence at 200 hPa (b) 500 hPa vertical velocity, (c) velocity potential and convergence at 200 hPa and (d) height-longitude plot of  $u$  and  $w$  averaged for equatorial belt ( $10^{\circ}\text{S}$ - $10^{\circ}\text{N}$ ) for MAM1

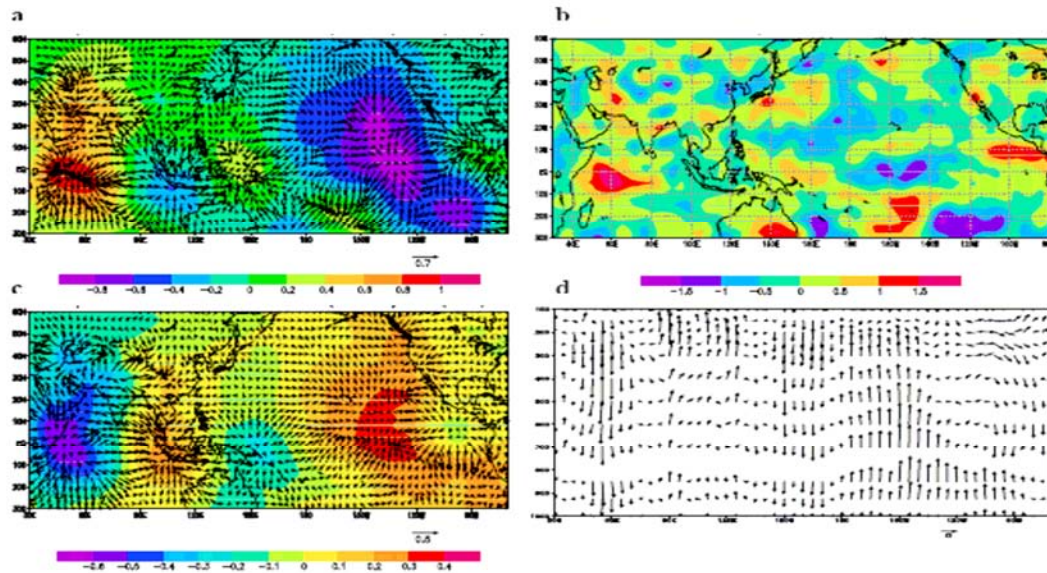


Figure 3.9: Strong minus weak TBO composite of (a) velocity potential and convergence at 200 hPa (b) 500 hPa vertical velocity, (c) velocity potential and convergence at 200 hPa and (d) height-longitude plot of  $u$  and  $w$  averaged for equatorial belt ( $10^{\circ}\text{S}$ - $10^{\circ}\text{N}$ ) for JJA1

### 3.4.2 Mean meridional circulation during TBO cycle

To understand the seasonal evolution of mean meridional circulation of the TBO composite analysis of stream function for strong minus weak monsoon years are carried out for TBO years from JJA-1 to JJA1

During the previous summer (JJA-1) of a strong monsoon, the composite gives two anomalous Hadley cells in the tropics. The negative anomalous cell at the southern hemisphere (SH) indicates increased mass transport to the south and positive cell in the northern hemisphere (NH) gives increased transport to north. Thus, during JJA-1 both the Hadley cells are intensified. The midlatitude cells are very weak. The NH Hadley cell starts to weaken by the autumn (SON-1). The negative cell in the northern hemisphere extends to entire NH tropics by the boreal winter (DJF-1). Throughout this time the SH Hadley cell has negative anomaly, indicating the presence of intensified cell. During the pre monsoon season (MAM0), the anomalous SH Hadley cell is positive, representing the weakening of the cell. A negative cell is seen close to the equator with lesser vertical extend. Ferrel cell is active in the northern hemisphere.

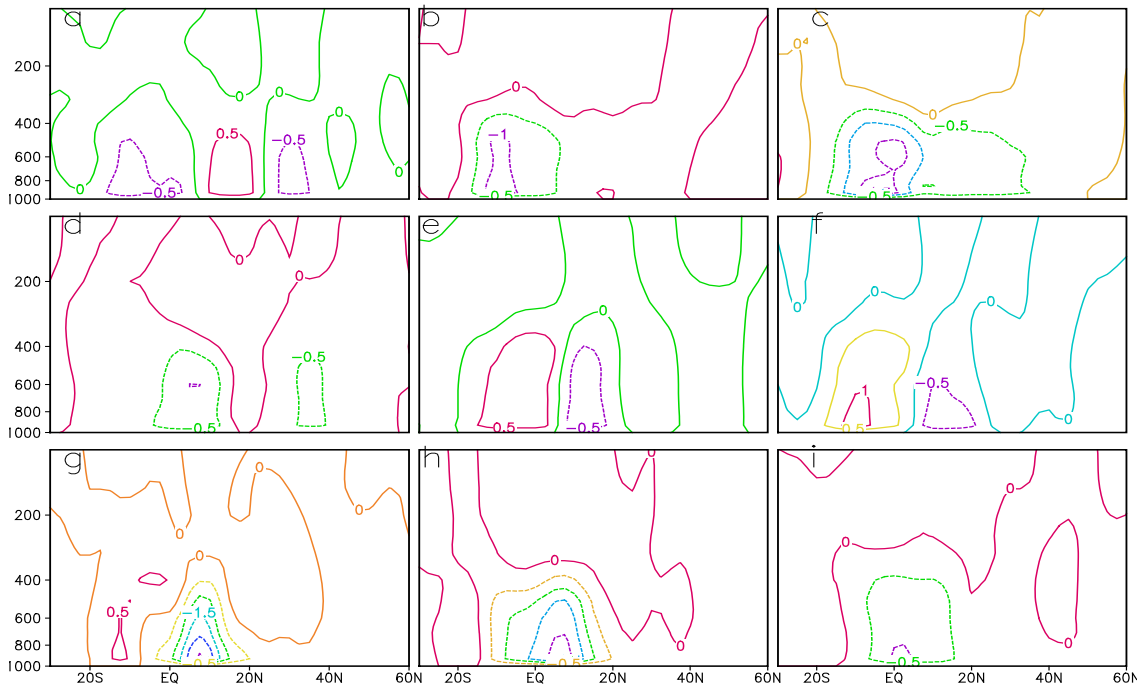


Figure 3.10: Strong minus weak composite of mean meridional circulation derived from stream function for seasons from JJA-1 to JJA1.

Throughout the strong monsoon season (JJA0), the Hadley cells are weak in both the hemispheres. The anomalous mass transport at the upper levels is directed towards the equator. The indirect Ferrel cells are also seen in both the hemispheres, but they are generally weak. After the strong monsoon season the northern hemisphere Hadley cell

anomaly reduces, while it strengthens in the southern hemisphere. Ferrel cell is absent in the southern hemisphere. During the boreal winter (DJF0) two equatorward mass transporting cells are seen in both the hemispheres, in which southern hemisphere cell is intense. Ferrel cell is seen in the northern hemisphere midlatitudes. Throughout the preceding spring (MAM1), only the northern hemisphere anomalous negative cell is present representing the weakened tropical circulation. During the next year of a strong monsoon (JJA1), the negative cell at the equator also weakens. This indicates that in the following summer season of TBO year anomaly is very small indicating a situation not far from normal.

Thus in the TBO composites, both the Hadley cells are strong during the weak monsoon prior to the strong monsoon year and it slightly changes to weak cell by JJA0. But the stream function anomaly is not reversing in the next strong to weak cycle.

### ***3.4.3 Local monsoon Hadley circulation during the TBO cycle***

The mean meridional circulation during the TBO years doesn't exhibit clear reversal of anomalies from JJA-1 to JJA0 and then to JJA1. So we concentrate on the TBO cycle of local monsoon Hadley circulation over the 60<sup>0</sup>E-95<sup>0</sup>E areas in the previous year (JJA-1), current monsoon (JJA0) and next year monsoon (JJA1) to know the modification of meridional circulation by TBO.

During the JJA-1 season, the local meridional circulation has anomalous ascending motion between the equator and 10<sup>0</sup>S. In southern hemisphere ascending motion prevails over 25<sup>0</sup>S to 35<sup>0</sup>S. The descending motion is present in the entire northern hemisphere tropics indicating weak circulation over the Indian monsoon region. During the strong monsoon (JJA0), upward motion anomaly is noted from equator to 30<sup>0</sup>N and downward motion is seen between equator and 10<sup>0</sup>S. Hence ascending motion is seen over the monsoon region and descending motion in the entire southern hemisphere. By the next monsoon (JJA1) anomalous downward motion is found over 10<sup>0</sup>S-25<sup>0</sup>N area and upward motion in southern hemisphere between 10<sup>0</sup>S-30<sup>0</sup>S.

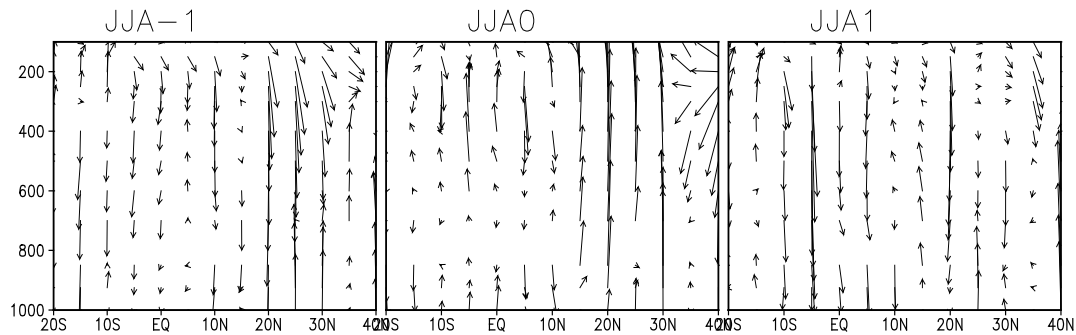


Figure 3.11: Height-latitude profile of  $v$  and  $w$  for three consecutive summer monsoon seasons averaged over  $60^{\circ}$ - $95^{\circ}$ E region.

In brief, the local meridional circulation over the Indian summer monsoon exhibits clear biennial cycle with anomalous ascending motion in strong years and anomalous descending motion in the preceding and the subsequent years.

### 3.4.4 Temporal variation of Local Hadley circulation

In the previous section, it has been noted that the local Hadley circulation represented by the vertical profiles of  $(v, -w)$  has a clear TBO tendency. In order to find whether this reversal of anomalies is preset in all strong and weak monsoons we have analyzed the time series of local Hadley circulation and monsoon rainfall. Local Hadley circulation is represented by an index called monsoon Hadley (MH) index as suggested by Goswami et al. (1999). MH index is a circulation index, defined as the meridional wind-shear anomaly (between 850 hPa and 200 hPa) averaged over the region  $70^{\circ}$ E- $110^{\circ}$ E,  $10^{\circ}$ N- $30^{\circ}$ N. The monsoon season standardized anomaly of MH index is plotted along with ISMR for the period 1950-2002 periods and is shown in figure 3.12.

From the figure 3.12 it is evident that both the MH index and ISMR shows a biennial oscillation. The MH index and ISMR has a correlation of 0.663. The index remains positive (negative) during the strong (weak) TBO years indicating close association of local meridional circulation with TBO.

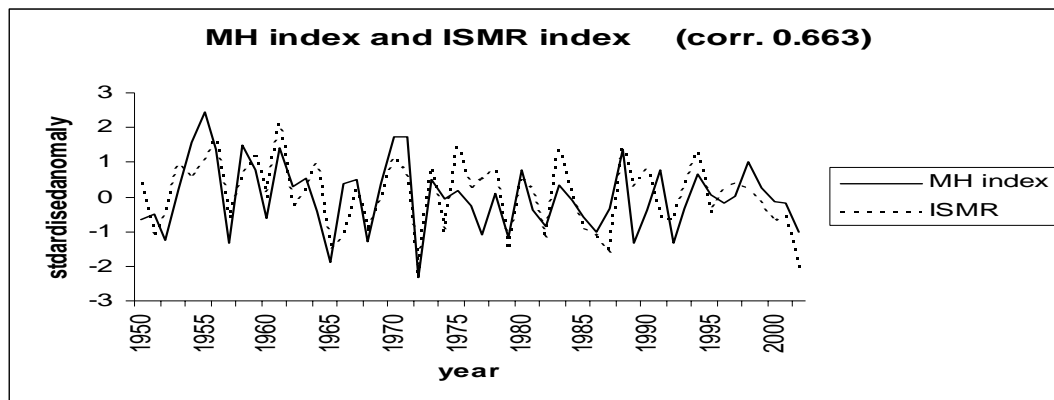


Figure 3.12 : Time series Monsoon Hadley index (full line) and ISMR index(dotted line). Indices are as defined in text.

### 3.5 Discussion and Conclusion

Convergence/divergence center in the lower and upper troposphere along with mid-troposphere upward/downward motion shows clear TBO cycle with weakening during weak monsoon and strengthening in strong monsoon. Lower level divergence and upper level convergence is over India and west Pacific in weak monsoon (JJA-1) with weakened Walker circulation indicated by downward motion over the east Indian Ocean and west Pacific. The upward motion anomaly in the west Indian Ocean along with east Pacific indicates an El Niño pattern of weak monsoon. The convergence/divergence centers start moving southeast and lower level divergence is over Australia in DJF-1 and Walker circulation remains weakened. By the spring season pattern reverses with low-level convergence and upper level divergence over southeast Asia. Equatorial Walker circulation starts strengthening by downward motion at extreme east in association with SST cooling in the extreme east Pacific in MAM0. Convergence appears over India by strong monsoon in JJA0 and divergence in east Pacific strengthens. Walker circulation has upward motion in west Indian Ocean and west Pacific and downward motion in east Indian Ocean and east Pacific. Thus equatorial western Indian Ocean remains convergent in both JJA-1 and JJA0.

After monsoon convergence center from Indian region moves southeast and Walker circulation has downward motion in western Indian Ocean and downward center comes in the eastern Indian Ocean. Convergence reaches over Australia by next winter. By

MAM1 Walker circulation has upward motion in the east Indian Ocean. By next summer divergence is over equatorial west Indian Ocean. Thus the convergence/divergence centers shows good biennial cycle associated with interannual variability of Indian summer monsoon, with divergence over India in JJA-1 changes to convergence by JJA0 and in JJA1 it is over equatorial west Indian Ocean. This pattern is in good agreement with SST pattern obtained earlier. The continuation of cool SST in the Indian Ocean in JJA1 may lead to divergence obtained in equatorial west Pacific, which was convergent in JJA-1.

During JJA-1 season mass transport from the equator to both the hemisphere are increased by intensified Hadley cells. The northern hemisphere Hadley cell starts weakening after the weak monsoon, but the SH cell remain strengthened upto the winter. By JJA0 both the cells are weakened. But after the strong monsoon also the cells remains weakened, making JJA0 to JJA1 transition insignificant. But the local monsoon circulation has upward motion in northern hemisphere tropics in the strong monsoon season and has downward motion in the previous and next year of JJA0. Thus biennial cycle is clear in both the transitions.



---

## **Influence of El Nino Southern Oscillation and Indian Ocean Dipole in biennial oscillation of Indian summer monsoon**

---

### **4.1 Introduction**

The main contributors to the interannual variability of Indian summer monsoon rainfall (ISMR) is the large scale forcing from El Nino Southern Oscillation (Webster and Yang, 1992; Ju and Slingo, 1995; Webster et al., 1998), tropical Tropospheric Biennial Oscillation (Meehl, 1997; Chang and Li, 2000; Meehl and Artblaster, 2002a; Meehl et al., 2003; Wu and Kirtman, 2004; 2007) and Indian Ocean Dipole (Saji et al., 1999; Webster et al., 1999; Ashok et al., 2004). During an El Niño event, the locus of maximum SST in the Pacific Ocean shifts eastward, bringing more precipitation over the central and eastern Pacific Ocean. During these periods the eastern Indian Ocean, Indonesia, and south Asia are in the subsiding part of the Walker circulation that has shifted eastward from its climatological position (Webster et al., 1998). Clearly, there is a connection between the Asian monsoon and ENSO, but it is not possible to predict the strength of the monsoon solely from the phase of ENSO, as these monsoon–ENSO correlations have variable lag-lead times (Webster and Yang, 1992). With regard to monsoon–ENSO relationships, Torrence and Webster (1999) noted the demise of ENSO-based predictive relationships in the 1920–1960 period. During the 1997/98 El Niño events, the Indian rainfall remained essentially normal (Webster et al., 1998;

Torrence and Webster, 1999). Kumar et al. (1999) gives the evidence of weakening of the reverse monsoon-ENSO relationship in recent decades.

Years of heavy Indian summer monsoon rainfall tend to be followed by years of diminished rainfall. This well-known biennial periodicity of monsoon rainfall is extensively related to tropospheric biennial oscillation (TBO), which appears in a wide range of atmospheric variables including rainfall, surface pressure, wind, and SST of tropical regions (Meehl, 1987). Meehl (1997), Meehl and Arblaster (2001; 2002a) described an air–sea negative feedback mechanism in which warm spring SSTs in the Indian Ocean enhance atmospheric convection. The ensuing stronger monsoon leads to greater than average wind strength, increased Ekman transports and vertical mixing, and higher heat loss by evaporation throughout the summer monsoon season, which causes subsequent cooling of the ocean surface. The low ocean temperatures persist for one year until the next summer season. The lowered SSTs are associated with less convection than the previous spring, producing weakened winds, reduced heat loss by evaporation, and less mixing, which leads to higher SSTs than the year before. The cycle is thus repeated. Clearly a better understanding of the ocean–atmosphere and land–atmosphere feedbacks that may give rise to the TBO can improve predictions of monsoon strength.

Indian Ocean Dipole mode (Saji et al., 1999) is the coupled ocean-atmosphere interaction mode in Indian Ocean, which may induce unusual rainfall not only in surrounding areas, but other parts of the globe also (Saji and Yamagata, 2003). Positive IOD is characterized by anomalously cool SST in the southeast equatorial Indian Ocean off Sumatra due to unique coastal upwelling and anomalous warming in the west equatorial Indian Ocean. Cool water in the east Indian Ocean gives easterly anomalies along the equator. This conditions develop in the boreal summer season and peak in boreal autumn season. The reverse situation is the negative Indian Ocean dipole mode.

An index to quantify the IOD has been defined (Saji et al., 1999) as the SST difference between the tropical western Indian Ocean ( $50^{\circ}\text{E}$ - $70^{\circ}\text{E}$ ,  $10^{\circ}\text{S}$ - $10^{\circ}\text{N}$ ) and the tropical southeastern Indian Ocean ( $90^{\circ}\text{E}$ - $110^{\circ}\text{E}$ ,  $10^{\circ}\text{S}$ -equator). Ashok et al. (2001) using a 41

month sliding correlation of both IOD index and *Nino3* SST with ISMR showed that correlations have decadal variations and in decades when IOD-ISMIR correlation is strong *nino3*-ISMIR correlation is weak and vice versa. The presence of a positive IOD has facilitated normal or excess rainfall over the Indian region during the summers, despite the simultaneous occurrence of the negative phase of the Southern Oscillation by bringing IOD induced convergence over Indian Ocean replacing the ENSO induced divergence there (Behera et al., 1999; Webster et al., 1999). On the other hand, during some years the prevailing negative IOD and El Niño have combinedly caused an anomalously deficit rainfall during the monsoon season. The ISMR anomalies also depend on the relative intensities of the IOD and the El Niño/La Niña events.

The period of ENSO is estimated to be of 3-7 years. So these unusually long period episodes may weaken the biennial signal (Reason et al., 2000). But there is enough evidence for the biennial tendency of the ENSO episodes (Kiladis and Van Loon, 1988; Kiladis and Dias, 1989; Rasmusson et al., 1990). Thus the definition of TBO years will include some of the ENSO onset years also. In addition, there are other years, including many Indian Ocean dipole (or zonal mode) events, that contribute to biennial transitions. Ropelewski et al. (1992) related the TBO to the southern oscillation. Meehl and Arblaster (2001, 2002a) projected Pacific Ocean SST as the major contributor for TBO mechanism. Based on modeling studies, Chang and Li (2000), Li et al. (2001), suggested that Indian Ocean alone can produce TBO transition for monsoon, but the TBO amplitude will be weaker. By including Pacific in the model the anomalies become more pronounced. Meehl et al. (2003) showed that with and without ENSO onset years, TBO cycle has only difference in the magnitude of anomalies. According to him there exist some other remote mechanisms like ENSO, which can contribute to biennial variability. Thus earlier studies have the opinion that with and without ENSO years there may be only a difference in magnitude of the observed anomalies in TBO composites. In fact TBO and ENSO signal strength is closer in magnitude in Indian Ocean than in Pacific (Reason et al., 2000). Almost all the previous studies explain the TBO cycle on the basis of ENSO biennial cycle. Yu et al. (2003) argued that Pacific Ocean SST anomaly is more important in in-phase Indian to Australian monsoon

transition, while Indian Ocean plays a dominant role in out of phase transition from Australian to Indian summer monsoon. Wu and Kirtman (2004) with the help of coupled GCM produced biennial cycle for wet minus dry years accompanied by ENSO years. They are of the opinion that there is biennial cycle that are not associated with ENSO, during which other factors like Indian Ocean SST anomaly may play a role and that should be studied separately. A power spectrum of the monthly Dipole Mode Index shows significant peaks in the 2–3-year range, and smaller peaks in the 3–5 year range.

Moreover according to Loschinger et al. (2003) ocean dynamics in the Indian Ocean is associated with springtime transitions as well as SST anomalies in the equatorial regions. Thus ocean dynamics which are associated with extremes of IOD is natural parts of TBO evolution. Large-scale meridional heat transport in the Indian Ocean modulates the north Indian Ocean SST on seasonal time scales and may be involved in interannual variability of Asian monsoon by affecting the heat content and SST anomalies as part of biennial cycle of SST modulation. Loschinger et al. (2003) hypothesized that Indian Ocean Dipole Zonal Mode and TBO as integral parts of self regulating systems of monsoons that are acted as negative feedbacks to keep the variability of monsoon both on annual and interannual scales. Thus TBO includes both ENSO and IOD years. But how these dynamic features of Pacific and Indian Ocean regulate TBO and interannual variability of Indian summer monsoon is not fully understood.

## **4.2 Objectives of the study**

Almost all the earlier studies were looking at the biennial oscillation of Indian summer monsoon on the basis of its interaction with the Pacific by ENSO. The Indian and Pacific Ocean processes are found to influence TBO and interannual variability of Indian summer monsoon. The present study analyses the modification of biennial cycle of Indian summer monsoon with ENSO and IOD, those represents the dynamic processes in the Pacific Ocean and Indian Ocean respectively.

### 4.3 Data and methodology

The present study uses zonal and meridional wind, 200 hPa velocity potential and vertical velocity obtained from National Center for Environmental Prediction /National Center for Atmospheric Research (NCEP/NCAR) reanalysis (Kalnay et al., 1996) for the period 1950-2005. NOAA outgoing longwave radiation (OLR) data set for the period 1974-2005 with a one year data gap at 1978 is used for studying the movement of atmospheric convection zones. Sea surface temperature for the study period is also obtained from NCEP. ISMR index, which is the area averaged June to September rainfall of 306 stations well distributed over India, (Parthasarathy et al., 1994) and updated for making it to period 1950-2005 is used to represent the strength of Indian summer monsoon in particular years.

By using ISMR value, we defined years as strong (weak) TBO year, if it has more (less) ISMR anomaly than the previous and following year. ENSO years are then identified from area averaged SST anomalies of *nino3.4* region ( $5^{\circ}\text{N}$ - $5^{\circ}\text{S}$ ,  $170^{\circ}$ - $120^{\circ}\text{W}$ ), whose five month running mean should be at least  $\pm 0.5^{\circ}\text{C}$  for two consecutive seasons after March- April- May season over the following one year period. In order to assess the effect of ENSO in interannual variability of Indian summer monsoon, TBO years are analysed separately for those associated with TBO (ENSO-TBO) and independent of TBO (normal TBO). Similarly the SST, wind and circulation features of TBO years in presence of IOD are also analysed. The analyses were carried out from present strong monsoon (JJA0), following autumn (SON0), winter (DJF0), and spring (MAM1) and next monsoon (JJA1).

### 4.4 Results

The ENSO-TBO years and IOD-TBO years are studied separately to investigate the role of ENSO and IOD on TBO. The years in which IOD and ENSO co-occurs are also analyzed here.

#### 4.4.1 Effect of ENSO on TBO

In order to investigate the effect of ENSO on TBO composite analysis of strong minus weak TBO years compared for TBO years both in presence and absence of ENSO. As

all the ENSO years are not TBO years, first the peculiarities of ENSO years are compared for all ENSO years using SST anomalies of *Nino3.4* region.

**4.4.1.1 Evolution of ENSO anomalies in the Pacific**

From the above method of defining TBO years we have 35 TBO years in the 56 year study period. In this 14 are associated with ENSO in the Pacific. Thus all the ENSO years are not TBO years. In order to investigate the peculiarities of ENSO years, which are TBO years we have made analysis of SST anomaly formation of ENSO years of 1950-2005 period in figure 4.1

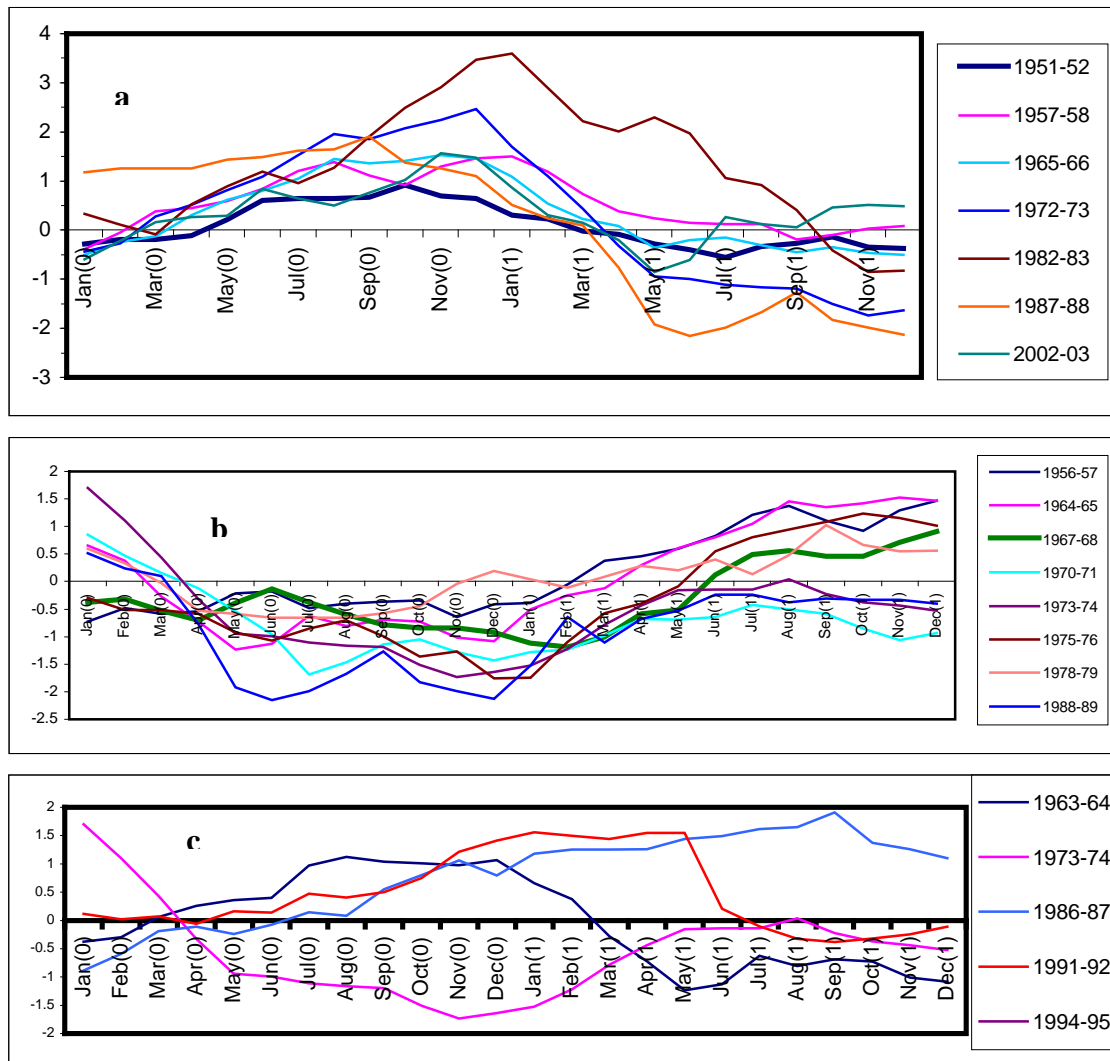


Figure 4.1: Time series of Nino3.4 region SST anomalies for years (a) TBO years associated with El Niña , (b) associated with La Niña and (c) ENSO years independent of TBO.

In the analysis onset time of ENSO is defined as the month in which the anomaly of the region is above  $\pm 0.5^{\circ}\text{C}$ . In the ENSO-TBO years the onset of ENSO (both El Nino and La Nina) is in any of the month (April or May) before the onset of Indian summer monsoon in June (figure 4.1 a and b). In other ENSO years the onset is at the time of onset of summer monsoon or later (see figure 4.1c). In all ENSO years the SST anomaly attains maximum by the next winter. The spring season is most important for the TBO associated with Indian summer monsoon. Thus onset of the ENSO must be in the spring season to influence the interannual variability of Indian summer monsoon through TBO mechanism.

#### **4.4.1.2 TBO mechanism in presence and absence of ENSO**

Strong minus weak composite of various oceans –atmosphere parameters for ENSO-TBO and normal TBO years are carried out from JJA0 to JJA1 and the results are presented in the form of comparison.

##### **4.4.1.2.1 SST pattern**

Figure 4.2 shows the TBO anomalies from JJA0 to JJA1 for ENSO-TBO (left panels) and normal TBO years (right panel). During the strong summer monsoon season (JJA0) entire north Indian Ocean is cooled in ENSO TBO years along with equatorial east and central Pacific and western Pacific is warm. But in the absence of ENSO, monsoon cooling is confined to Arabian Sea, Bay of Bengal and equatorial east Indian Ocean. In Pacific Ocean anomalies are reverse in absence of ENSO with cool west Pacific and warm east Pacific. In the post monsoon season (SON0), anomalies strengthens in both the cases.

By the boreal winter (DJF0) entire Indian Ocean is cooled and cooling from equatorial east Pacific reaches extreme west if TBO is associated with ENSO in the Pacific. But in the absence of ENSO, cooling in the north Indian Ocean decreases and confines to west side only and warming in the east Pacific reaches extreme west. Cooling continues to next spring (MAM1) in the Indian Ocean and extreme east Pacific starts warming in presence of ENSO, while entire east and central Indian Ocean is warm in normal TBO

years and equatorial west Pacific and extreme east Pacific starts cooling. Indian Ocean remains cool for next year summer (JJA1) of TBO year in presence of ENSO and warming in the east Pacific extends west. In the absence of ENSO the north and southeast Indian Ocean is warm and cooling from the east Pacific extends to central Pacific.

Thus the evolution and movement of TBO anomalies are different in both these cases. In TBO scale, Pacific Ocean anomalies are opposite in both the cases and the effect of monsoon cooling is confined to oceanic regions close to land region and upto winter only. The ENSO-TBO pattern resembles all TBO cases

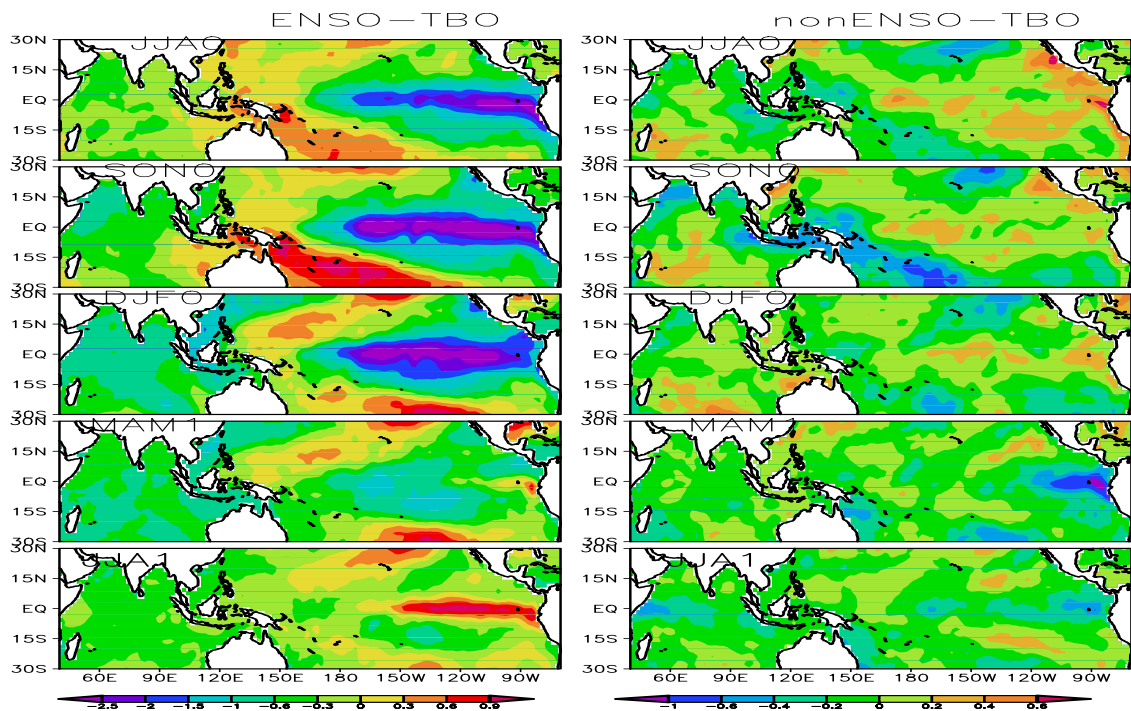


Figure 4.2: Strong minus weak TBO year composite of SST for seasons from JJA0 to JJA1. Left panel for TBO years, which are ENSO onset years also and right panel for non-ENSO TBO years

#### 4.4.1.2.2 850 hPa wind pattern

The strong minus weak composite of 850 hPa wind for ENSO-TBO and normal TBO for the present summer (JJA0), following winter (DJF0) and next summer (JJA1) is given in figure 4.3. During JJA0 westerlies in the north Indian Ocean are stronger in the absence of ENSO. In these case the westerlies doesn't extend to north of Australia



during boreal winter. Thus southeast movement of anomalies is absent in non-ENSO TBO years. But by next summer wetsrelies reverse to easterlies in north Indian Ocean and Indian subcontinent.

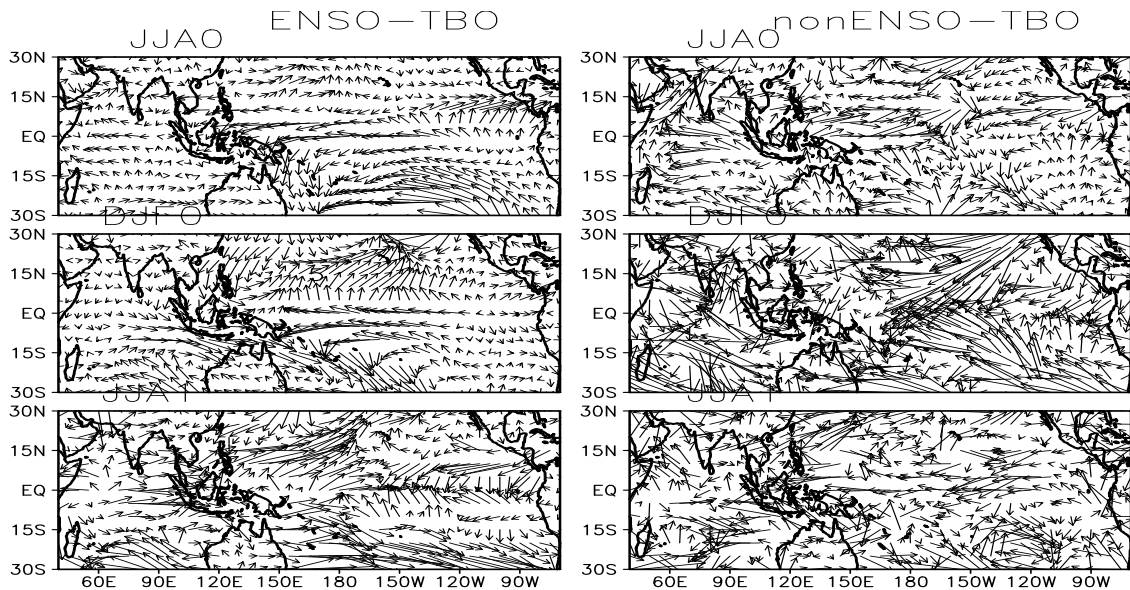


Figure 4.3: strong minus weak TBO year composite of wind at 850 hPa for TBO year summer (JJA0), coming winter (DJF0) and next year summer (JJA1).

#### 4.4.1.2.3 Sea level pressure (SLP) pattern

Figure 4.4 illustrates the TBO cycle of SLP in presence and absence of ENSO from JJA0 to JJA1. During the summer season of strong TBO year (JJA0), SLP is low over India and entire Indian Ocean extending to Indonesia and Australia in the presence of ENSO. In normal TBO years SLP lowers in these regions, but the low pressure center is northwest of India. By the boreal winter (DJF0) the minimum SLP anomaly moves to Australia and northwest Pacific making Indian to Australian monsoon transition in ENSO-TBO years. In the absence of ENSO, the low pressure region is in the western Indian Ocean and northwest Pacific Ocean and SLP is high over Australian monsoon region. By the next year summer (JJA1) SLP is high over India and western Indian Ocean and is low in the east Pacific in the presence of ENSO. But in the absence of ENSO SLP remains low over India and western Indian Ocean in JJA1.

Thus the transition and reversal of SLP anomalies are possible in presence of ENSO only for TBO years

#### ***4.4.1.2.4. 200 hPa velocity potential and convergence***

200 hPa velocity potential and convergence pattern for seasons from JJA0 to JJA1 is shown in figure 4.5. Negative anomaly of velocity potential in the upper level is associated with convergence and upward motion in the lower levels.

Upper level divergence is over India and west Indian Ocean in JJA0 indicating upward motion over Indian monsoon region and downward motion over east Pacific when ENSO is present along with TBO. In normal TBO years, the upward motion center in the equatorial Pacific over dateline is stronger than that over the Indian monsoon region. Downward motion is over the extreme east Pacific and equatorial east Indian Ocean. In the post monsoon season (SON0) upward motion zone moves to Indonesian region and downward motion center is over the equatorial east Pacific for ENSO-TBO years. The southeast movement of anomalies are absent for TBO in the absence of ENSO onset years and convergence/divergence centers remains as such in the post monsoon. The convergence center extends to northwest Pacific from Australian monsoon region making Australian monsoon strong in DJF0 for ENSO-TBO composites. But absence of ENSO brings divergence over Australia, making in phase Indian to Australian monsoon transition weak in the absence of ENSO.

By the next spring (MAM1) convergence zone moves further east in Pacific and divergence appears over equatorial Indian Ocean for ENSO-TBO years. In the absence of ENSO convergence is over African region and divergence is over extreme east Pacific. During the next summer monsoon (JJA1) convergence associated with TBO-ENSO is in the east Pacific and divergence is in the western Indian Ocean. If ENSO years are removed, pattern remains as MAM1 with convergence in the African region and divergence in the east Pacific.

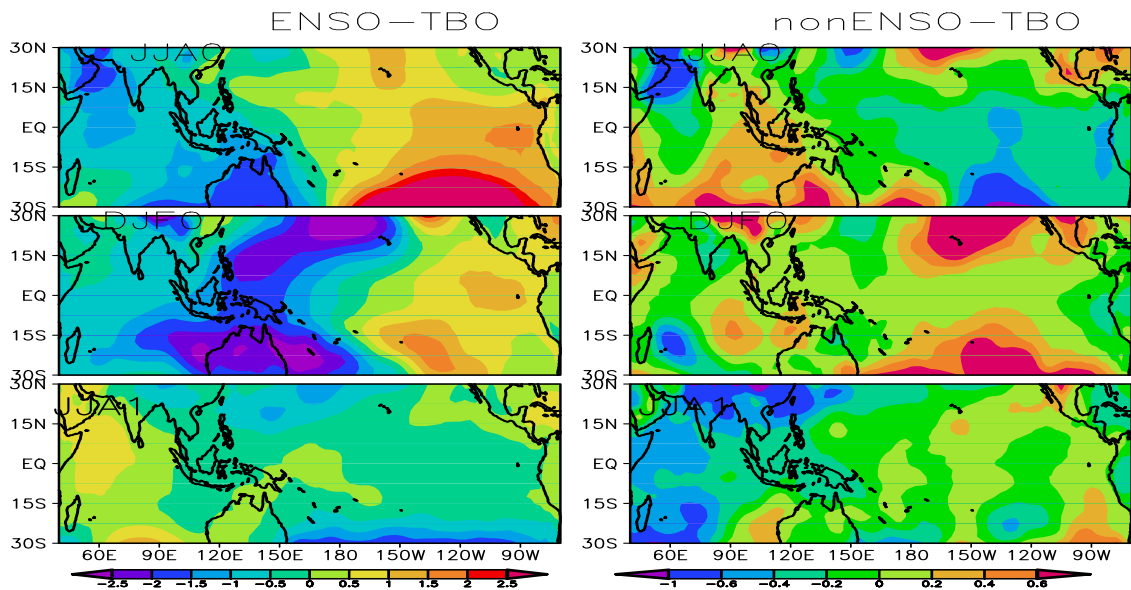


Figure 4.4: Strong minus weak TBO year composite of SLP for seasons from JJA0 to JJA1. Left panel for TBO years, which are ENSO onset years also and right panel for non-ENSO TBO years

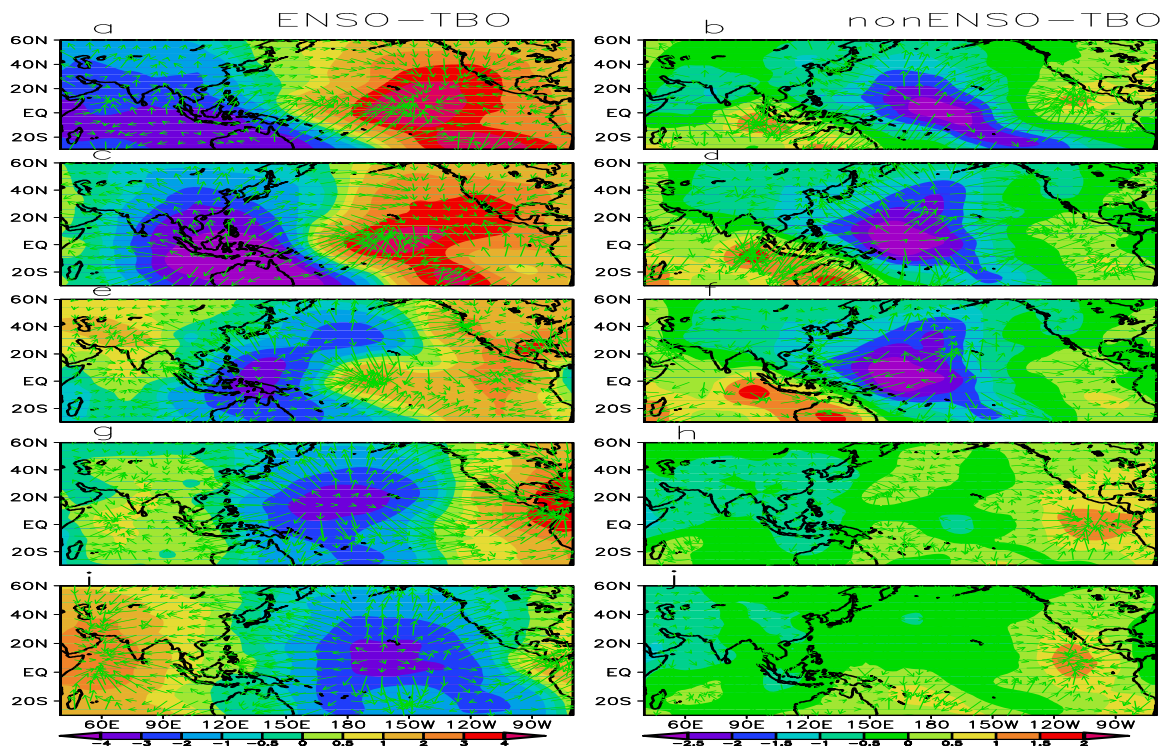


Figure 4.5: Strong minus weak TBO year composite of 200 hPa velocity potential (shaded) and convergence(vector) for seasons from JJA0 to JJA1. Left panel for TBO years, which are ENSO onset years also and right panel for non-ENSO TBO years

#### 4.4.1.2.5 Convection anomalies and its propagation

Figure 4.6 shows the Hovmuller diagram showing the movement of north Indian Ocean OLR anomalies in TBO cycle. During ENSO only TBO years, convection starts in the western Indian Ocean by the beginning of strong TBO year and strengthens by onset of monsoon in June. The convection anomalies propagates eastward and by the next year weak monsoon the convection reaches close to dateline and convection is absent in the Indian Ocean region. Thus the TBO cycle is completed and convection moves from Indian region to central Pacific from strong TBO to weak TBO year. But in the absence of ENSO, convection starts in the extreme west Indian Ocean by onset of strong monsoon and it also moves east and by next year summer it is at 120°E, ie., in the Indian Ocean region itself. Thus in both the presence and absence of ENSO, convection anomalies associated with Indian monsoon reverses, but its movement from one TBO to next year is different in both the cases

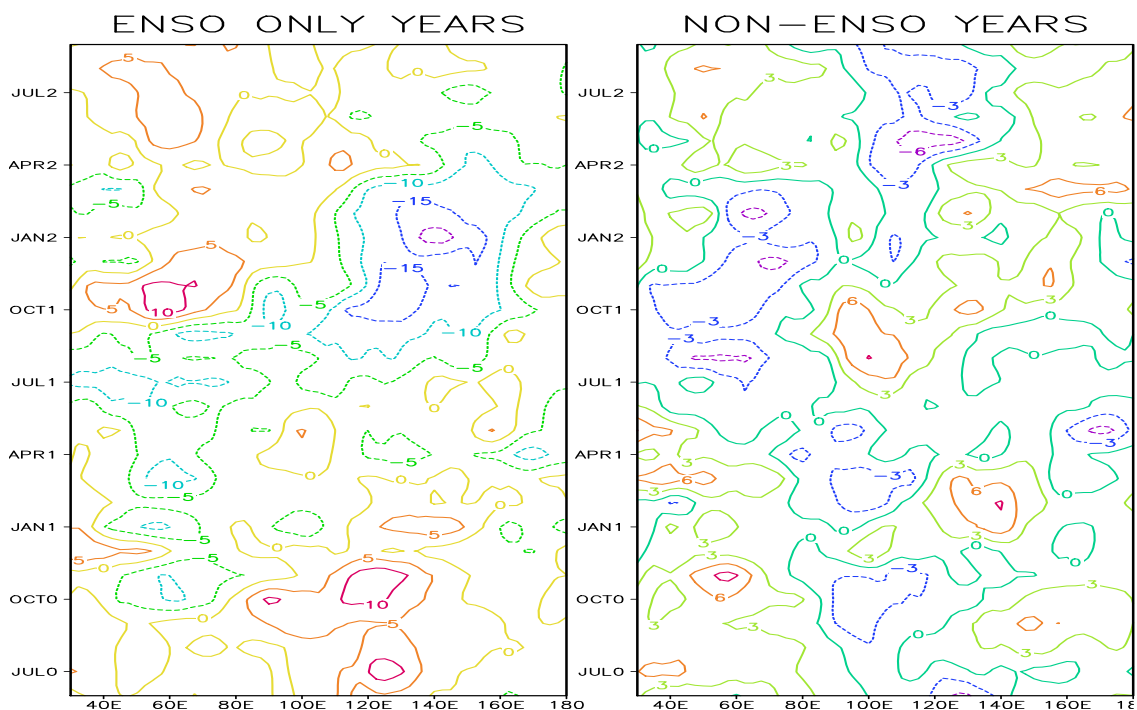


Figure 4.6: Time- longitude diagram for strong-minus weak TBO year composite of OLR in the north Indian Ocean (equator to 25°N) for ENSO-TBO (left) and non ENSO TBO (right) years, Months with zero indicates previous year, 1 current TBO year and 2 next year for both strong and weak TBO years

#### 4.4.1.2.6 Effect of ENSO on summer season atmospheric circulation cells

The summer season equatorial ( $10^{\circ}\text{S}$ - $10^{\circ}\text{N}$ ) zonal circulation for TBO year and year after the TBO is shown in figure 4.7. Equatorial Walker circulation has upward motion anomalies in the Indian Ocean and west Pacific in the positive phase of TBO associated with strong Indian summer monsoon (JJA0) in the presence of ENSO in the Pacific Ocean. In the absence of ENSO equatorial region over Indian Ocean has downward motion and upward motion at dateline and downward motion is seen in the extreme east Pacific.

During the next summer season (JJA1) ENSO-TBO years has downward motion in the western Indian Ocean and west Pacific and downward motion in the eastern Indian Ocean and east Pacific. But in the absence of ENSO, Indian region between  $60^{\circ}\text{E}$  and  $100^{\circ}\text{E}$  has upward motion anomalies and downward motion in the western and central Pacific (lower panels of figure 4.7). Thus the upward motion in the equatorial Indian Ocean in strong phase of TBO is the effect of ENSO.

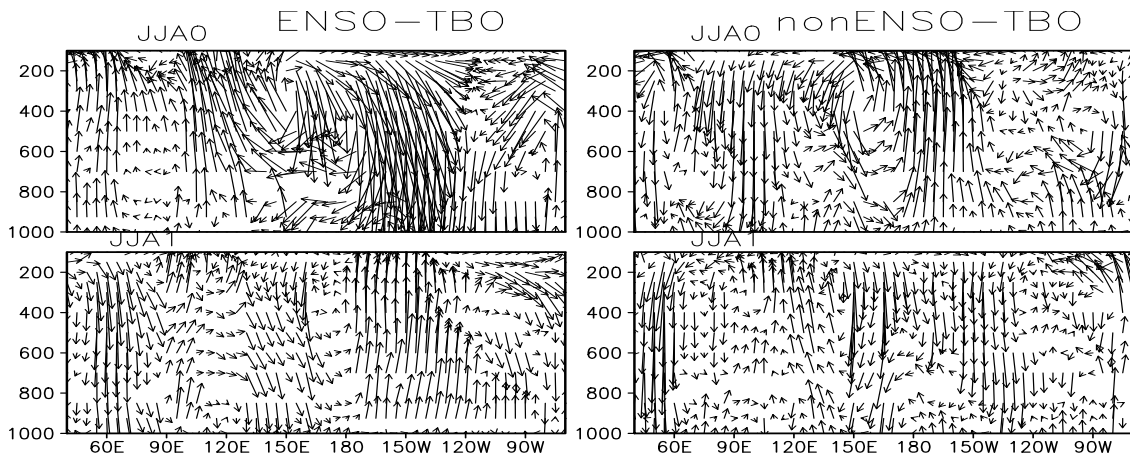


Figure 4.7: height-longitude profile of zonal wind and negative of vertical velocity averaged over  $10^{\circ}\text{S}$ - $10^{\circ}\text{N}$  for JJA0 and JJA1, indicating equatorial zonal circulation.

Local Hadley circulation over monsoon region ( $60^{\circ}$ - $95^{\circ}\text{E}$ ) for three monsoon seasons, JJA-1, JJA0 and JJA1 is illustrated in figure 4.8 from the vertical profile of meridional wind and vertical velocity. The Local Hadley circulation over the Indian monsoon longitudes has upward motion in the tropics between  $5^{\circ}\text{S}$  and  $30^{\circ}\text{N}$  and downward

motion south of  $5^{\circ}\text{S}$  in presence of ENSO for strong TBO year. In the absence of ENSO in the Pacific, downward motion exists between  $5^{\circ}\text{S}$  and  $10^{\circ}\text{N}$  and upward movement is observed from  $10^{\circ}\text{N}$  to  $40^{\circ}\text{N}$ . In the preceding year summer anomalies reverses in both the cases with downward motion from  $5^{\circ}\text{S}$  to  $30^{\circ}\text{N}$  in presence of ENSO and upward motion close to equator and downward motion in the region between  $10^{\circ}\text{N}$  and  $40^{\circ}\text{N}$  in absence of ENSO.

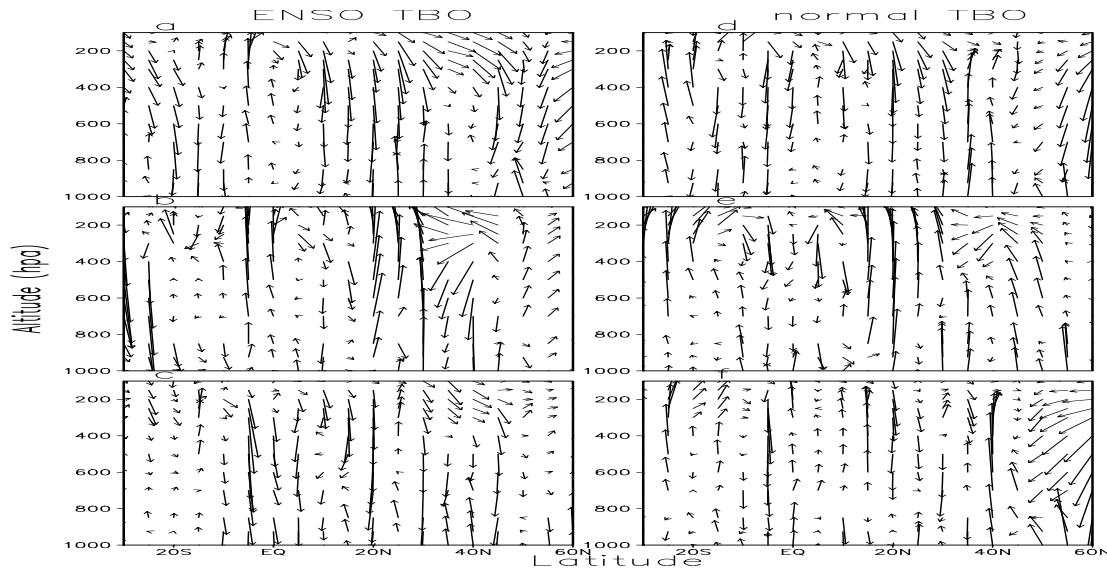


Figure 4.8: height-longitude profile of meridional wind and negative of vertical velocity averaged over  $60^{\circ}\text{-}95^{\circ}\text{E}$ , indicating local Hadley circulation for three consecutive summer seasons. Left panel for ENSO-TBO years and (a), (b) and (c) for JJA-1, JJA0 and JJA1 and (d), (e) and (f) are their counter parts in the absence of ENSO

Thus the local Hadley circulation between the equatorial Indian Ocean and Indian monsoon region plays a role in TBO in the absence of ENSO. When ENSO is present, it brings additional upward/downward motion in the equatorial Indian Ocean and that over the monsoon region is similar in both the situations.

#### 4.4.2 Role of IOD in TBO

In the 56 year period from 1950-2005 we have 10 positive dipole years and 9 negative dipole years. But in the 10 positive dipole years, four of them (1961, 1967, 1994, 1997) are associated with strong TBO years and another three (1972, 1982, 2002) are associated with weak TBO and 1963, 1986 and 1991 are independent of TBO. Similarly for negative IOD also we have 1960, 1974, 1992 are associated with negative TBO and

1956, 1975 and 1988 are associated with strong TBO years and 1971, 1984 and 1996 are detached from TBO. Thus the interaction of TBO and IOD are two-fold. IOD years are associated with both ENSO and non ENSO TBO years. In presence of ENSO, both TBO and IOD are in opposite phase and in absence of ENSO IOD and TBO are in same phase.

#### ***4.4.2.1 In- phase and out of phase association of TBO and IOD***

As the influence of IOD is two fold in TBO, TBO cycle is analysed separately for strong minus weak TBO composites, in which strong (weak) TBO is associated with strong (weak) IOD and strong (weak) TBO is associated with weak (strong) IOD years. The later case is associated with La Niña/El Niño years also. The results are presented in the form of comparison of these two cases for individual season from the TBO year summer to next year summer for SST, wind and 200 hPa vertical velocity.

During the monsoon season when TBO and IOD are strong, monsoon cooling confines to ocean region close to India and Indonesia and other regions are warm along with east Pacific. Upward motion is over east Pacific and west Indian Ocean regions. Westerlies in the north Indian Ocean extends to equatorial Pacific and easterlies are strong in the equatorial Indian Ocean (see left panels in figure 4.9). During the summer monsoon season when strong TBO is associated with weak IOD, entire Indian Ocean SST is cool and convergence is over India and Indian Ocean regions. Westerlies are strong in the north Indian Ocean and easterlies are present in the south Indian Ocean and maximum easterlies are over the equatorial Pacific (right panel of figure 4. 9).

After the strong monsoon, cooling in north Indian Ocean decreases and convergence in the western Indian Ocean moves to southwest Indian Ocean when both TBO and IOD are in same phase as seen in figure 4.10. Easterlies are strong in the equatorial east Indian Ocean and westerly maximum moves to east Pacific. Entire Indian Ocean and east and central Pacific regions are warm and convergence is over Indonesia in the TBO years with IOD and ENSO. Westerly maximum moves southeast and easterlies in the central and east Pacific

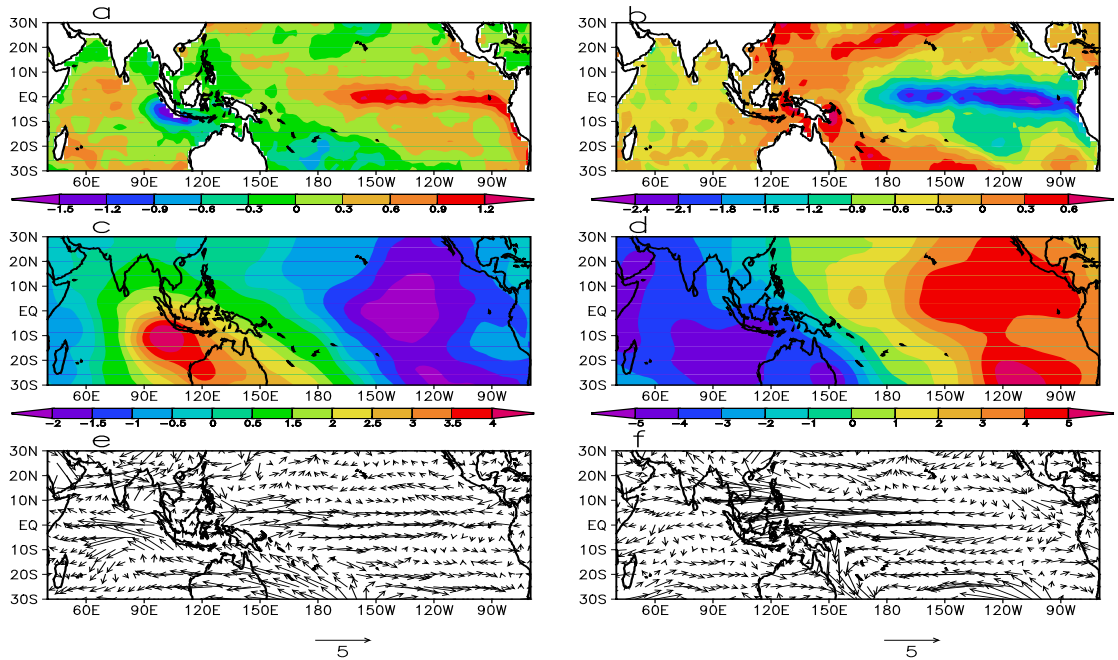


Figure 4.9: JJA0 strong-weak anomalies for TBO cycle in presence of IOD. Left side of figure for in phase IOD and TBO (a) SST, (c) 200 hPa velocity potential (e) 850 hPa wind and right panel for out of phase relationship of same parameters

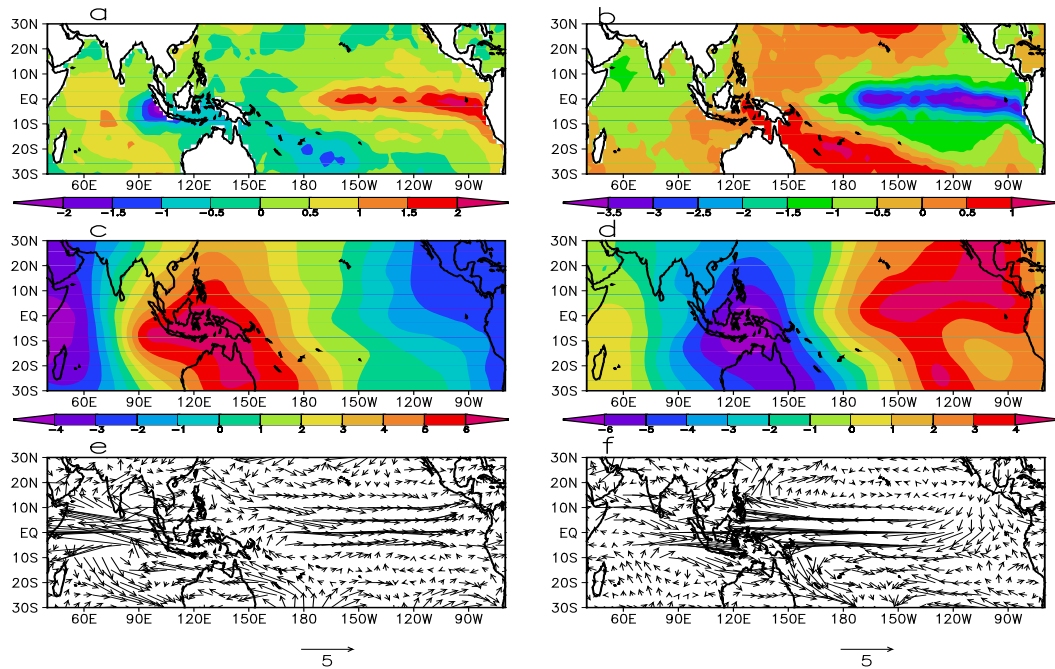


Figure 4.10: SON0 strong-weak anomalies for TBO cycle in presence of IOD. Left side of figure for in phase IOD and TBO (a) SST, (c) 200 hPa velocity potential (e) 850 hPa wind and right panel for out of phase relationship of same parameters



The in-phase and out-of phase association of TBO and IOD for the boreal winter season DJF0 is shown in figure 4.11. During the boreal winter following the strong monsoon (DJF0), Indian and Pacific Oceans are warm and convergence is over southwest Indian Ocean in the inphase transition of both TBO and IOD. Easterlies remains in the southeast Indian Ocean and north of Australia and westerlies are in the extreme east Pacific (figure 4.11, left panels). Entire Indian Ocean is cool along with equatorial Pacific and convergence is over Australia and west Pacific in the boreal winter after strong monsoon when TBO and IOD are in opposite phase (figure 4.11b). Westerly anomalies reach north of Australia and easterlies are in the eastern Indian Ocean.

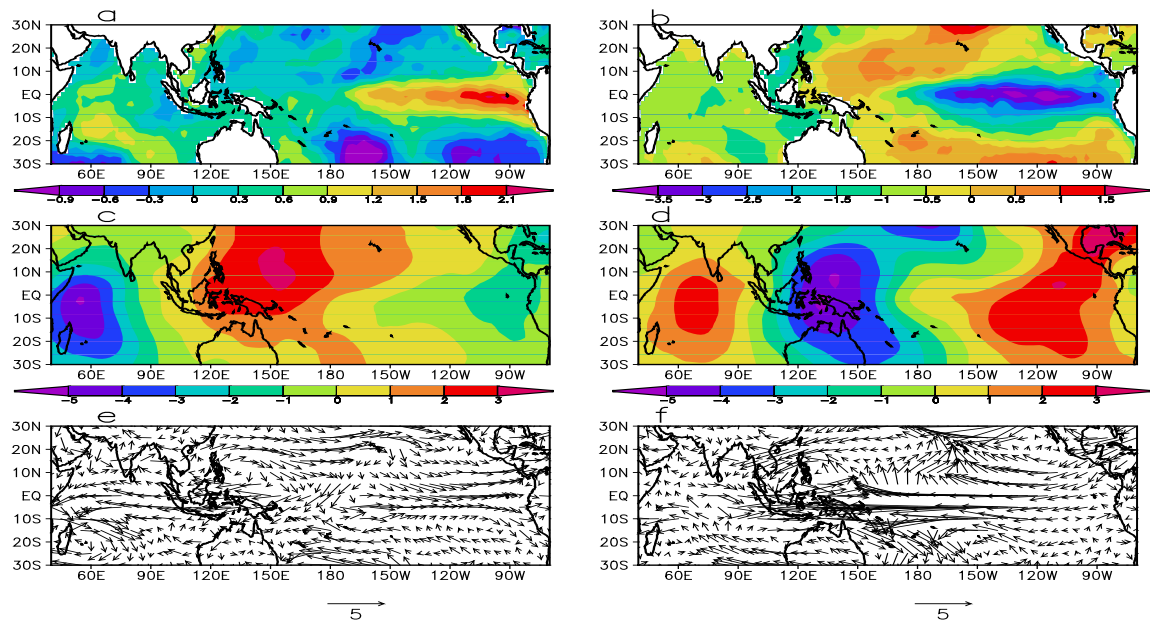


Figure 4.11: DJF0 strong-weak anomalies for TBO cycle in presence of IOD. Left side of figure for in phase IOD and TBO (a) SST, (c) 200 hPa velocity potential (e) 850 hPa wind and right panel for out of phase relationship of same parameters

In the next year spring season (MAM1), when TBO and IOD are in same phase, Indian Ocean is warm along with equatorial Pacific and convergence is at extreme southeast Pacific. Easterlies are seen over equatorial Indian Ocean and west Pacific (see figure 4.12, left panels). In opposite phase TBO and IOD, cooling continue in both the Indian and Pacific Oceans and convergence moves to north central Pacific. Westerlies also

move to west Pacific shifting easterlies further east and easterlies are seen over Indian subcontinent (figure 4.12, right panels).

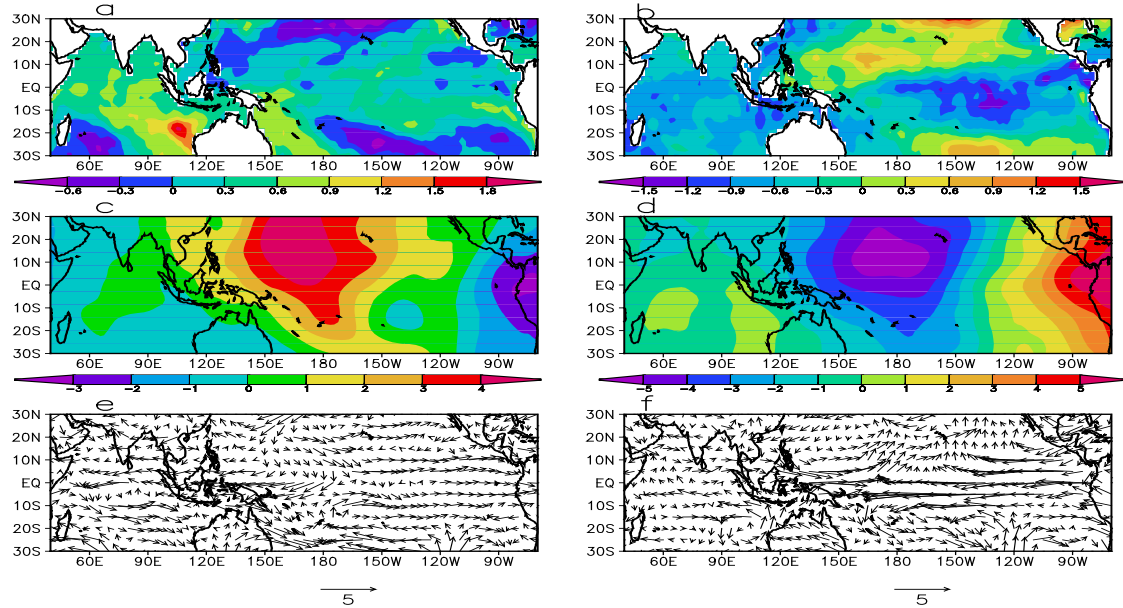


Figure 4.12: MAM1 strong-weak anomalies for TBO cycle in presence of IOD. Left side of figure for in phase IOD and TBO a) SST, c) 200 hPa velocity potential e) 850 hPa wind and right panel for out of phase relationship of same parameters

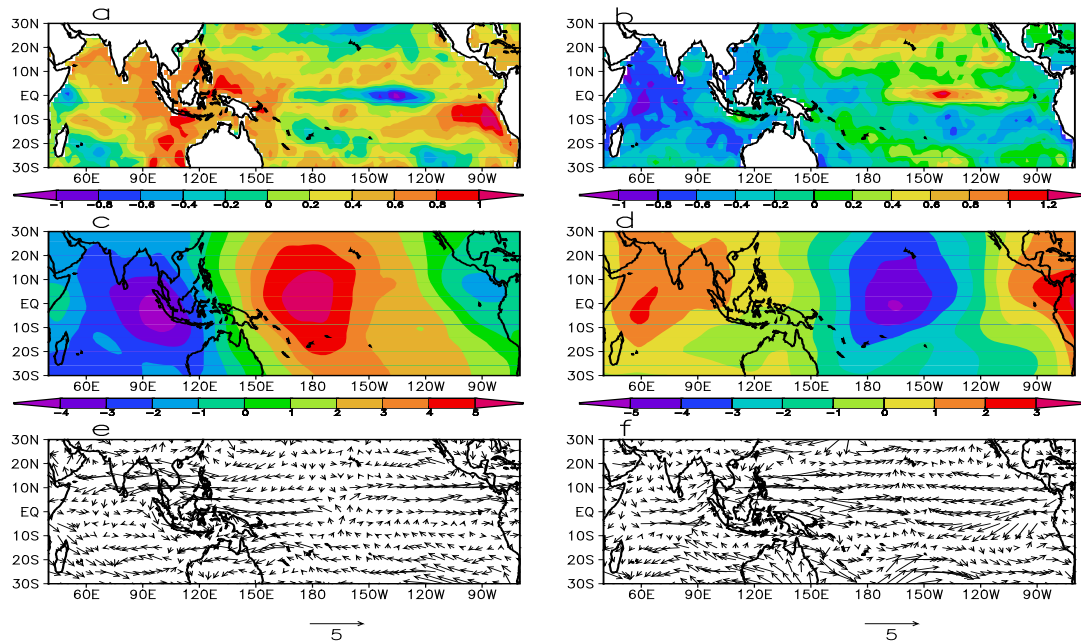


Figure 4.13: JJA1 strong-weak anomalies for TBO cycle in presence of IOD. Left side of figure for in phase IOD and TBO (a) SST, (c) 200 hPa velocity potential (e) 850 hPa wind and right panel for out of phase relationship of same parameters

In the next year monsoon of in phase TBO and IOD, Indian Ocean is warm along with west Pacific and east Pacific and convergence is over equatorial east Indian Ocean (figure 4.13 a and c). Easterlies are seen over India and in the west Pacific Ocean. In out of phase JJA1 season, Indian Ocean is still cool and east Pacific is warm and convergence is over central Pacific in presence of both IOD and ENSO. Westerlies are seen in the equatorial Indian Ocean and west Pacific.

Thus the cyclic evolution and movement of TBO scale anomalies are different according to the phase of IOD. When IOD and TBO is in same phase ENSO is also absent and in reverse association, ENSO is absent. Pacific Ocean SST and Walker circulation anomalies are opposite in both the cases, while lower level wind and SST in the north Indian Ocean has slight changes only.

#### **4.4.3 TBO cycle in the absence of both ENSO and IOD (pure TBO years)**

In this section the possibility of TBO cycle in the absence of both these Indian Ocean and Pacific Ocean phenomena are investigated for SST, velocity potential and wind for JJA0 to JJA1 with the same method used for above analysis and is presented in figure 4.14 and 4.15.

Along with the onset of strong monsoon Indian Ocean cools close to land and southeast region. Westerlies strengthen over western Indian Ocean and India and easterlies are in the equatorial Indian Ocean. Convergent anomalies are seen over India with center in the northwest Pacific and divergence is over southeast Indian Ocean and northeast Pacific. Central and southwestern Indian Ocean is still warm in the SON0 and warm center in the east Pacific moves to central region. Westerly maximum moves to northwest Pacific and southeast Indian Ocean and convergence is in the northwest Indian Ocean. Entire Indian Ocean is not cooled in the preceding winter. Westerly maximum is over the Australian region, though weak westerlies are seen in western Indian Ocean. But downward motion is seen over the north of Australia. East Pacific also cool in the MAM1 season along with the north Indian Ocean. South Indian Ocean has westerly anomalies and north equatorial region has easterly anomalies and

equatorial Indian Ocean is convergent. North Indian Ocean is cool in the next monsoon season and easterlies are strong in the north Indian Ocean and upward motion center is over southeast Pacific, though Indian region is convergent.

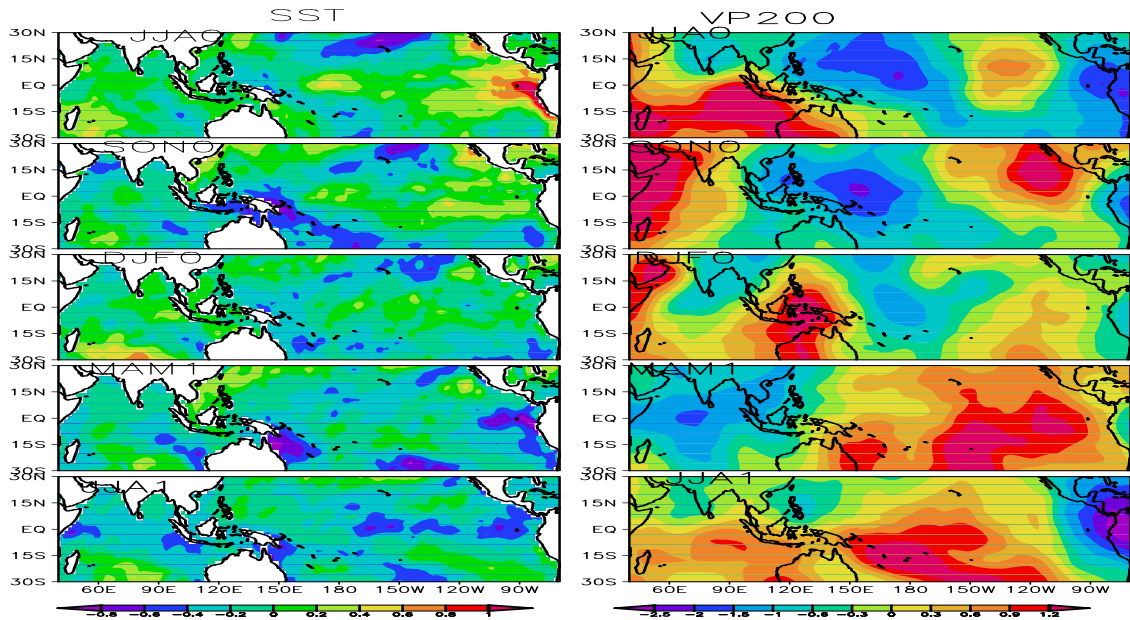


Figure 4.14: strong minus weak composite of SST (left panel) and 200 hPa velocity potential (right panel) for pure TBO (both ENSO and IOD are absent) years

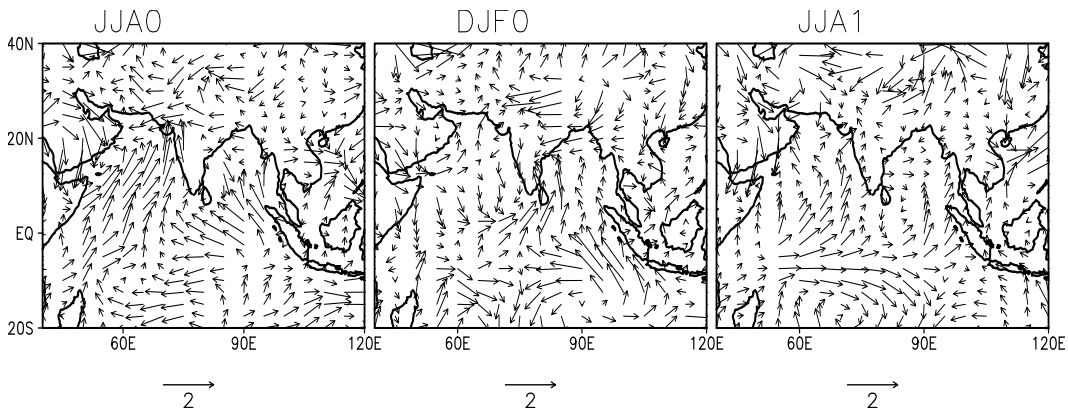


Figure 4.15: strong minus weak composite of 850 hPa wind over Indian Ocean region for pure TBO years

### 4.5 Discussion and summary

The present chapter identifies the difference in evolution of anomalies associated with TBO in presence of ENSO and IOD. ENSO years with spring onset only can affect the

interannual variability of Indian summer monsoon associated with TBO. The theory of TBO by Meehl and Arblaster (2002a) stresses the spring season processes give rise to monsoon transition in the next summer. The condition in Pacific during spring season affects TBO than the maximum anomaly of ENSO. Monsoon cooling will not distribute to the entire north Indian Ocean in absence of ENSO and its southeast movement to entire Indian Ocean by next winter is controlled by ENSO. Pacific Ocean SST anomalies are opposite in ENSO-TBO and normal TBO years and warms by weak TBO in absence of ENSO (Pillai and Mohankumar 2007). Southeast movement of westerly anomaly to Australian monsoon region from north Indian Ocean is controlled by ENSO. Biennial Oscillation of SLP over India and Indian Ocean in the interannual variability of monsoon is possible only with the presence of ENSO. Convergence and upward motion strengthens over equatorial Pacific close to dateline in summer and post monsoon season in the absence of ENSO and divergence appears over Australia in the winter season. Equatorial Walker circulation has downward (upward) motion in the equatorial Indian Ocean in strong (weak) monsoon season in the absence of ENSO. Local Hadley circulation between the Indian monsoon region and adjacent ocean is present in absence of ENSO only for strong/weak monsoon. Eastward movement of equatorial convection anomalies is limited to Indian Ocean region only in the absence of ENSO as illustrated in Pillai and Mohankumar 2007.

Thus local SST in the Indian Ocean close to Indian monsoon region, monsoon convection, and local Hadley circulation has biennial cycle in the absence of ENSO and forces interannual variability of Indian summer monsoon. At the same time large-scale features affecting Indian monsoon like Pacific Ocean SST anomalies, SLP, Walker circulation etc is modulated by ENSO making its biennial transition and in phase Indian to Australian monsoon transition. By Meehl et al (2003), Indian to Australian monsoon linkage is through large scale east-west circulation with eastern Walker cell links Indian and Australian monsoon to dynamics in the Pacific and western Walker cell connects Indian and Australian monsoon to dynamical processes in the Indian Ocean. Thus the convection movement from Asian to Australian monsoon connects Indo-Pacific Oceans. Similarly the persistence of anomalies in the Indian Ocean is not observed in the

absence of ENSO. Our present observation of TBO cycle for Indian Ocean SST and local processes supports Wu and Kirtman (2007) who through the modeling study produced TBO after suppression of Pacific Ocean. Thus the biennial cycle observed for Indian Ocean parameters can produce interannual variability of Indian summer monsoon in absence of ENSO. But many properties of TBO like in-phase Indian to Australian monsoon transition is not observed.

The interaction of IOD with TBO is twofold for interannual variability of Indian summer monsoon. In presence of El Nino (La Nina) in the Pacific, negative (positive) TBO is associated with positive (negative) IOD and in absence of El Nino/La Nina TBO and IOD are in same phase. The in-phase TBO and IOD SST anomalies look like non ENSO TBO composites discussed earlier in this chapter. The SST, convergence and wind anomalies of out of phase TBO-IOD composite looks like ENSO-TBO cases, indicating that in both these cases ENSO is the dominant factor. Walker circulation and Pacific Ocean SST anomalies are opposite in TBO-IOD in phase and out of phase association.

According to Ashok et al (2004), when a strong IOD is associated with El Nino, its influence on monsoon is reduced by both poles of IOD. An anomalous divergence is induced in east Indian Ocean and divergence over west Pacific and convergence over India by positive IOD. But in the case of monsoon variability governed by TBO, associated with positive (negative) IOD and El Nina (La Nina), SST pattern looks similar to TBO-ENSO composite, which include both IOD-ENSO and non-IOD ENSO years. Convergence/divergence pattern is also similar in JJA0 and SON0 of La Nina (El Nina) is associated with negative (positive) IOD in strong (weak) TBO years. But in DJF0, upper level convergence of equatorial Indian Ocean is strengthened in IOD only ENSO-TBO years and the upper level divergence in the west Pacific shifts northward in next two seasons.

The SST composite of IOD only TBO and non-ENSO TBO cases is comparable, though the anomaly is strong in the IOD only TBO cases. But the convergence/divergence pattern is different in both the cases. In IOD only TBO years convergence is in the east Pacific from JJA0 to MAM1 and is in the equatorial east Indian Ocean by JJA1. In IOD

only TBO case, only one Walker circulation cell with one convergent center and one divergent center is present. But in the case of non-ENSO TBO, the central Pacific always remains convergent and more than one pair of convergent/divergent centers is obtained. Thus in the case of IOD only TBO years, the convergence/divergence associated with IOD dominates the TBO and in when associated with ENSO, it dominates over IOD.

In the absence of both these dynamic processes in both the Indian and Pacific Ocean, SST and wind pattern has biennial cycle (pure TBO years). SST pattern of JJA0 to DJF0 resembles the TBO pattern in the absence of ENSO. But when IOD is present the warming of the Indian Ocean in the next phase starts in the MAM1 itself. But in pure dipole years Indian Ocean is cool in the MAM1 season and starts warm by JJA1 only. But convergent/divergent centers have no biennial cycle in absence of ENSO and IOD.

---

# Investigation of Common Mode of Variability in Boreal Summer Intraseasonal Oscillation and Tropospheric Biennial Oscillation

---

## 5.1 Introduction

The Asian summer monsoon is one of the most vigorous and energetic of all large-scale phenomena and influences global circulation during northern summer. Monsoon is developed as response to the gradients in large scale heating distribution arising from surface heating of Asian continent (Krishnamurthi and Ramanathan, 1982) and through atmosphere latent heating associated with convection over warm pool of west Pacific and Indonesia (Lau et al., 1988). Thus it is closely related to seasonal cycle. This annual monsoon has substantial variability on interannual time scale, which has a major role in life and economy of India and southeast Asia. Understanding of the dynamic forcing of interannual variability of Indian summer monsoon is central to success in seasonal and longer term prediction.

These dynamic forcing includes extensively studied inverse relationship with El Nino Southern Oscillation (Yasunri, 1990; Webster and Yang, 1992; Ju and Slingo, 1995). Biennial oscillation in monsoon rainfall is also a factor and is related to biennial oscillation found in various atmospheric and oceanic variables including precipitation, surface pressure, tropospheric winds and sea surface temperature, defined as tropospheric biennial oscillation (Meehl, 1997; Meehl and Arblalaster, 2002a; b). The effect of ENSO on monsoon interannual variability is discussed in detail by many investigators. It is also shown that the relationship has weakened reasonably (eg. Kumar



et al., 1999). The TBO is also studied in detail and major theories are given in chapter 1 and TBO cycle is explained in previous chapters also.

Another source for the intrannual variability of Asian monsoon strength is interannual changes in intraseasonal variability (Sperber et al., 2000). Monsoon exhibits strong intraseasonal variability, characterised by active/break cycles (eg: Gadgil and Asha, 1992) with dominant periods between 10-20 days and 30-60 days and affects monthly or seasonal means for a particular year. During monsoon season, there are two preferred locations of convection over Indian longitudes, one over continent and another over equatorial Indian Ocean (Sikka and Gadgil 1980). The transition of inter tropical convergence zone (ITCZ) from oceanic to the northward continent region has time scale of 30-60 day in some year. Krishnamurthi and Bhalme (1976) noted 10-20 day variability in various parameters describing monsoon during normal rainfall years and in cloudiness data over monsoon region by Yasunari (1979).

During the active phase of 30-60 day mode, convection is enhanced significantly over Indian subcontinent, extending to Bay of Bengal, maritime continent and to west Pacific. Convection suppressed in the equatorial Indian Ocean and plains of Indo-China extending to northwest tropical Pacific. In 10-20 day mode, convection is enhanced over Indian subcontinent and eastern equatorial Indian Ocean and convection is suppressed in the south Bay of Bengal and over land and ocean modulated simultaneously, spatial pattern of OLR is more regional and dominated by east-west structure and 15 day mode contribute to about 25% of intraseasonal oscillation. (Annamali and Slingo, 2001).

In 30-60 day mode, cross equatorial flow is increased at 850 hPa and western Indian Ocean turning into westerlies over Arabian Sea. In the upper level (200 hPa) anticyclone over north India extending to Pakistan with increased upper level northerlies turning to easterlies over northern and equatorial Indian Ocean. Thus enhanced lower and upper level flow strengthens local Hadley circulation. Strong upper level westerlies over Pacific shows strengthened east-west Walker circulation.

Eventhough the relationship between interannual variability and intraseasonal oscillation of monsoon is poorly understood; there is some evidence that intrannual variability of ISO activity may influence seasonal mean monsoon strength. Fennessy and Shukla (1994) showed that spatial structure of interannual variability and the interseasonal oscillation are quite similar. Ferranti et al., 1997 showed that monsoon fluctuations within a season and between different years have a common mode of variability with a bimodal meridional structure in precipitation. Palmer (1994) put forward the hypothesis that perturbations to subseasonal variability control the intrannual variability should correspond. Goswami et al. (1998) also observed spatial structure of ISO mode and that of dominant mode of interannual mode are similar.

But Annamali et al. (1999) showed that unlike early studies, there was no common dominant mode, which describes monsoon variability on interannual and intraseasonal time scales. But the boundary forcing like ENSO influence intraseasonal behavior of monsoon. Goswami and Ajayamohan (2000) suggested that ISO and interannual variability of monsoon have a common mode of spatial variability for low level winds and low-level vorticity.

## **5.2 Objective of the study**

ISO has a quasi-biennial periodicity in interannual time scale. TBO is the biennial scale oscillation of tropical atmosphere and ocean. The present study looks for the existence of common mode between ISO frequency and TBO scale frequency for convection and lower level wind associated with Indian summer monsoon.

## **5.3 Data and methodology**

The main data sets used for the study include daily and monthly data sets of NCEP/NCAR reanalysis (Kalnay et al, 1996) like 850 hPa zonal and meridional wind and NOAA OLR. The NCEP data sets are for the period 1960-2005 and OLR is from 1974-2005, with a data gap in the year 1975. Daily rainfall data from India meteorological department in  $1^{\circ} \times 1^{\circ}$  resolution over Indian region (Rajeevan et al., 2005) is also used. ISMR index (Parthasarathy et al., 1994) is used to identify strong

and weak TBO years. Wavelet analysis of daily summer monsoon rainfall averaged over Indian monsoon region is performed to understand the dominant periodicities in TBO years. After filtering the daily data sets into 10-20 day and 30-60 day frequencies, EOF analysis is carried out to investigate the dominant spatial patterns. EOF analysis of both TBO filtered and unfiltered June to September season is also carried out. Variance of prominent EOF patterns are calculated to understand the strength of ISO and TBO in each year and composite analysis of active minus break periods for daily data and strong minus weak TBO year composite for TBO years were also carried out.

## **5.4 Results**

### **5.4.1 Wavelet analysis of TBO years**

Strong and weak TBO years are selected from ISMR index, whose anomaly is greater (lesser) than previous and next year is defined as a strong (weak) TBO year. Wavelet analysis of daily rainfall over India during summer season is carried out and that for strong TBO years are shown in figure 5.1. The wavelet power spectrum of individual years shows dominant periodicities of different time scales. Most of the years have a low frequency and high frequency variations in the significant level. In the case of strong TBO years, which are associated with La Nina most of the years like 1964, 1967, 1970, 1973 etc have only one dominant frequency with peak at almost 40 day period. But year 1956 has 10-20 day and 30-60 day periodicity and 1975 and 1988 has periodicity at 30 and 60 day periods. But the strong TBO years in the absence of La Nina like 1951, 1959, 1978, 1980, 1991, 1994, 1997 has two periodicities one with peak around 20 day and other in 45 or 60 day periods. But the years like 1961 and 1983 has only one dominant peak at 35 day.

In the case of weak TBO years, almost all the years both in presence and absence of ENSO, has two periodicities one in between almost 15-25 days and other at 40-60 days (see figure 5.2). In some El Nino-TBO years like 1972, 1982 has only one significant peak at 50-60 day periods. Thus in the TBO years the low and high frequency variations are present. So the datasets need to be filtered into two frequencies one at 10-20 day and

30-60 day periodicities and these two periodicities need to be investigated for TBO years

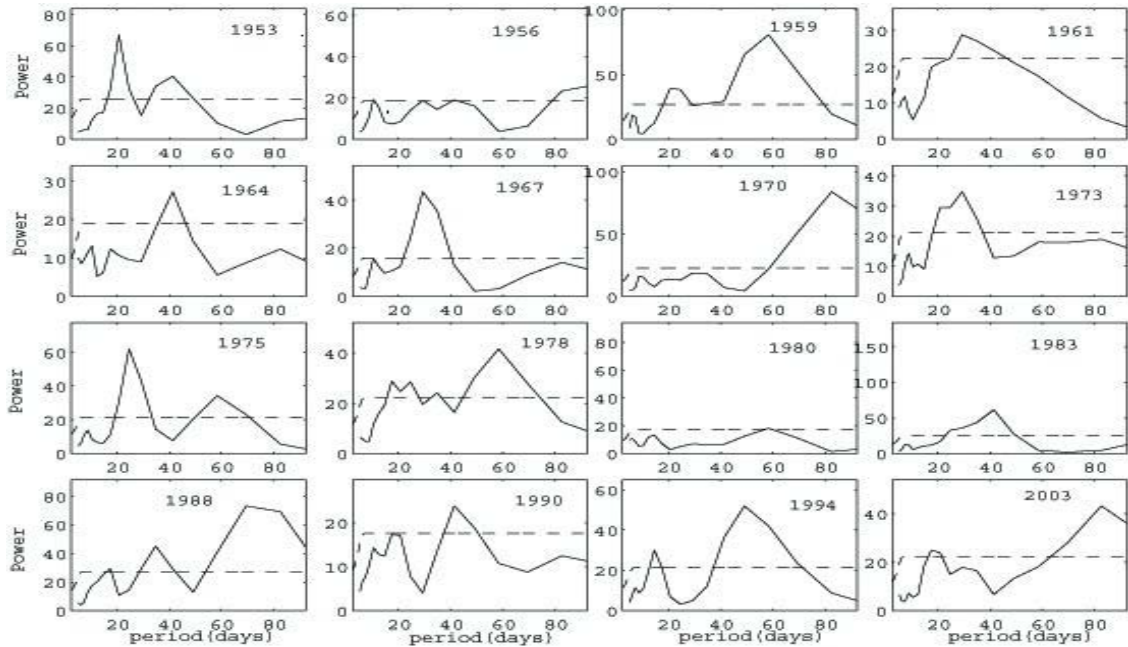


Figure 5.1: wavelet power spectrum of daily rainfall over Indian monsoon region for strong TBO years. Dotted line indicates 95% significance level

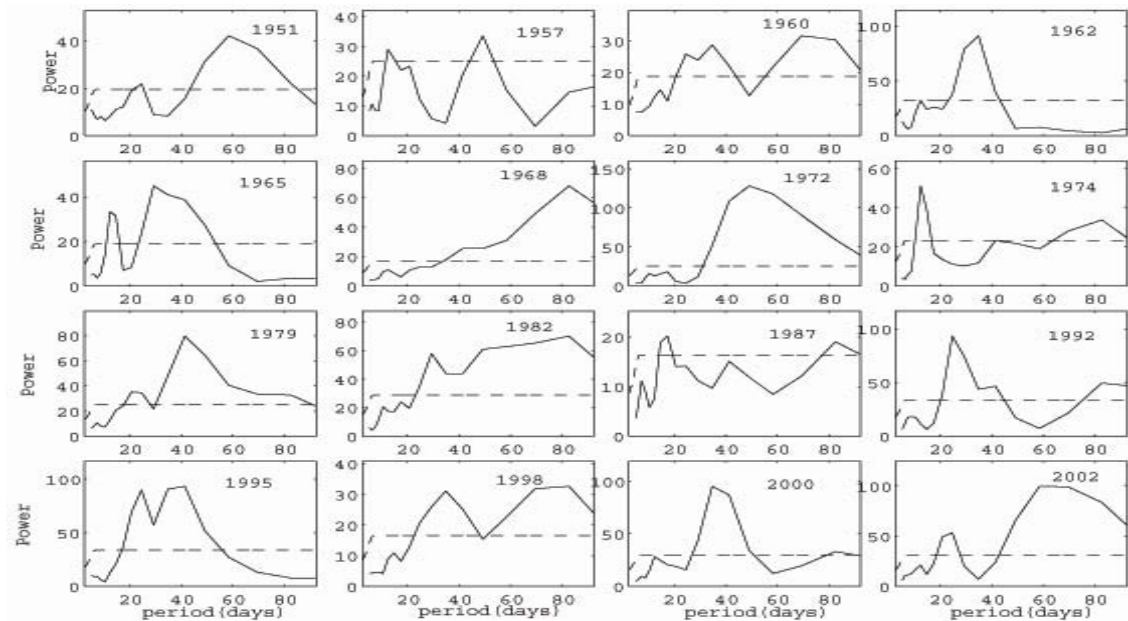


Figure 5.2: wavelet power spectrum of daily rainfall over Indian monsoon region for weak TBO years. Dotted line indicates 95% significance level

## 5.4.2 Dominant pattern of ISO and TBO

In order to investigate the dominant mode of intraseasonal variability, the EOF analysis of 10-20 day filtered and 30-60 day filtered summer seasonal OLR and zonal wind over the Indian and Indian Ocean region in between  $20^{\circ}\text{S}$ - $30^{\circ}\text{N}$ ,  $40^{\circ}\text{E}$ - $120^{\circ}\text{E}$  were carried out.

### 5.4.2.1 OLR

Spatial pattern of first four EOFs of daily in 30-60 day filtered, 10-20 day filtered and TBO filtered monthly OLR are seen in figure 5.3. The first two prominent patterns of 30-60 day filtered OLR has convective pattern over India, Arabian Sea and Bay of Bengal extending to northwest Pacific and reduced convection over rest of equatorial Indian Ocean. The EOF1 of 10-20 day pattern has convection over India, Arabian Sea and east equatorial Indian Ocean. In the second pattern Bay of Bengal is convective instead of equatorial east Indian Ocean. In the TBO filtered case, convection is enhanced over India, Arabian Sea and Bay of Bengal along with equatorial east Indian Ocean. The second pattern has convection over India, Arabian Sea and Bay of Bengal region.

In figure 5.3, EOF1 of 10-20 day filtered and TBO filtered OLR looks alike with convection over Arabian Sea, India and equatorial east Indian Ocean. But in the TBO case in addition to this the Bay of Bengal is also convective. Second EOF of both these windows looks alike with convection over Arabian Sea, India and Bay of Bengal. Thus the spatial pattern is comparable in these cases.

Wavelet analysis of time series of first two EOFs in both 10-20 day and 30-60 day filtered OLR is shown in figure 5.4. First and second pattern of 10-20 day filtered OLR has periodicity around 2.5 years, indicating TBO scale variability. In the 30-60 day filtered OLR also has a periodicity in 2.5 year for EOF1. But the periodicity changes to 3 year for EOF2

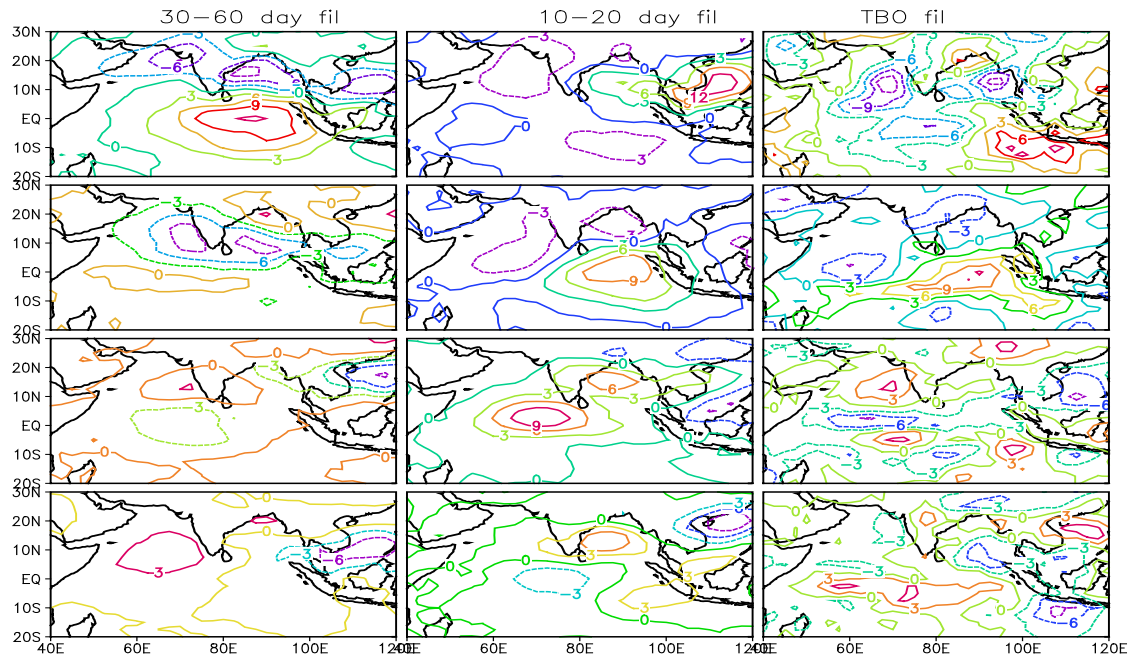


Figure 5.3: Spatial pattern of first Four EOFs of 30-60 day filtered daily, 10-20 day filtered daily and TBO filtered monthly OLR data sets for June to September season.

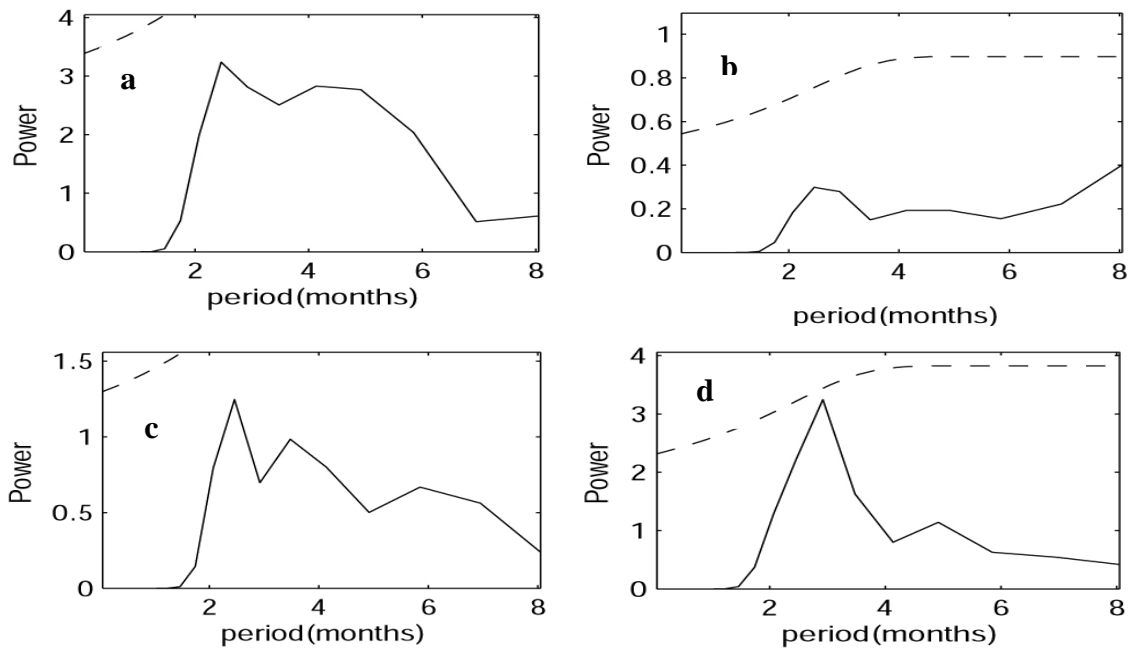


Figure 5.4: Wavelet analysis of first two PC's of daily OLR of June to September seasonal mean for 1974-2005. (a) and (b) for PC1 and PC2 for 10-20 day filtered and (c) and (d) for 30-60 day filtered OLR.

Thus both spatial pattern and time series of 10-20 day filtered OLR resembles TBO scale OLR pattern and corresponds to TBO scale variations.

The average time series of first two prominent patterns for 10-20 day filtered OLR for strong and weak TBO years and their variance are shown in the figure 5.5. In both strong and weak TBO years, the first EOF leads the second EOF by more than 5 days. The variance of both the first and second pattern has maximum value in June for strong TBO years and for weak TBO years the maximum is in the second half of June and the decreases and increases by July last and remains strengthened in the first half of August. Variance of both patterns coincides in both strong and weak TBO years. In the case of 30-60 day filtered OLR, second EOF leads the first EOF in both strong and weak TBO years. The variance remains strengthened one month from about almost 15<sup>th</sup> June to 15<sup>th</sup> July for both EOF1 and EOF2.

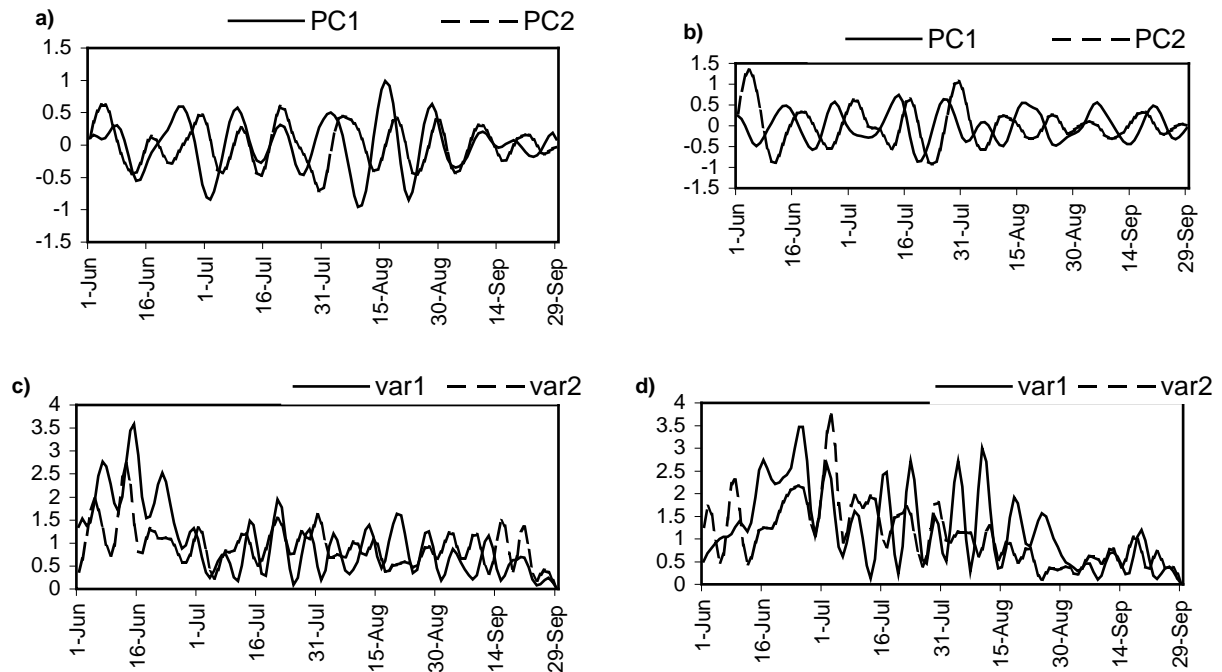


Figure 5.5: Time series of first two prominent EOFs (PC1 and PC2) for (a) strong TBO composites (b) weak TBO composites and (c) and (d) corresponds to their respective variance for 10-20 day filtered summer season (June to September) daily OLR .

Figure 5.6 indicates the time series and variance for 30-60 day filtered OLR. In this case, the PCs are not coherent for strong TBO years and in weak TBO years both the EOF has difference of a few days. The variance is maximum for EOF1 in July last and

August first week and is in the middle of June for EOF2. For weak TBO years also the maximum value of variance of both the PCs are not coinciding.

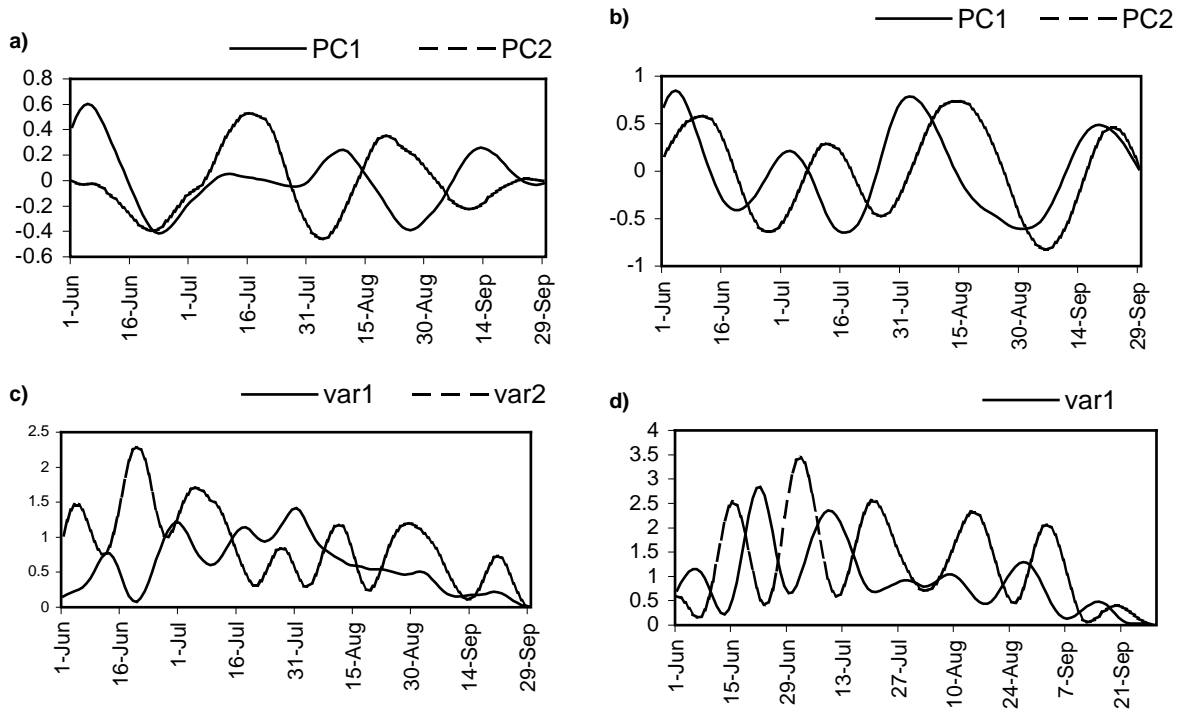


Figure 5.6: Similar as figure 5.4, except for 30-60 day filtered daily OLR data.

#### 5.4.2.2 Zonal wind at 850 hPa

Figure 5.7 shows the spatial pattern of first four EOFs of both 30-60 day filtered (left panel), 10-20 day filtered (middle panel) daily zonal wind and TBO scale filtered (right panel) at 850 hPa. The first pattern of 30-60 day filtered case has westerly anomalies over India and Arabian Sea and Bay of Bengal region and easterlies in the equatorial region and south of equator. The pattern is reversed for EOF2. The 10-20 day filtered u wind has westerly anomalies over Indian region and Arabian Sea and Bay of Bengal. But the maximum value is over Bay of Bengal extending to northwest Pacific Ocean. Easterly anomalies exist south of equator. The second pattern has westerly anomalies between equator and  $20^{\circ}\text{N}$  and easterlies above and below that. The EOF1 of TBO filtered U wind has westerly anomalies over India and adjacent seas and easterlies in the equatorial Indian Ocean. But westerly maximum is over the Bay of Bengal extending to



northwest Pacific Ocean. The second pattern has westerly anomalies between  $10^{\circ}\text{N}$  and  $20^{\circ}\text{N}$  and easterlies above and below that. Thus from both these figures EOF1 and EOF2 of both 10-20 day filtered daily 850 hPa  $U$  wind and monthly TBO filtered  $U$  wind has comparable spatial pattern.

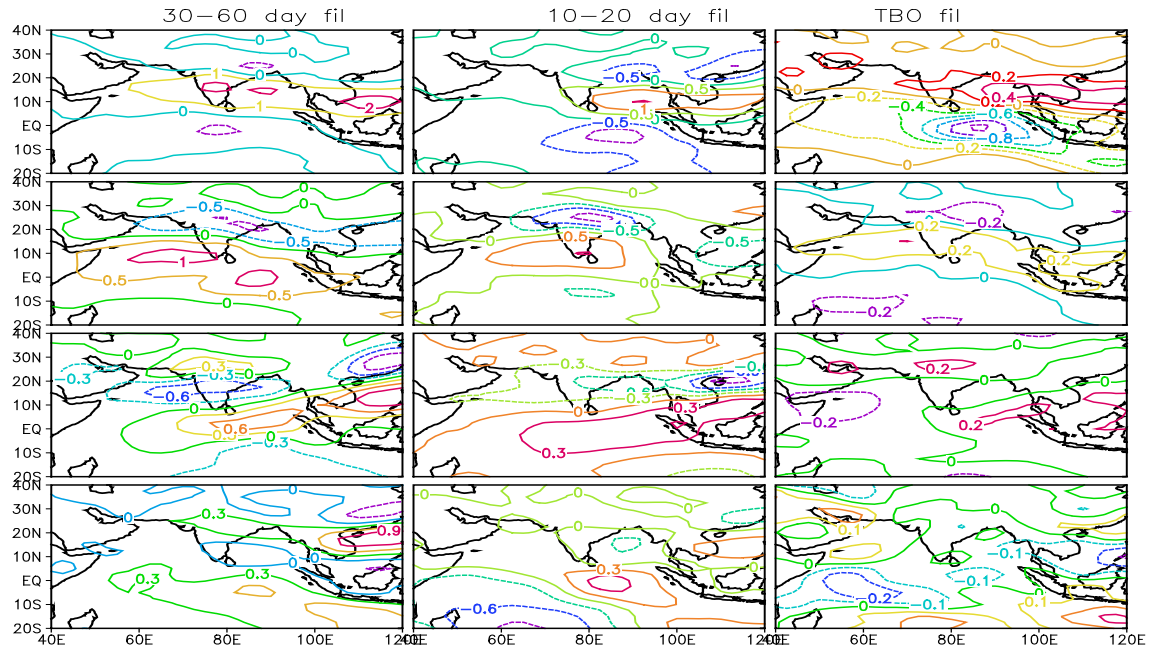


Figure 5.7: Spatial pattern of first Four EOFs of 30-60 day filtered daily, 10-20 day filtered daily and TBO filtered monthly zonal wind at 850 hPa for June to September season.

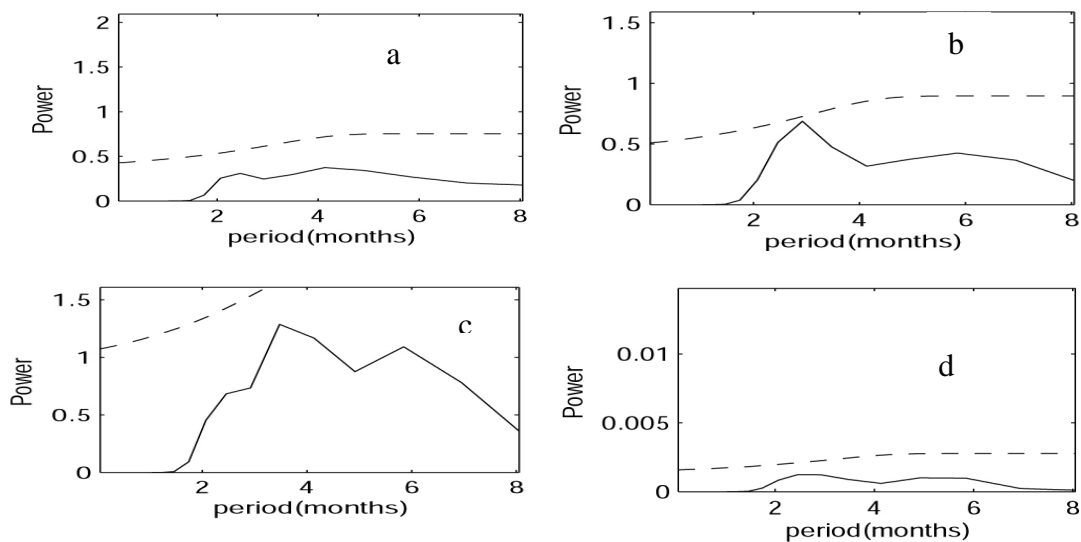


Figure 5.8: Wavelet analysis of first two PCs of daily zonal wind at 850 hPa of June to September seasonal mean for 1960-2005. (a) and (b) for PC1 and PC2 for 10-20 day filtered and (c) and (d) for 30-60 day filtered  $U$  at 850 hPa

Figure 5.8 indicates the wavelet analysis of time series of first two prominent patterns of 10-20 day filtered and 30-60 day filtered zonal wind at 850 hPa. The EOF1 of 10-20 day filtered daily U has a periodicity of around 2.5 year. But for EOF2 it shifts to almost 3 year. In the case of 30-60 day filtered daily U wind has periodicity of about 2-5 year and the peak is not clear for second EOF. Thus both spatial pattern and time series of 10-20 day filtered 850 hPa zonal wind resembles TBO scale pattern and corresponds to TBO scale variations

The variance and average of first two EOFs of 10-20 day filtered daily U at 850 hPa for the strong and weak TBO years are shown in figure 5.9. For both the strong and weak TBO years, the first two EOFs are coherent, but has a phase change of 3-4 days. The variance of strong TBO years has maximum in the second half of June and then decreases and then strengthen from July last to mid August. But the variance of weak TBO years increases upto second half of July and then decreases. For the 30-60 day filtered zonal wind variance is not coherent for TBO years (figure 5.10). The variance of most prominent mode attains maximum by July last or in the beginning of August. But the variance of EOF2 is maximum 15 days ahead of that of EOF1.

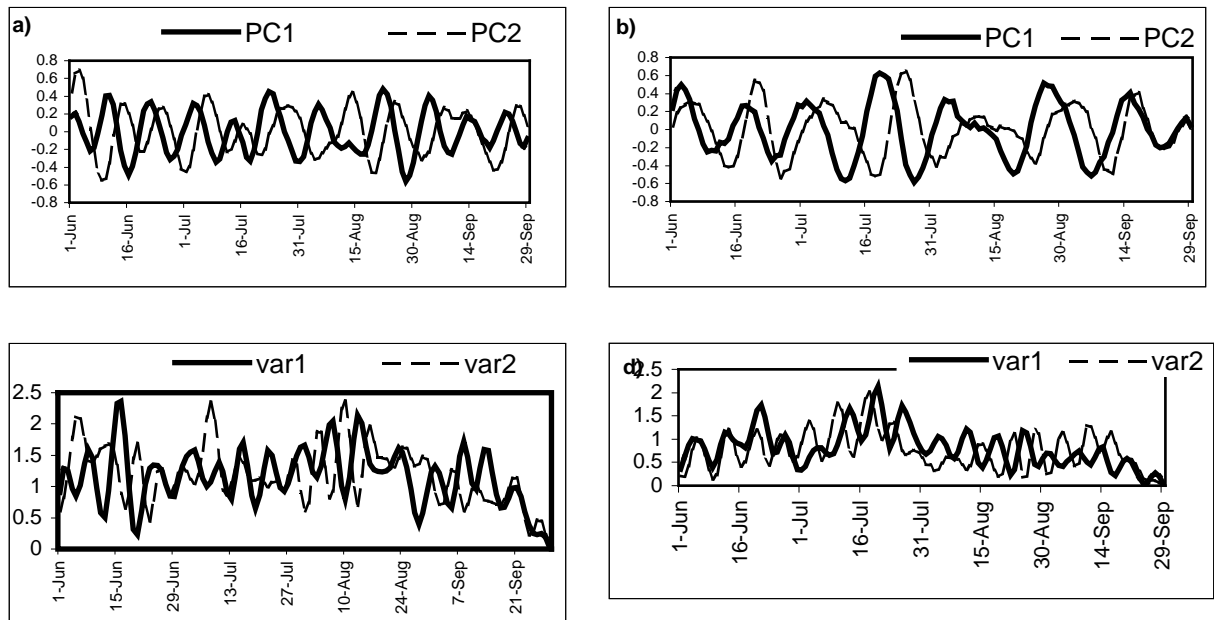


Figure 5.9: Time series of first two prominent EOFs (PC1 and PC2) for a) strong TBO composites b) weak TBO composites and c) and d) corresponds to their respective variance for 10-20 day filtered summer (June to September) daily zonal wind at 850 hPa.

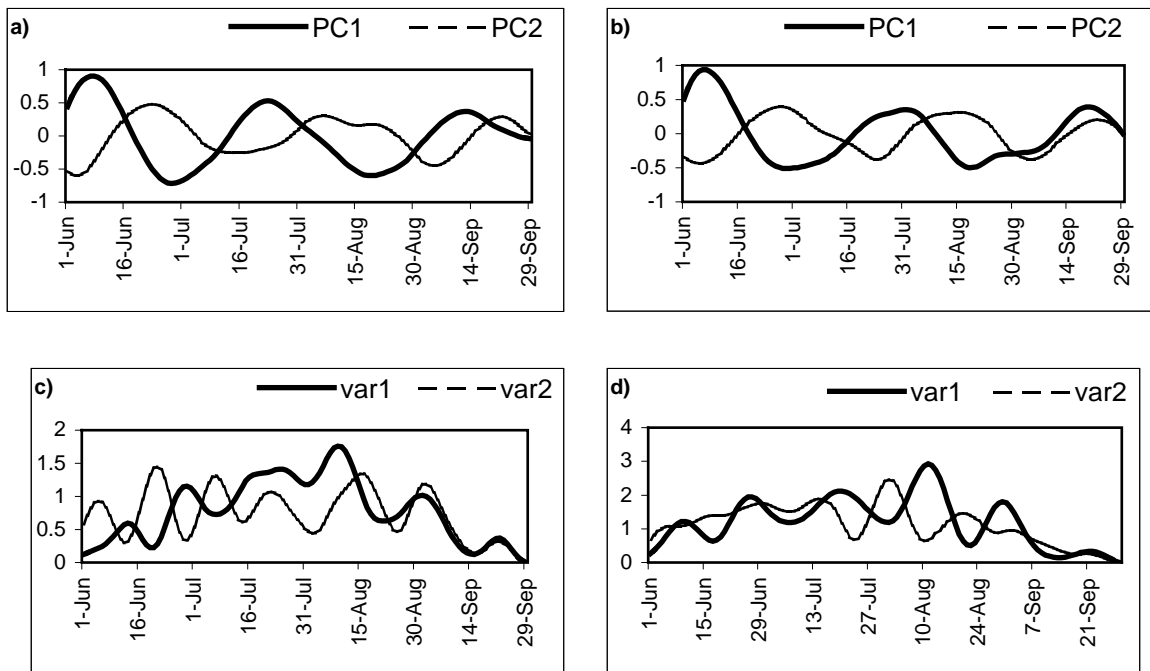


Figure 5.10: same as figure 8, but for 30-60 day filtered summer season (June to September) zonal wind at 850 hPa

Thus the 10-20 day variance of both the first two prominent EOFs are coherent in TBO, both strong and weak for OLR and zonal wind at 850 hPa and spatial patterns are almost similar with TBO scale pattern

### 5.4.3 Propagation of convection in TBO years

The eastward and northward propagation of both 10-20 day filtered and 30-60 day filtered OLR is analyzed for some selected strong and weak TBO years, which include both ENSO-TBO and non-ENSO TBO. In the analysis 1988 is a strong TBO year with La Nina onset in the Pacific and 1987 is a weak TBO year co occurred with El Nino. 1994 is strong TBO and 1995 is a weak TBO both in the absence of ENSO in Pacific.

Latitude wise and longitude wise propagation of convection for La Nina-strong TBO year summer 1988 is shown in figure 5.11. In the Lanina- TBO year (1988) over the Indian longitudes ( $60^{\circ}\text{E}$ - $100^{\circ}\text{E}$ ) the northward propagation of anomalies are evident in both 10-20 day and 30-60 day scale OLR. The northward propagation of anomalies are throughout the season in 30-60 day scale and is in June-July months for 10-20 day scale as seen from figure 10a. Similarly eastward propagation of convection anomalies in the

equatorial Indian Ocean ( $10^{\circ}\text{S}$ - $10^{\circ}\text{N}$ ) is also evident in both the cases. But it is more prominent and persists throughout the summer is in the 30-60day scale.

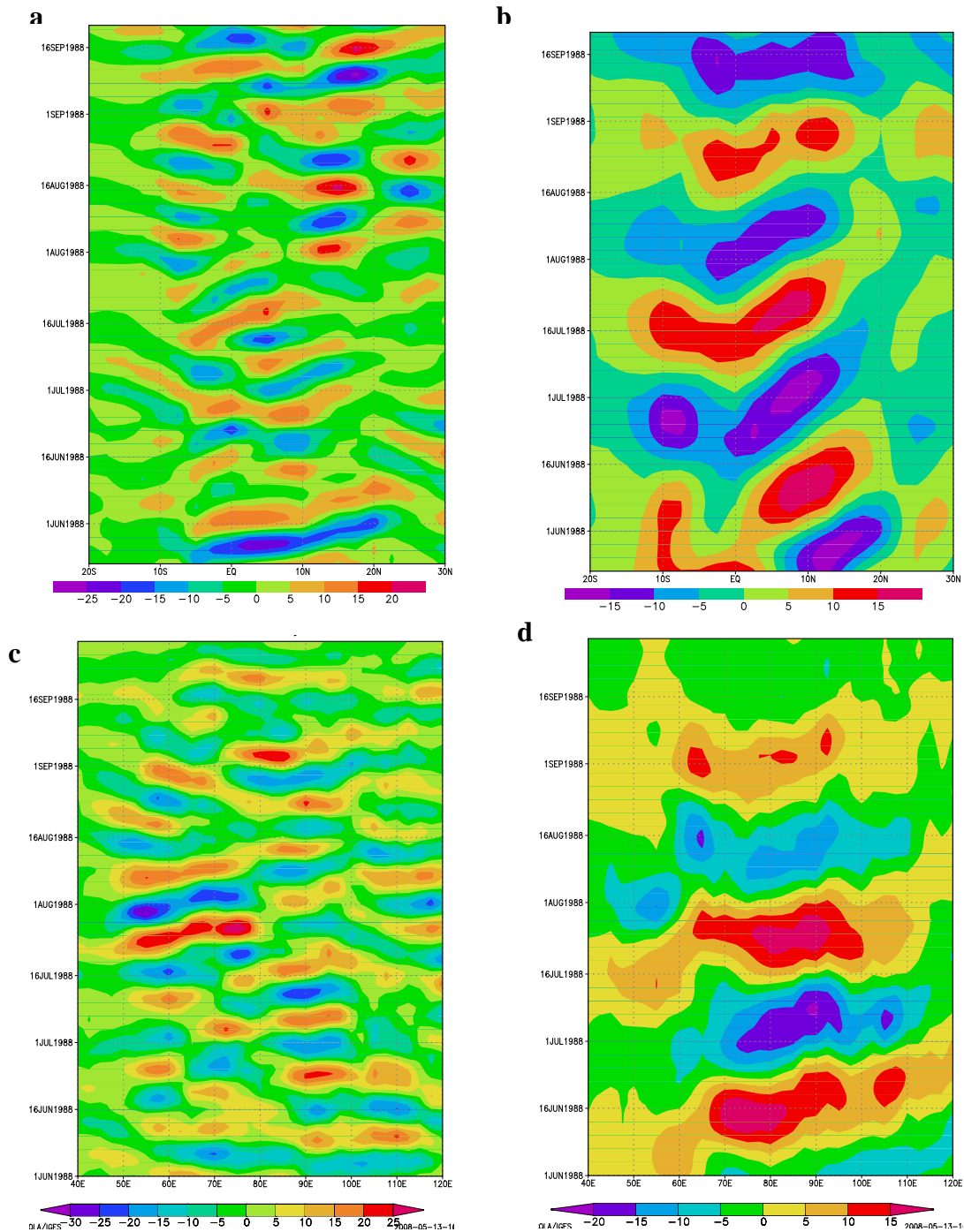


Figure 5.11: Hovmuller diagram of daily OLR for 1988 (a) time-latitude diagram for 10-20 day filtered OLR, (b) similar as a, but for 30-60 day filtered OLR, (c) time-longitude diagram for 10-20 day filtered OLR, (d) same as c, but for 30-60 day filtered OLR.

Figure 5.12 represents a El Nina-weak TBO year (1987) summer season propagation of OLR. In this case, northward propagation is not prominent in the 10-20 day band as seen in the figure 5.12a and is strong in the 30-60 day scale. Similarly for eastward propagation in the equatorial Indian Ocean is also clear in the 30-60 day band than 10-20 day scale in the entire summer season

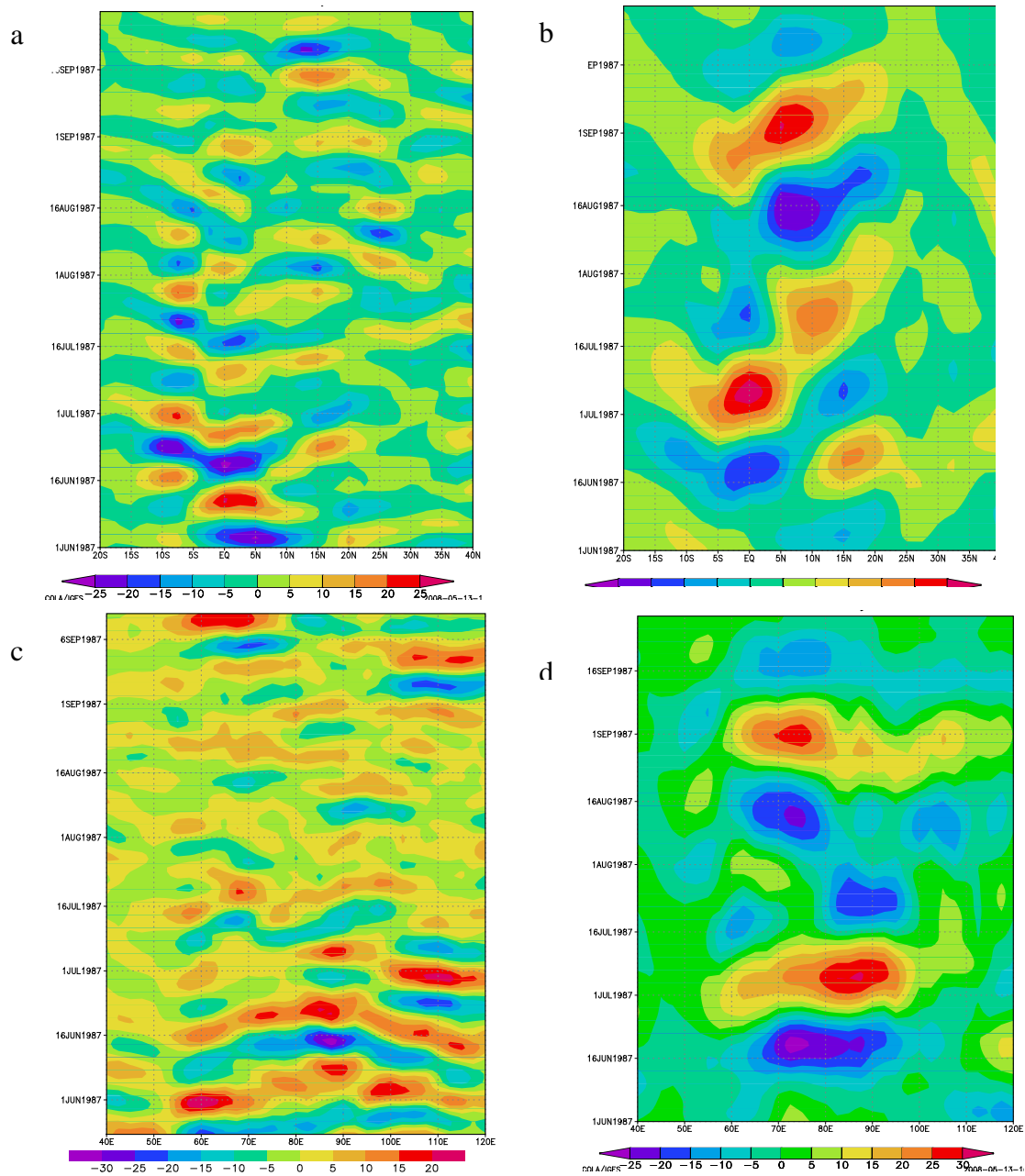


Figure 5.12: Hovmuller diagram of daily OLR for 1987 a) time-latitude diagram for 10-20 day filtered OLR, b) similar as a, but for 30-60 day filtered OLR, c) time-longitude diagram for 10-20 day filtered OLR, d) same as c, but for 30-60 day filtered OLR.

In the case of strong TBO year in the absence of La Nina the northward propagation is not prominent in both 10-20 day and 30-60 day scale OLR. But 10-20 day filtered OLR has eastward propagation in the equatorial Indian Ocean region, which is not evident in the case of 30-60 day scale OLR (see figure 5.13 )

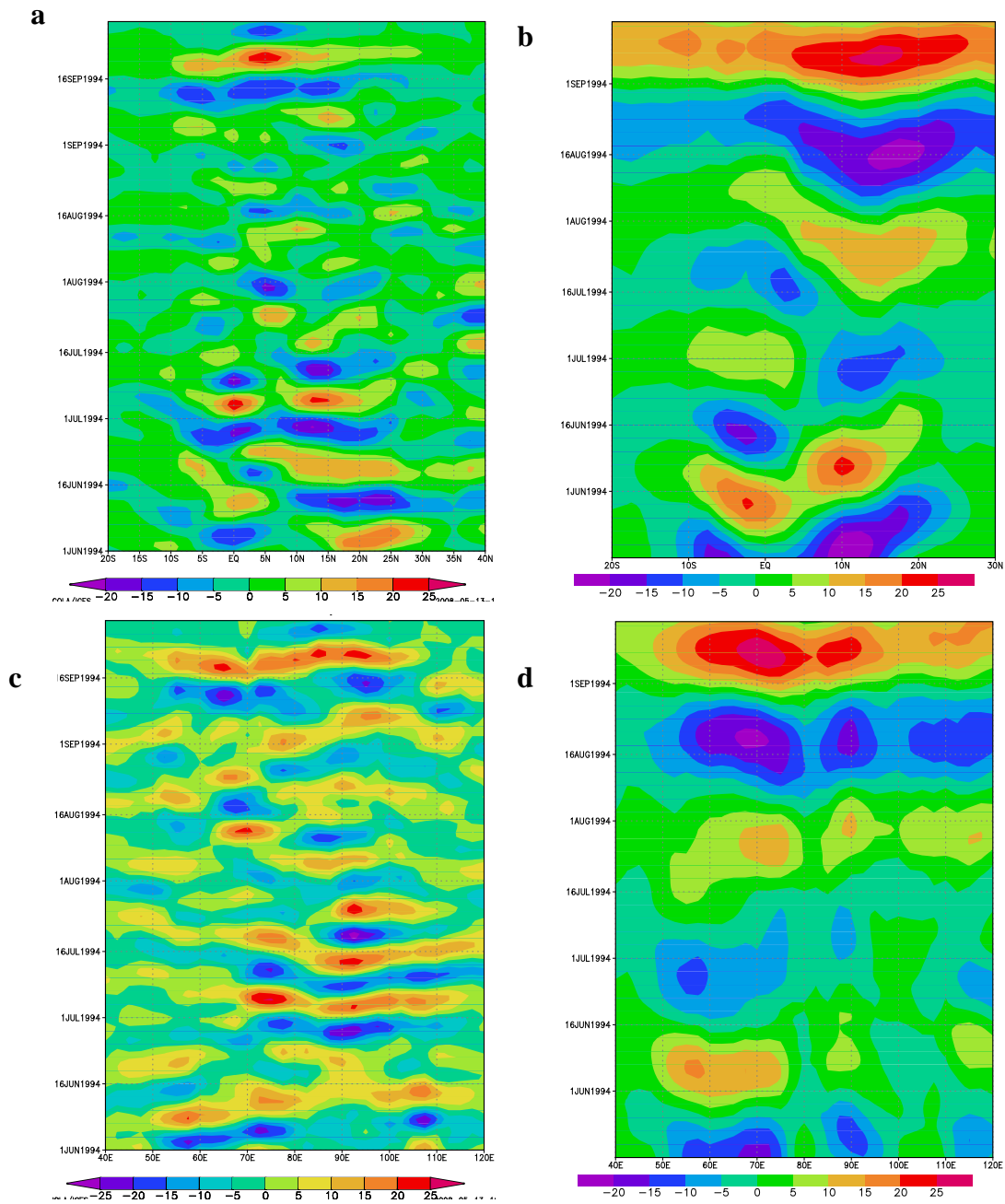


Figure 5.13: Hovmuller diagram of daily OLR for 1994 (a) time-latitude diagram for 10-20 day filtered OLR, (b) similar as a, but for 30-60 day filtered OLR, (c) time-longitude diagram for 10-20 day filtered OLR, (d) same as c, but for 30-60 day filtered OLR.

In the case of weak TBO year in the absence of El Nino (1995) also northward propagation of convection is seen in 10-20 day filtered and 30-60 day filtered OLR in the beginning and end of the summer season only (see figure 5.14 a and 5.14 b). But 10-20 day mode has eastward propagation in the equatorial Indian Ocean during the entire season for 10-20 day mode (figure 5.14 c and 5.14 d).

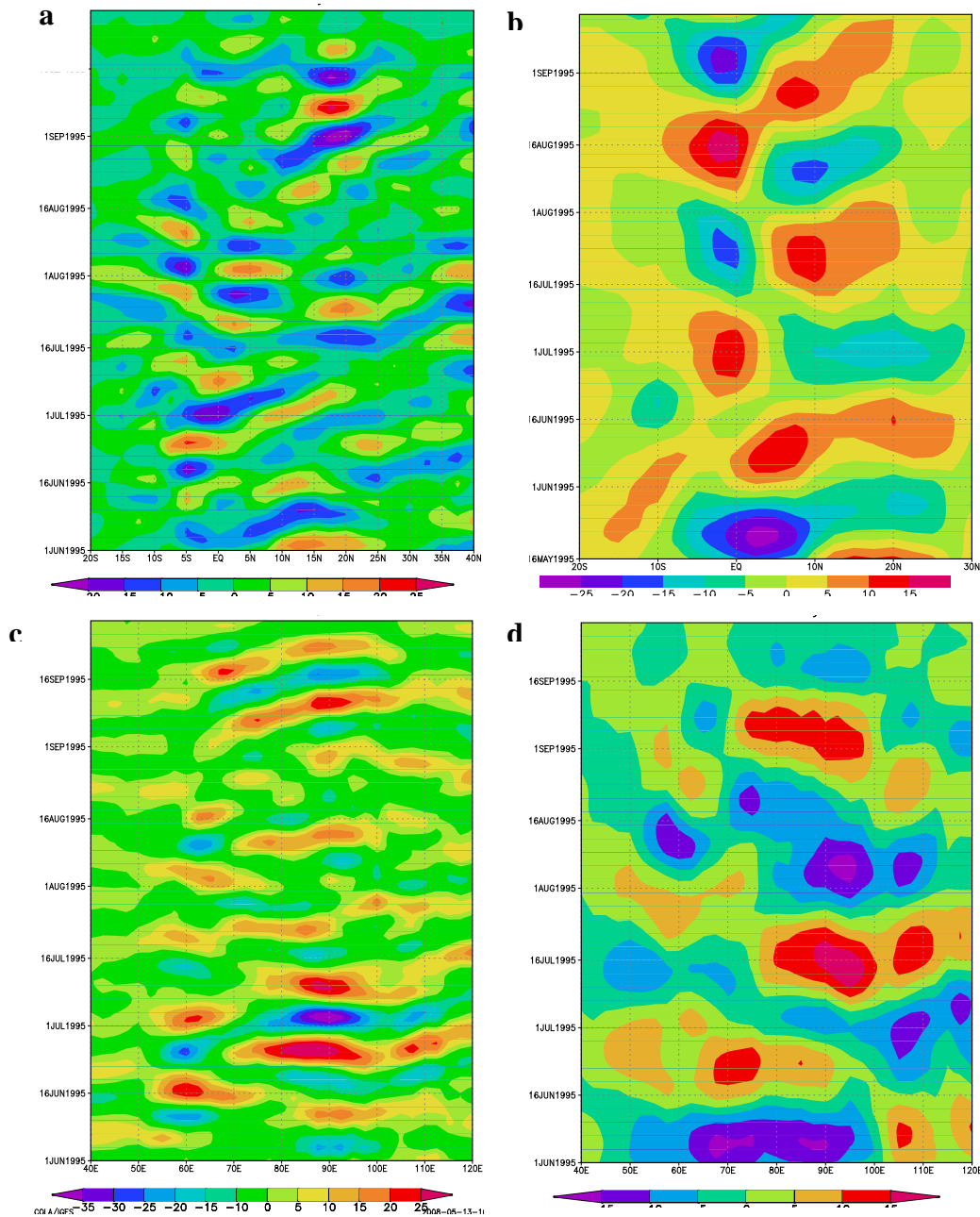


Figure 5.14: Hovmuller diagram of daily OLR for 1995 (a) time-latitude diagram for 10-20 day filtered OLR, (b) similar as a, but for 30-60 day filtered OLR, (c) time-longitude diagram for 10-20 day filtered OLR, (d) same as c, but for 30-60 day filtered OLR.

Thus 10-20 day mode has eastward propagation in TBO years and is prominent in the absence of ENSO. The 30-60 day mode has northward and eastward propagation in the presence of ENSO only for TBO years. The eastward propagation of anomalies, which is associated with TBO is observed in the 10-20 day mode in both ENSO-TBO and non-ENSO TBO years.

## 5.5 Conclusion

The present chapter analyses the prominent modes of boreal summer intraseasonal oscillation associated with TBO years. Indian summer monsoon rainfall shows both low and high frequency variations in most of the TBO years. In our analysis first prominent pattern of OLR in both 10-20 day and 30-60 day scale corresponds to active minus weak composite of Annamali and Slingo (2001) in both these scales. In TBO mode we have strong convection over India, Arabian Sea, Bay of Bengal and central-east Indian Ocean. In daily mode 10-20 day has increased convection in all these areas except the east part of Bay of Bengal. At the same time 30-60 day mode has increased convection over India and Bay of Bengal. Second mode of 10-20 day and TBO scale OLR is similar. For zonal wind at lower troposphere westerly anomalies are seen over India in both 10-20 day mode and 30-60 day mode and also in TBO scale during summer monsoon season. But in 10-20 day mode and TBO mode maximum westerly is shifted to Bay of Bengal and northwest Pacific. Thus 10-20 day scale OLR and 850 hPa zonal wind has almost similar spatial pattern with TBO scale and has a periodicity of about 2.5 year on the interannual time scales.

In the case of OLR, 30-60 day scale also has periodicity between 2.5 and 3 years. But for zonal wind it is between 3-6 years in 30-60 day scale. The first two PC's and its variance are coherent in the TBO years for 10-20 day filtered OLR and zonal wind. According to Slingo et al, (1999), when one mode is associated with some phenomena, the PC's must be similar and its variance must be coinciding. These all points out the spatial and temporal scale similarly of 10-20 day scale boreal summer intraseasonal oscillation and TBO scale interannual oscillation.



According to Anamali and Slingo (2001) large scale circulation is enhanced in 30-60 day scale and local Hadley circulation is enhanced in 10-20 day scale and is regional in character. It is found that in TBO years, local Hadley circulation is strengthened, especially in the absence of ENSO. The 10-20 day scale convection exhibits eastward propagation in TBO years, especially in the absence of ENSO in the Pacific Ocean. Thus the 10-20 day interseasonal oscillation is associated with TBO induced interannual variability of Indian summer monsoon, than 30-60 day mode.

---

# Linkage of Stratospheric QBO and Tropospheric Biennial Oscillation of Asian-Australian Monsoon System

---

### 6.1 Introduction

Quasi- biennial oscillation (QBO) described by Reed et al. (1961), is a remarkable regular oscillation of the zonal wind between easterlies and westerlies in the equatorial stratosphere with a mean periodicity of about 28 to 29 months. During the one half of this period, easterlies propagate from upper stratosphere to lower stratosphere and during the other half they are replaced by westerly winds. The alternating wind regimes develop at the top of the lower stratosphere and propagate downwards at about 1 km per month until they are dissipated at the tropical tropopause. Westerly shear zones (in which westerly winds increase with height) descend more regularly and rapidly than easterly shear zones. The amplitude of the easterly phase is about twice as strong as that of the westerly phase. At the top of the vertical QBO domain, easterlies dominate, while at the bottom, westerlies are more likely to be found. The amplitude of  $\sim 20 \text{ ms}^{-1}$  is nearly constant from 5 to 40 hPa but decreases rapidly as the wind regimes descend below 50 hPa. (Baldwin et al., 2001).

Lindzen and Holton (1968) showed that QBO could be driven by a broad spectrum of vertically propagating gravity waves (including phase speeds in both westward and eastward directions) and that the oscillation arose through an internal mechanism involving a two-way feedback between the waves and the background flow. The first

part of the feedback is the effect of the background flow on the propagation of the waves (and hence on the momentum fluxes). The second part of the feedback is the effect of the momentum fluxes on the background flow. Holton and Lindzen (1972) assume random forcing by wave energy of eastward moving Kelvin waves and westward moving Rossby-gravity waves from upper troposphere, which interacts with the zonal mean flow in the lower stratosphere will give rise to QBO. But in actual case these forcing has strong seasonal dependence. This mechanism indicates linkage between the tropospheric disturbances and the QBO in the zonal winds of the lower stratosphere.

The QBO exhibits a clear signature in temperature, with pronounced signals in both tropics and extratropics. The tropical temperature QBO is in thermal wind balance with the vertical shear of the zonal winds (Andrews et al., 1987). Besides the equatorial maximum in QBO temperature, there is a coherent maxima over  $20^{\circ}$ – $40^{\circ}$  latitude in each hemisphere, which are out of phase with the tropical signal.

Many observational studies reported the presence of a similar quasi-biennial oscillation in many ocean-atmosphere parameters in the tropical region. These include tropospheric winds, temperature, Indian summer monsoon, tropical sea surface temperature (SST), southern oscillation etc (eg; Nicholls, 1978; Rasmusson et al., 1990; Ropeleswki et. al., 1992; Goswami, 1995; Terray 1995; Meehl, 1997). This biennial oscillation observed in the tropical regions, especially over the Indo-Pacific region is known as Tropospheric Biennial Oscillation (TBO). The mechanism of TBO is believed to be quite different from that of stratospheric QBO. Details of TBO and factors controlling TBO are described in the chapter 1 of the thesis. Coupled climate interactions between ocean and atmosphere contribute to a mechanism that produces biennial variability (TBO) in the troposphere and upper ocean in the tropical Indian and Pacific Ocean regions. Detailed explanation of TBO including the role of northwest Pacific warm pool in TBO is given Li et al. (2006).

Because the QBO has its maximum amplitude over the equator, it is natural to inquire whether this oscillation has any effect on the underlying tropical troposphere. But the

zonal wind and temperature anomalies of the QBO do not penetrate significantly below the tropopause. The temperature QBO at the tropopause is small relative to the annual cycle. It is known that the tropical troposphere has a quasi-biennial oscillation of its own, uncorrelated with the stratospheric QBO (Yasunari, 1985; Gutzler and Harrison, 1987; Kawamura, 1988; Lau and Sheu, 1988; Moron et al., 1995; Shen and Lau, 1995). Unlike the stratospheric QBO, the “tropospheric QBO” is irregular in time, asymmetric in longitude and propagates slowly eastward.

Yasunari (1989) suggested a possible link between biennial oscillations in the stratosphere and troposphere over the Asian monsoon region and SST in the equatorial Pacific using station data from Singapore and Pacific SST. Ropelewski et al. (1992) identified the association of stratospheric QBO with interannual variability of coupled air-sea system. Many studies have identified significant relationship between the phases of QBO in the zonal wind in the lower stratosphere (30 hPa) and percentage departure of monsoon rainfall of India. Mukherjee et al., (1985) showed that strong easterly (westerly) phase of the QBO is associated with weak (strong) monsoon. Meehl (1997) emphasizes the role of Asian summer monsoon on TBO. Sathiyamurthy and Mohanakumar (2000) related the TBO and QBO of zonal wind and temperature over an equatorial Indian station. Thus both these oscillation (QBO and TBO) are linked to the Indian summer monsoon separately. But no physical explanation is available so far for the possible linkage between stratospheric QBO and Tropospheric Biennial Oscillation. Thus both these oscillation (QBO and TBO) are linked to the Indian summer monsoon separately. Mohankumar and Pillai (2008) observed the unique structure of zonal wind over Indian monsoon region in TBO cycle

## **6.2 Objectives of the study**

The present study is an attempt to identify the characteristics of biennial variation of the stratosphere and troposphere and the possible interaction between these two areas over the Indian monsoon region and north Australian monsoon region, as these two monsoon regions are vigorously involved in TBO. The study further extends to find the

interaction of QBO and TBO associated with the annual cycle of Indian summer monsoon.

### 6.3 Data and methodology

In the present study zonal wind and temperature data for 23 vertical levels from 1000 hPa to 1 hPa for the period 1960-2002 obtained from European Center for Medium range Weather Forecast (ECMWF) have been used for the investigation of vertical structure of entire troposphere and lower stratosphere. A full description of ECMWF reanalysis (ERA) is available from Gibson et al., (1996, 1997). Indian summer monsoon rainfall (ISMR) data, which is the area averaged June to September rainfall of 306 stations well distributed over India, has been taken from Parthasarathy et al., (1994) and updated for making it to period 1960-2002 is used to define TBO years.

Indian monsoon area considered for the study is confined between the latitudes  $10^{\circ}\text{N}$  and  $30^{\circ}\text{N}$  and longitudes between  $65^{\circ}\text{E}$  and  $95^{\circ}\text{E}$  and Australian monsoon region  $5^{\circ}\text{S}$  and  $15^{\circ}\text{S}$  and longitudes  $105^{\circ}$  to  $135^{\circ}\text{E}$ . Gridded data of ECMWF is averaged over these areas considered for investigating the vertical structure. These data sets are filtered into biennial scale using a band pass filter developed by Murakami (1979). TBO years are identified using ISMR as done in the chapter 2 of the thesis. Then the vertical structure is studied for the composite of years satisfying the above criteria for ISMR. A Pearson cross correlation analysis is carried out in order to understand the speed of propagation of zonal wind and temperature anomalies and also their relationship with SST anomalies of Pacific and Indian Ocean SST in biennial scale. For sufficiently long data series of  $x$  and  $y$ , the general lag  $-k$ , Pearson cross-correlation coefficient between them is

$$(r_{xy})_k \approx \frac{\sum_{i=1}^{n-k} [(x_i - \bar{x})(y_{i+k} - \bar{y})]}{\left[ \sum_{i=1}^{n-k} (x_i - \bar{x})^2 \sum_{i=k+1}^n (y_i - \bar{y})^2 \right]^{1/2}} \quad \dots 6.1$$

## 6.4 Results

### 6.4.1 Wavelet analysis of zonal wind over Indian monsoon region

In order to identify the dominating frequencies of zonal wind, wavelet analysis is carried out for monthly mean zonal winds at different levels of troposphere and lower stratosphere. The Morlet wavelet is used and the transform is performed in Fourier space using the method described in Torrence and Compo (1998).

The power spectrum over Indian monsoon region is shown in figure 6.1. In the monsoon region annual oscillation is the major periodicity throughout the entire height ranging from 1000 hPa to 10 hPa. In the entire troposphere only the annual variation is present with maximum power at 100 hPa. Along with the annual oscillation QBO is also predominant in the lower stratosphere. Quasi-biennial periodicity starts at 70 hPa, though it is well below significant level and it becomes significant from 50 hPa onwards. The ratio of QBO to annual oscillation peaks at 30 hPa. The dominance of annual cycle in the troposphere winds over the Indian monsoon region is due to the effect of annually occurring southwest monsoon in this region.

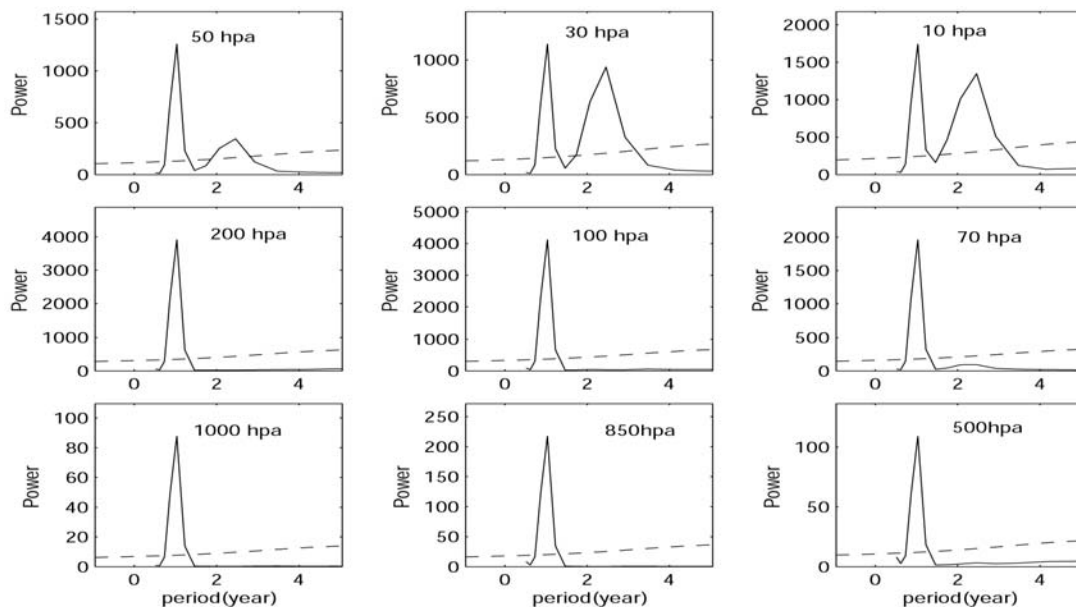


Figure 6.1: Wavelet power spectrum of monthly mean zonal wind at different levels over Indian monsoon region. Dotted line indicates 95% significance level.

Thus in order to study the troposphere-stratosphere interaction in the biennial scale, the prominent annual frequency must be removed from the data.

### 6.4.2 Zonal wind structure in QBO scale

The time series of QBO filtered zonal wind over India and Australian monsoon region are presented here.

#### 6.4.2.1 Indian monsoon region

The time series of the vertical profile of zonal wind over the Indian monsoon region is depicted in figure 6.2. In the lower stratosphere, zonal wind propagates downward. The downward propagation of zonal wind anomalies weakens on reaching the tropopause level, but it extends to the lower troposphere. In some years, the stratospheric maximum extends to the troposphere, especially from 1980's. In both the troposphere and stratosphere the zonal wind anomalies reverses their direction year by year indicating a biennial oscillation.

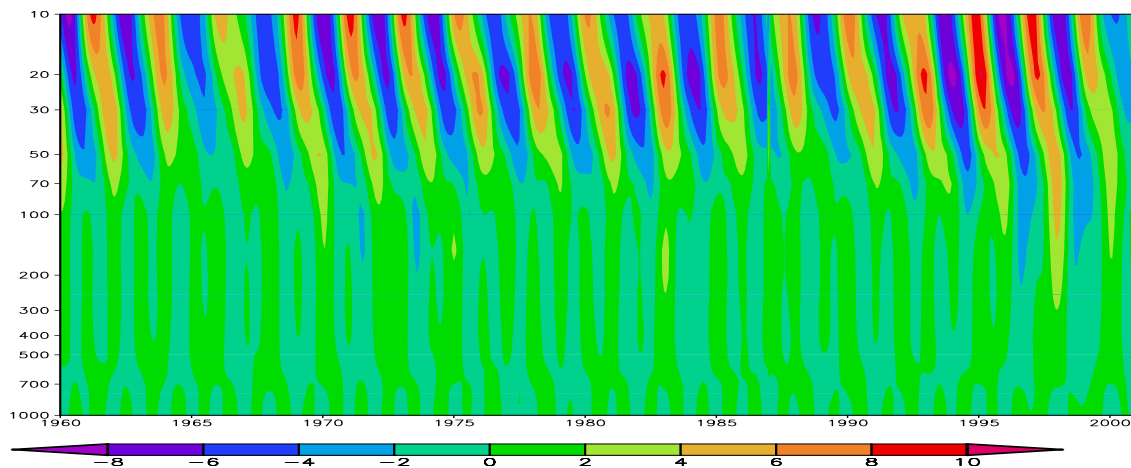


Figure 6.2: Time-height plot of zonal wind over Indian monsoon region. Height is in pressure units

#### 6.4.2.2 Australian monsoon region

The time series from 1960-2000 over Australian monsoon region is given in figure 6.3. Over Australian monsoon region the lower stratosphere has easterly/westerly structure extending upto 70 hPa and then weakens and anomalies are larger than over Indian monsoon region. Another maximum anomaly region is found in the surface, which also

alters year by year and it propagates upwards and anomalies are very weak in the middle and upper troposphere.

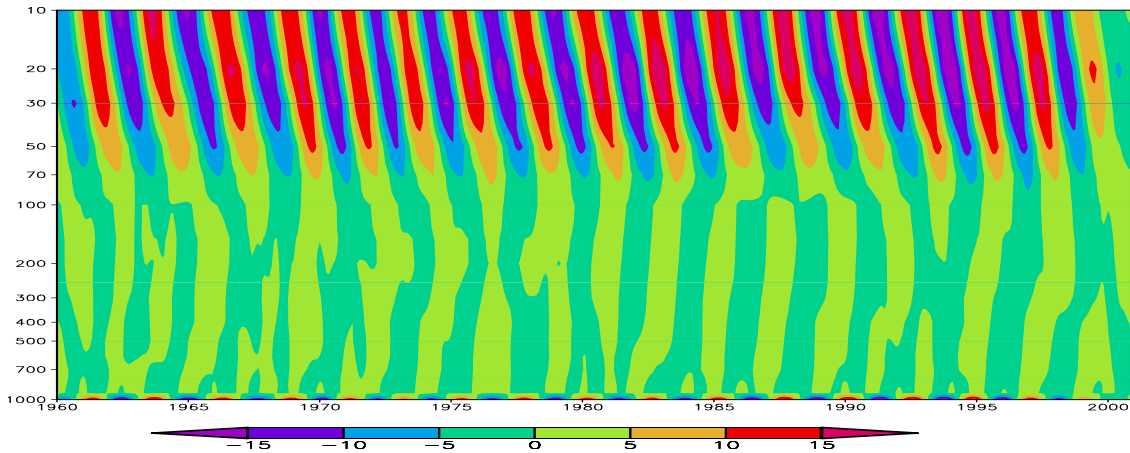


Figure 6.3: Time-height plot of zonal wind over Australian monsoon region. Height is in pressure units

Thus in both these monsoon regions QBO propagation is almost similar, but is more intense over Australian monsoon region. The interaction with troposphere is different in both the regions. A surface maximum is seen over the Australian monsoon region.

### 6.4.3 Propagation of zonal wind anomalies in QBO scale

Pearson cross correlation analysis is carried out for both Indian and Australian monsoon region with 20 hPa wind and that at different levels in order to understand the time taken to reach the effect of lower stratospheric winds at different levels. Similar correlation analysis is carried out for tropospheric winds at selected levels with that at levels just below that to get the interaction of zonal winds at troposphere.

#### 6.4.3.1 Indian monsoon region

20 hPa wind has lead correlation of 1 month with that at 30 hPa (correlation coefficient is about 0.97) ie, it takes one month to reach 30 hpa level and about 6 months to reach 50 hpa (cc is 0.83). It will reach at 70 hPa by another two months. It has lead correlation of 12 months with 100 hPa (0.31). Thus zonal wind from 20 hPa reaches tropopause level by about a year time period. Correlation with heights from 200 to 500 hpa is less than 0.2 always. It has a positive lead correlation of 4 months (0.3) with zonal wind at



700 hPa and another 16 month negative correlation (-0.3) also. Similarly with 850 also has +0.3 at 3 months lead and -0.3 with 11 months lead. Correlation is less than 0.2 for 925 and surface with 20 hPa wind leading the lower level by about 5 months.

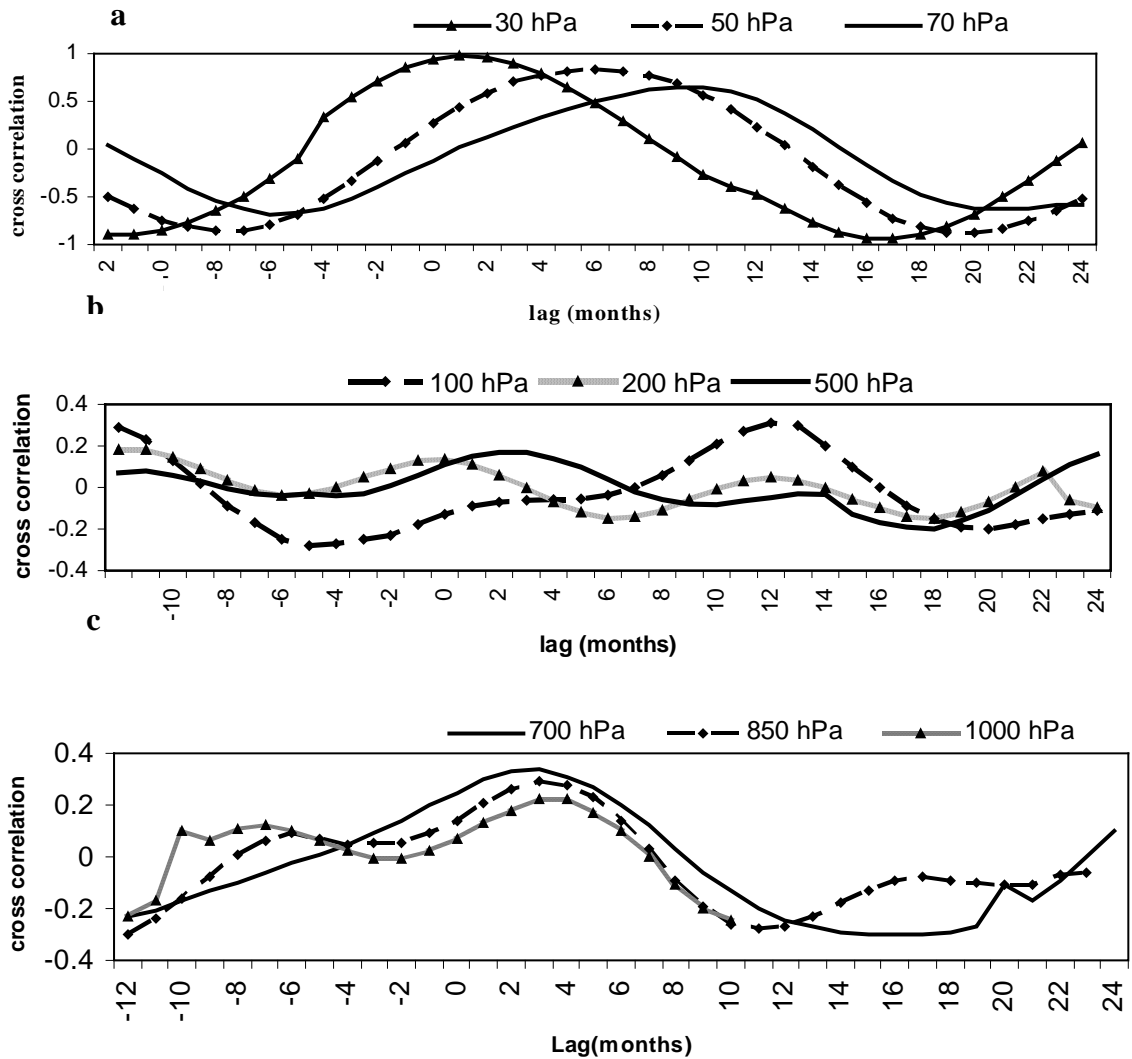


Figure 6.4: Cross correlation of zonal wind at 20 hPa with that at different levels below.

In order to examine clearly the propagation of anomalies in troposphere we have made similar correlation for tropospheric winds with that at just lower levels and is seen in figure 6.5. Zonal wind spreads from 100 hpa to 200 hpa (max correlation 0.94 is with zero lag) and from 200 to 300 also it spreads with zero lag(0.99) . From 300 to 500 also it spreads (0.94). From 500 hpa to 700 hpa it takes 2 months (0.7) and takes one month to reach 850 hpa (0.61). It again spreads to 925 hpa(0.98) and from there to

surface(0.99). Thus the wind spreads quickly from 100 hPa to 500 hPa (ie, zero lag) and from there to 700 hPa it moves slowly taking 2 months to reach 700 hPa and then spreads to surface.

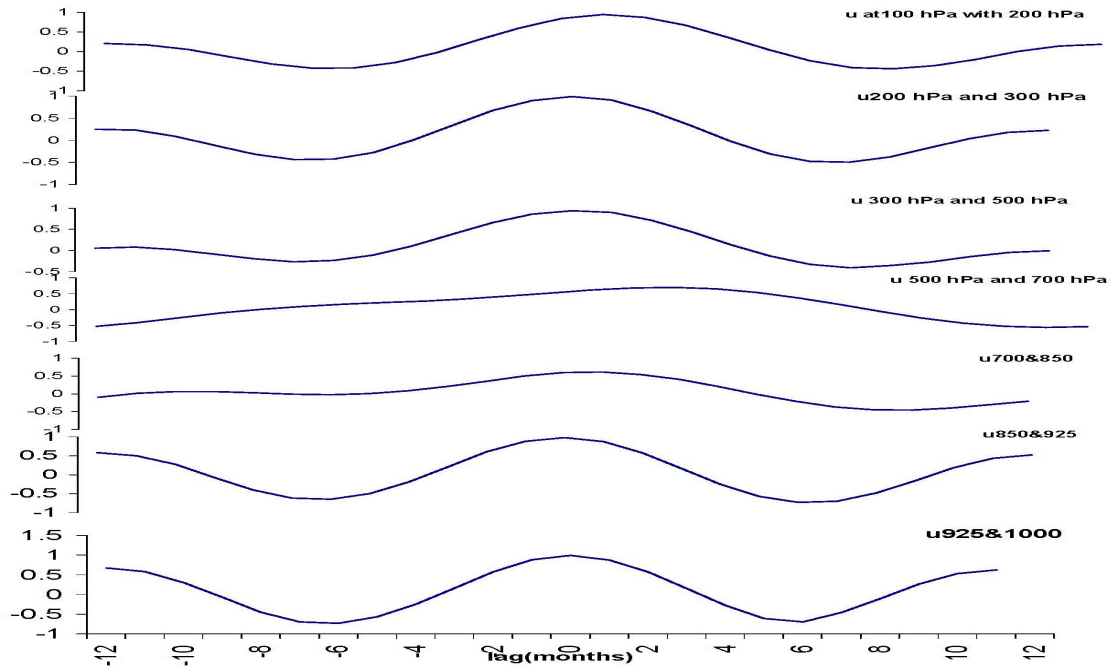


Figure 6.5: cross correlation of tropospheric winds with that at level below that

### 6.4.3.2 Australian monsoon region

Similar cross correlation analysis is carried out for the zonal wind over Australian monsoon region and the maximum correlation value and lead/lag of 20 hPa with lower levels is given in table 6.1. Here zonal wind at 20 hPa reaches 30 hPa by 2 months (0.99) and with another five months it will reach at 50 hPa (0.97). Within a period of nine months wind from 20 hPa will reach at 70 hPa and it spreads quickly to upper troposphere. Thus zonal wind from 20 hPa will reach the tropopause level three months earlier than that at Indian monsoon region. Correlation pattern reverses in the upper and middle troposphere level here. This reversal of correlation indicates upward propagation of anomalies from troposphere. 20 hPa zonal wind has a lag of 2 months with that of 200 hPa wind (0.3) and the lag is 4 months with 300 hPa. Correlation is negligible upto 850 hPa and surface has a lag correlation of 4 months (-0.26) with surface wind. This

means that westerly (easterly) phase of surface wind leads the easterly (westerly) phase of 20 hPa by four months. Thus in both these monsoon areas, downward movement of stratospheric winds are different in lower stratosphere and propagation is opposite in troposphere.

Table 6.1: cross correlation of 20 hPa zonal wind over Australia with that at lower levels. Months with + sign indicates 20 hPa wind leads the other and negative indicate lag.

U20/levels (hPa)	Lag/lead (months)	Correlation
50 hPa	+7	0.97
100 hPa	+9	0.4
500 hPa	+24	0.22
850 hPa	-3	-0.22
1000 hPa	-3	-0.26

Table 6.2: cross correlation of zonal winds of different levels at troposphere with that just below.

Levels	Lag/lead (months)	Correlation
100 hPa with 200 hPa	0	0.65
200 hPa with 300 hPa	-1	0.87
300 hPa with 500 hPa	-1	0.6
500 hPa with 850 hPa	-1	0.82
850 hPa with 925 hPa	0	0.98
925 hPa with 1000 hPa	0	0.99

Over the Australian monsoon region, zonal wind at 100 hPa has zero lag with that at 200 hPa. But 200 hPa wind has one month lag with 300 hPa and this one month lag is present upto 700 hPa wind. Lower troposphere wind has no lag with that at lower levels as seen in table 6.2.

#### 6.4.4 Vertical profile of zonal wind during the TBO years

In order to investigate the stratosphere-troposphere interaction associated with biennial oscillation of ISMR, composite analysis of strong minus weak TBO year, which are defined earlier, is performed from previous year to next year of a strong/weak TBO year.

##### 6.4.4.1 Indian monsoon region

Figure 6.6 is the vertical structure of zonal wind anomalies over Indian monsoon region during TBO cycle. In the Indian summer monsoon region, the stratosphere has downward motion from upper to lower levels and it reverses its sign by the next year. Instead of dissipating at the upper troposphere, the anomalies propagate downwards to troposphere. But the propagation speed varies at different levels. It spreads between lower and middle troposphere and then propagates slowly to 700 hPa level by about nine months, with speed of 0.3 km/month and then extends to lower level quickly. The westerly anomalies seen over the upper stratosphere during the weak monsoon propagates to lower level by the next strong monsoon and easterly anomalies from the stratosphere come to the upper troposphere.

The zonal wind pattern shows three distinct layers in the troposphere. The upper region (above 500 hPa), where zonal wind extends quickly, then a transition region, which lies between 700 and 500 hPa and the bottom region, from 700 hPa to surface. Easterly anomalies prevail in the bottom region during the weak monsoon year. In the upper region westerlies are seen till the spring season before the positive phase of TBO and are replaced by easterlies and continue to the next year spring. The transition layer slowly transits the upper region to the bottom region over the monsoon area, which takes a period of about six months. The existence of the transition zone is quite unique in the monsoon area.

Another interesting fact noted over the monsoon area is that the zonal wind structure remains the same phase in the entire troposphere during the winter season (November-February), which changes its phase in the next year. In figure 6.6, it can be seen that the previous winter season of an active monsoon year, the entire troposphere from surface

to the tropopause level exhibits westerly anomalies. This westerly phase is completely replaced by easterly phase in the next year of a strong monsoon year. Clear downward propagation of easterlies and westerlies from the stratosphere to the troposphere is seen over the monsoon region.

As reported by the earlier observational studies, it is evident in the fig.6.6 that westerlies in the lower troposphere and easterlies in the upper troposphere is an indicator of a strong monsoon year. In a weak monsoon year, TBO has its easterly phase in the lower troposphere and westerly component in the upper troposphere. This biennial tendency has a strong influence in the monsoon circulation. When the TBO exhibits westerly in the lower troposphere it activates the low level jet (LLJ) circulation, there by intensifying the monsoon circulation. Similarly the easterly anomalies in the upper level enhances the speed of the tropical easterly jet stream (TEJ), which is present about 14 km height over the monsoon region. The intensity and location of TEJ is very much related with the monsoon activity. When TBO is in the opposite phase, the easterlies in the lower troposphere reduce the LLJ and westerlies in the upper troposphere oppose TEJ and both these effects weaken the monsoon circulation.

It can be also seen that the stratospheric QBO has got direct link with the TBO during the monsoon season. Westerly anomalies in the lower stratosphere are transferred to the upper troposphere during the previous year of an active monsoon year. The westerly wind regime is then slowly and steadily transferred to the lower troposphere by the transition layer. In the case of a weak monsoon year, we can see similar transport of the easterly regime from the lower stratosphere to the upper troposphere and then to the lower troposphere. This characteristic supports the role of stratospheric winds on troposphere in biennial scale.

#### ***6.4.4.2 Over Australian monsoon region***

In the Australian monsoon region also easterly anomalies are seen at the lower stratosphere during the previous year of strong TBO year and it propagates downwards and reaches tropopause level (100 hPa) within a year. At the same time the upper and middle troposphere has westerly anomalies and lower level has easterlies from July

onwards. The easterlies formed propagate upward to upper troposphere by next year April and interacts with downward propagating QBO easterlies at the upper troposphere. At the same time westerlies are formed in the lower stratosphere and propagates downward and westerlies forms in the lower stratosphere by next June, which is strong TBO year and next cycle with reverses anomalies starts.

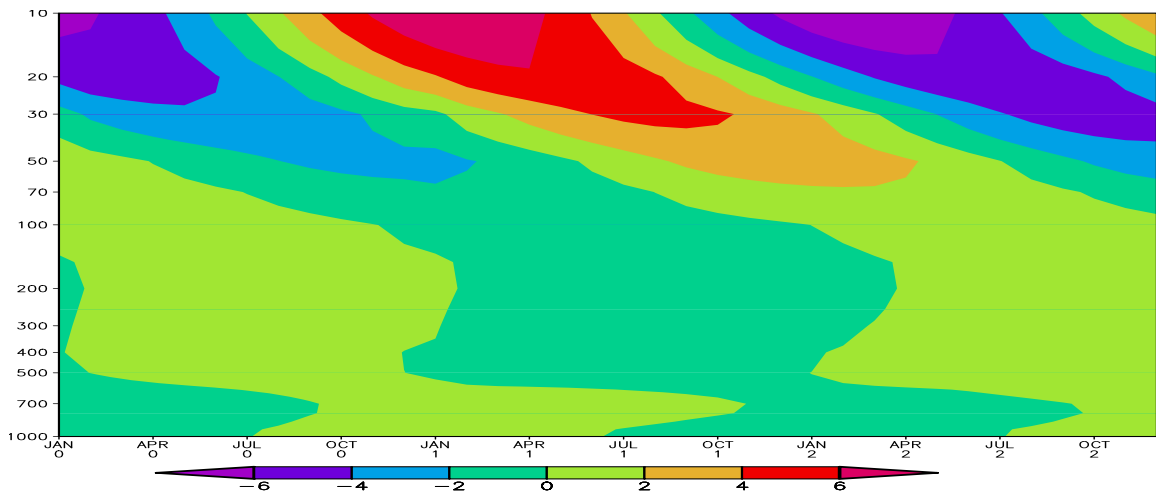


Figure 6. 6: Time –height plot of zonal wind anomalies over the Indian monsoon region (averaged over  $10^{\circ}\text{N}$ - $30^{\circ}\text{N}$ ,  $65^{\circ}\text{E}$ - $95^{\circ}\text{E}$ ) for strong minus weak TBO years composites, from previous year to next year of reference monsoon. Months with 0 correspond to previous year, with 1 to current TBO year and 2 to the next year.

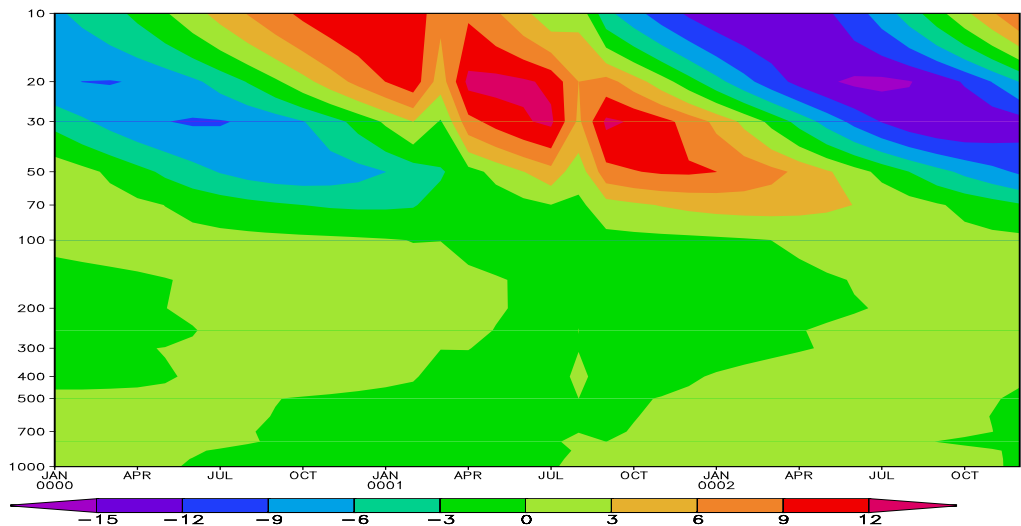


Figure 6.7: Time –height plot of zonal wind anomalies over the Australian monsoon region (averaged over  $5^{\circ}\text{S}$ - $15^{\circ}\text{S}$ ,  $105^{\circ}\text{E}$ - $135^{\circ}\text{E}$ ) for strong minus weak TBO year composites.

Thus during a strong (weak) TBO year Australian monsoon season (December to February) westerlies (easterlies) are seen in the lower troposphere and stratosphere and propagates to upper troposphere and interacts there.

#### **6.4.5 Zonal temperature anomalies in TBO cycle**

As the zonal wind over these regions showed difference in structure in order to assess the dynamic features of these regions, we analyzed the temperature structure in these regions by similar composite analysis.

##### **6.4.5.1 Indian monsoon region**

Over the Indian monsoon region, the lower troposphere levels have negative temperature anomalies in the previous year upto April month with maximum cooling anomalies over the troposphere region between 500 hPa to 200 hPa (see figure 6.8). But in the upper troposphere the negative anomalies are seen upto June. Positive anomalies sets in the lower troposphere along with the onset of weak monsoon and propagates to midtropshere and attains maximum in between 500 and 200 hPa by next spring season before the strong monsoon. Cool temperature anomalies are seen in the lower stratosphere at this time. The pattern reverses with the onset of strong monsoon with cooling in the troposphere. Thus in the Indian monsoon region, we have temperature maximum in the mid-troposphere and at lower stratosphere of almost similar intensity as seen in figure 6.8.

##### **6.4.5.2 Australian monsoon region**

Vertical temperature in TBO scale over Australian monsoon region is shown in figure 6.9. In the Australian monsoon region cold anomalies in the lower stratosphere in the weak TBO year propagate downward and reach 100 hPa by next year boreal summer monsoon. At this time warm anomalies are seen in the troposphere (figure 6.9). Then the negative anomalies propagate downwards to lower troposphere. Surface was cool from the January itself and it mixes with upward moving negative anomalies below 850 hPa. This anomaly maximum in the lower level is the difference of Australian monsoon pattern from the equatorial pattern

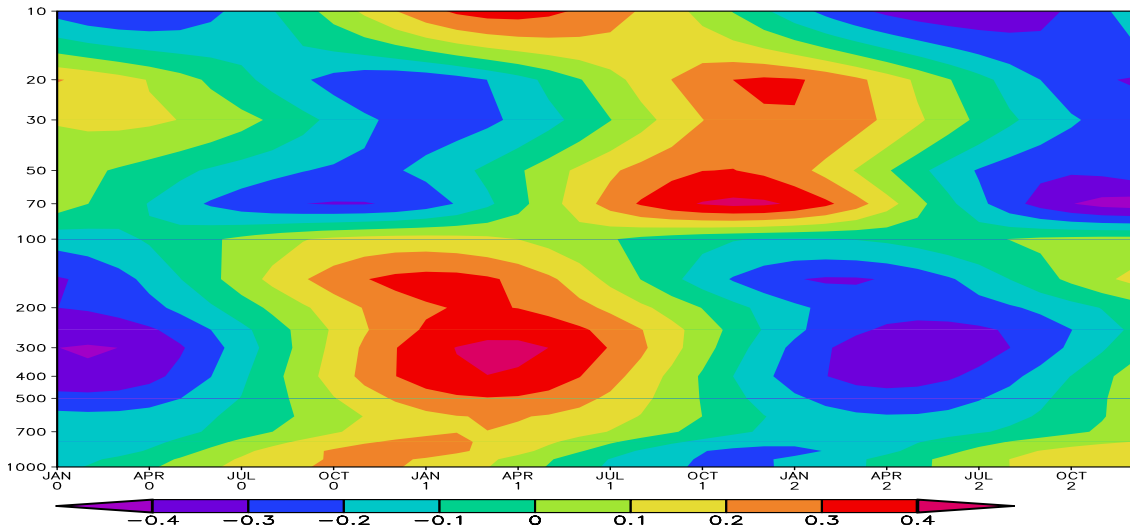


Figure 6.8 : Time –height plot of zonal temperature anomalies over the Indian monsoon region (averaged over 10<sup>0</sup>N-30<sup>0</sup>N, 65<sup>0</sup>E-95<sup>0</sup>E) for strong minus weak TBO years composites.

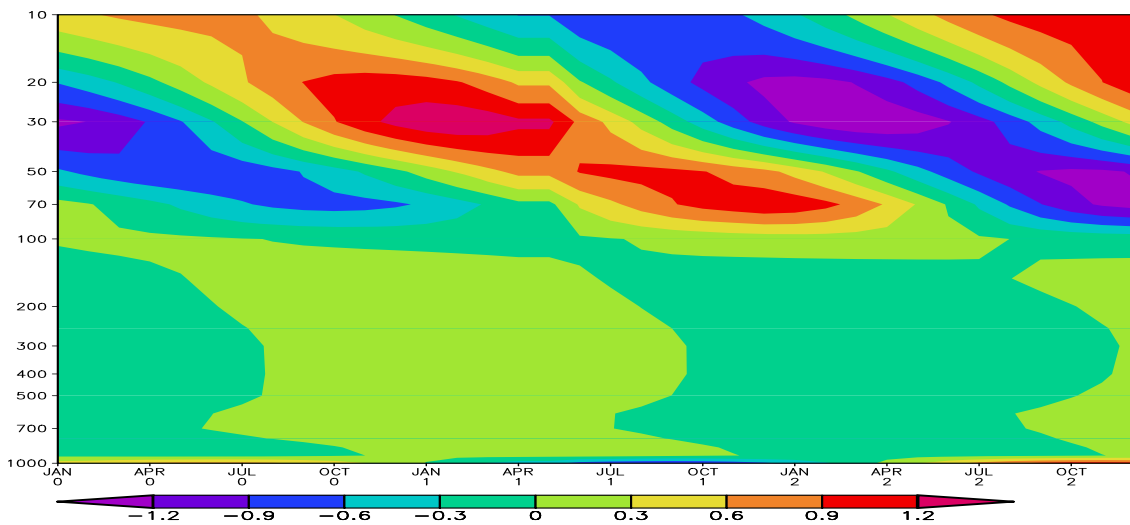


Figure 6.9: Time –height plot of zonal temperature anomalies over the Australian monsoon region (averaged over 10<sup>0</sup>N-30<sup>0</sup>N, 105<sup>0</sup>E-135<sup>0</sup>E) for strong minus weak TBO years composites, from previous year to next year of reference monsoon. Months with 0 correspond to previous year, with 1 to current TBO year and 2 to the next year

### 6.4.6 Relationship between zonal wind over India and Australia with sea surface temperature in TBO cycle

Figure 6.10 below shows the time series of wind at different levels over India and Australia and SST anomalies for strong minus weak composites of TBO cycle from



previous year (months with  $-1$ ) to the next year (months with  $+1$ ) of strong TBO year (months with  $0$ ). The pattern over Indian monsoon region is given in figure 6.10a and b. In lower levels (1000 hPa and 850 hPa) of the troposphere, wind anomaly over Indian monsoon region becomes westerly by boreal winter and attains maximum with strong monsoon and become easterly in the next winter season. Middle troposphere (500 hPa) pattern is opposite to the lower level pattern with positive maximum during weak monsoon and it becomes negative along with the spring season before the strong monsoon and negative maximum is after the onset of strong monsoon. 100 hPa wind becomes negative by winter and maximum value is during July and again becomes positive by next march. At 20 hPa, zonal wind anomaly becomes westerly after the weak monsoon and attains maximum by April and reverses sign by next winter.

Over the Australian monsoon region, surface winds have easterly anomalies in the previous year and maximum easterly is in the previous year winter and becomes westerly by September and westerly anomaly maximum is at the time of strong Australian monsoon (January of next year). 850 hPa also has similar pattern. Mid-troposphere level also has similar pattern, but delayed by four months (figure 6.10c). 100 hPa has opposite pattern of surface anomalies. 20 hPa has westerlies from the previous year September of strong TBO year and attains maximum during the spring season of strong TBO year and starts reversing at the time of onset of strong monsoon over Australia.

SST anomalies in the north Indian Ocean ( $0-25^{\circ}\text{N}$ ,  $60^{\circ}-100^{\circ}\text{E}$ ) becomes positive before the weak monsoon and attains its maximum value in the winter season before the strong monsoon and continues to spring and reverses sign by the onset of the strong monsoon and completes the next half in next one year (see figure 6.10d). The south Indian Ocean ( $0-15^{\circ}\text{S}$ ,  $85^{\circ}-100^{\circ}\text{E}$ ) warms after the weak monsoon attaining maximum warming in the following spring season and cools in the post monsoon season. The *Nino3.4* region ( $10^{\circ}\text{S}-10^{\circ}\text{N}$ ,  $170^{\circ}-120^{\circ}\text{W}$ ) SST anomaly remains positive from the beginning of previous year and attains maximum in the October month and reverses by the onset of monsoon and remains cool till the end of next weak monsoon.

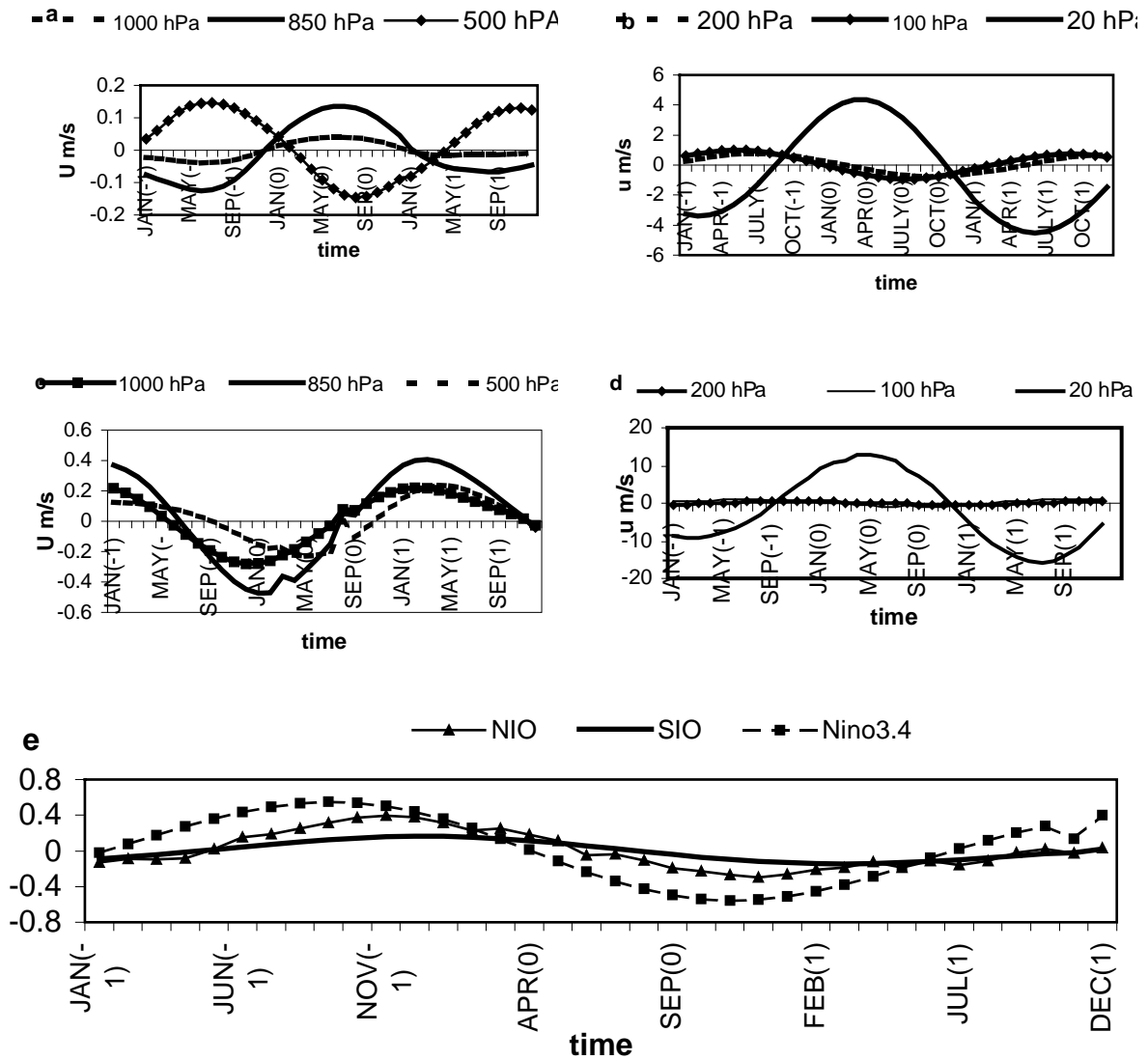


Figure 6.10: Strong minus weak composite of a) ,b) zonal wind over Indian monsoon region, c) over Australian monsoon region and d) SST over north Indian Ocean, south Indian Ocean and equatorial east Pacific. Months with (-1) denotes previous year, 0 current TBO year and +1 next year.

The cross relationship of zonal wind over India and SSTs of both Indian and Pacific Ocean regions are analyzed by Pearson cross correlation analysis of zonal wind at different levels and SSTs of north Indian Ocean (NIO), Southeast Indian Ocean (SEIO) and east equatorial Indian Ocean (Nino3.4) and is shown in figure 6.11. Zonal wind at

20 hPa has insignificant correlation with NIO SST. In the case of 100 hPa wind, the cross correlation is maximum with a lead of 3 months and for 500 hPa it is four month. That is zonal wind at 100 hPa and 500 hPa becomes westerly/easterly a season ahead of north Indian Ocean warming starts. Correlation is insignificant in the surface levels also. Zonal wind at 20 hPa has 1 month lead over SEIO SST (0.28) and the lead increases to two months (0.65) for 100 hPa and is again reduced to one month for midtroposphere level zonal wind. Surface wind has two month lead over SEIO SST. Zonal wind at 20 hPa has lag correlation of 6 months (-0.45) with *nino3.4* SST. 100 hPa has lead correlation of 1 month (0.45) and 500 hPa has 2 month lead (0.66). 700 hPa has 1 month lag (-0.64). Lower levels have negligible correlations (<0.15).

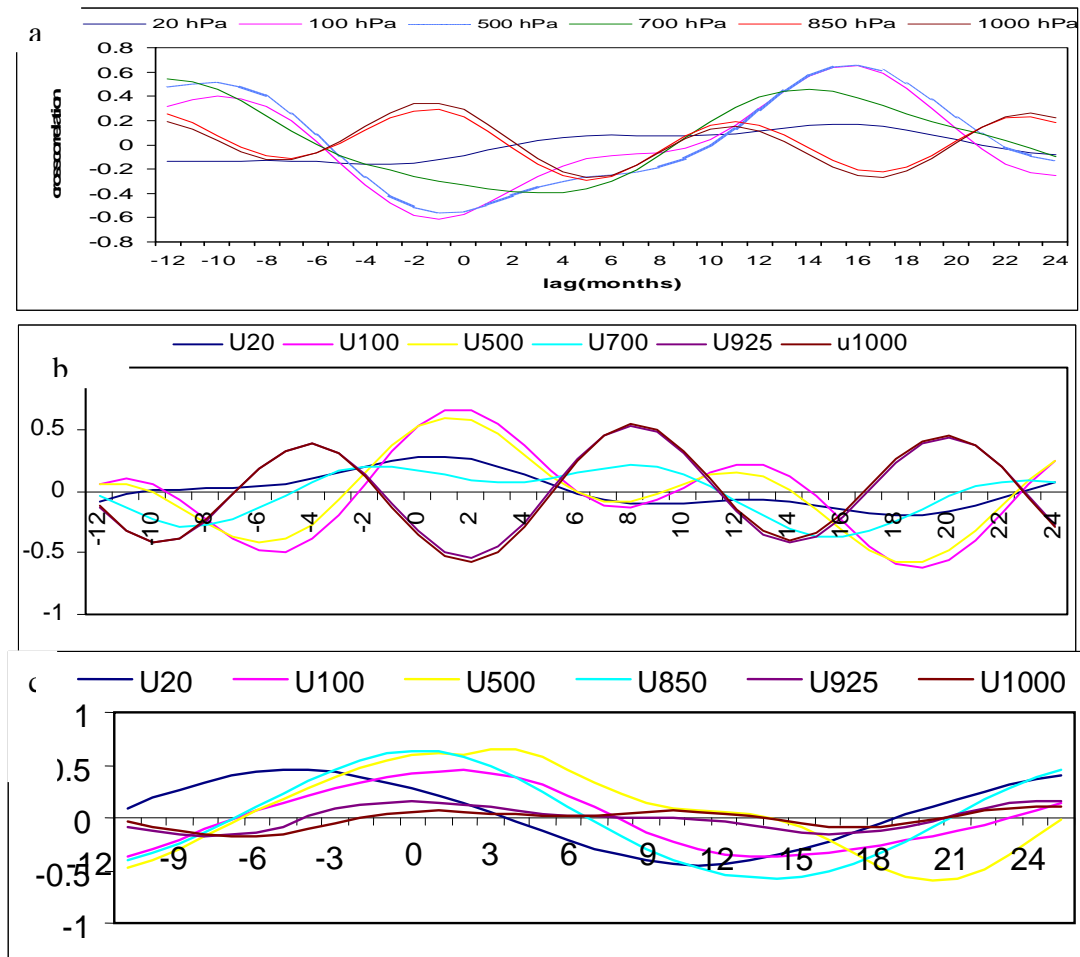


Figure 6.11: cross correlation of a) north Indian Ocean SST, b) Southeast Indian Ocean SST and c) Nino3.4 region SST anomalies with zonal wind at different levels over Indian monsoon region.

It is well known that the autumn season SST anomalies over the southeast Indian Ocean (SEIO) and east Pacific SST (*Nino3.4*) anomalies are important for Australian monsoon in TBO cycle. So the cross correlation of zonal wind over Australian monsoon region is analyzed with SEIO and *Nino3.4* SST anomalies in QBO scale. Lower troposphere winds has a lag of 11 months (0.65) and lead of 14 months with SEIO SST anomalies and lag reduces to 5 months (0.55), for 500 hPa and it has a lead of 15 months also (0.5). 100 hPa has 11 month lag with SEIO SST (0.35). Lower stratosphere has negligible correlation with SEIO SST anomalies. Surface wind has 3 month lag (-0.63) with *Nino3.4* SST (both are in opposite phase) and is four month for 850 hPa (-0.71). Midtroposphere wind leads *Nino3.4* SST by four months (0.64). 100 hPa has one month and 20 hPa has seven month lag with *Nino3.4* SST anomalies.

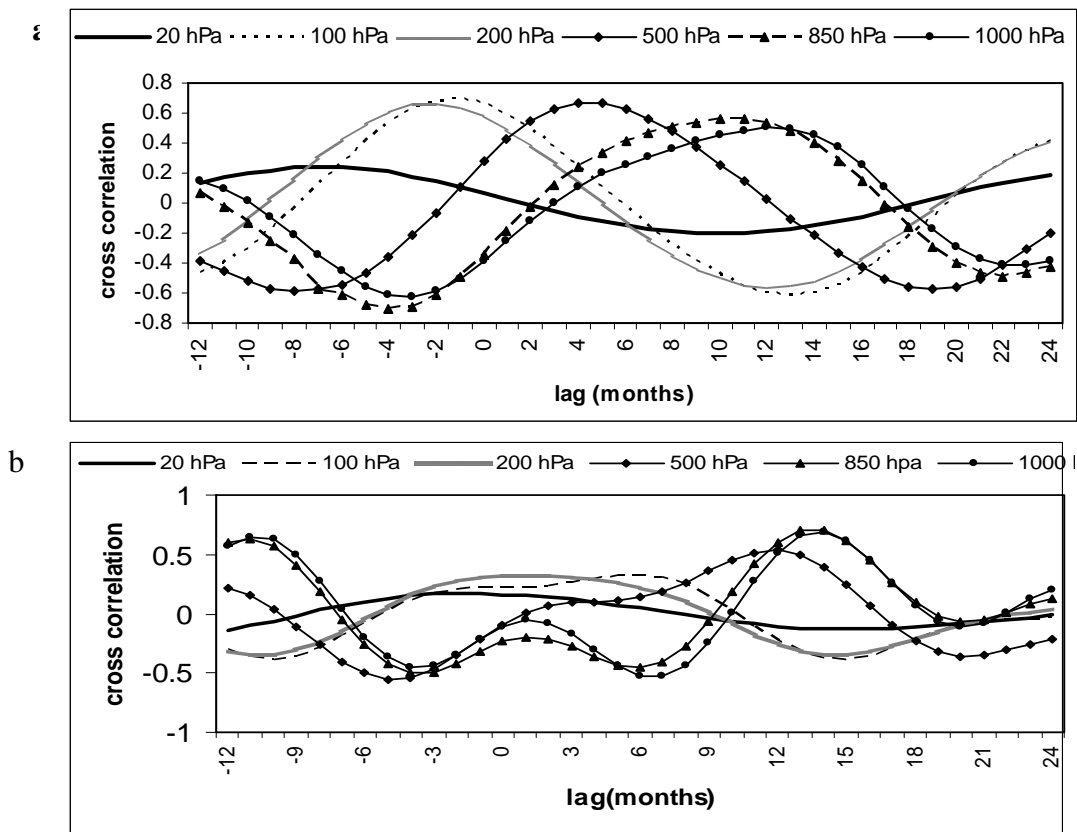


Figure 6.12: cross correlation of a) Southeast Indian Ocean SST and b) *Nino3.4* region SST anomalies with zonal wind at different levels over Australian monsoon region.

### 6.4.7 Effect of QBO on ISMR in biennial time scale

Peculiarities of zonal wind and temperature structure over Indian monsoon are observed in earlier sections. For zonal wind the QBO scale maximum is in lower stratosphere, while for temperature maximum is between 500 hPa and 200 hPa. The effect if these maxima in Indian summer monsoon are analysed with the help of correlation analysis between ISMR and maximum region U wind and temperature time series.

#### 6.4.7.1 Lower stratospheric winds and ISMR

Lag-lead correlation analysis has been carried out between the zonal wind at 30 hPa (u30) and 50 hPa (u50) with ISMR index on biennial time scale. Figure 6.13 shows the correlation from January of the previous year to the next year December of a monsoon season. A significant negative lag correlation exists between u50 over India and ISMR with maximum value of -0.5 at the pervious December. It is interesting to note that the correlation is negligible during the early phase of monsoon and the positive correlation dominates in the later months of the monsoon and attains the maximum in the early month of next year. Similar analysis is also carried out between u30 hPa and ISMR. In this case the correlation becomes positive in the previous winter season before the monsoon and the simultaneous correlation becomes highly significant (0.6). The maximum lag correlation is in the previous year monsoon.

It is also noted that the anomaly of the summer monsoon is very much associated with the phase of QBO at 50 hPa during the previous winter season. During the winter season, before an active monsoon year, the QBO is in its easterly phase at 50 hPa level and in opposite phase for weak monsoon years. The association becomes very strong during the TBO years of Indian summer monsoon. The zonal wind anomaly at 30 hPa level also shows a strong association to the summer monsoon activity over the Indian subcontinent. It appears that the lower stratosphere interact with tropospheric circulation, especially over the monsoon region.

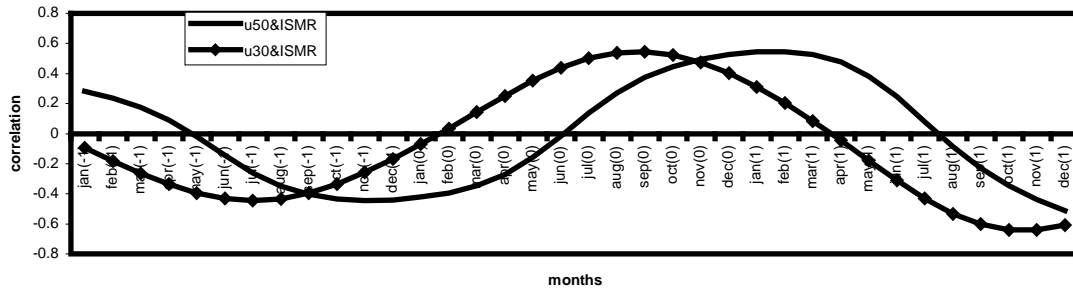


Figure 6.13 : Correlation of Indian summer monsoon rainfall with zonal wind at 30 and 50 hPa levels over Indian monsoon region from previous year (-1) to next year(1) of a reference monsoon (0)

**6.4.7.2 Upper troposphere temperature and Indian summer monsoon rainfall**

A Lag-lead correlation of the average temperature of maximum area (500 hPa to 200 hPa) with ISMR index is carried out on the biennial scale for 1950-2002 TBO years. Figure 6.16 shows the correlation from the previous year (months with -1) January to next year (months with +1) December of strong TBO year (months with 0). The correlation becomes positive after the weak monsoon and attains positive during the March before the strong monsoon it peaks (0.73) and then reverses after the strong monsoon. From the figure 6.8 we saw that the temperature at this level has maximum positive value in the spring season before the strong monsoon and negative maximum in the spring season of weak monsoon. The correlation maximum is also this time. Thus the temperature maximum at this region has prominent relationship with monsoon rainfall over India.

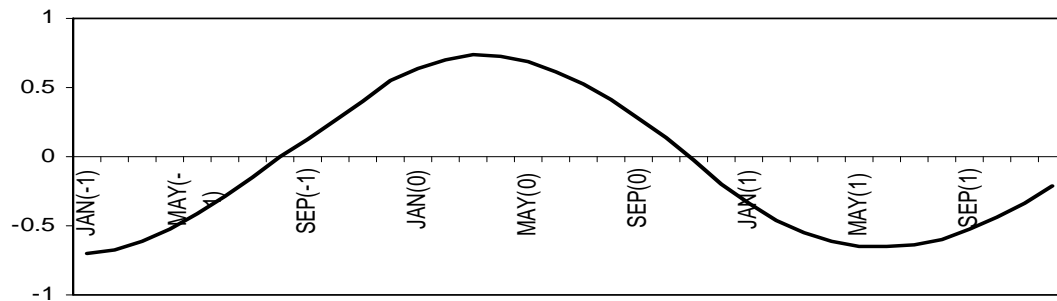


Figure 6.14: Correlation of zonal temperature averaged over 500 to 200 hPa over India with ISMR index from previous year (-1) to next year (+1) of monsoon (0).

## 6.5 Discussion

Both the QBO scale time series and cross correlation analysis indicates the downward propagation of zonal wind from the lower stratosphere to tropopause over Indian and Australian monsoon region. It takes one year to reach tropopause from 20 hPa level over Indian monsoon region and only ten months over Australian monsoon region. Over the Indian monsoon region, the stratosphere winds propagate to the troposphere, though weakened at tropopause level. In TBO cycle this pattern is very clear with three different layers in the troposphere. In the Australian monsoon region pattern is different with downward propagation in the lower stratosphere and upward propagation in the lower troposphere and interaction is at the tropopause level. Temperature pattern over the Indian monsoon region is also peculiar with additional source (sink) in the middle and upper troposphere region, which strengthens in the spring season. The spring season anomaly is important for the TBO mechanism.

In TBO cycle, 20 hPa westerly maximum is at spring season before monsoon and 1000 hPa maximum is during summer, with a three month lead for 20 hPa as observed in Pearson cross correlation. 20 hPa wind has insignificant correlation with North Indian Ocean SST, but 100 and 500 hPa leads north Indian Ocean SST by a season. 20 hPa zonal wind leads southeast Indian Ocean SST by one month and equatorial east Pacific SST leads stratosphere zonal wind by six months. Thus warm SST in the equatorial east Pacific facilitates the zonal wind at 20 hPa six months later. This 20 hPa zonal wind affects southeast Indian Ocean SST a month after. Southeast Indian Ocean SST, which attained maximum warming in the March season before the strong Indian summer monsoon influences the surface Australian summer monsoon wind in the beginning of next calendar year. The relationship of SEIO SST reverses at tropopause level. At the same time equatorial east Pacific SST has 3 month lead over Australian monsoon surface winds with correlation of  $-0.63$ . The negative correlation indicates that cool SST in the east Pacific affects the westerlies over Australian monsoon region, a season earlier. The 20 hPa wind over Indian and Australian monsoon region has similar pattern over both Indian and Australian monsoon region indicating the absence of southeast

movement in the stratosphere, which is major property of TBO in the troposphere. By the above mechanism QBO scale zonal winds and TBO scale SST are correlated with a cyclic processes in the Indo-Australian monsoon region and topical Indo-Pacific Oceans.

## 6.6 Conclusion

The QBO in lower stratosphere wind and temperature is evident in both Indian and Australian monsoon region for TBO cycle. The downward propagating stratospheric zonal winds penetrate deep into the troposphere over the Indian monsoon region, while downward propagating stratospheric zonal winds and upward propagating winds from the lower troposphere meet in the upper troposphere over Australian monsoon region. Propagation of zonal wind anomalies over the Indian monsoon region at different levels is with different speed. An additional source (sink) of temperature is present in between the middle and upper troposphere over Indian monsoon region a season before strong (weak) monsoon. Zonal winds over Indian ant middle and upper troposphere have lead correlation with north Indian Ocean SST, while 20 hPa wind leads southeast Indian Ocean SST. Southeast Indian ocean SST affects the surface wind of Australian summer monsoon season. The east Pacific SST leads lower stratosphere zonal wind of both Indian and Australian monsoon region. Thus QBO scale zonal wind over Indian and Australian monsoon region is closely related to tropical Indian and Pacific Ocean SST anomalies in TBO scale.



---

## **Effect of late 1970's Climate Shift on Interannual Variability of Indian Summer Monsoon Associated with TBO**

---

### **7.1 Introduction**

Biennial variability has been identified as one of the major modes of interannual oscillation in the troposphere in the various parts of the tropical Indian and Pacific regions. (Trenberth, 1975; Mooley and Parthasarathy, 1984; Kawamura, 1988; Lau and Sheu, 1988; Rasmusson et al., 1990; Ropelewski et. al, 1992). This biennial variability in the troposphere is named as tropospheric biennial oscillation (TBO, Meehl, 1997; Meehl and Arblaster, 2001) in order to differentiate it from the stratospheric QBO. TBO includes periods of both persistence and transitions. The persistence is reflected in the same sign of anomalies between the Indian summer monsoon and following Australian summer monsoon (Meehl, 1987). The transition occurs in northern spring for Indian summer monsoon and northern fall for Australian summer monsoon. The transition between the years is characterized by large-scale coupled land-atmosphere-ocean interactions in the Indian and Pacific Ocean regions (Meehl, 1997). Different mechanism proposed to explain the formation and characteristics of TBO are described in chapter 1. At present TBO is considered as the result of large scale coupled interaction between land-atmosphere-ocean in the Indo-Pacific region and SST anomalies of both these oceans has major role in TBO and it includes Asian and Australian monsoon.

The tropical climate system has undergone many secular changes on interdecadal timescales as the climate shift occurred in 1976. Along with the climate shift, significant increase in SST was found in the tropical central and eastern Pacific and

Indian Ocean and these changes were linked to enhanced tropical convective activity (Nitta and Yamada, 1989; Wang, 1995). Following this climate shift in the tropical Pacific, many properties of ENSO, such as frequency, intensity and the direction of propagation have changed (Trenberth, 1990; Wang, 1995). In addition, the ENSO period appears to have increased to five years since the 1980's. Clarke et al. (2000) put forward the idea that the 1976 climate shift influences the relationship between Indian Ocean SST and Indian summer monsoon. The long-recognized negative correlation between Indian monsoon rainfall and ENSO has weakened rapidly during recent decades. Many previous studies have explored the possible reasons for the weakening of the ENSO-monsoon relationship (Webster and Palmer, 1997; Kumar et al., 1999; Chang et al., 2001; Kinter et al., 2002). Kumar et al. (1999) pointed out the southeastward shift in the Walker circulation anomalies of ENSO after the 1976 climate shift and increased surface temperature over Eurasia in winter and spring as reasons for the weakening of ENSO-monsoon relationship. Kinter et al. (2002) related the change in monsoon-ENSO relationship to changes in the atmospheric circulation over the entire Pacific Ocean, which entered a new regime about 1976. The difference in monsoon evolution associated with ENSO and the ENSO-monsoon relationship before and after the climate shift is described in Annamalai and Liu (2005). Terray et al. (2005) stressed the increased role of southeast Indian Ocean in monsoon-ENSO relationship from the late 1970's onwards.

The monsoon rainfall itself has decadal variations as observed by Torrence and Webster (1999). The strength of TBO is modulated by interdecadal variability, weakening in some decades and strengthening in other (Torrence and Webster, 1999). Thus it will be interesting to investigate the effect of 1976 climate shift in TBO and its interaction with monsoon. More over most of the studies on TBO (eg: Meehl and Arblaster 2001; 2002a) used data sets after 1976 to study the properties of TBO

## **7.2 Objective of the study**

All of the previous studies on climate shift were concentrated on the changes of El Nino properties and the monsoon-ENSO relationship. Like ENSO, the strength of TBO is also modulated by interdecadal variability, weakening in some decades and

strengthening in other. Whereas the ENSO involves ocean-atmosphere processes mainly in the Pacific, TBO involves larger scales with Asian–Australian monsoon and entire tropical Indian and Pacific Ocean basins. So the basic state changes associated with Pacific Ocean climate shift can have an influence in the biennial variability of monsoon also. As the regime shift of 1976 affected the basic state parameters like tropical SST, it may cause definite changes on the parameters, which depend on the air sea interaction processes in the tropical regions. This chapter analyses the TBO cycle of Indian summer monsoon before and after climate shift. It also addresses the role of ENSO and local Indian Ocean process in TBO and Asian–Australian monsoon relationship on the context of climate regime shift.

### **7.3 Data and methodology**

The basic datasets used in this study include vertical velocity at 500 hPa, sea level pressure and 200 hPa velocity potential, latent heat flux obtained from the National Center for Environmental Prediction/ National Center for Atmospheric Research (NCEP/NCAR) reanalysis (Kalnay et al., 1996) for the 1950-2005 period. NCEP SST and Indian summer monsoon rainfall (ISMR) index (Parthasarathy et al., 1994) are also used. India Meteorological Department gridded rainfall data (Rajeevan et al., 2005) is also used to analyze the rainfall pattern in both the periods.

Changes occurred to prominent modes of variabilities of Indian summer monsoon rainfall and ocean-atmosphere parameters of the Indo-Pacific region due to climate shift are identified with the help of empirical orthogonal function (EOF) analysis. EOF analysis has been carried out for Indian Ocean ( $30^{\circ}\text{S}$ - $30^{\circ}\text{N}$ ,  $40^{\circ}\text{E}$ - $120^{\circ}\text{E}$ ) seasonal SST anomalies, summer season velocity potential at 200 hPa of the Indo-Pacific area ( $30^{\circ}\text{S}$ - $60^{\circ}\text{N}$ ,  $40^{\circ}$ - $80^{\circ}\text{E}$ ), and Indian region ( $6.5^{\circ}\text{N}$ -  $35^{\circ}\text{N}$ ,  $67^{\circ}\text{E}$ - $100^{\circ}\text{E}$ ) monsoon rainfall. The 25 year time period from 1951 to 1975 is denoted as PRE76 and the next 25 year period from 1978 to 2002 as POST76. The period after 2002 is avoided as some changes in pattern are reported after 2002 for some of the parameters. The spectral analysis of the time series of the each prominent mode were carried out in both the periods to identify the changes in periodicities associated with climate shift.

TBO years and ENSO years are defined as in earlier chapters from ISMR index and *nino3.4* SST anomalies. According to the above definitions of TBO and ENSO, we have 15 TBO years in the PRE76 period like 1953, 1956, 1959, 1961, 1964, 1970, 1973 (strong TBO years) and 1951, 1957, 1960, 1962, 1965, 1968, 1972, 1974 (weak TBO years), in which 4 are associated with El Nino onset years (1951, 1957, 1965, 1972) and another 4 with La Nina onset years (1956, 1964, 1970, 1973). In the POST76 period we have 14 TBO years (1978, 1980, 1983, 1988, 1990, 1994, 1997 (strong TBO) and 1979, 1982, 1987, 1992, 1995, 2000, 2002 (weak TBO) in which only 4 is associated with El Nino onset years (1982, 1987, 1997, 2002) and 1988 with La Nina. Strong minus weak composite analysis is carried out for TBO years with and without ENSO from the onset of a strong Asian monsoon at the summer season denoted as JJA0 to next year summer (JJA+1) separately for both the PRE76 and POST76 periods. Latent heat flux and low-level moisture convergence data sets of NCEP/NCAR reanalysis are also used to identify the role of local processes in monsoon transition in both the epochs.

## **7.4 Results**

### **7.4.1 EOF analysis**

EOF analysis is carried out for Indian Ocean SST, 200 hPa velocity potential, Indian summer rainfall etc to investigate the prominent pattern of these parameters in these two epochs to assess the difference in pattern before and after climate shift.

#### **7.4.1.1 Seasonal Indian Ocean SST anomalies**

Figure 7.1 below shows the time series of prominent pattern (EOF1) of seasonal SST anomalies of Indian Ocean SST for spring, summer, autumn and winter season from 1951-2002. From the time series it is evident that Indian Ocean has clear warming trend from late 1970's for all the four seasons. Thus with the climate regime shift in the Pacific, Indian Ocean SST also changed from a cold epoch to a warm epoch.

The EOF analyses of seasonal SSTs of Indian Ocean in both the periods were carried out separately and wavelet analysis of PC's of both the periods identifies the prominent frequencies in both the periods. The figure 7.2 shows the prominent periodicities of first three EOFs of spring season SST in two epochs. In the figure

first two patterns shifted to lower frequency in the POST76 period and variance of these are reduced significantly. The third EOF has both 2-3 year and 3-7 year periodicity in the PRE76 period and after shift the 2-3 year periodicity peak just shifted, but variance gets increases with climate shift.

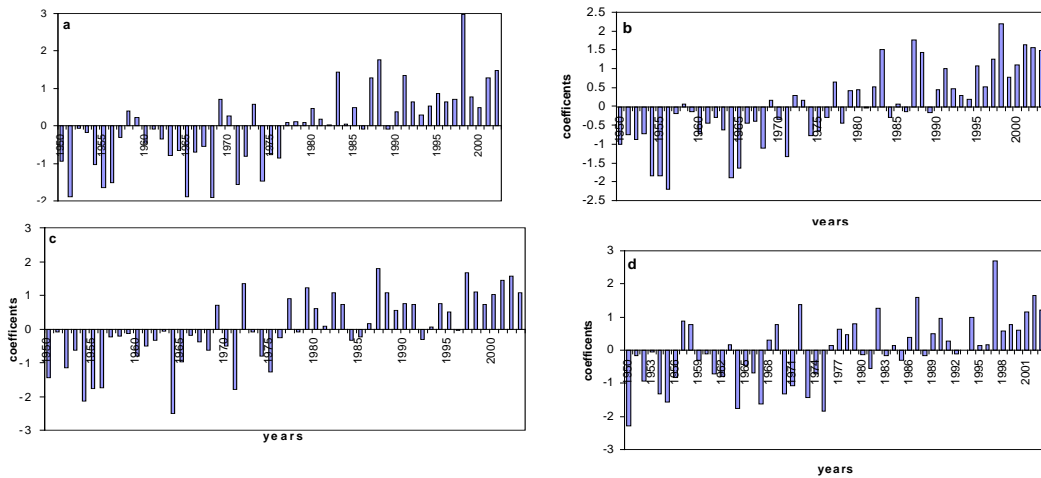


Figure 7.1: Time series of first EOF (PC) of Indian Ocean (30°S-30°N, 40°-120°E) SST anomalies for different seasons (a) spring (MAM) (b) summer (JJA) (c) autumn (SON) and (d) winter (DJF).

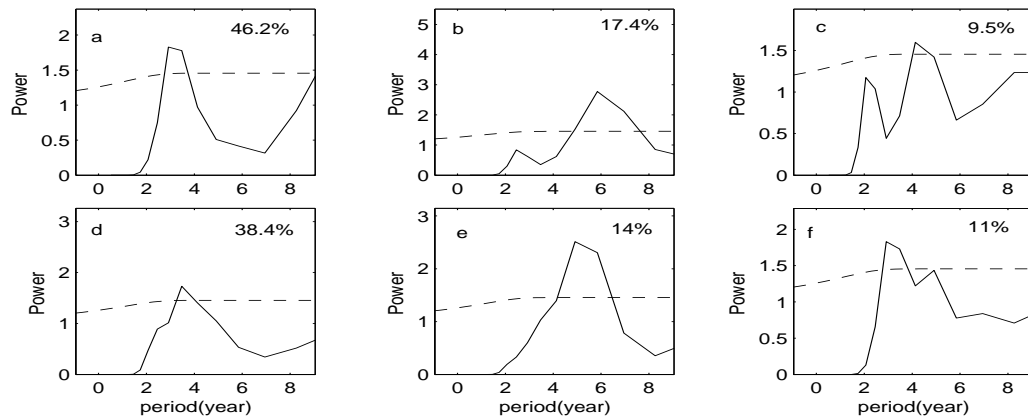


Figure 7.2: wavelet global spectrum of PC's of spring season SST anomalies of Indian Ocean. (a) PC1 for PRE76 period, (b) PC2 for PRE76, (c) PC3 for PRE76. (d), (e) and (f) for POST76 periods. Variance of each PC in percentage is marked in the top right corner and 95% significant level is marked with dotted lines.

In the summer season also first two patterns are shifted to lower frequency along with climate shift and variance also reduced. The third pattern changes to a periodicity between 2 and 3.5 year with increased variance (see figure 7.3).

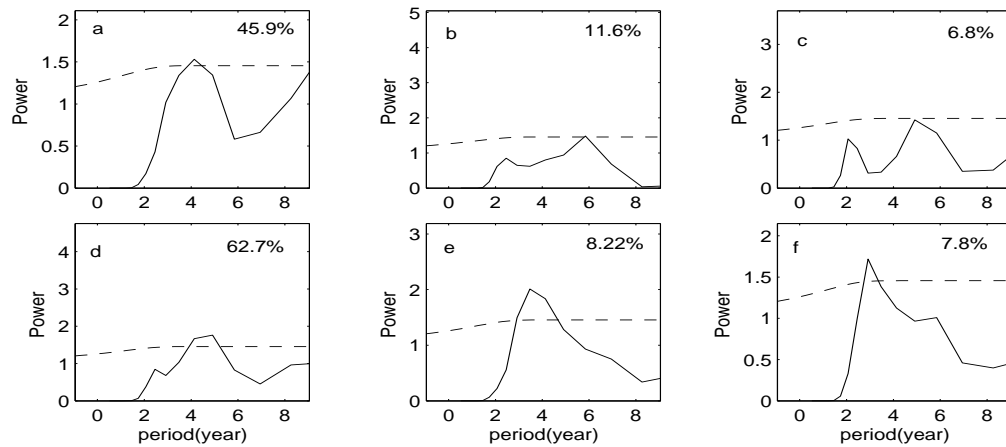


Figure 7.3: wavelet global spectrum of PC's of summer season SST anomalies of Indian Ocean. (a) PC1 for PRE76 period, (b) PC2 for PRE76, (c) PC3 for PRE76. (d), (e) and (f) for POST76 periods. Variance of each PC in percentage is marked in the top right corner and 95% significant level is marked with dotted lines.

In the autumn season (SON) variance is increased for third PC only and it has a significant periodicity between 2-4 year period for Indian Ocean SST anomalies in figure 7.4.

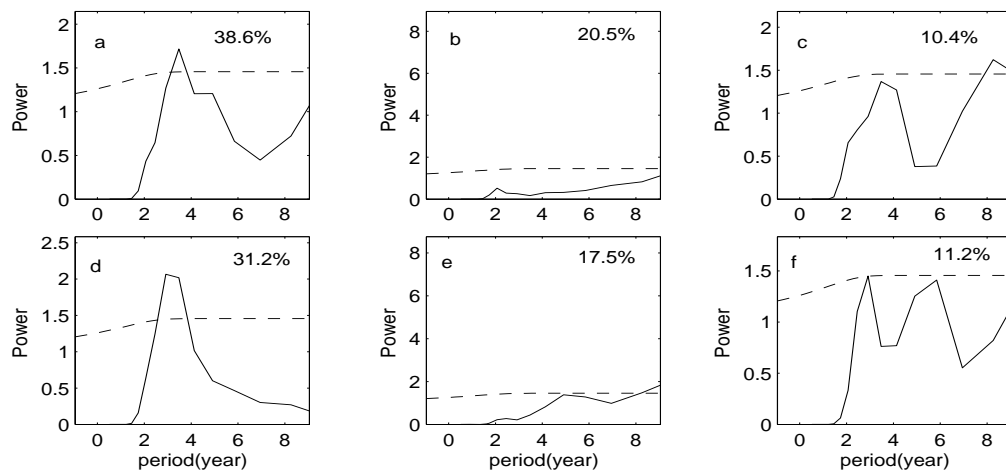


Figure 7.4: wavelet global spectrum of PC's of autumn season SST anomalies of Indian Ocean. a) PC1 for PRE76 period, b) PC2 for PRE76, c) PC3 for PRE76. d, e and f for POST76 periods. Variance of each PC in percentage is marked in the top right corner and 95% significant level is marked with dotted lines.

In the winter season, the periodicity of both PC1 and PC2 is 2-6 year in both the epochs. But the variance is reduced for first PC and is increased for second one. The third pattern shifted to about 3 year periodicity after the climate shift and variance is increased with climate shift as seen from figure 7.5.

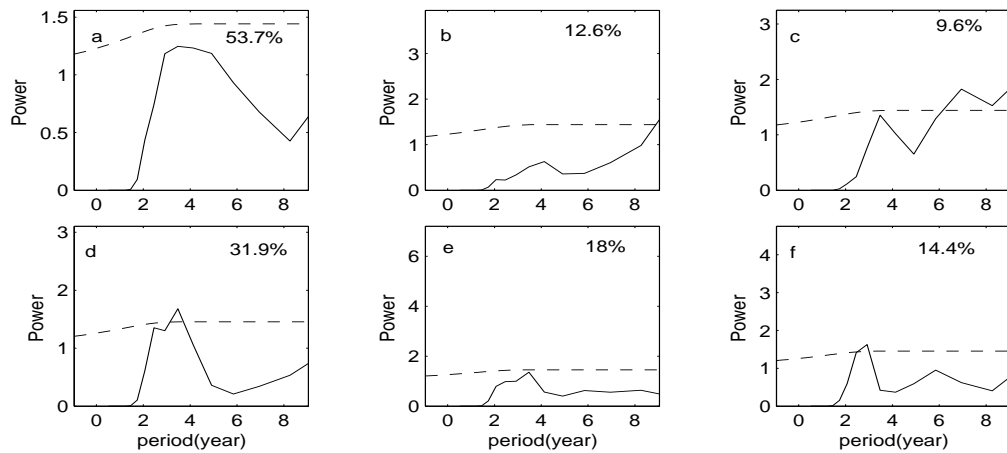


Figure 7.5: wavelet global spectrum of PC's of winter season SST anomalies of Indian Ocean. a) PC1 for PRE76 period, b) PC2 for PRE76, c) PC3 for PRE76. d, e and f for POST76 periods. Variance of each PC in percentage is marked in the top right corner and 95% significant level is marked with dotted lines.

#### 7.4.1.2 Summer season velocity potential at 200 hPa

The changes in the periodicity and variance of velocity potential at 200 hPa identifies the changes associated with Walker circulation linking Indo-Pacific regions and is shown in figure 7.6.

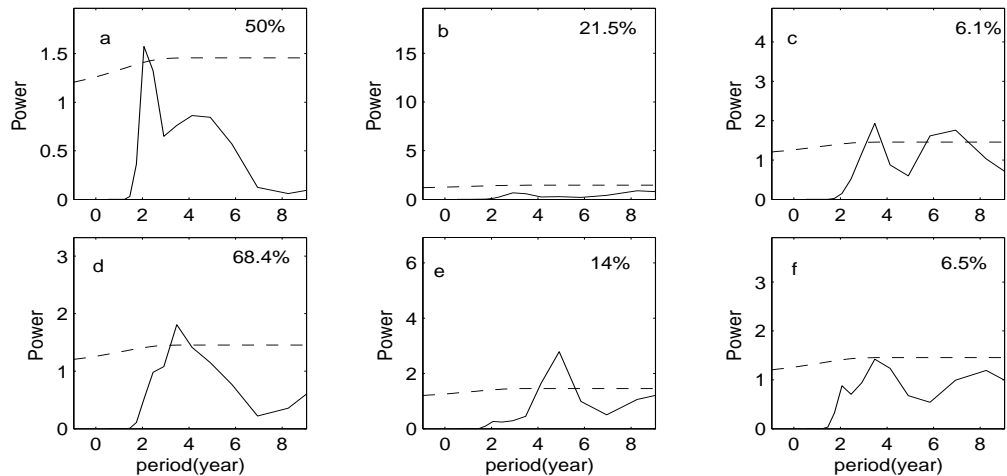


Figure 7.6: wavelet global spectrum of PC's of summer season 200 hPa velocity potential anomalies. (a) PC1 for PRE76 period, (b) PC2 for PRE76, (c) PC3 for PRE76. (d), (e) and (f) for POST76 periods. Variance of each PC in percentage is marked in the top right corner and 95% significant level is marked with dotted lines.

In the PRE76 period, the first EOF has biennial periodicity and explained 50% of the total variance. After the climate shift the variance increased to 68.4%, but frequency shifted to 2-6 year. The second pattern also shifted to lower frequency with reduced

variance. The third pattern has biennial periodicity after the climate shift, but is well below significant level.

#### 7.4.1.3 Indian summer monsoon rainfall anomalies

The EOF analysis of summer season rainfall over the Indian monsoon region is carried out for both the PRE76 and POST76 periods separately. The wavelet of first three PC's and its variance is given in the figure 7.7 for both the epochs. The first EOF has a periodicity between 2 and 3.5 in both the time periods and its variance is reduced from 30% to 23% with climate shift. The second pattern has a low frequency in the PRE76 period and it shifted to biennial frequency after 1976. But the variance of the pattern is reduced from 20% to 13%. The variance of the third pattern increased from 9% to 10%, but periodicity shifted to lower frequency range.

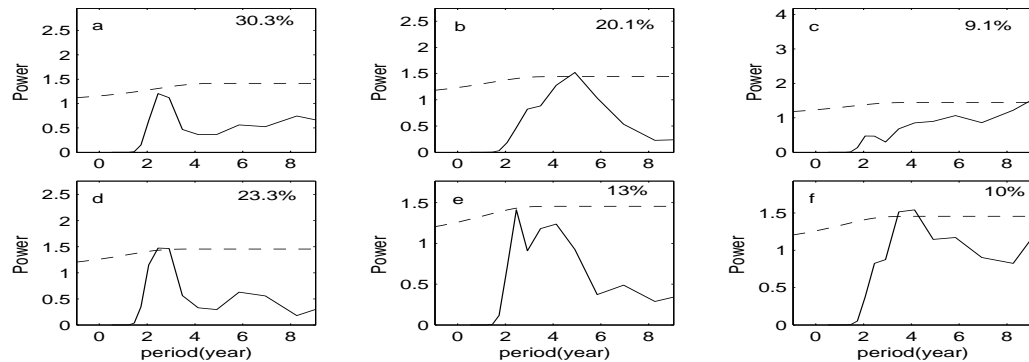


Figure 7.7: wavelet global spectrum of PC's of summer season 200 hPa velocity potential anomalies. (a) PC1 for PRE76 period, (b) PC2 for PRE76, (c) PC3 for PRE76. (d), (e) and (f) for POST76 periods. Variance of each PC in percentage is marked in the top right corner and 95% significant level is marked with dotted lines.

Thus both the Indian summer monsoon rainfall and Indian Ocean SST has biennial periodicity in both the epochs, while it is not appearing as a prominent periodicity for Walker circulation in the POST76 era. This may be the influence of ENSO, which shifted to longer time periods along with the climate shift. As the biennial periodicity for rainfall is evident in both the epochs, the TBO cycle associated with interannual variability of Indian summer rainfall is analysed in both the epochs in the next section

#### 7.4.2 TBO mechanism before and after the shift

The TBO mechanism is presented for both the PRE76 and POST76 periods separately as in the form of strong minus weak TBO year composites. SST, velocity



potential and divergence at 200 hPa over the Indo-Pacific regions are used to represent the large scale features associated with TBO and moisture convergence and local Hadley circulation over the Indian region and adjacent Ocean are used to analyse the local processes in both the epochs. The results are presented in the form of composite analysis from strong summer monsoon (JJA0) to next year summer (JJA1).

#### ***7.4.2.1 SST composite***

Strong minus weak TBO year composite of SST for both the PRE76 period and POST76 period is shown in figure 7.8. In figure left panels are for PRE76 and right one for POST76 epochs.

Along with the onset of strong monsoon in JJA0, cooling in the Indian Ocean confines to north Indian Ocean for PRE76 TBO years, while the north and southeast Indian Ocean is cool in the POST76 TBO years (figure 7.8 top panels). In the Pacific Ocean, the cooling in the eastern region extends to central Pacific in the 1951-1975 period, while cooling starts in the central equatorial Pacific itself in POST76 period. Prior to 1976 cooling in the Indian Ocean extends to the equator by SON0 and the negative anomaly from the equatorial east Pacific extended to west. But in the POST76 period Indian Ocean remains as such and the negative anomaly extends both eastward and westward from the central Pacific. In the PRE76, entire Indian Ocean is cooled in the boreal winter season DJF0 and the anomalies persist to next seasons. Cooling in the DJF0 is confined to the Arabian Sea and equatorial eastern Indian Ocean and negative in the Pacific extends to both sides of the equator in the POST76 period.

Extreme southeast Indian Ocean is warm in the MAM1 season of POST76 period. In the POST76 period the extreme east Pacific cools only by MAM1, while it was started cooling before the strong monsoon in PRE76 periods. In the next monsoon season (JJA1), before the shift entire Indian Ocean was cool, but Oceans adjacent to Indian continent and south Indian Ocean is warm in the POST76 era and cooling in the equatorial Pacific still persists. Thus biennial reversal of SST anomalies from JJA0 to JJA1 is evident in the Indian Ocean after the shift, while in the Pacific it was clear before the shift.

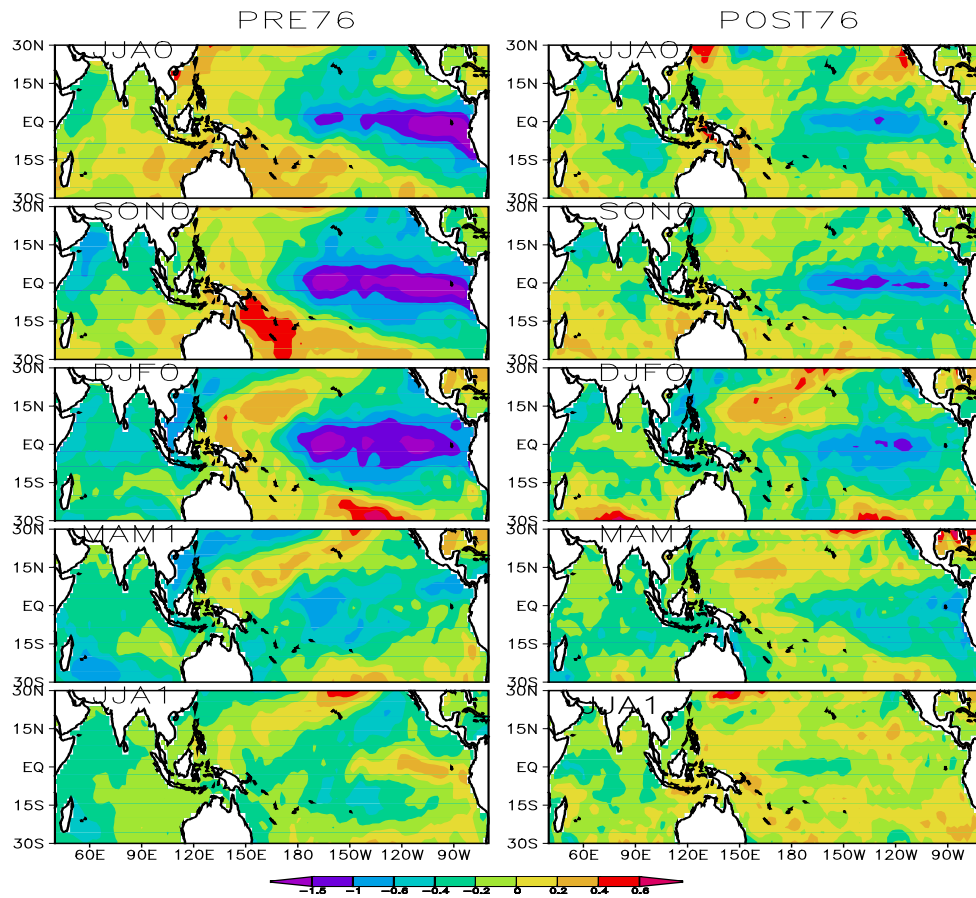


Figure 7.8: Strong minus weak TBO year composite of SST for PRE76 (1951-1975) and POST76 (1978-2002) period.

#### 7.4.2.2 Velocity potential at 200 hPa

Upper troposphere (200 hPa) velocity potential can be used as a good indicator for Walker circulation. Upper level convergence/divergence coincides with lower level divergence/convergence and so centers of upward motion can be identified from figure 7.9. During the strong monsoon season, the entire Indian Ocean was the area of divergence at 200 hPa before 1976 (figure 7.9a). After 1976 climate change, southeast Indian Ocean turns to be an area of convergence for TBO years and convergence in the east Pacific moves further east (figure 7.9b). After the monsoon the anomalies moves southeast from Indian region in both the epochs. But in the POST76 period center of divergence moves to west Pacific instead of concentrating over Indonesian region and convergent center appears over western Indian Ocean as seen from the figure 7.9d. In the boreal winter of second period (1978-2002) TBO

years, the divergent center is over east of Australia whereas it was over north of Australia in the first period. By the next spring divergence center appears over Indian region after 1976. During JJA1 upper level convergence is over western Indian Ocean in both periods, but after the shift, divergence center appears over eastern Pacific.

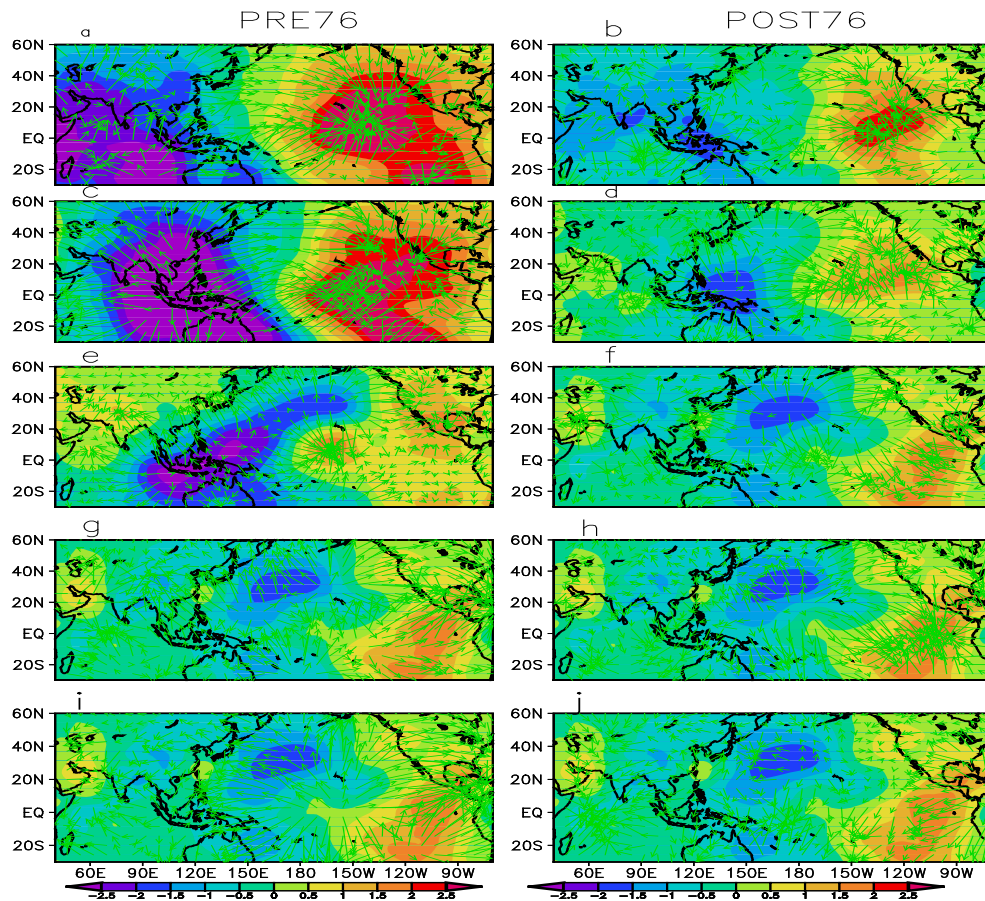


Figure 7.9: Strong minus weak TBO year composite of 200 hPa velocity potential and wind convergence for PRE76 (1951-1975) and POST76 (1978-2002) period. (a) for JJA0, (c) for SON0, (e) for DJF0, (g) for MAM1 and (i) for JJA1 of PRE76 period and (b), (d), (f), (h), (j) for these seasons in PST76 period

#### 7.4.2.3 Local Hadley circulation of summer monsoon.

The local Hadley circulation between the Indian continental region and the equatorial ocean has significant role in the monsoon circulation. The local Hadley circulation is represented by the vertical velocity at 500-hPa level in figure 7.10. The negative value represents upward motion and positive indicates downward motion. In both the periods upward motion is over India and downward anomalies are over

north Indian Ocean for strong TBO years indicating strong local circulation between India and adjacent oceans. During next year, downward motion is seen over India and adjacent oceans for all TBO years of 1951-1975 period making local Hadley circulation insignificant. After the shift, JJA1 has opposite pattern to that of JJA0. Thus the role of local Hadley circulation in both the phases of TBO (positive and negative) is evident after the climate shift.

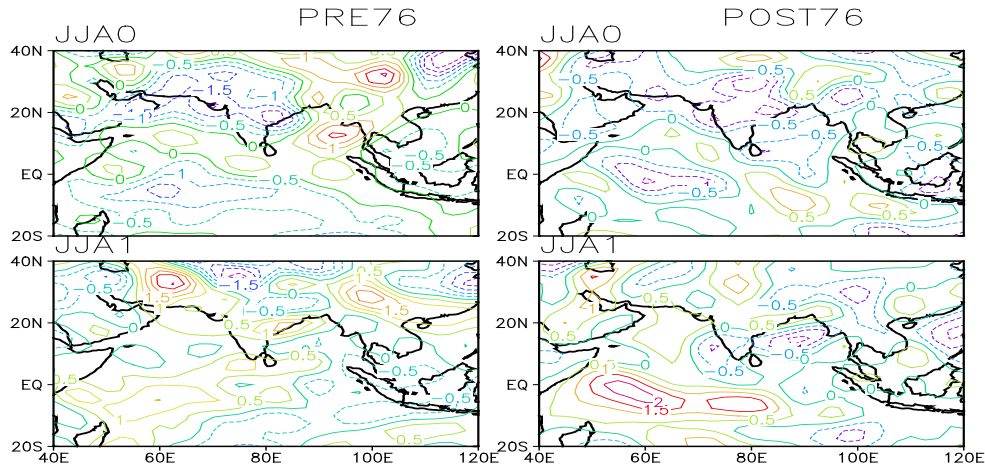


Figure 7.10: Strong minus weak TBO year composite of vertical velocity at 500 hPa for PRE76 (1951-1975) and POST76 (1978-2002) period.

**7.4.2.4 Moisture convergence associated with biennial cycle of monsoon**

Moisture convergence over Indian monsoon region is analyzed from three season earlier to monsoon for both the epochs in figure 7.11 for TBO composite.

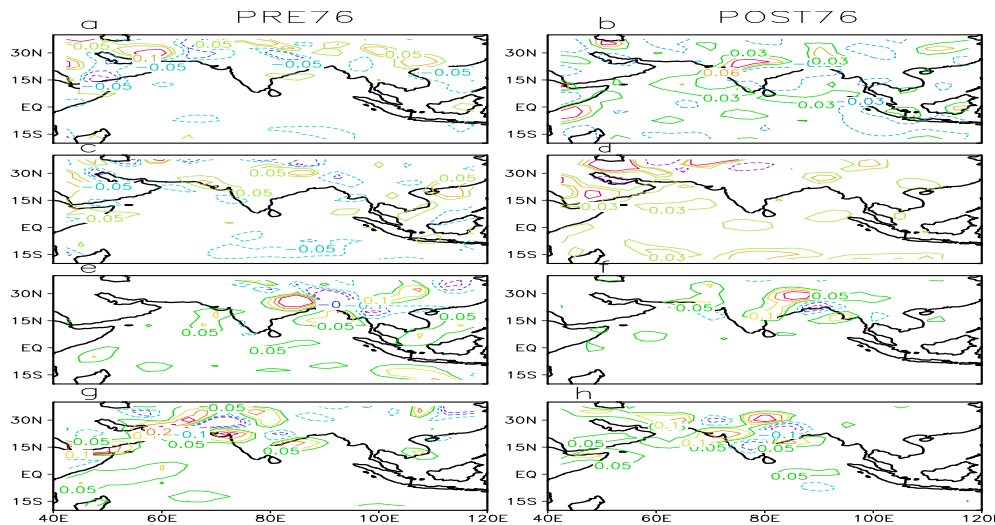


Figure 7.11: strong minus weak TBO year composite of moisture convergence anomalies in the PRE76 and POST76 period. Figure a and b for SON-1, c and d for DJF-1, e and g for MAM0 and g and h for JJA0.

Eventhough convergent anomaly is present over India in both the epochs from SON-1 for TBO years, in the post climate shift era, the convergent center appears over the central Indian region (see figure 7.11b). In the following boreal winter season it was over western side of Indian region in the PRE76 period (figure 7.11c), but after the shift convergence is located over Arabian Sea and eastern part of India (figure 7.11d). Moisture convergence is seen over the western as well as eastern side of India in the spring season and also in the monsoon season in both the epochs (see figure 7.11e-h). Thus after the climate shift, moisture convergence over India is one season earlier than the PRE76 period.

### **7.4.3 Effect of ENSO on TBO cycle**

A similar analysis of TBO years in the absence of ENSO will help us to understand the role of ENSO in modulating the TBO cycle in both these epochs. For this, the TBO years which coincide with ENSO onset years in the Pacific are excluded from the analysis.

#### **7.4.3.1 SST composites**

SST composite of strong minus weak non-ENSO (normal) TBO years in both the PRE76 and POST76 periods are shown in the figure 7.12. During the strong monsoon season, equatorial eastern Indian Ocean is also cooled in the absence of ENSO for PRE76 TBO years and the cooling in the east Pacific confines to extreme east. Cooling spreads in the entire north Indian Ocean by SON0 and it moves to equatorial and south Indian Ocean by next spring, MAM1. Cooling in the west Pacific moves to central Pacific by December for the PRE76 non-ENSO TBO years and entire equatorial Pacific is cooled during MAM1. After the shift removal of ENSO has only effect in the central Pacific making it warm upto spring in figure 7.12 (right panel). In MAM1 north Indian Ocean is not cooled completely in absence of ENSO in both the epochs and cooling in Pacific confines to extreme east. During the next year monsoon (JJA1) removal of ENSO makes Arabian Sea and Bay of Bengal warm and east Pacific cool in the PRE76 epochs. After the climate shift, only the equatorial region is cool in the Indian Ocean and east Pacific Ocean warms when ENSO years are not included. Anomalies increase with the removal of ENSO

in both these periods. Thus it indicates that in the POST76 period the effect of ENSO on TBO is limited to central Pacific only.

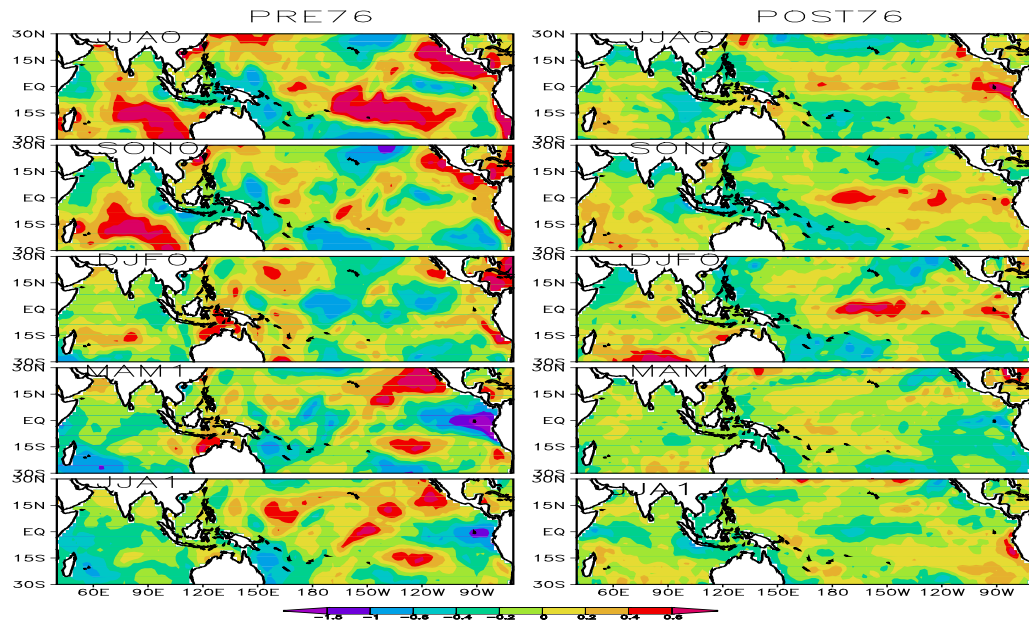


Figure 7.12: Same as figure 7.8, but for TBO years which are not ENSO onset years only included

#### 7.4.3.2 Velocity potential at 200 hPa.

In the absence of ENSO, convergent anomaly didn't extend entire Indian Ocean and center of divergence is shifted towards west in the preceding seasons of strong monsoon in the PRE76 strong TBO years. Throughout these periods the ENSO onset years has no significant effect on the anomaly pattern after the 1976 TBO years. During strong monsoon of normal TBO of PRE76 period, upper level divergence center over Indian Ocean is confined to western Indian Ocean and another feeble one appears over central Pacific. Convergence is located over Australia and extreme east Pacific. After the shift divergent center appears over central Pacific and convergence strengthens over southeast Indian Ocean. (figure 7.13b).

In the POST76 era, in the absence of ENSO, the convergence moves to north of Australia and that over central Pacific shifts towards east after the monsoon (figure 7.13c), while convergence center appears over southeast Indian Ocean (figure 7.13d). In the following winter season normal TBO years has additional center of convergence over southwestern Indian Ocean in the PRE76 period. In the POST76

period convergence over the west Pacific strengthens shifting the divergent center east (figure 7.13f). The following spring has not much change in the absence of ENSO in both the epochs. During the next year summer (JJA1), upper level convergence in the Indian Ocean is not seen in PRE76 period and after shift convergent center in the southwest Indian Ocean extends east (figure 7.13j).

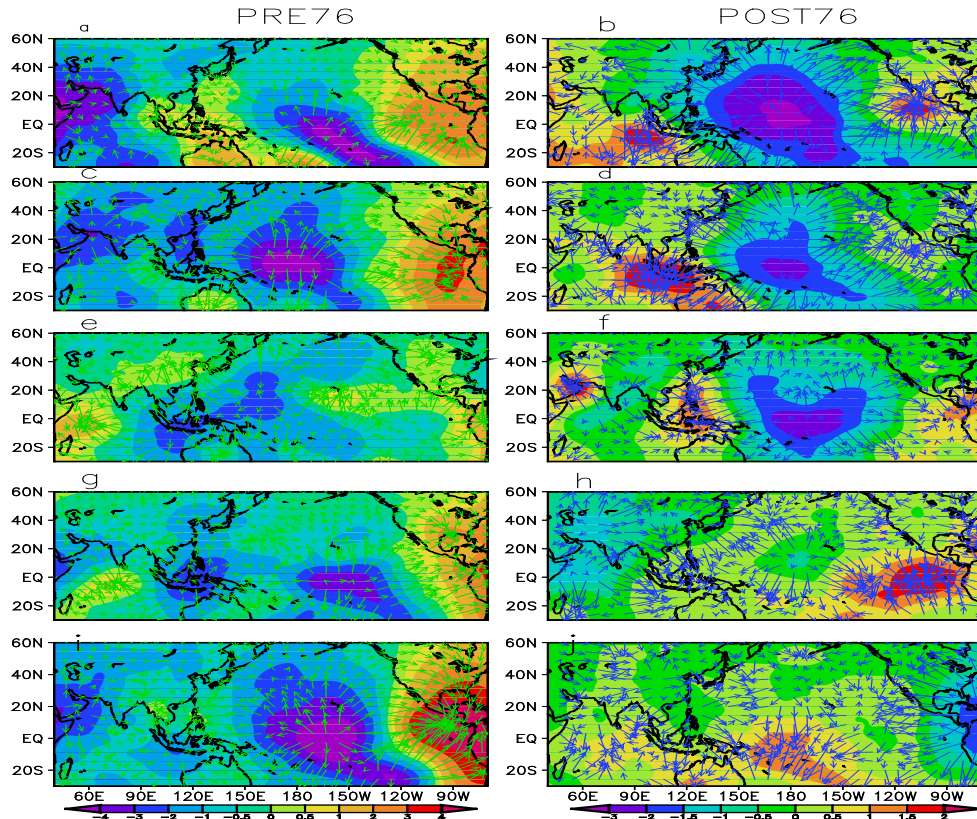


Figure 7.13: same as figure 7.9, but for non-ENS TBO years are only considered for composites.

#### 7.4.3.3 Local Hadley circulation and moisture convergence

Local Hadley circulation of JJA0 and JAJ1 for non ENSO-TBO years in both PRE76 and POST76 periods is shown in Figure 7.14. Local Hadley circulation pattern has not shown much change during JJA0 before and after the shift. But during the next year monsoon absence of ENSO brings opposite centers in ocean and land regions for PRE76 period making local Hadley circulation prominent. ENSO has no effect in the pattern in the POST76 period. The absence of ENSO thus makes local Hadley circulation prominent in PRE76 TBO cycle and after the shift ENSO has no role in local Hadley circulation.

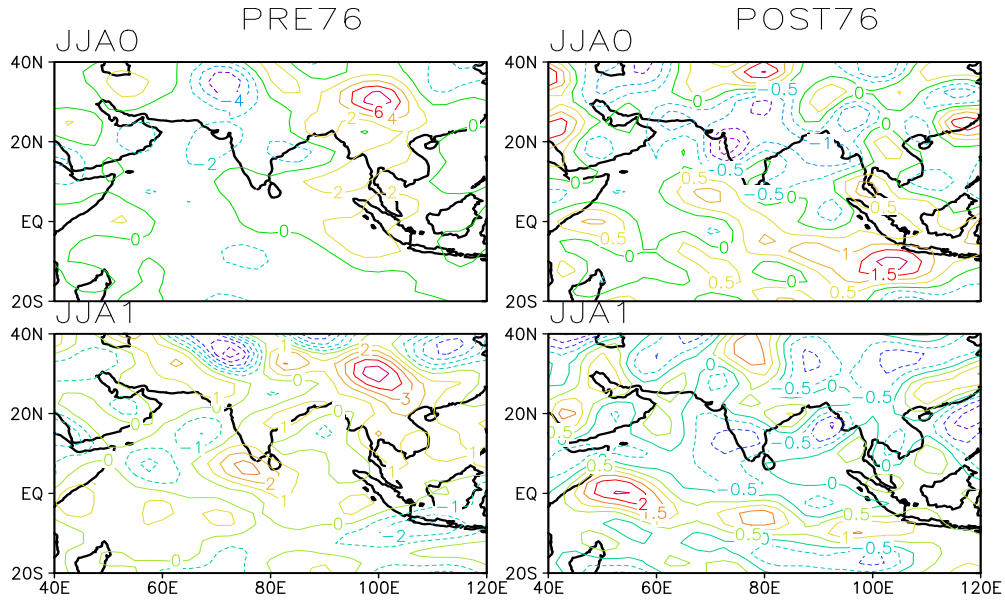


Figure 7.14: same as figure 7.10, but composite is made from TBO years independent of ENSO

During normal TBO (non ENSO TBO) years low level moisture convergence appears over India by previous year September itself in the PRE76 period and it continues in the remaining seasons. POST76 patterns are similar both in presence and absence of ENSO (see figure 7.15). Thus in the absence of ENSO convergence starts a season earlier in the PRE76 period.

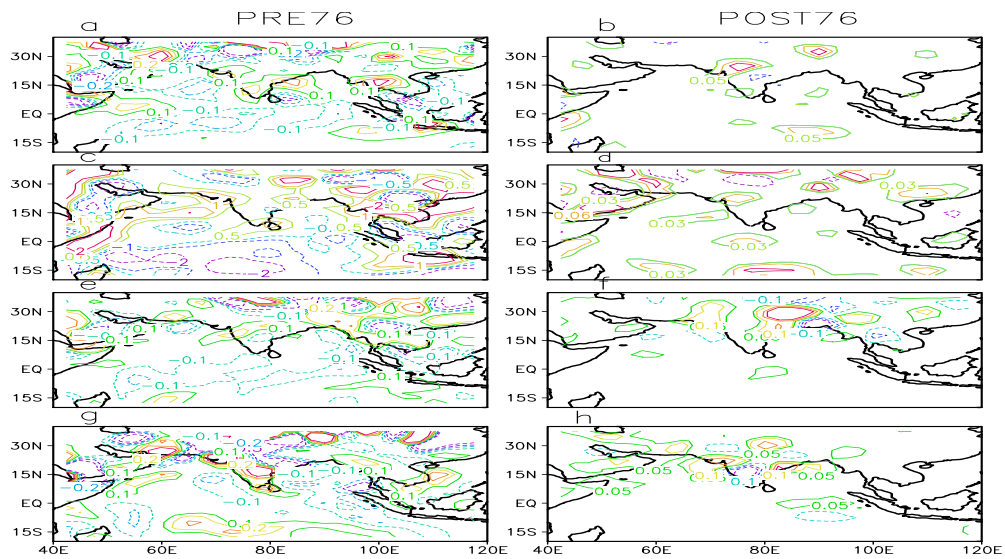


Figure 7.15: same as figure 7.11, but composite is made from TBO years independent of ENSO



It indicates that the absence of ENSO makes local processes strong in the PRE76 period and the effect of ENSO itself is reduced after the climate shift.

### **7.5 Asian–Australian monsoon relationship**

Composite analysis shows difference in the in-phase movement of anomalies from Indian monsoon to Australian monsoon in both the epochs. The relationship between the Indian and Australian summer monsoon is analysed with the help of circulation indices. The circulation index used by Webster and Yang (1992) (represented as WY monsoon index), which is defined as the vertical shear of zonal wind between 850 hPa and 200 hPa averaged over the area  $5^{\circ}\text{N}$ – $20^{\circ}\text{N}$  and  $40^{\circ}\text{E}$ – $110^{\circ}\text{E}$  for summer monsoon season. Australian summer monsoon is represented by 850 hPa zonal wind anomaly averaged over  $2.5^{\circ}\text{S}$  to  $15^{\circ}\text{S}$ ,  $110^{\circ}\text{E}$ – $150^{\circ}\text{E}$  for DJF season, which is named as AU index by Hung and Yanani (2004). A 21-year sliding correlation between WY index of summer season and next winter AU index is used to realize the changes in the association between Indian summer monsoon and Australian summer monsoon. The sliding correlation increases to maximum value by 1970's and after late 1970's it decreases and becomes very low.

Since the correlation is very low with the unfiltered indices, we applied a band pass filter (Murakami, 1979) to separate the indices in both TBO (2-3 year) and ENSO (3-7 year) windows and is shown in figure 7.16. In the TBO window, the correlation coefficient is almost constant from 1960 to 1980, with significant value of 0.76 (as the data sets are filtered in both the scales, its degrees of freedom decreases and correlation above 0.42 becomes 95% significant). After 1980 the correlation decreases considerably and even drops to below 0.4. At the same time in the ENSO scale the correlation becomes positive by early 1960 only and the maximum is after climate shift (0.8) and remains significant. Thus the in phase transition from Indian to Australian monsoon is more significant in the ENSO scale after the climate shift and ENSO is a main factor for in phase transition.

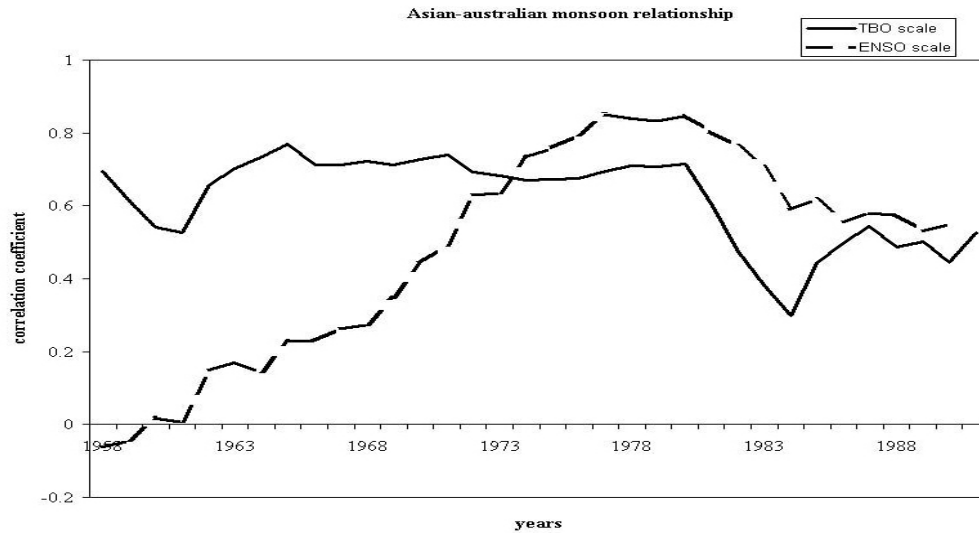


Figure 7.16: 21 year sliding correlation of boreal summer WY index and boreal winter Au index in TBO and ENSO scale.

### 7.6 SST–latent heat flux relationship in Indian Ocean

In this section SST tendencies (difference in SST anomalies between two consecutive seasons) are with latent heat flux to investigate the relationship between them in the Indian Ocean region. In the PRE76 period, SST tendency of summer season (JJA0-MAM0) shows cooling trend in the entire Indian Ocean except extreme southeast. The latent heat flux anomaly of spring season has positive anomalies in the Indian Ocean except entire eastern region and extreme west of Arabian Sea. At the same time, after the shift SST tendency is positive in the central and southwest Indian Ocean and latent heat flux anomalies are negative in these areas. In the PRE76 era cooling tendency continues to the next season. At this time, positive latent heat flux confined to the equatorial and southwest Indian Ocean (see figure 7.17 top panel). But after shift though cooling is confined only to north Indian Ocean, the opposite relationship of SST tendency and latent heat flux is maintained, except at extreme northwest Indian Ocean (figure 7.17 bottom section).

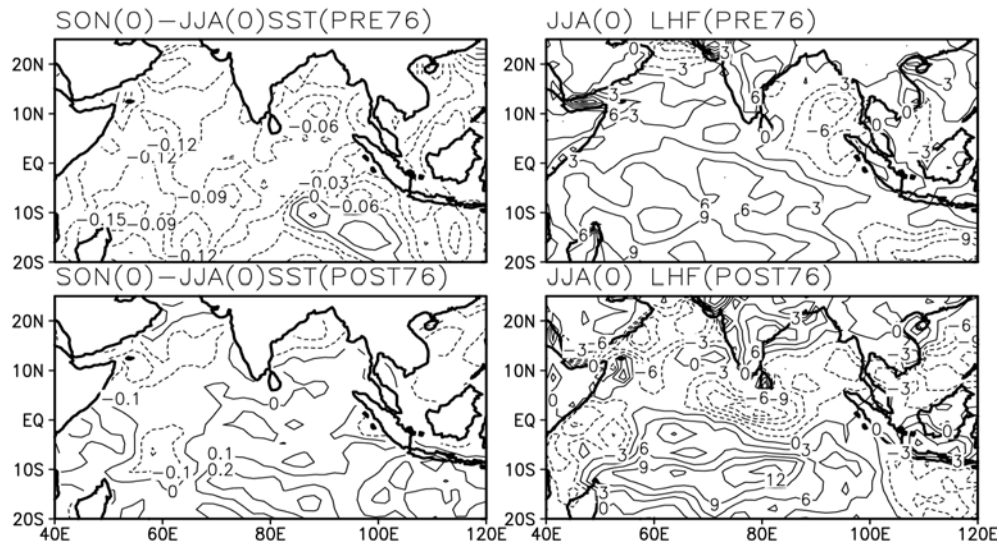


Figure 7.17: SST tendency of post monsoon season (left side) and monsoon season latent heat flux anomalies in both PRE and POST76 period for TBO years

### 7.7 Discussion

Composite analysis identifies distinct cycles for TBO years in both the epochs. Complete warming/cooling of Indian Ocean before monsoon is not observed after 1976. In the pre-climate shift period (1951-1975), reversal of anomalies in the Pacific starts a season earlier to monsoon while it is with the monsoon after 1976 and is seen in Indian Ocean and central Pacific. Instead of extreme east Pacific, anomalies develop in the central Pacific and extend both eastward and westward after the regime shift. This change in propagation was earlier reported by Annamalai and Liu (2005) for El Niño years. The present analysis captures the difference in pattern for TBO in the presence and absence of ENSO in PRE76. But after the shift ENSO has no role in both in-phase (Indian monsoon to Australian monsoon) and out-of-phase (Australian monsoon to Indian monsoon) transitions of Indian Ocean and only alter the in-phase transition of Pacific Ocean. The shift therefore made ENSO almost insignificant for TBO transition of SST anomalies. After the climate shift southeast movement of anomalies are also seen, but it moves to southwest Pacific by autumn season instead concentrating over Indonesia.

Non-ENSO SST anomalies are stronger after the shift. Terray et al. (2005) pointed out that SST anomalies in the southeast Indian Ocean (SEIO;  $72^{\circ}\text{E}$ - $122^{\circ}\text{E}$  and  $4^{\circ}\text{S}$ - $26^{\circ}\text{S}$ ) has biennial periodicity both before and after 1976 and after 1976 it has major

role in the monsoon-ENSO relationship. In the TBO years an anomaly center comes over the SEIO after 1976, but it is close to equator and has same anomalies as north Indian Ocean. In chapter 4 of the thesis, it is found that ENSO years with spring onset only has influence on TBO. Analyzing the nino3.4 SST anomalies of ENSO years shows that after the shift onset is changed to summer season for almost all the ENSO years (refer figures 4.1). This stresses the reduced role of ENSO after shift.

After the shift, lower level convergence appears over the Indian Ocean two seasons earlier than summer monsoon itself and the divergence over the eastern Indian Ocean is shifted further east. The anomalous ascending branch of Walker cell (represented by anomalous upper level divergence) in the winter season along with that at east Pacific can be considered as the thermodynamic effect of Indian Ocean SST opposing the ENSO forcing from Pacific (Li and Zhang, 2002). In the in-phase transition from Indian to Australian monsoon, the convergent anomaly from the Indian region concentrated over the southwest Pacific after the shift and even divergence comes over Australia in the normal TBO years of 1978-2002 periods. Thus the Indian to Australian transition of convergence is due to the effect of ENSO and with the shift the in-phase transition is weakened. In both the cases lower level convergence appears over the western Indian Ocean by next monsoon, while the convergent center over the eastern Pacific moves west after 1976. After the climate shift, the central Pacific always remains convergent and SST pattern and convergent/divergent centers are well matching in both the epochs. All these observational evidences indicate that the role of Pacific Ocean is reduced in biennial oscillation of Indian summer monsoon.

Composite analysis of latent heat flux has opposite patterns in both the periods and after the shift the latent heat flux anomalies looks similar with presence and absence of ENSO. According to Yu and Rienecker (1999), the latent heat flux explains the changes in SST in most of the tropical Indian Ocean except in the Arabian Sea and Bay of Bengal. If SST changes are introduced by latent heat flux, reduction in latent heat flux can cause progressive warming over tropical Indian Ocean. Our comparison of SST tendency and latent heat flux anomalies agrees well with Yu and Rienecker (1999) for the TBO years after the climate shift and for normal TBO

years before the shift. Apart from the latent heat flux, local Hadley circulation and moisture convergence also has increased role in TBO after the climate shift.

After the climate shift, the dependence of SST tendency on latent heat flux, appearance of convergent anomaly very early, and ascending branch of Walker cell in the Indian Ocean two seasons before the monsoon etc after the climate shift points out the increased role of Indian Ocean processes and reduced effect of ENSO on TBO associated with Indian summer monsoon.

### **7.8 Conclusion**

The TBO cycle for SST, Walker circulation, latent heat flux, local Hadley circulation etc are presented for time periods before and after climate shift. From the composite analysis of above parameters it is found that the TBO cycle from a strong monsoon to next year weak monsoon is different in PRE76 and POST76 periods. All TBO and non ENSO TBO patterns were different in the PRE76 period, indicating dominant role of Pacific Ocean in TBO cycle. Though the TBO cycle is evident in both ENSO-TBO and non-ENSO-TBO years, formation and movement of anomalies are different in PRE76 period. But in the POST76 period the effect of ENSO to the TBO are reduced much for all the parameters and is felt only in the central Pacific. The Asian to Australian monsoon transition is weakened in the recent decades on biennial scale and is strong only in ENSO scale. The climate shift had made the local processes over the Indian Ocean dominant for TBO transition of Indian summer monsoon. Local Hadley circulation between Indian continent and adjacent oceans are prominent after the climate shift. SST tendency in the Indian Ocean is in close association with Indian Ocean latent heat flux anomalies after climate shift. Local moisture convergence over Indian region starts a season earlier and became more effective in the POST76 period. Thus, the importance of Indian Ocean and its local effects gained upper hand in the biennial transition of Indian summer monsoon over the remote effect from the Pacific Ocean, after the climate shift.

### Summary and Conclusion

---

The socio-economic progress of a country like India strongly depends on agricultural sector and related industries and thereby to the timely and sufficient summer monsoon rainfall. So understanding of the variabilities of the summer monsoon is very important. In the different scales of variabilities, interannual variability is most extensively studied. The interannual variability of summer monsoon corresponds to biennial scale and multi-year scale variability. The biennial scale monsoon variability is related to tropospheric biennial oscillation (TBO) and the multi-year variability to El Nino Southern Oscillation (ENSO). The relationship of interannual variability of monsoon to ENSO is established earlier, though the reverse relationship is weakening in recent decades. Different mechanisms involving coupled ocean-atmosphere processes in the Indo-Pacific regions are proposed to explain the mechanism of TBO. But the monsoon-TBO interaction, effect of Pacific and Indian Ocean dynamics on TBO, relationship with stratospheric QBO and boreal summer ISO like factors are not studied in detail. The present thesis analyses the above factors of TBO with the help of NCEP/NCAR reanalysis data sets, ISMR index, Indian monsoon rainfall and zonal wind and temperature of ECMWF.

Though the interannual variability of Indian summer monsoon rainfall corresponds to biennial scale (TBO) and low frequency ENSO scale, the rainfall distribution is different in both these cases. In TBO scale, rainfall is enhanced over India, Bay of Bengal and just south of the equator during a strong monsoon and reverses in the weak

monsoon. But in ENSO scale, strong monsoon year has increases rainfall over India and north Indian Ocean and decreases in the next weak year. Indian Ocean SST has similar anomalies in both the scales with warm anomaly before strong monsoon and starts reversing with onset of monsoon. But east Pacific starts cooling in the spring season in TBO scale and central Pacific has opposite anomalies in both the scales. The warm anomaly of Indian Ocean contributes to widespread rainfall over India, Bay of Bengal and western parts in TBO scale and it confined to western Indian Ocean only in ENSO scale. SST and wind anomalies are southeast propagating in TBO scale. SST, wind and SLP like parameters shows biennial oscillation along with convection from a weak to strong and then back to weak Indian monsoon transition. In phase Indian to Australian and out of phase Australian to Indian monsoon transition is evident for TBO years. Indian Ocean fluxes also show biennial oscillation. Atmospheric circulation—both zonal and meridional- is also associated with TBO and interannual variability of Indian summer monsoon. Convergence/divergence centers and associated upward motion migrates southeast along with convection in the Indo-Australian monsoon region. Equatorial Walker circulation and local Hadley circulation gets strengthened during strong Indian summer monsoon and weakened in the next cycle.

TBO years encompasses most of the ENSO onset years in the Pacific Ocean. But the ENSO years, which has onset before the summer monsoon is only contributing to TBO associated monsoon variability. Both ocean-atmosphere parameters in the tropical Indo-Pacific region has different type of evolution and TBO cycle during the interannual variability of Indian summer monsoon, which are associated with ENSO and independent of ENSO. In presence of ENSO, almost entire Indian Ocean is cooled during strong monsoon season, while in absence of ENSO cooling confined to ocean region adjacent to land masses. Pacific Ocean SST anomalies are opposite in both the cases. Southeast movement of anomalies from Indian region to Australian monsoon region is controlled by ENSO in the Pacific. Biennial oscillation of Pacific Ocean SST, SLP and convergence/divergence are strong in the presence of ENSO only. The biennial cycle of Indian Ocean SST, wind, local processes like monsoon local Hadley circulation between Indian land masses and equatorial Ocean are evident in the interannual

monsoon variability in absence of ENSO. Thus in ENSO years remote effect dominates TBO and monsoon cycle and in absence of ENSO local processes itself can produce TBO and associated monsoon variability.

The effect of Indian Ocean dynamic processes (ie, Indian Ocean Dipole) is in phase in the absence of ENSO and out of phase in the presence of ENSO. In presence of ENSO IOD-TBO pattern resembles ENSO-TBO for SST and Walker circulation. Inphase TBO-IOD pattern resembles the non-ENSO SST pattern of Indian Ocean and Pacific Ocean SST and Walker circulation is opposite for inphase and out of phase TBO-IOD interactions. Thus ENSO dominates the out of phase TBO-IOD related monsoon transitions and IOD dominates in-phase TBO-IOD monsoon transition. But Indian Ocean SST and lower level wind over Indian Ocean can produce TBO transition associated with interannual variability of Indian summer monsoon in absence of both ENSO and IOD.

In most of the TBO years a low frequency and high frequency mode is observed for summer season Indian monsoon rainfall. The first mode of 10-20 day filtered OLR and 850 hPa zonal wind has spatial coherence with TBO scale OLR and wind and has quasi-biennial periodicity in interannual time scales. The variance of first two prominent modes is coherent for 10-20 day scale convection and wind for TBO years.

Though two different mechanisms are responsible of stratospheric QBO and tropospheric TBO, interaction of lower stratosphere and troposphere is evident for TBO years over Indian and Australian monsoon region. Over the Indian monsoon region the stratospheric zonal wind extends to lower troposphere, creating three different layers in the troposphere in TBO years and shows interannual variation associated with monsoon variation. The zonal temperature has an additional source (sink) in the midtroposphere level over Indian monsoon region in the spring season before a strong (weak) Indian summer monsoon. The lower stratosphere wind and midtroposphere spring season temperature has good predictive relationship with monsoon rainfall over India. Over the Australian monsoon region along with the downward propagation of zonal winds from the lower stratosphere an upward propagation from the lower troposphere also takes



place and both these interact in the tropopause level. Zonal wind over India and Australian monsoon region are related with TBO scale SST anomalies of both Indian and equatorial east Pacific Ocean.

Indian summer rainfall has biennial characteristics, though ENSO like external monsoon regulating factors changes to lower frequency after the climate regime shift of 1976. Along with the climate shift, effect of ENSO to the SST, wind and convergence/divergence over Indian Ocean region is reduced and is confined to the equatorial central and east Pacific Ocean regions. Indian Ocean latent heat flux and local Hadley circulation has increased role in the interannual variability of monsoon controlled by TBO. The inphase Indian to Australian monsoon transition is weakened after the climate regime shift.

Thus the TBO-Indian summer monsoon relationship is through both ocean and atmosphere processes and is modulated by both ENSO and IOD and is related to stratospheric QBO. TBO can produce interannual variability of Indian summer monsoon both in the presence and absence of ENSO, with different interactions. When ENSO is present in the Pacific, the remote effect dominates the TBO and in absence of ENSO, the TBO is confined to Indian Ocean and Indian Ocean fluxes and local circulation dominates the interannual monsoon variability. Effect of Indian Ocean dipole to monsoon-TBO cycle is suppressed by ENSO, when both IOD and ENSO co-exist. Boreal summer Intraseasonal oscillation and stratospheric QBO gets modified in TBO years. Climate regime shift of 1976 weakened in phase Indian to Australian monsoon transition by reducing the effect of ENSO in TBO and local processes in the Indian Ocean dominated TBO and TBO producing interannual variability of Indian summer monsoon.

### **8.1 Scope of future work**

The present study illustrates the biennial oscillation in different ocean-atmosphere parameters associated with interannual variability of Indian summer monsoon rainfall. It also accounts the role of different processes like ENSO, IOD, QBO and ISO in the monsoon variability during the TBO years. But the study can be extended further to

understand the more features of TBO and its role in ENSO-Monsoon biennial cycle and interactions. This is very much in need for the accurate understanding of interannual variability of monsoon and its prediction, which is the main goal. Modelling studies are very much needed for the more studies of TBO cycle. The modeling studies with interactive Pacific and Indian Ocean combine and separately can produce the TBO cycle in presence and absence of ENSO and separate analysis are needed to analyse the cycle both in presence and absence of ENSO. Different atmospheric and ocean parameters are analysed in the present study to explain the TBO in presence and absence of ENSO. But the modeling results will be able to analyse this for an extended time and more parameters like fluxes and ocean heat storage, mixed layer depth and the produced tropical rainfall. Then the biennial cycle of TBO and that of ENSO and IOD can be separated from the analysis. These modeling studies will enable to study the interannual variability of Indian summer monsoon irrespective of ENSO in the Pacific.

## REFERENCES

- Andrews, D. G., Holton, J. R. and Leovy, C.B. 1987. Middle Atmosphere Dynamics, Academic Press, San Diego.
- Annamalai, H. and Liu, P. 2005. Response of Asian summer monsoon to changes in El Nino properties. *Quart. J. Roy. Meteor. Soc.*, 131, 805-831.
- Annamali, H. and Slingo, J. M. 2001. Active/break cycles: diagnosis of the intraseasonal variability of Asian monsoon. *Climate Dyn.*, 18, 85-102.
- Annamali, H., Slingo, J. M., Sperber, K. R. and Hodges, K. 1999. The mean evolution and variability of Asian summer monsoon: comparison of ECMWF and NCEP/NCAR Reanalysis. *Mon. Wea. Rev.*, 127, 1157-1186.
- Ashok, K., Guan, Z. and Yamagata, T. 2001. Influence of the Indian Ocean Dipole on the relationship between the Indian monsoon rainfall and ENSO. *Geophys. Res. Lett.*, 28, 4499-4502.
- Ashok, K., Guan, Z., Saji, N. H. and Yamagata, T. 2004. On the individual and combined influences of the ENSO and the Indian Ocean Dipole on the Indian Summer Monsoon. *J. Climate.*, 17, 3141-3154.
- Baldwin, M. P., Gray, L. J., Dunkerton, T. J., Hamilton, K., Haynes, P. H., Randel, W. J., Holton, J. R., Alexander, M. J., Hirota, I., Horinouchi, T., Jones, D. B. A., Kinnersley, J. S., Marquardt, C., Sato, K. and Takahashi, M. 2001: The Quasi-Biennial Oscillation. *Rev. Geophys.*, 39, 179-229.
- Barnett, T. P. 1991. The interactions of multiple time scales in the tropical climate system. *J. Climate.*, 4, 29-285.
- Barnett, T. P., Dümenil, L., Schlese, U. and Roeckner, E. 1989: The effect of Eurasian snow cover on regional and global climate variations. *J. Atmos. Sci.*, 46, 661-685.
- Behera, S. K., Krishnan, S. and Yamagata, T. 1999. Unusual ocean-atmosphere conditions in the tropical Indian Ocean during 1994. *Geophys. Res. Lett.*, 26, 3001-3004.
- Bjerknes, J. 1969. Atmospheric teleconnection from the equatorial Pacific. *Mon Wea. Rev.*, 97, 163-172
- Brankovic, C., Palmer, T. N., and Ferranti, L. 1994. Predictability of seasonal atmospheric variations. *J. Climate.*, 7, 217-237.
- Brier, G. W. 1978. The quasi-biennial oscillation and feedback processes

- in the atmosphere–ocean–earth system. *Mon. Wea. Rev.*, 106, 938–946.
- Chang, C. P. and Li, T. 2000. A theory for the tropical tropospheric biennial oscillation. *J. Atmos. Sci.*, 57, 2209–2224.
- Chang, C. P., Harr, P. and Ju, J. 2001. Possible roles of Atlantic circulation on the weakening Indian monsoon rainfall-ENSO relationship. *J. Climate.*, 14, 2376-2388.
- Chao, C. W. and Chen, B. 2001. Origin of monsoon. *J. Atmos. Sci.*, 58, 3497-3507.
- Charney, J. G. and Shukla, J. 1981. Predictability of monsoons. Monsoon Dynamics, J. Lighthill and R.P. Pearce, Eds., Cambridge University Press, 99-109.
- Chung, C. and Nigam, S. 1999: Asian summer monsoon-ENSO feedback on the Cane-Zebiak model ENSO. *J. Climate.*, 12, 2787-2807.
- Clarke, A. J., Cole, J. A. and Webster, P. J. 2000. Indian Ocean SST and Indian summer rainfall: predictive relationship and their decadal variability. *J. Climate.*, 13, 2503-2519
- Clarke, A. J., Liu, X. and Gorder, S.V. 1998. Dynamics of the biennial oscillation in the equatorial Indian and far western Pacific Oceans, *J. Climate.*, 11, 987-1001.
- Dima, I. M. and Wallace, J. M. 2003. On the seasonality of the Hadley cell. *J. Atmos. Sci.*, 60, 1522-1527.
- Fasullo, J. and Webster P.J. 1999. Warm pool SST variability in relation to the surface energy balance. *J. Climate.*, 12, 1292-1305.
- Fennessey, M. J. and Shukla, J. 1994. GCM simulations of active and break monsoon periods. In proceedings of international conference on monsoon variability and prediction. Trieste. WMO/TD 619, WCRP-84 vol.2, 576-585.
- Ferranti, L., Slingo, J. M., Palmer, T. N., and Hoskins, B. J. 1997. Relations between interannual and intraseasonal monsoon variability as diagnosed from AMIP integrations. *Quart. J. Roy. Meteor. Soc.*, 123, 1323-1357.
- Flohn, H. 1957. Large-scale aspects of the “summer monsoon” in south and east Asia, *J. Meteor. Soc. Japan.*, 35, 180-186.
- Gadgil, S. and Asha, G. 1992. Intraseasonal variation of Indian summer monsoon. *J. Meteor. Soc. Japan.*, 70, 517-527.
- Gibson, J. K., Kallberg, P. and Uppala, S. 1996. The ECMWF Reanalysis (ERA) Project. *ECMWF Newsl.*, 73, 7-17.

- Gibbson, J. K., Kallberg, P., Uppala, S., Hernandez, A., Nomura, A. and Serrano, E. 1997. ECMWF Reanalysis project Rep.Ser.1, ECMWF, United Kingdom.
- Goswami, B. N. 1995. A multiscale interaction model for the origin of the tropospheric QBO. *J. Climate.*, 8, 524–534.
- Goswami, B. N. 1998. Interannual variations of Indian summer monsoon in a GCM: External conditions versus internal feedbacks, *J. Climate.*, 11, 501-522.
- Goswami, B. N. and Ajayamohan, R. S. 2000. Intraseasonal oscillation and interannual variability of the Indian summer monsoon. *J. Climate.*, 14, 1180-1198.
- Goswami, B. N. and Shukla, J. 1984. Quasi-periodic oscillations in a symmetric general circulation model. *J. Atmos. Sci.*, 41, 20-37.
- Goswami, B. N., Krishnamurthi, V. and Annamali, H. 1999. A broad scale circulation index for the interannual variability of Indian summer monsoon. *Quart. J. Roy. Meteor. Soc.*, 125, 611
- Goswami, B. N., Sengupta, D. and Suresh Kumar, G. 1998. Intraseasonal oscillations and interannual variability of surface winds over the Indian monsoon region, *Proc. Indian. Acad. Sci.* 107, 45-64.
- Gutzler, D. S. and Harrison, D. E. 1987. The structure and evolution of seasonal wind anomalies over the near-equatorial eastern Indian and western Pacific oceans, *Mon. Wea. Rev.*, 115, 169–192.
- Harzallah, R. and Sadourny, R. 1997. Observed lead-lag relationships between Indian summer monsoon and some meteorological variables. *Climate Dyn.*, 13, 635–648.
- Holton, J. R. 1992. An introduction to dynamic meteorology. Third edition, Academic press, USA.
- Holton, J. R. and Lindzen, R. S. 1972. An updated theory for the quasi-biennial cycle of tropical stratosphere. *J. Atmos. Sci.*, 37, 2200-2208.
- Hou, A. Y. and Lindzen, R. S. 1992. The influence of the concentrated heating on the Hadley circulation. *J. Atmos. Sci.*, 49, 1233-1241.
- Hung, C. W. and Yanani, M. 2004. Factors contributing to onset of Australian summer monsoon. *Quart. J. Roy. Meteor. Soc.*, 130: 739-758.
- Ju. J. and Slingo. J. 1995. The Asian summer monsoon and the ENSO. *Quart. J. Roy. Meteor. Soc.*, 121, 1133-1168.
- Kalnay, E., and co-authors. 1996. The NCEP/NCAR reanalysis project,

*Bull.Amer. Meteor.Soc.*, 77, 437- 471.

- Kawamura, R. 1988. Quasi-biennial oscillation modes appearing in the tropical sea water temperature and 700 mb zonal wind, *J. Meteor. Soc. Japan.*, 66, 955–965.
- Kawamura, R., Matsuura, T. and Iizuka, S. 2001. Role of an equatorially asymmetric mode in the Indian Ocean in the Asian summer monsoon-ENSO coupling. *J. Geophys. Res.*, 106, 4681–4693.
- Kiladis, G. N., and Diaz, H. F.1989. Global climatic anomalies associated with extremes in the Southern Oscillation. *J. Climate.*, 2, 1069-1090.
- Kiladis, G. N. and van Loon, H. 1988. The Southern Oscillation. Part VII: Meteorological anomalies over the Indian and Pacific sectors associated with the extremes of the oscillation. *Mon. Wea. Rev.*, 116, 120–136.
- Kim, K. M. and Lau, K. M. 2001. Dynamics of monsoon induced biennial variability in ENSO. *Geophys. Res. Lett.*, 28, 315-318.
- Kinter, J. L., Miyakoda, K. and Yang, S. 2002. Recent changes in connection from Asian monsoon to ENSO. *J. Climate.*, 15, 1203-1215.
- Kirtman, B. P. and Shukla, J. 2000. On the influence of the Indian summer Monsoon on ENSO, *Quart. J. Roy. Meteor.Soc.*, 126, 213-239.
- Kitoh, A., Yukimoto, S. and Noda, A. 1999. ENSO-monsoon relationship in the MRI coupled GCM. *J. Meteor. Soc. Japan.*, 77, 1221–1245.
- Krishnamurthi, T. N. 1971. Tropical east-west circulation during northern summer. *J. Atmos. Sci.*, 28, 1342-1347.
- Krishnamurthi, T.N., and Bhalme, T. 1976. Oscillations of a monsoon system,1 Observational aspects, *J. Atmos. Sci.*, 33, 1937-1943.
- Krishnamurthi, T. N., and Ramanathan, Y. 1982. Sensitivity of monsoon onset to differential heating. *J. Atmos. Sci.*, 39, 1290-1306.
- Kumar, K. K., Rajagopalan, B. and Cane, M. A. 1999. On weakening relationship between Indian monsoon and ENSO, *Science* 284. 2156-2159.
- Lau, K. M. and Sheu, P. J. 1988. Annual cycle, quasi biennial oscillation, and Southern Oscillation in global precipitation. *J. Geophys. Res.*, 93, 10975–10988.
- Lau, N. C. and Nath, M. J. 2000. Impact of ENSO on the variability of the Asian-Australian monsoons simulated in GCM experiments, *J.*

*Climate.*, 13, 4287-4309.

- Lau, K. M., Yang, G. and Shen, S. H. 1998. Seasonal and intraseasonal climatology of summer monsoon rainfall over east Asia. *Mon. Wea. Rev.*, 116, 18-37.
- Li, C. and Yan, M. 1996. The onset and interannual variability of Asian summer monsoon in relation to land-sea thermal contrast. *J. Climate.* 9, 358-375.
- Li, T. and Zhang, Y. 2002. Processes that determine the quasi-biennial and lower frequency variability of the south Asian monsoon. *J. Meteor. Soc. Japan.*, 80, 1149–1163.
- Li, T., Liu, P., Fu, X., Wang, B. and Meehl, G. A. 2006. Spatiotemporal structure and mechanism of tropospheric biennial oscillation in Indo-Pacific Warm Ocean regions. *J. Climate.*, 19, 3070-3087.
- Li, T., Tam, C. W. and Chang, C. P. 2001. A coupled air–sea monsoon oscillator for the tropospheric biennial oscillation. *J. Climate.*, 14, 752– 764.
- Lindzen, R. S. and Holton, J. R. 1968. A theory of the quasi-biennial Oscillation. *J. Atmos. Sci.*, 25, 1095–1107.
- Lindzen, R. S. and Hou, A. .1988. Hadley circulation for zonally averaged heating centered off the equator. *J. Atmos. Sci.*, 45, 2417-2427
- Lorenz, E. 1967. The nature and theory of the general circulation of the atmosphere. *WMO publ.* No 218, FP. 115, Geneva.
- Loschnigg, J. and Webster, P.J. 2000. A coupled ocean–atmosphere system of SST modulation in the Indian Ocean. *J. Climate.*, 13, 3 342–3360.
- Loschnigg, J., Meehl, G. A., Arblaster, J. M., Compo, G. P. and Webster, P. J. 2003. The Asian Monsoon, the tropospheric biennial oscillation and the Indian Ocean Dipole in the NCAR CSM *J. Climate.*, 16, 1617-1642.
- McCreary, J. P. and Anderson, D. L. T. 1991. An overview of coupled ocean atmosphere models of El Niño and the Southern Oscillation. *J. Geophys. Res.*, 96, 3125-3150.
- Meehl, G. A. 1987. The annual cycle and interannual variability in the tropical Pacific and Indian Ocean region. *Mon. Wea. Rev.*, 115, 27-50.
- Meehl, G. A. 1993. A coupled air–sea biennial mechanism in the tropical Indian and Pacific Ocean regions: Role of the ocean. *J. Climate.*, 6, 31–41
- Meehl, G. A. 1994. Coupled land–ocean–atmosphere processes and South

- Asian monsoon variability. *Science*, 266, 263–267.
- Meehl, G. A. 1997. The south Asian monsoon and the tropospheric biennial oscillation. *J. Climate*, 10, 1921–1943.
- Meehl, G. A. and Arblaster, J. M. 2001. The tropospheric biennial oscillation and Indian monsoon rainfall. *Geophys. Res. Lett.*, 28, 1731–1734.
- Meehl, G. A. and Arblaster, J. M. 2002a. The tropospheric biennial oscillation and Asian-Australian monsoon rainfall. *J. Climate.*, 15, 722–744.
- Meehl, G.A. and Arblaster, J.M., 2002b. Indian monsoon GCM experiments testing tropospheric biennial oscillation transition conditions. *J. Climate.*, 15, 923–944.
- Meehl, G.A., Arblaster, J.M., and Loschinger, J. 2003. Coupled-ocean-atmosphere dynamical processes in tropical Indian and Pacific oceans and the TBO. *J. Climate.*, 16, 2138–2158.
- Mohankumar, K. and Pillai, P.A. 2008. Stratosphere-Troposphere interaction associated with Biennial oscillation of Indian summer monsoon. *J. Atmos. Solar Terrestrial Physics*, 77, 764–773
- Mooley, D.A. and Parthasarathy, B. 1983. Indian summer monsoon and El-Nino. *PAGEOPH*, 121, 339–352
- Mooley, D. A. and Parthasarathy, B. 1984. Fluctuation in all-India summer monsoon rainfall during 1871–1985, *Clim. Change*, 6, 287–301.
- Moron, V., Fontaine, B. and Roucou, P. 1995. Global equatorial variability of 850- and 200-hPa zonal winds from rawinsondes between 1963 and 1989, *Geophys. Res. Lett.*, 22, 1701–1704.
- Mukherjee, B. N, Indria, K., Reddy, R. S., and Ramana Murthy, B. H. V. 1985. Quasi-biennial oscillation in stratospheric zonal winds and Indian summer monsoon. *Mon. Wea. Rev.*, 107, 1581–1588.
- Murakami, M. 1979. Large-scale aspects of deep convective activity over the GATE data. *Mon. Wea. Rev.*, 107, 994–1013.
- Nellin, J. D., Battisti, D. S., Hirst, A. C., Jin, F. F., Wakata, Y., Yamagata, T. and Zebiak, S.E. 1998. ENSO theory. *J. Geophys. Res.*, 103, 14262–14290
- Newell, R. E., Kidson, J. W., Vincent, D. G. and Boer, G. J. 1972. The general circulation of the tropical atmosphere. Vol.1, Cambridge: MIT press, 258.
- Nicholls, N. 1978. Air–sea interaction and the quasi-biennial oscillation. *Mon. Wea. Rev.*, 106, 1505–1508.



- Nitta T. and Yamada. S. 1989. Recent warming of tropical sea surface temperature and its relationship to the northern hemisphere circulation. *J. Meteor. Soc. Japan.*, 67, 375-383.
- Ogasawara, N., Kitoh, A., Yasunari, T. and Noda, A. 1999. Tropospheric biennial oscillation of ENSO-monsoon system in the MRI coupled GCM. *J. Meteor. Soc. Japan.*, 77, 1247-1270.
- Oort, A. H. and Rasmusson, E. M. 1970. On the annual variation of monthly mean meridional circulation. *J. Climate.*, 13, 3969-3993.
- Oort, A. H., and Yienger, J. J. 1996. Observed interannual variability in Hadley circulation and its connection to ENSO. *J. Climate.* 9 2751-2767.
- Palmer, T. N. 1994. Chaos and predictability in forecasting the monsoon. *Proc. Indian. Nat. Sci. Acad.* 60. No.1. 57-66.
- Parthasarathy, B., Munot, A. A. and Kothwalae, D. R. 1994. All India monthly and seasonal rainfall series, 1871-1993. *Theoret. Appl. Climatol.*, 49, 217-224.
- Philander, S.G. 1990. El Niño, La Niña and the southern oscillation. Academic press, London, 289.
- Piexoto, J. P., and Oort, A. H. 1992. Physics of climate. New York: American Institute of Physics, 520.
- Pillai, P.A. and Mohankumar, K 2007. Tropospheric biennial oscillation of Indian summer monsoon with and without El-nino southern oscillation. *Int. J. Climatol.*, 127, 2095-2101
- Pillai, P.A and Mohankumar, K 2008. Local Hadley circulation over Asian monsoon region associated with Tropospheric biennial oscillation. *Theorl. Appl. Climatol.* 91, 171-179
- Rajeevan, M., Bhate, J., Kale, J. D and Lal, B. 2005. Development of a high resolution daily gridded rainfall data for the Indian region, India Meteorological Department, Met. Monograph Climatology No. 22/2005, pp. 26.
- Ramage, C.S. 1971 Monsoon Meteorology, Acedemic Press, New York, 6.
- Rasmusson, E. M. and Carpenter, T. H. 1983. The relationship between eastern equatorial Pacific sea surface temperature and rainfall over India and Sri Lanka, *Mon. Wea. Rev.*, 111, 517- 528.
- Rasmusson, E. M., Wang, X., and Ropeleswki, C. 1990. The biennial component of ENSO vatiability. *J. Mar. Sys.* 1, 71- 96.
- Reason, W. C., Allen, R. J., Lindesay, J. A. and Ansell, T. J. 2000. ENSO and climatic signals across the Indian ocean basin in global

- context: Part1. Interannual composite patterns. *Int. J. Climatol.* 20, 1285-1327.
- Reed, R. J., Campbell, W. J., Rasmussen L. A. and Rogers, D. G. 1961. Evidence of downward propagating annual wind reversal in the equatorial stratosphere. *J. Geophys. Res.*, 66, 813-818.
- Ropelewski, C. F., Halpert, M. S. and Wang. X. 1992. Observed tropospheric biennial variability and its relationship to Southern Oscillation. *J.Climat.*, 5, 594-614.
- Saji, N. H. and Yamagata, T. 2003. Structure of SST and surface wind variability during Indian Ocean dipole events: COADS observations. *J. Climate.*, 16, 2735-271
- Saji, N. H., Goswami, B. N., Vinayachandran, P. N. and Yamagata, T. 1999. A dipole mode in the tropical Indian Ocean. *Nature*, 401,360–363.
- Sathiyamurthy, V. and Mohanakumar, K. 2000. Characteristics of tropospheric biennial oscillation and its possible association with stratospheric QBO. *Geophys. Res. Lett.*, 27, 669-672.
- Shen, S. and Lau, K. M. 1995. Biennial oscillation associated with the east Asian summer monsoon and tropical sea surface temperature. *J. Meteor. Soc. Japan.*, 73, 105-124.
- Shukla, J. 1981. Dynamical predictability of monthly means. *J. Atmos. Sci.*, 38, 2547-2572.
- Shukla, J. 1987. Interannual variability of Monsoon, in Monsoons, edited by J.S Fein and P.L Stephens, John Willey, New York, 399-464
- Sikka, D. R. 1980. Some aspects of large-scale fluctuations of summer monsoon rainfall over India in relation to fluctuations in planetary and regional scale circulation parameters, *Proc. Ind. Acad. Sci.*, 89,179-195.
- Sikka, D., and Gadgil, S. 1980. On the maximum cloud zone and the ITCZ over Indian longitudes during southwest monsoon. *Mon. Wea. Rev.*, 108,1840-1853.
- Slingo, J. 1987. The development and verification of a cloud prediction scheme for the ECMWF model. *Quart. J. Roy. Meteor. Soc.* 113, 899-927.
- Slingo, J. M. and Annamali, H. 2000. 1997:The El Niño of the century and the response of the Indian summer monsoon. *Mon. Wea. Rev.*, 128, 1778-1797.
- Soman, M. K., and Slingo, J. M. 1997. Sensitivity of the Asian summer monsoon to aspects of the sea surface temperature anomalies in

- the tropical Pacific Ocean. *Quart. J. Roy. Meteor. Soc.*, 123, 309–336.
- Sperber, K. R, Slingo, J. M. and Annamali, H. 2000. Predictability and the relationship between subseasonal and interannual variability during asian summer monsoon. *Quart. J.Roy. Meteor. Soc.* 126, 2545-2574.
- Terray, P.1995. Space-time structure of monsoon interannual variability. *J.Climate.*, 8, 2595-2619.
- Terray, P, Dominiak, S. and Delecluse, P. 2005. Role of the southern Indian Ocean in the transitions of the monsoon-ENSO system during recent decades. *Climate Dyn.*, 24, 169-195.
- Tomita, T. and Yasunari, T.1993. The two types of ENSO. *J. Meteor. Soc. Japan.*, 71, 273–284.
- Tomita, T. and Yasunari, T. 1996: Role of the northeast winter monsoon on the biennial oscillation of the ENSO/monsoon system. *J. Meteor. Soc. Japan.*, 74, 399–413.
- Torrence, C. and Compo, G.P.1998. A practical guide to wavelet analysis. *Bull. Amer. Meteor. Soc.*, 79, 61-78.
- Torrence, C. and Webster, P.J.1999. Interdecadal changes in ENSO-Monsoon system. *J.Climate.*, 12, 2679-2690.
- Trenberth, K.E. 1975. A quasi-biennial standing wave in the southern hemisphere and interactions with sea surface temperature. *Quart. J. Roy. Meteor. Soc.*, 101, 55-74.
- Trenberth, K. E., 1990: Recent observed interdecadal climate changes in the Northern Hemisphere. *Bull. Amer. Meteor. Soc.*, 71, 988–993..
- Trenberth, K. E., Stepaniak, D. P. and Caron, J. M. 2000. The global monsoon as seen through the divergent atmospheric circulation. *J. Climate.*, 13,3969–3993.
- Vernekar, A. D., Zhou, J. and Shukla, J. 1995. The effect of Eurasian snow cover on the Indian monsoon. *J. Climate.*, 8, 248-266.
- Wang, B. 1995. Interdecadal changes in El Niño onset in the last four Decades. *J.Climate.*, 8, 267-285.
- Wang, B., and Xie, X. 1997. A model for the boreal summer intraseasonal oscillation. *J.Atmos.Sci.*, 54,71-86
- Wang, B., Wu, R. and Li, T. 2003. Atmosphere–Warm Ocean Interaction and Its Impacts on Asian–Australian Monsoon Variation. *J. Climate.*, 16, 1195-1211.
- Wang, C. 2002. Atmospheric circulation cells associated with El Niño-

- Southern Oscillation. *J. Climate.*, 15, 399-419.
- Webster, P.J. 1987 The Elementary Monsoon in Monsoons, edited by J.S Fein and P.L Stephens, John Willey, New York, 3-32.
- Webster, P.J., and Palmer, T. N. 1997 The past and future of El Nino. *Nature*, 390.562-564
- Webster, P.J., and Yang, S. 1992. Monsoon and ENSO. Selectively interactive system. *Quart.J.R.Meteor.Soc.*, 118, 877-926.
- Webster, P.J., Magana V.O., Palmer, T.N, Shukla, J., Tomas, R.A., Yanai, M. and Yasunari, T. 1998. Monsoons: Processes, predictability and the prospects for prediction. *J. Geophys. Res.*, 103, 14451-14510
- Webster, P.J., Moore, A.M., Loschinger, J.P. and Leben, R.R. 1999. Coupled ocean-atmosphere dynamics in the Indian ocean during 1997-98. *Nature*, 401, 356-360.
- Wu, R. and Kirtman, B.P. 2004. The tropospheric biennial oscillation of ENSO-monsoon system in an interactive ensemble coupled GCM. *J. Climate.*, 17 1623-1640.
- Wu, R., and Kirtman, B.P. 2007. Role of Indian Ocean in biennial transition of Indian summer monsoon. *J.Climate.*, 20, 2147-2164.
- Xie, P., and Arkin, P.A. 1997. Global precipitation: A 17 year monthly analysis based on gauge observations, satellite estimates and model outputs. *Bull. Amer.Meteor.Soc.*, 78, 2539-2558.
- Yang, S., Lau, K.M., and Rao, M.S., 1996. Precursory signals associated with the interannual variability of the Asian summer monsoon, *J. Climate.*, 9, 949- 964.
- Yang, S., Lau, K.M., and Sankar-Rao, M. 1996: Precursory signals associated with the interannual variability of the Asian Monsoon. *J. Climate.*, 9, 949-964.
- Yasunari, T. 1979. Cloudiness fluctuations associated with the northern hemisphere summer monsoon. *J. Meteor. Soc. Japan.*, 57, 227-242
- Yasunari, T. 1985. A possible link of the QBO between the stratosphere, troposphere and sea surface temperature in the tropics. *J.Meteor. Soc. Japan.*, 67, 483-493.
- Yasunari, T. 1987. Global structure of the El-Niño/Southern Oscillation. Part I: El-Niño composites. *J. Meteor. Soc. Japan.*, 65, 65-80.
- Yasunari, T. 1989. A Possible Link of the QBOs Between the Stratosphere, Troposphere and Sea Surface Temperature in the Tropics. *J. Meteor. Soc. Japan.*, 67, 483-493.

- Yasunari, T. 1990 Impact of Indian monsoon on the couple atmosphere/ ocean systems in the tropical Pacific, *Met. Atmos. Phys.*, 44, 29-41
- Yasunari, T. 1991. The monsoon year - a new concept of the climate year in the tropics. *Bull. Amer. Meteorol. Soc.*, 72, 1331-1338.
- Yasunari, T., and Seki, Y. 1992. Role of the Asian monsoon on the interannual variability of the global climate system. *J. Meteor. Soc. Japan* 70, 177-189.
- Yasunari, T., Kitoh, A. and Tokioka, T. 1991: Local and remote responses to excessive snow mass over Eurasia appearing in the Northern spring and summer climate—A study with the MRI-GCM. *J. Meteor. Soc. Japan*, 69, 473-487.
- Yu, J.Y., Weng, S.P., and Farrara, J.D, 2003. Ocean roles in TBO transition of Indian- Australian monsoon system. *J. Climate.*, 16. 3072-3080.
- Yu, L, and Riencker, M.M. 1999. Mechanism of the Indian Ocean warming during 1997-1998 El Niño. *Geophys. Res. Lett.*, 26. 735-738.

## List of Publications

### a) International journals

- 1) **Prasanth A Pillai** and K Mohankumar (2007) *Tropospheric biennial oscillation of Indian summer monsoon with and without El-nino southern oscillation*. *International journal of climatology* vol27 issue 15 pages 2095-2101
- 2) **Prasanth A Pillai** and K Mohankumar (2007) *Seasonal modification of Walker Circulation Cells associated with Tropospheric Biennial Oscillation cycle*. *Meteorology and Atmospheric Physics* (under review).
- 3) **Prasanth A Pillai** and K Mohankumar (2008) *Local Hadley circulation over Asian monsoon region associated with Tropospheric biennial oscillation*. *Theoretical and applied climatology* vol 91 pages 171-179 DOI 10.1007/s00704-007-0305-5
- 4) K Mohankumar and **Prasanth A Pillai** (2008) *Stratosphere-Troposphere interaction associated with Biennial oscillation of Indian summer monsoon*. *Journal of Atmospheric and Solar-Terrestrial Physics* Vol 77 Pages 764-773. DOI:10.1016/j.jastp.2007.12.001
- 5) **Prasanth A Pillai** and K Mohankumar (2008) *Role of TBO and ENSO scale Ocean-Atmosphere interaction in the Indo-Pacific region on Asian summer monsoon variability*. *Theoretical and applied climatology*, DOI 10.1007/s00704-008-0053-1
- 6) **Prasanth A Pillai** and K Mohankumar (2008) *Effect of late 1970's climate shift on Tropospheric Biennial Oscillation- Role of local Indian Ocean processes on Asian Summer monsoon*. *International journal of climatology* (accepted).
- 7) **Prasanth A Pillai** and K Mohankumar (2008) *Common mode of variability of boreal summer intraseasonal oscillation and tropospheric biennial oscillation*, *Dynamics of Atmospheres and Oceans* (under review)
- 8) **Prasanth A Pillai** and K Mohankumar (2008) *Individual and combined influence of El Nino Southern Oscillation and Indian Ocean Dipole in Tropospheric Biennial Oscillation*. *Quarterly Journal of Royal Meteorological Society* (communicated)
- 9) **Prasanth A Pillai** and K Mohankumar (2008) *Possible link of stratospheric QBO with TBO associated with Indian-Australian monsoon system*. *Journal of Atmospheric and Solar-Terrestrial Physics* (Submitted)

b) **Proceedings of seminars**

*International*

- 1) **Prasanth A Pillai** and K Mohankumar (2007) *Tropospheric Biennial Oscillation of Indian summer monsoon independent of El-Nino Southern Oscillation.*, IUGG2007, Perigue 2007 July
- 2) **Prasanth A Pillai** and K Mohankumar(2007) *Effect of Climate change in the late 1970's on Tropospheric Biennial Oscillation.*, IUGG2007, Perigue 2007 July
- 3) **Prasanth A Pillai** and K Mohankumar(2007) *Evidence of increase in tropospheric biennial oscillation of Indian summer monsoon after the late 1970's climate shift.* international conference "Celebrating monsoon" at IISC, Bangalore July2007
- 4) K Mohanakumar and **Prasanth A Pillai**(2008) **Stratosphere-Troposphere coupling over Indian monsoon region.** COSPAR 2008 July, Canada
- 5) **Prasanth A Pillai** and K Mohankumar(2008) *QBO-TBO interaction over monsoon regions: A Global Perspective.* COSPAR 2008 July, Canada
- 6) K Mohanakumar, **Prasanth A Pillai** and Rajesh J (2008) *Stratosphere-Troposphere interaction over a tropical monsoon region*, SPARC 2008 September, Italy
- 7) K Mohanakumar, **Prasanth A Pillai** and Nithin Viswambaran (2008) *Stratospheric Variability : Before and after late 1970's climate shift.* SPARC 2008 September, Italy

*National seminars*

- 1) **Prasanth A Pillai** and K Mohankumar (2006)*Coupled ocean-atmosphere processes affecting Indian summer monsoon on TBO and ENSO scale.* ATMOCIN06,
- 2) **Prasant A Pillai** and K Mohankumar (2007) *Atmospheric circulation associated with Tropospheric Biennial Oscillation.* Tropmet2007, Pune.
- 3) **Prasanth A Pillai** and K Mohankumar(2007) *Tropospheric Biennial Oscillation of Indian summer monsoon without El-Nino southern oscillation* METOC2007, Cochin.

## List of Abbreviations

ASM	Asian Summer Monsoon
CMAP	Climate Prediction Centre Merged Analysis Project
DJF-1	Boreal winter season (previous year December, current year January and February) of a strong/ weak TBO year.
DJF0	Boreal winter season (December of TBO year, January and February of next year) after TBO year
ECMWF	European Centre for Medium Range Weather Forecast
ENSO	El Nino Southern Oscillation
EOF	Empirical Orthogonal Function
IAV	Inter annual variability
IOD	Indian Ocean Dipole
ISMR	Indian Summer Monsoon Rainfall
ISO	Intraseasonal Oscillation
ITCZ	Inter Tropical Convergence Zone
JJA-1	Previous year summer (June to August) of a strong/weak TBO year
JJA0	Summer season of TBO year
MAM0	Spring season (March to May) of a strong/weak TBO year
MAM1	Next year spring season of TBO year
NCAR	National Centre for Atmospheric Research
NCEP	National Centre for Environmental Prediction
NOAA	National Ocean atmosphere Administration
OLR	Outgoing Long Wave Radiation
PC	Principal Component
QBO	Quasi-Biennial Oscillation
SLP	Sea Level Pressure
SON-1	Autumn season (September to November) before a TBO year
SON0	Autumn season of a TBO year
SPCZ	South Pacific Convergence Zone
SST	Sea Surface Temperature
TBO	Tropospheric Biennial Oscillation